

UNITED KINGDOM · CHINA · MALAYSIA

# Design and synthesis of lugdunin analogues as macrocyclic peptide antibiotics

Ta Chi, Su

Thesis submitted to the University of Nottingham for the degree of Doctor of Philosophy

Apr 2024

## **Abstract**

Due to the overuse of antibiotics, bacteria have become increasingly resistant to many different antibiotics, resulting in antibiotic-resistant strains such as *methicillin-resistant Staphylococcus aureus* (MRSA) and *vancomycin-resistant S. aureus* (VRSA). It also makes the clinical treatment of bacterial diseases more difficult and leads to an increased mortality rate. The development of new classes of antibiotics has remained stagnant for a long time. In 2016, lugdunin, a new natural product from *Staphylococcus lugdunensis* which is presented in the human nostrils, was found to display potent antimicrobial activity against antibiotic-resistant strains of *S. aureus* (MIC =  $1.5 \mu g/ml$  against MRSA). Thus, the project aims to design a focused series of lugdunin analogues and to determine their antimicrobial activities against different strains of *S. aureus*.

To synthesize lugdunin and its analogues, the Fmoc-based solid phase peptide synthesis (Fmoc-SPPS) was used. Moreover, various types of solid supports (resin) were investigated and used to optimize the reaction. For the total synthesis of lugdunin and analogues thereof, threonine-glycine (TG) resin was used as the most effective resin due to several advantages, such as high yields and simple operation. A modified TG resin was then prepared by the pre-loading of different Fmoc-amino aldehydes, which in turn were prepared from their corresponding Fmoc-amino acids by a one-pot procedure involving 1, 1'-carbonyldiimidazole (CDI)-activation followed by diisobutylaluminium hydride (DIBAL-H)-mediated reduction.

To determine the importance of each amino acid residue to the antimicrobial activity, alanine scanning was first introduced. Then, to establish a preliminary structure-activity relationship (SAR), several analogues were synthesized, such as the installation of modified amino acids, including D-phenylalanine and D-tryptophan at position-6 and L-norvaline, L-norleucine, *N*-

methyl-L-valine, *N*-methyl-L-leucine, L-tryptophan, L-cyclopropylalanine and L-homoleucine at position 7.

For the antimicrobial assessment, different strains of *S. aureus* including SH1000 and USA300 JE2 were used to investigate the antibacterial activity. Amongst all the evaluated compounds, lugdunin (IC $_{50} = 27.58 \pm 0.62 \,\mu\text{M}$ ), (Leu) $^7$ -lugdunin (IC $_{50} = 6.88 \pm 0.75 \,\mu\text{M}$ ), (L-*N*-Me-Val) $^7$ -lugdunin (IC $_{50} = 25.49 \pm 0.18 \,\mu\text{M}$ ) and (D-Trp) $^6$ -lugdunin (IC $_{50} = 19.74 \pm 0.27 \,\mu\text{M}$ ) showed good-to-high antibacterial activity against *S. aureus* USA300 JE2. Then, the three analogues were further evaluated against several other strains of *S. aureus*, including Mu50, Newman and PM64. The analogue (Leu) $^7$ -lugdunin was found to be the most potent analogue tested to date, displaying typically 4-fold higher potency than the synthesized lugdunin.

Following the results of antimicrobial activity tests, an SAR study of lugdunin at position 6 and 7 was established. At position 7, it is found that a linear side chain is more potent than a cyclic/aromatic side chain. Moreover, four carbon atoms are found to be the most suitable length of the side chain. In the contrast, a cyclic/aromatic side chain showed more potent activity than a linear side chain at position 6. Future work will focus on further analogues with the modification and substitution at position 7, time-kill assay and also antimicrobial tests against different bacteria.

# Acknowledgement

First and foremost, I want to extend my heartfelt gratitude to my supervisor Professor Weng C Chan whose patient guidance, valuable suggestions and constant encouragement make me understand the project and the process of PhD research. He has always provided a good learning and research environment for me to well develop my enthusiasm for research.

I would like to acknowledge my co-supervisor Professor Michael Stocks, internal assessor Professor Peter Fischer, and the generous funding from the Vice-Chancellor Scholarship.

I would like to express my sincere gratitude to all my colleagues as well as C22 lab mates Vivian, Paulina, James, Leonardo, Rebecca, Emanule, Lei and Ryan. Their advice and support help me all over the first year of study. I am also grateful to colleagues from other labs especially, Yen Ju, Zhi Yuan, Ruiling, Louis and Chia Yang for their friendship and invaluable help while working in the lab. Many thanks to Lee Hibbett, Christophe and Ewan for the assistance in NMR, LC/MS/MS and microbiological work in C69.

To all my friends since high school in Taiwan, thanks for the continuous support and accompany while I was writing my thesis.

Last but not least, I would like to express my special and forever thanks to my parents and my little sister, whose care and support motivate me to move on and funded for the PhD. They always encourage me and make me never give up during the past four years. Without them, I could not have the opportunity to study abroad. Thus the successful completion of this thesis is especially dedicated to them.

# **Abbreviations**

ACTH Adrenocorticotropic hormone

AMPs Antimicrobial peptides

AMR Antimicrobial resistance

Boc *t*-Butyloxycarbonyl

Boc<sub>2</sub>O Di-*tert*-butyl dicarbonate

br Broad

Cbz Carboxybenzyl

CDC Centers for Disease Control and Prevention

CDI 1,1'-Carbonyldiimidazole

1-[1-(Cyano-2-ethoxy-2-oxoethylideneaminooxy)-dimethylamino-

COMU morpholino]-uronium hexafluorophosphate

CoNS Coagulase-negative Staphylococcus

CPA Cyclopropylalanine

d Doublet

DBF Dibenzofulvene

DCC Dicyclohexylcarbodiimide

DCM Dichloromethane

dd Doublet of doublet

DEAD Diethyl azodicarboxylate

DIBAL-H Diisobutylaluminium hydride

DIC Diisopropylcarbodiimide

DIPEA *N,N*-Diisopropylethylamine

DMF Dimethylformamide

DMP Dess-Martin periodinane

DMSO Dimethyl sulfoxide

dt Doublet of triplet

Eap Extracellular adherence protein

EDC 1-Ethyl-3-(3-dimethylaminopropyl)carbodiimide

EDTA Ethylenediaminetetraacetic acid

ENaC Epithelial sodium channel

Fmoc 9-Fluorenylmethyloxycarbonyl

Fnbp A Fibronectin-binding protein A

Fnbp B Fibronectin-binding protein B

GISA Glycopeptide-intermediate Staphylococcus aureus

1-[Bis(dimethylamino)methylene]-1*H*-1,2,3-triazolo[4,5-*b*]pyridinium 3-

HATU oxide hexafluorophosphate

3-[Bis(dimethylamino)methyliumyl]-3*H*-benzotriazol-1-oxide

HBTU hexafluorophosphate

Hla α-Hemolysin

HOAt 1-Hydroxy-7-aza-benzotriazole

HOBt 1-Hydroxy-benzotriazole

HPTS 8-Hydroxypyrene-1,3,6-trisulfonic acid trisodium salt

HRMS High-resolution mass spectrometry

IC<sub>50</sub> Concentration required to achieve 50% inhibition

Isd A Iron-regulated surface determinant A

LB Luria Bertani

MDR Multidrug-resistant

MDRP Multiple-drug-resistant Pseudomonas aeruginosa

MIC Minimal inhibitory concentration

MoA Mode of action

M.p. Melting point

MRSA Methicillin-resistant Staphylococcus aureus

MβLs Metallo-β-lactamases

NEAT Near-iron transporter

NHP *N*-Hydroxy peptide

NHS *N*-Hydroxysuccinimide

NRAPs Nonribosomal antibacterial peptides

NRPs Nonribosomally peptides

NRPSs Nonribosomal peptide synthetases

OD Optical density

ORD Optical rotatory dispersion

PI Propidium iodide

PISP Penicillin-intermediate resistant *S. pneumonia* 

POPC 1-Palmitoyl-2-oleoyl-sn-glycero-3-phosphocholine

PTC Phase-transfer condition

PTSA *p*-toluenesulfonic acid

7-Azabenzotriazol-1-yloxy)tripyrrolidinophosphonium

PyAOP hexafluorophosphate

PyBOP Benzotriazol-1-yloxy)tripyrrolidinophosphonium hexafluorophosphate

[Ethylcyano(hydroxyimino)acetato-O<sup>2</sup>]tri-1-

PyOxim pyrrolidinylphosphoniumhexafluorphosphate

r.t. Room temperature

SAR Structure-activity relationship

SBLs Serine β-lactamases

SCVs Small-colony variant

SEs Staphylococcal enterotoxins

SPPS Solid-phase peptide synthesis

t Triplet

TES Triethylsilane

TFA Trifluoroacetic acid

THF Tetrahydrofuran

TIPS Triisopropylsilane

TNF $\alpha$  Tumor necrosis factor  $\alpha$ 

 $t_{\rm R}$  Retention time

VRE Vancomycin-resistant enterococci

VRSA Vancomycin-resistant S. aureus

# **Table of contents**

Ał	ostract	i
Ad	cknowledgement	iii
Ał	Abbreviationsi	
1.	Introduction	1
	1.1 Development of antimicrobial agents	1
	1.2 Gram-positive bacteria.	4
	1.2.1 Staphylococcus aureus	7
	1.2.2 Epidemiology and pathology	8
	1.2.3 Invasion strategies of <i>S. aureus</i>	10
	1.2.4 Treatments for <i>S. aureus</i> infection	14
	1.2.4.1 β-lactam antibiotics	14
	1.2.4.2 Aminoglycosides	20
	1.2.4.3 Quinolones	22
	1.2.4.4 Macrolides	24
	1.2.4.5 Vancomycin and VRSA	25
	1.3 Peptide medicines	27
	1.3.1 Introduction of peptide medicines	27
	1.3.2 Antimicrobial peptides	30
	1.3.3 Ribosomally synthesized peptides	32
	1.3.3.1 Ribosomally synthesized peptides from natural sources	32
	1.3.3.2 Mechanism of ribosomally synthesized AMPs	33
	1.3.3.3 Challenges in development of ribosomally synthesized AMPs	34
	1.3.4 Non-ribosomally synthesized peptides	35
	1.3.4.1 Introduction to non-ribosomally synthesized peptides	35

	1.3	3.4.2 Non-ribosomally synthesized peptides as antimicrobial agents36
	1.4 Lugd	unin – an overview41
	1.4.1	Background of lugdunin
	1.4.2	Antimicrobial activity and MoA of lugdunin
	1.4.3	Research on lugdunin analogues and SAR study
	1.4.4	Interaction between lugdunin and bacterial membrane resulting in proton
		translocation
	1.5 Aims	and objectives63
2.	Total syn	thesis of lugdunin69
	2.1 Synthe	esis of lugdunin69
	2.2 An ov	erview of synthetic strategies
	2.3 Solid-	phase peptide synthesis (SPPS)
	2.3.1	An overview of peptide synthesis
	2.3.2	Introduction of solid-phase peptide synthesis (SPPS)75
	2.3.3	Introduction of Fmoc-SPPS76
	2.3.4	Solid supports (resin) for Fmoc-SPPS
	2.3.5	Introduction of peptide macrocyclization79
	2.3.6	Peptide coupling reagents80
	2.3	3.6.1 Carbodiimides81
	2.3	3.6.2 Aminium/uronium salts82
	2.3	3.6.3 Phosphonium salts83
	2.4 Synthe	esis of thiazolidine dipeptide84
	2.4.1	Synthesis of amino aldehyde84
	2.4.2	Optical rotation study
	2.4.3	Synthesis of thiazolidine dipeptide90

	2.5 Synth	esis of lugdunin	91
	2.5.1	Synthesis of lugdunin by Weinreb AM resin	91
	2.5.2	Synthesis of lugdunin by Thr-Gly functionalized Rink TG resin	94
	2.5.3	Purification by RP-HPLC	97
	2.6 Concl	usions	99
3.	Synthesis	s and alanine-scanning of (Ala) <sup>7</sup> -lugdunin	101
	3.1 Synthe	esis of (Ala) <sup>7</sup> -lugdunin	101
	3.1.1	Synthesis of (Ala) <sup>7</sup> -lugdunin by 2-Cl-Trt chloride resin	101
	3.1.2	Synthesis of (Ala) <sup>7</sup> -lugdunin by TG resin	102
	3.2 Alanii	ne-scanning of (Ala) <sup>7</sup> -lugdunin	105
	3.2.1	Introduction of alanine scanning	105
	3.2.2	Synthesis of compounds <b>3.11-3.15</b>	108
3	3.3 Conclus	sions	109
4.	Synthesis	s of Fmoc-N-methyl amino acids and Fmoc-L-homoleucine	111
	4.1 Introd	uction of N-methyl amino acids	111
	4.2 Repor	ted synthetic strategies to N-methyl amino acids	112
	4.2.1	<i>N</i> -methylation via α-bromo acids	112
	4.2.2	N-methylation via a Mitsunobu reaction	113
	4.2.3	N-methylation via base-mediated alkylation	114
	4.2.4	N-methylation via an oxazolidinone intermediate	115
	4.3 Synth	esis of Fmoc-L-homoleucine via Ni(II)-Gly-BPB complex	118
	4.3.1	Chiral glycine equivalent approach	118
	4.3.2	Total synthesis of Ni(II)-Gly-BPB complex	119

	4.3.2.1 Synthesis of <i>N</i> -benzyl-( <i>S</i> )-proline
	4.3.2.2 Synthesis of chiral ligand (S)-2-[N'-(N-
	benzylprolyl)amino] benzophenone (BPB)121
	4.3.2.3 Synthesis of Ni (II)-Gly-BPB complex
	4.3.2.4 Alkylation of Ni (II)-Glycine-BPB complex122
	4.3.2.5 Disassembly of the alkylated Ni (II)-Glycine-BPB complex and N-Fmoc-
	protection reaction
	4.4 Conclusions
5.	Lugdunin analogues with modifications at position 6 and 7
	5.1 Synthesis of lugdunin analogues with modification at position 7127
	5.1.1 Strategy for the design of lugdunin analogues
	5.1.2 Synthesis of the lugdunin analogues with linear/branched side chain128
	5.1.3 Synthesis of the lugdunin analogues with cyclic/aromatic side chain132
	5.1.4 Synthesis of the lugdunin analogues with <i>N</i> -methylated amino acids134
	5.1.5 Synthesis of the lugdunin analogues (L-threonine) <sup>7</sup> -lugdunin137
	5.2 Synthesis of lugdunin analogues with modification at position 6
	5.3 Synthesis of lugdunin analogues with combined modification at position 6 and 7141
	5.4 Conclusions
6.	Antibacterial assessment of lugdunin and analogues thereof
	6.1 Introduction
	6.2 Antimicrobial activity of lugdunin and its analogues against <i>S. aureus</i> 146
	6.2.1 Growth inhibition and broth microdilution assays

	6.2.2	Structure-activity relationships study of lugdunin and the analogu	es against S.
		aureus	150
	6.2	2.2.1 SAR study of alanine-scanning	150
	6.2	2.2.2 SAR study of analogues modified at position 7	150
	6.2	2.2.3 SAR study of analogues modified at position 6	152
	6.2.3	Broth microdilution of selected analogues	153
	6.3 Concl	usions	154
7.	General c	conclusions and future work	159
•		al conclusions	
	7.1 Gener 7.1.1	Synthesis of Fmoc- <i>N</i> -methyl amino acids	
	7.1.2	Synthesis of Fmoc-L-homoleucine	
	7.1.3	Total synthesis of lugdunin and analogues thereof	
	7.1.4	Antimicrobial assessment of lugdunin and analogues thereof	
	7.1.5	A brief overview on SAR study	
		e work	
		Further investigation into the residue at position 7	
	7.2.2	Evaluation of lugdunin analogues by time-kill assay	
	7.2.3	Determination of Log <i>P</i> values for synthesized compounds	
		nary	
	7.5 Sullin	iai y	179
8.	Experime	ental	
	8.1 Metho	ods and materials	181
	8.2 Exper	imental for Chapter 2	183
	8.3 Exper	imental for Chapter 3	194

	8.4 Experimental for Chapter 4	200
	8.5 Experimental for Chapter 5.	207
	8.6 Biological evaluations of lugdunin and analogues	233
9.	References	235
	Appendix	273

# Chapter 1

#### Introduction

#### 1.1 Development of antimicrobial agents

Antimicrobial agents have played a vital role in the clinical treatment of infectious diseases and hence profoundly affected the destiny of human beings. <sup>1,2</sup> However, mankind is now facing a countercharge due to the appearance of infectious diseases caused by antibiotic-resistant bacteria. Currently, antibiotic-resistant bacteria have left mankind with a serious problem to deal with in the clinic. <sup>3</sup> With inappropriately chosen antimicrobial agents, the therapy may not achieve the best effect, and moreover can result in the exacerbation of the disease. <sup>4,5</sup> In addition, the excessive use of broad-spectrum antibiotics is known as the key reason for causing the spread of multidrug-resistant bacteria. <sup>6</sup>

Owing to the problem of increasing antibiotic-resistant bacterial strains, antibiotic choices for infection control have become increasingly limited and more expensive. Therefore, it is important to have a complete understanding of the mechanisms and patterns of bacterial resistance and to further engage in the development of new drugs or therapy. Furthermore, increased effort to promote the proper prescription of antimicrobial agents is needed to preserve antibiotics which are currently in use in the clinic. At present, a few antimicrobial agents with a novel mode of action (MoA) are coming onto the market. Since the first antibiotic, penicillin, was found in 1928, many antibiotics have been discovered or synthesized (Figure 1.1). However, no new antibiotics have been brought through to the clinic from the discovery stage over the past decade. In the current status, due to the wide spread of multidrug-resistant bacteria, options for treatment with antibiotics are limited, and the number of brand-new drugs placed on the market is decreasing.

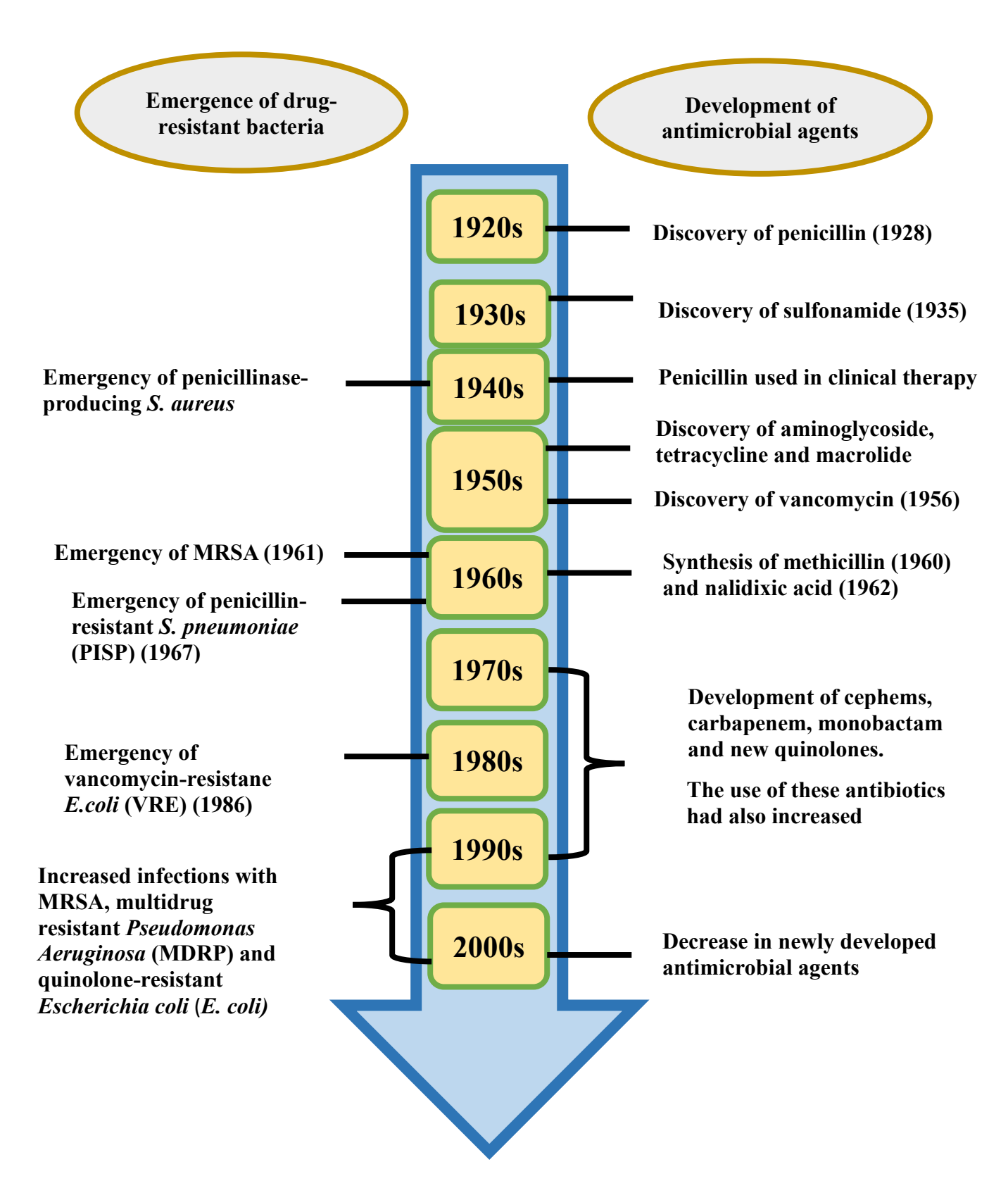


**Figure 1.1** Historical development of antimicrobial agents.<sup>1</sup> The figure shows the impact of drug-resistant bacteria and the discovery of all generations of antimicrobial agents during the past century. The development of novel antimicrobial agents has dramatically decreased since 2000 while the cases of drug-resistant bacteria are still increasing.

Therefore, the first step to resolve the issue of resistant bacteria could focus on the proper use

of the existing antibiotics and the effort to minimize the transmission and spread of resistant bacteria through appropriate infection control.<sup>11</sup>

Nevertheless, we are currently facing a reality that the discovery of novel antimicrobial agents with unique MoA is truly urgent.<sup>12</sup> As mentioned before, the number of new antimicrobial agents being brought to the market has undergone a steady decline. So far, to solve the problem, efforts have been made on the modification of existing antimicrobial agents or the development of new ones.<sup>13</sup> However, during the past four decades, a few new groups of antibacterial agents, such as oxazolidinones, diarylquinolines and streptogramins have been marketed and most of them are for the treatment of Gram-positive bacterial infections.<sup>14</sup>

There are several reasons for the decrease in the development of new antimicrobial agents. For example, most of the obvious targets for antibacterial activity which allow selective toxicity have already been discovered. Moreover, current new approaches, such as the exploitation of microbial genomics and high-throughput screening, have not led to the expected discovery of an abundance of new agents. Since the 1990s, owing to the consolidation in the pharmaceutical industry, a reduction of around 70 reasonable-sized companies with research and development (R&D) efforts in the antibacterial area to less than a dozen, has also taken a toll. It is estimated that only a few of the companies in the USA and Europe are maintaining active R&D programmes for antimicrobial agents. The lack of interest by big pharma in antibacterial agents is related to a number of factors, including the many generic antibacterial agents currently on the market that still have varying degrees of effectiveness and that are considered first lines of therapy by many public health authorities. There is a tendency to place new expensive agents on reserve status, largely as a matter of cost containment. Moreover, the duration of treatment with antibacterial agents is limited, which means that these agents are

less profitable to big pharma than drugs for treatment of cancer, and neurological, psychological, musculoskeletal or cardiovascular diseases, which are often given chronically and yield higher prices in some instances. Finally, a number of regulatory issues have also made it difficult to bring new agents to the market, particularly in the USA, including the fact that the US Food and Drug Administration (FDA) has recently shown a tendency to 'shift goalposts' for approval criteria for antimicrobial agents and has raised significant issues regarding the need to carry out placebo-controlled trials for patients with serious bacterial infections. <sup>15</sup>

To develop new antimicrobial agents, peptide antibiotics are frequently regarded as an important source of new drugs. <sup>16-18</sup> Naturally occurring antimicrobial peptides are thus recognized as a potential source for pharmaceutical research and the development of modern medicines. <sup>19</sup> As mentioned before, the discovery of novel antibiotics is necessary and urgent, therefore, the aim of the project reported in this thesis is to develop potentially new antibiotics with potent activity and unique MoA. Lugdunin is a potent peptide antibiotic first reported in 2016. <sup>20</sup> Thus, the project will focus on synthetic approaches to lugdunin and analogues thereof, and their design and antimicrobial assessment against various strains of the opportunistic human pathogen, *Staphylococcus aureus*.

## 1.2 Gram-positive bacteria

Bacteria can easily be distinguished and classified into two categories based on the result of the Gram stain test because of the different physical and chemical properties of the cell walls.<sup>21</sup> The Gram staining test, which was introduced in 1884 by Christian Gram, a Danish microbiologist is now the most common method.<sup>22</sup> Under the observation of an optical microscope, a blue-purple color will be seen for Gram-positive bacteria due to their thick mesh-

like cell wall while it appears red for Gram-negative bacteria after the general procedure (Figure 1.2).<sup>23</sup>

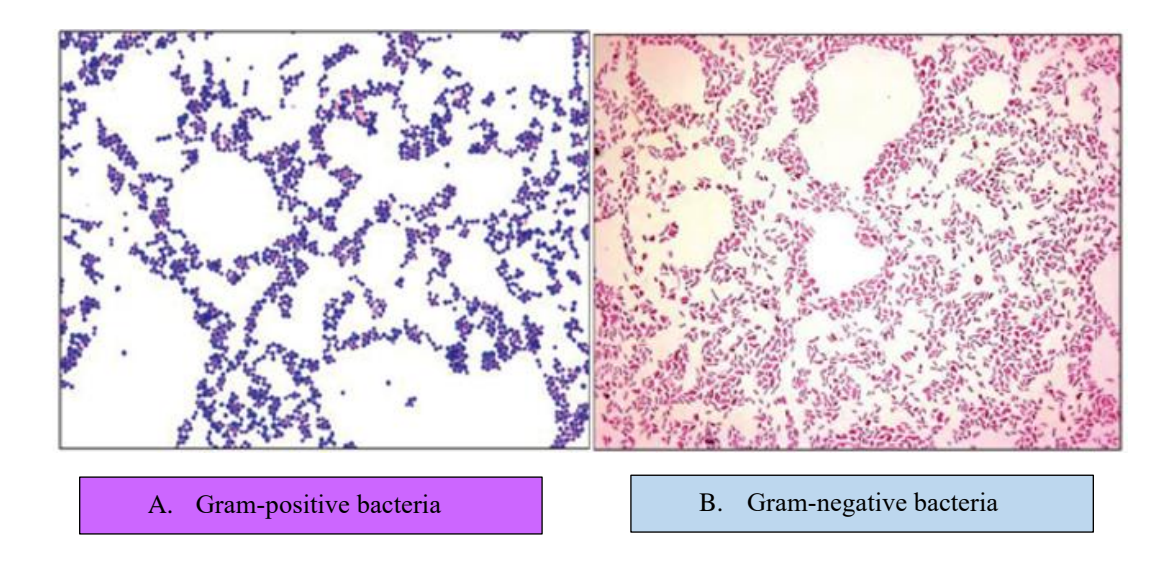


**Figure 1.2** Gram staining test for Gram-positive (A) and Gram-negative bacteria (B). Thick cell wall retains the crystal violet stain, whereas the Gram-negative cell wall loses the color as it is washed away (Figure obtained from Thairu *et al.*).<sup>24</sup>

Despite the difference in their peptidoglycan layer, Gram-positive bacteria are known to be more sensitive to specific antibiotics that interact with targets in the cell wall because of the lack of an outer membrane (Figure 1.3).<sup>25</sup> In general, several characteristics can be found in Gram-positive bacteria, such as lipoteichoic acids which are related to adherence, smaller periplasm and thicker peptidoglycan layer.<sup>26</sup> Moreover, rigid cell walls are generated from the cross-linking of peptidoglycan chains by DD-transpeptidase.<sup>27</sup>

To differentiate bacterial species and observe the cell shape, Gram staining is also a convenient and useful tool.<sup>21</sup> Based on several factors, such as the staining, antibiotic susceptibility testing, physiological tests, growth requirement and macroscopic tests, the bacteria can subsequently be classified (Figure 1.4).<sup>28</sup> *Staphylococcus aureus*, a member of the family of staphylococci, is one of the most important bacterium causing infectious diseases.

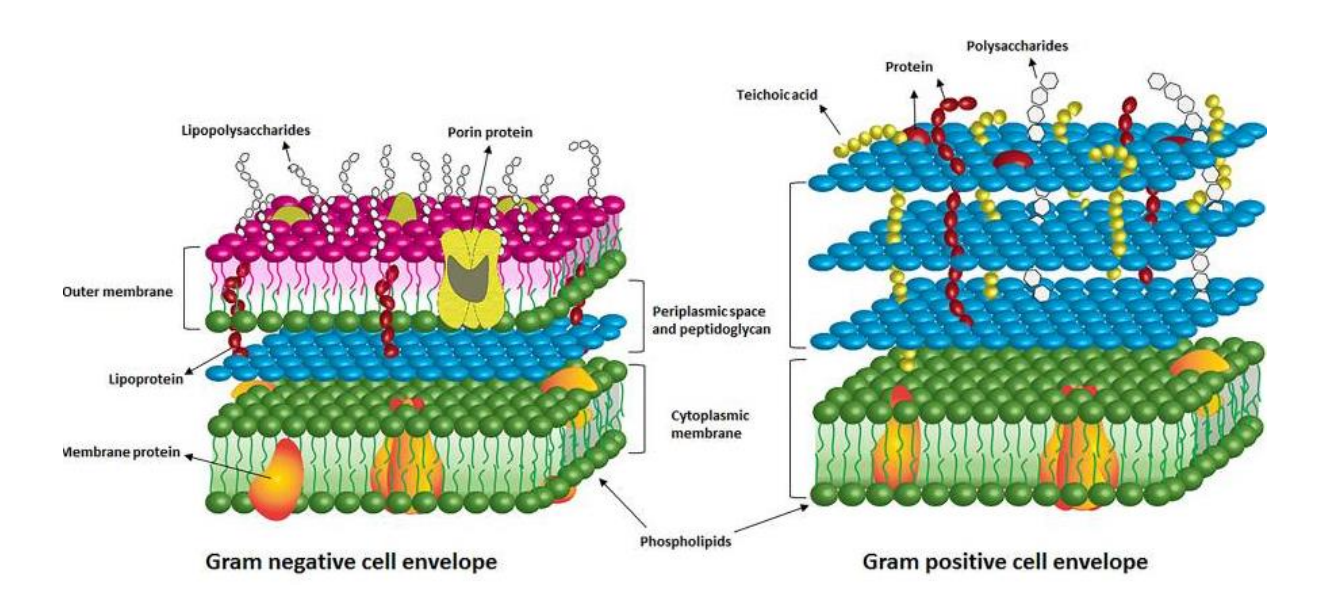


**Figure 1.3** Cell structure of Gram-negative (left) and Gram-positive (right) bacteria. The thicker peptidoglycan layer and the lack of the outer membrane can be seen in the Gram-positive cell envelope (Figure obtained from Liu, Yao *et al.*).<sup>29</sup>

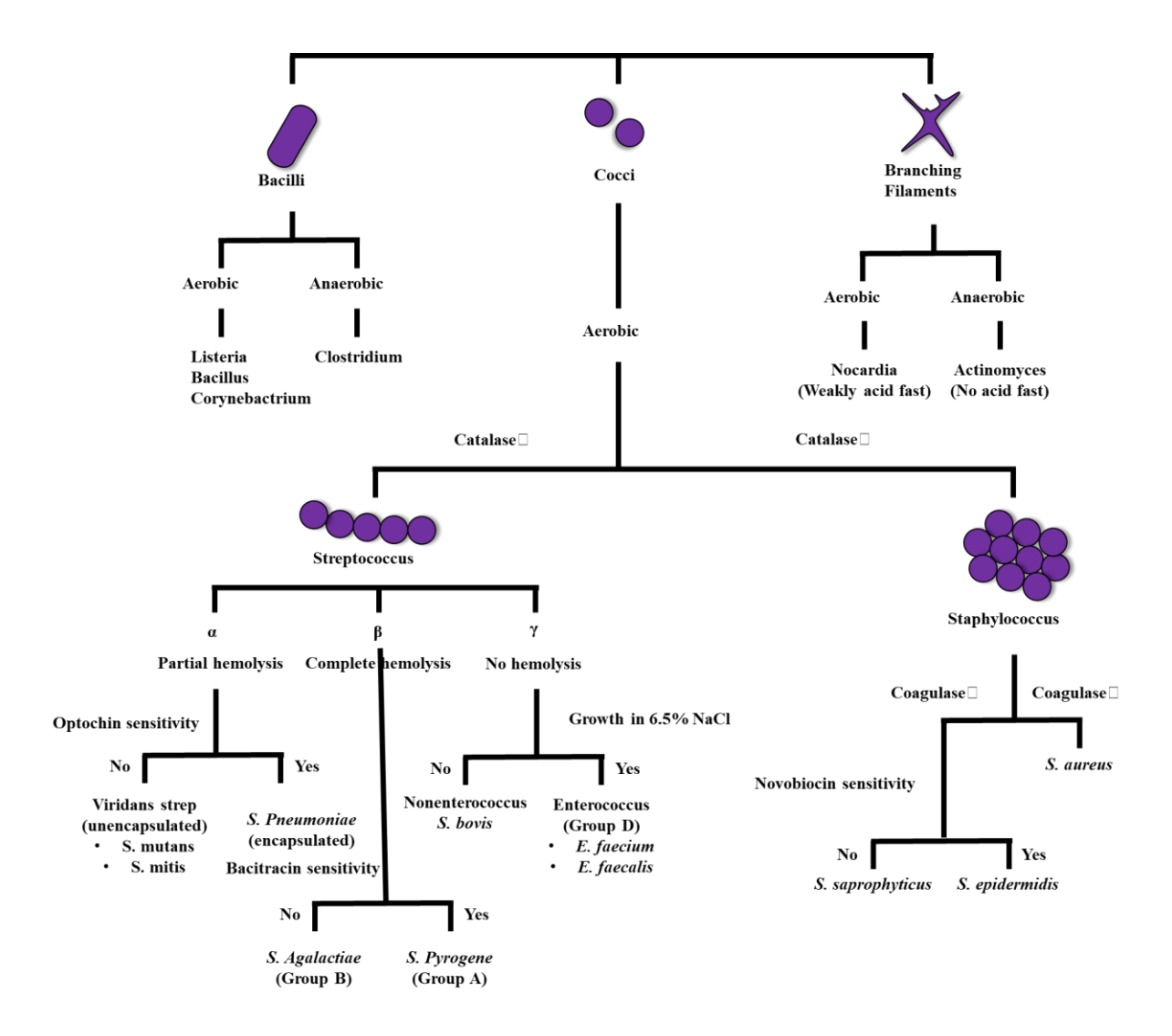


Figure 1.4 Classification and subdivision of G(+) bacteria (Figure obtained from Rea et al.).

# 1.2.1 Staphylococcus aureus

In 1881, *Staphylococcus* spp. was discovered to cause wound infections from an abscess surgery performed by Sir Alexander Ogston.<sup>30</sup> In 1884, *Staphylococcus aureus* which was separated and isolated from *Staphylococcus albus* was then identified by the German scientist Friedrich Julius Rosenbach.<sup>31</sup> Since 1940s, infections caused by *S. aureus* have been thought to be the most virulent.<sup>32</sup>

*S. aureus* is a Gram-positive bacterium which is widely distributed and found almost everywhere, particularly on the skin of humans and other animals.<sup>33,34</sup> About 60% of the human population is estimated to be colonized by *S. aureus* and 20-30% of humans are persistent carriers.<sup>35,36</sup> Although the nose is found to be the most favourable site for colonization by *S. aureus*, the bacteria can also survive on the skin and in the environment for a long time.<sup>36</sup> As a facultative anaerobe, oxygen is not necessary for their survival. With the ability to produce surface proteins which facilitate the adherence to host tissues and the secretion of toxins, *S. aureus* can cause mild to severe infections.<sup>37</sup>

### 1.2.2 Epidemiology and pathology

According to the statistics, around 20-30% of the human population are long-term *S. aureus* carriers.<sup>36,38</sup> Several illnesses can be caused by *S. aureus*, from slight skin infections to life-threatening diseases, including pneumonia, endocarditis, respiratory tract infection, meningitis, bacteremia, and sepsis.<sup>39,40</sup>

It is also one of the major causes of infection after surgery. Each year in the USA, around one in 31 patients in hospitals acquire *S. aureus* infection and one-tenth die from it.<sup>41-43</sup> In the UK, more than 9000 cases of *S. aureus* bacteremia were reported in 2014.<sup>44</sup> In 2016, there were 18.2 cases per 100,000 people reported.<sup>44</sup> In the latest report from the UK government, 1 person out of every 100,000 had a methicillin-resistant *Staphylococcus aureus* (MRSA) bacteraemia in 2021. In contrast in 2022, 22 people out of every 100,000 had MRSA bacteraemia.<sup>45</sup> Furthermore, people with diabetes, heart diseases or injection medicine users are at a higher risk of infection.<sup>38</sup>

In broad terms, the consequences of antibiotic resistance can be severe and result in a tremendous influence on morbidity and mortality. It also without doubt imposes a financial

burden for patients and the public health systems. 6,46 For example, in the U.S. an average of 45% of microorganisms found in surgical site infections are resistant to the clinically used antibiotics. 47 It was also found that patients with infections caused by multidrug-resistant (MDR) microorganisms have a higher chance of poor outcome and death, and thus more medical resources will be needed and consumed. 48,49 It has been reported that among the patients with *Klebsiella pneumoniae* (*K. pneumonia*) bacteremia, a two-fold higher risk of death was found in those whose infection was caused by carbapenem-resistant strains of *K. pneumonia* compared to the susceptible strains. 50 Meanwhile, it was estimated by the hospitals in the U.S. that approximately an extra 10,000–40,000 US dollars were spent on the treatment of infections caused by antibiotic-resistant bacteria versus antibiotic-susceptible strains in 2015. 51

According to the statistics reported by the Centers for Disease Control and Prevention (CDC) in the U.S., there are at least 2 million infections caused by antibiotic-resistant bacteria every year, and furthermore resulted in 23,000 deaths and \$55-70 billion in economic impact each year. <sup>52-54</sup> In Europe, it was estimated that around 33,000 people die from MDR-induced bacterial infections every year, and along with an annual cost of 1.5 billion EUR. <sup>55-57</sup>

The route of *S. aureus* infections is mainly via the infected wound or personal objects.<sup>58</sup> Cleaning hands and bodies often is an effective measure to prevent infection, however *S. aureus* can have a long incubation period in the human body and remain undetected for several years.<sup>59</sup> Once symptoms begin to appear, it may take a few weeks to fully recover from the infection, and the disease can even be deadly without proper treatments.<sup>60,61</sup>

### 1.2.3 Invasion strategies of *S. aureus*

As a facultative intracellular bacterium, the adherence of S. aureus to the skin and nasal cavity of humans with its specific secreted factors is the first step of invasion. <sup>62,63</sup> This process is also regarded as the crucial pathogenesis step of S. aureus. 64,65 These secreted factors play an important role in the ability of S. aureus to withstand the immune response of hosts and further aid its colonization. 66-68 Figure 1.5 shows the examples of secreted factors produced by S. aureus. Among them, fibronectin-binding protein A (Fnbp A) and fibronectin-binding protein (Fnbp B) can bind to fibronectin and fibrinogen, subsequently stimulating the colonization.<sup>69,70</sup> Iron-regulated surface determinant A (Isd A) is a multifunctional surface protein found in S. aureus. 71,72 It is also known as the factor contributing to the resistance of S. aureus. The high binding affinity of Isd A to heme-iron from hemoglobin had been mapped to the near-iron transporters (NEAT) domain. 73,74 According to the investigations, the C-terminal domain of Isd A was thought to be related to the survival of S. aureus on the human body. 75,76 The hydrophilic nature of the C domain was found to be the reason for the bacterial resistance to potent anti-staphylococcal agents, such as human skin fatty acids. 72,77 Staphylococcal enterotoxins (SEs) will reduce the host immune response and are thought to be related to several clinical symptoms, such as nausea and vomiting. 78-80

Aureolysin is an extracellular metalloprotease that acts to cleave various host immune components and proteins.  $^{81-83}$  A major pathway by which aureolysin contributes to infection is by inactivating certain targets within the complement system. In the pathways of complement activation, there is a target for the protease to modulate.  $^{84}$  Aureolysin has also been noted to lead to overstimulation of neutrophils that ultimately results in neutrophil death. Aureolysin cleaves and inactivates protease inhibitor  $\alpha_1$ -antichymotrypsin and partially inactivates  $\alpha_1$ -antitrypsin. The cleavage of  $\alpha_1$ -antitrypsin generates a fragment that is chemotactic to

neutrophils, and the cleavage of both protease inhibitors causes deregulation of neutrophilderived proteolytic activity.<sup>85</sup> The extracellular adherence protein (Eap) is known to be associated with a lot of interactions within proteins. These interactions will promote the initiation and propagation of diseases caused by *S. aureus*.<sup>86,87</sup>

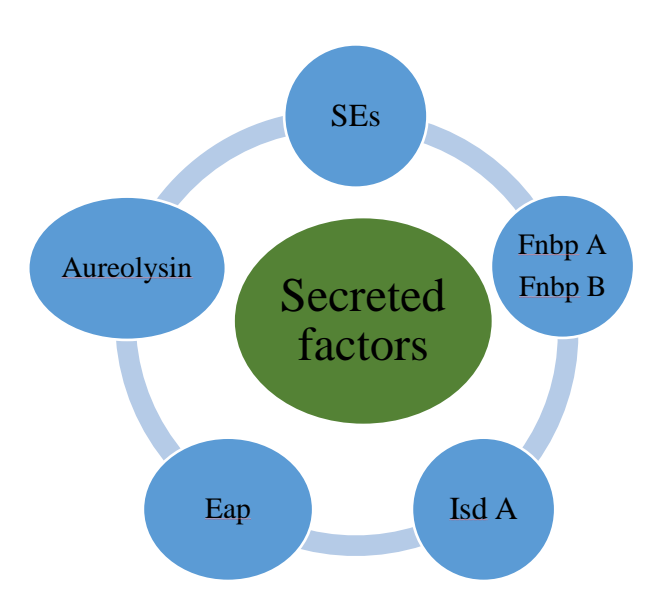


**Figure 1.5** Secreted factors produced by *S. aureus*. SEs indicates Staphylococcal enterotoxins which act both as potent gastrointestinal toxins, as well as superantigens that stimulate non-specific T-cell proliferation. Aureolysin effectively inhibits phagocytosis and killing of bacteria by neutrophils. Eap indicates extracellular adherence protein which is found as an extracellular protein of *S. aureus*. Isd are iron-regulated surface proteins which are responsible for heme scavenging from hemoproteins. Fnbp indicates fibronectin-binding protein which might contribute to virulence via host cell attachment, invasion, and interference with signaling pathways.

After the host adhesion and colonization, *S. aureus* can then penetrate the cell and reside in certain areas. <sup>60,88</sup> The toxin factors of *S. aureus* are thought to play a key role in helping the bacteria to enter and live in the cell. <sup>89</sup> Here, the function of these toxin factors will be briefly discussed. The  $\alpha$ -toxin, also named  $\alpha$ -hemolysin (Hla), is known as a member of the family of pore-forming toxins. Produced by *S. aureus*, it is the main component that leads to the toxicity to the living cells. <sup>90,91</sup> The  $\alpha$ -toxin can penetrate the host cell membrane, induce apoptosis and then result in the death of bacterial cells. <sup>92,93</sup> So far,  $\alpha$ -toxin-induced apoptosis is

known to be mediated through various pathways in different cell types, including intrinsic and extrinsic pathways. However, tumor necrosis factor  $\alpha$  (TNF $\alpha$ ) is the only cytokine that has demonstrated importance in  $\alpha$ -toxin-triggered apoptosis. Given its propensity to oligomerization,  $\alpha$ -toxin could exert a more profound influence on cell death than apoptosis. <sup>94</sup> As a major toxin of *S. aureus*,  $\alpha$ -toxin has multiple functions aside from pore-formation, but its exact pro-apoptotic role needs further investigation. The apoptosis-inducing abilities of  $\alpha$ -toxin in different cell types and the underlying mechanisms remain complex, and more cell types should be selected to determine the range of apoptotic roles of  $\alpha$ -toxin. <sup>95</sup> The  $\beta$ -toxin is a neutral sphingomyelinase which is also secreted by *S. aureus*. With the function to hydrolyze sphingomyelin which is a type of sphingolipid found in animal cell membranes,  $\beta$ -toxin can assist  $\delta$ -toxin to accumulate in the hydrophobic ceramide domains. <sup>96</sup> Under the cooperation of  $\beta$ -toxin and  $\delta$ -toxin, *S. aureus* can easily penetrate the host cell membrane (Figure 1.6). <sup>97</sup>

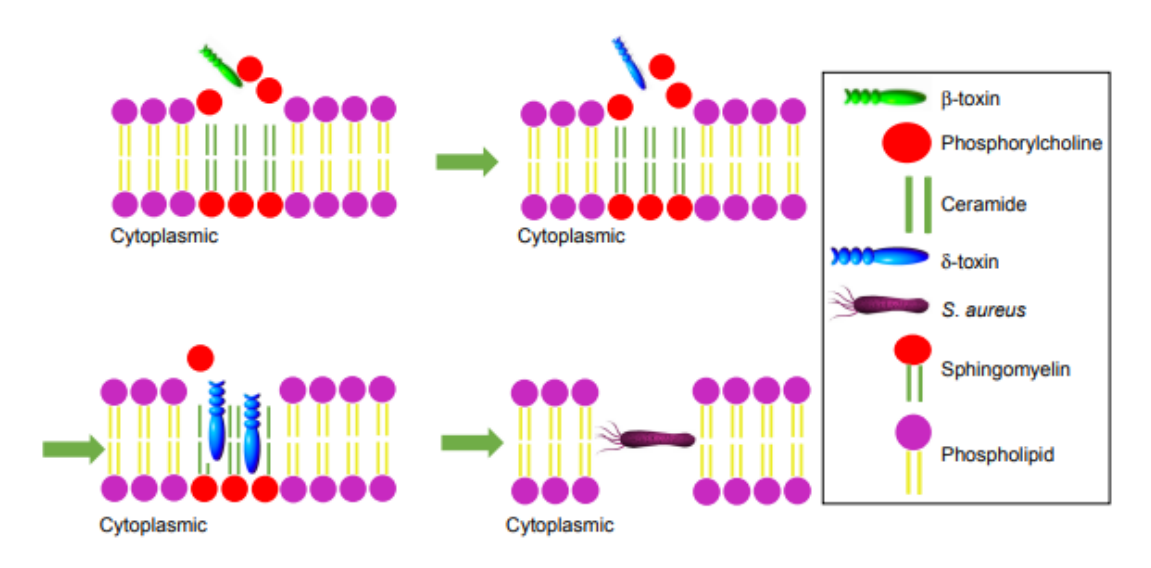


**Figure 1.6** The diagram indicates how *S. aureus* penetrates cell membranes through the help of β-toxin and δ-toxin. Sphingomyelin is hydrolyzed by β-toxin, enabling the accumulation of δ-toxin in the hydrophobic ceramide domains and the bacteria eventually permeabilize the cytomembrane (Figure obtained from Zhou *et al.*).<sup>61</sup>

After endocytosis, with the assistance of specific factors generated by S. aureus, the fusion of

lysosome and phagosome can be prevented (Figure 1.7). <sup>98,99</sup> When the host cell is successfully invaded, *S. aureus* small-colony variant (SCVs) can then help the persistence of bacteria. SCVs are a naturally occurring, slow-growing subpopulation with distinctive phenotypic characteristics and pathogenic traits. SCVs are defined by mostly non-pigmented and non-haemolytic colonies which are approximately 10 times smaller than the parent strain. The recovery of SCVs from clinical specimens was first described around 100 years ago. However, the connection of this phenotype to persistent and recurrent infections has only been appreciated in recent years. <sup>100</sup> SCVs have also been reported to be related to the antimicrobial resistance of *S. aureus*, re-infection, and chronic infections. <sup>101</sup> In the mid-1990s, the clinical importance of SCVs that are defective in electron transport gained considerable attention, and SCVs were linked to persistence and relapsing human infections. <sup>102</sup> Subsequently, clinical SCVs were frequently isolated from humans with persistent and relapsing infection, including septicemic arthritis, osteomyelitis, unmanageable wound infections, or cystic fibrosis following antimicrobial therapy with gentamicin or trimethoprim–sulfamethoxazole. <sup>103-105</sup>

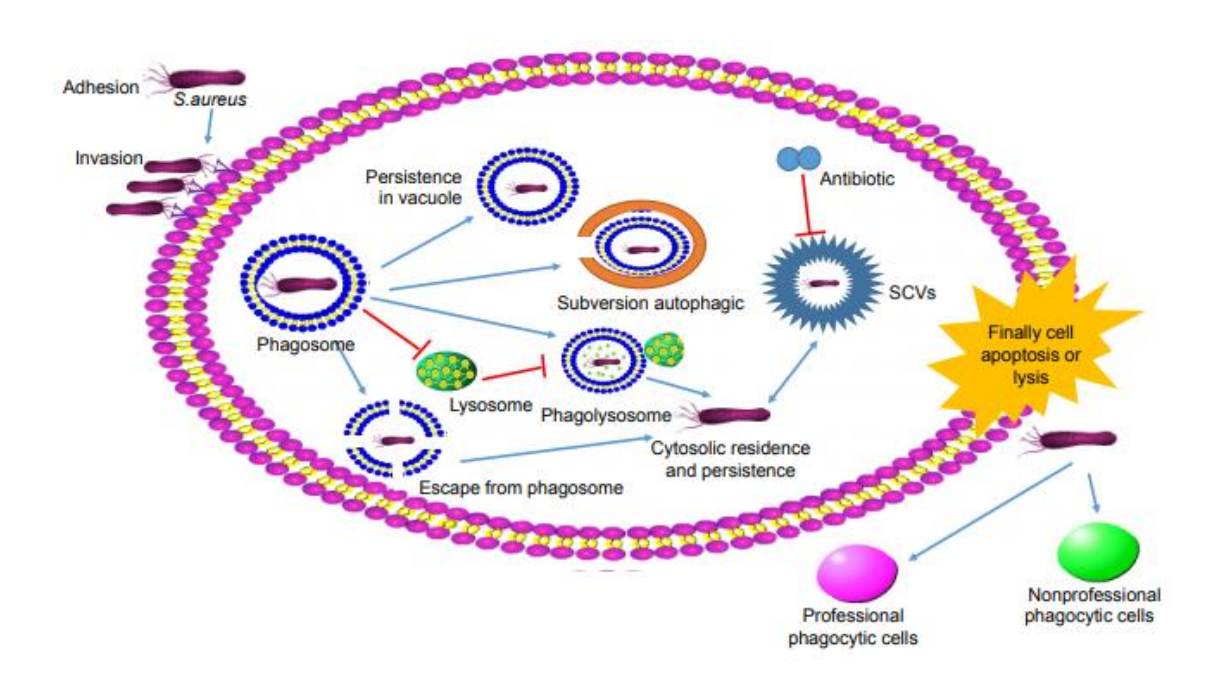


Figure 1.7. The figure shows how host cell is infected by Staphylococcus aureus. After endocytosis,

some bacteria can inhibit the fusion of phagosomes and lysosomes or escape from phagosomes by using various virulence factors and mechanisms (Figure obtained from Zhou *et al.*). <sup>61</sup>

#### 1.2.4 Treatments for S. aureus infection

#### **1.2.4.1** β-lactam antibiotics

The  $\beta$ -lactam antibiotics contain a  $\beta$ -lactam ring as their core structure that is combined with a heterocyclic ring, incliding a thiazolidine ring in penicillin such as penicillin G (1.1) and penicillin V (1.2), or a six-membered dihydrothiazine ring in cephalosporins such as cephalexin (1.3) and cefaclor (1.4) (Figure 1.8). 9,106,107 The antimicrobial activity, pharmacokinetics and the stability to  $\beta$ -lactamase can be determined by the  $R/R_1$  group in the amino acyl side chain which is attached to the β-lactam ring. 108,109 The β-lactam antibiotics work by inhibiting bacterial cell wall biosynthesis. 109,110 The β-lactam ring can cause the malfunction of the enzyme DD-transpeptidase by binding inhibiting generation to it and the of peptidoglycan cross-linkages. 110 As a result, the balance between cell wall formation and degradation is disrupted, leading to the death of the bacterial cell. Statistically, more than 50% of clinically used antibiotics are still β-lactam antibiotics.<sup>3</sup> However, resistance to these agents has gradually become a common and severe problem.

**Figure 1.8**. Penicillins (top left) with a  $\beta$ -lactam fused to thiazolidine core structure and cephalosporins (top right) with a  $\beta$ -lactam fused to six-membered dihydrothiazine core structure, which are exemplified by penicillin G (**1.1**) and penicillin V (**1.2**), and cephalexin (**1.3**) and cefaclor (**1.4**), respectively.

The  $\beta$ -lactamases are the major cause of bacterial resistance to  $\beta$ -lactam antibiotics. The function of  $\beta$ -lactamases is to cleave the  $\beta$ -lactam ring of the penicillin molecule, thereby inactivating the antibiotic. Following the Ambler sequence-based system<sup>111</sup>,  $\beta$ -lactamases can be divided into four distinct classes, termed A, B C and D. Figure 1.9 shows the 3-D crystal structures of these four classes of  $\beta$ -lactamases. Among them, classes A, C and D are found to possess active-site serine  $\beta$ -lactamases (SBLs) while class B comprises a heterogeneous group of zinc metallo- $\beta$ -lactamases (M $\beta$ Ls). <sup>112,113</sup>

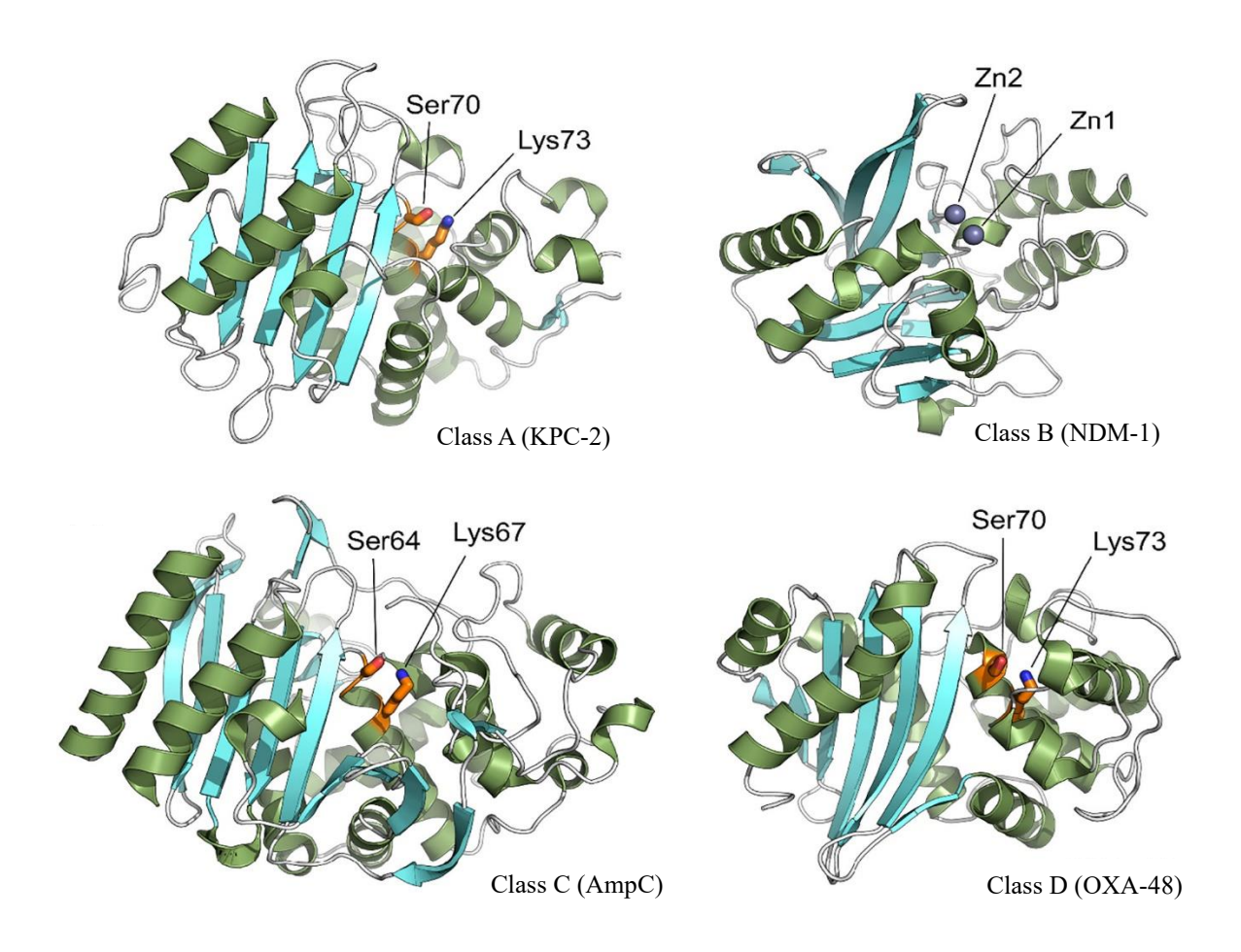


**Figure 1.9** The crystal structures of four classes of β-lactamases including Class A KPC-2 (PDB 5ul8), Class B NDM-1 (PDB 5zgy), Class C AmpC (PDB 1ke4) and Class D OXA-48 (PDB 3hbr). Catalytic important residues of serine-β-lactamases are colored orange, and the metallo-β-lactamase zinc ions are shown as gray spheres (Figure obtained from Tooke *et al.*).  $^{112}$ 

Scheme 1.1 shows the mechanism how SBLs employ the serine as the reaction nucleophile and hydrolyze β-lactams via a covalent acyl enzyme intermediate. General base B1 activates Ser for nucleophilic attack on the amide carbonyl carbon (C7) generating a covalent acyl enzyme via a tetrahedral oxyanionic acylation transition state. General base B2 activates incoming deacylating water molecules for nucleophilic attack on the acyl enzyme carbonyl liberating the penicilloate product via a tetrahedral deacylation transition state.<sup>113</sup>

**Scheme 1.1**. Mechanistic overview of serine  $\beta$ -lactamases react with penicillin. The identities of general bases B1 and B2 vary between  $\beta$ -lactamase classes. 113

Base

MβLs are the main mechanism of resistance to carbapenems. Clinically approved inhibitors of MβLs are currently unavailable as their design has been limited by the incomplete knowledge of their mechanism. Scheme 1.2 shows the general mechanism of carbapenem hydrolysis by binuclear class B metallo- $\beta$ -lactamases. <sup>112</sup> A Zn-bridging hydroxide will firstly be displaced by substrate binding to a terminal position enabling attack upon the scissile carbonyl. Then an anionic intermediate with negative charge delocalized around the pyrroline ring reacts either by protonation at C2 by bulk water generating the  $\Delta$ 1 pyrroline or at N4 by incoming water at the bridging position generating the  $\Delta$ 2 pyrroline product. <sup>112</sup>

Scheme 1.2. Proposed mechanism for carbapenem hydrolysis by binuclear class B metallo- $\beta$ -lactamases.<sup>112</sup>

In the UK, over 90% of *S. aureus* strains have become tolerant to penicillin, and the situation is similar worldwide. <sup>114</sup> Previously, this has led to the increasing clinical use of  $\beta$ -lactamase-resistant antibiotics, such as methicillin (**1.5**) and oxacillin (**1.6**) (Figure 1.10).

Figure 1.10 Structures of methicillin (1.5) and oxacillin (1.6).

Methicillin (1.5) is a semi-synthetic β-lactam antibiotic which was first discovered in 1960. Methicillin is well-known due to its resistance to penicillinase, a type of β-lactamase generated by penicillin-resistant bacteria. With the functional group *ortho*-dimethoxyphenyl attached to the carbonyl group of the penicillin, the improvement in the ability to resist β-lactamase was observed. The reason is thought to be associated with the side-chain steric hindrance, which causes the intolerance of the enzymes.  $^{117}$ 

Despite the discovery of penicillinase-resistant β-lactam antibiotics, the first case of methicillin-resistant *Staphylococcus aureus* (MRSA) was found in England in the 1960s.<sup>118</sup> MRSA is regarded as a significant pathogen relative to the development of antimicrobial resistance (AMR).<sup>119</sup> The emergency of MRSA is spread worldwide, and hence development of new antimicrobial agents remains a big challenge.<sup>120</sup>

## 1.2.4.2 Aminoglycosides

The aminoglycosides are traditionally effective against Gram-negative bacteria.<sup>121</sup> They are isolated from the *Streptomyces* genus, and hence are named with the suffix *-mycin*, whereas those that are derived from *Micromonospora* are named with the suffix *-micin*.<sup>122,123</sup> Aminoglycosides are currently used for numerous infection types in clinical settings due to several advantages, such as broad-spectrum activity and rapid bactericidal action.<sup>121,124</sup> Since the discovery of streptomycin (1.7) (Figure 1.11) in 1944, aminoglycosides have become a milestone of antimicrobial chemotherapy.<sup>125</sup> They were also known as the first antibiotics used routinely in the clinic, including neomycin (1.8), gentamicin A (1.9) (Figure 1.12). The core structure of aminoglycosides is characterized by an amino sugar which is attached to a dibasic aminocyclitol through a glycosidic linkage.<sup>121,126</sup> The mode of action of aminoglycosides is the inhibition of protein synthesis,<sup>121</sup> by binding to the Aminoacyl site (A site) on the 16S ribosomal RNA of the 30S ribosome.<sup>121,126,127</sup> Typically, the A-site binds the incoming tRNA with the complementary codon on the mRNA.

However, the increasing resistance to aminoglycosides has led to the development of novel aminoglycosides. Arbekacin (1.10) and plazomicin (1.11) (Figure 1.13) were thus designed and synthesized to deal with the problem of resistance without the loss of potency against multidrug-resistant (MDR) pathogens.<sup>121</sup>

Streptomycin 1.7

Figure 1.11 Structure of streptomycin (1.7).

Figure 1.12 Chemical structures of neomycin (1.8) amd gentamicin A (1.9).

$$H_2N$$
 $H_2N$ 
 $H_2N$ 

Figure 1.13 Chemical structures of arbekacin (1.10) amd plazomicin (1.11).

#### 1.2.4.3 Quinolones

Since the first discovery of quinolones in the 1960s, their antibacterial activity has aroused the interests of generations of scientists.<sup>3</sup> Several features can be found in this class of antibiotics, such as high potency, broad spectrum, good bioavailability and lower risk of side-effects.<sup>3</sup> Among them, nalidixic acid was the first synthetic quinolone with an alternative structure to the others (Figure 1.14).<sup>128,129</sup> Nalidixic acid (1.12) is used primarily against Gram-negative bacteria, and is clinically used for the treatment of urinary tract infections caused by *Escherichia coli* and *Klebsiella*.<sup>130</sup> Norfloxacin and ciprofloxacin, which contain a fluorine atom in their chemical structure, are members of the fluoroquinolone family (Figure 1.15). They are frequently used against both Gram-negative and Gram-positive bacteria.<sup>131</sup>

#### Nalidixic acid 1.12

Figure 1.14 Structure of nalidixic acid (1.12). The core structure is a naphthyridone, not a quinolone.

Figure 1.15 Structures of norfloxacin (1.13) and ciprofloxacin (1.14).

The quinolones act by inhibiting DNA synthesis, preventing replication, and thus leading to bacterial death. <sup>132</sup> Specifically, they inhibit the activity of the topoisomerase II, topoisomerase IV, and DNA gyrase. <sup>132</sup> Topoisomerases are nuclear enzymes that play essential roles in DNA replication, transcription, chromosome segregation, and recombination. Topoisomerase II protein is important for DNA replication, chromosome build-up and chromosome isolation. Inhibitors of topoisomerase II are essential medications for the chemotherapy of numerous neoplasms, including lung malignancy, testicular tumor, lymphomas and sarcomas. <sup>133</sup> Topoisomerase II breaks and passes double stranded DNA through the nick to allow relaxation of supercoiled DNA. Topoisomerase IV is one of two Type II topoisomerases in bacteria, the other being DNA gyrase. Like gyrase, topoisomerase IV can pass one double-strand of DNA through another. DNA gyrase is an essential bacterial enzyme that catalyzes the ATP-dependent

negative super-coiling of double-stranded closed-circular DNA. Generally speaking, the activity of quinolones against Gram-positive bacteria is linked to inhibition of DNA gyrase and the inhibition of topoisomerase IV is more relevant to Gram-negative bacteria. 134

#### 1.2.4.4 Macrolides

Macrolide antibiotics were first introduced in the 1950s with their bacteriostatic effects on bacteria. The archetype, erythromycin was isolated from the soil bacterium *Streptomyces erythraeus*. In the 1970s to 1980s synthetic derivatives of erythromycin (1.15), such as clarithromycin (1.16) were developed (Figure 1.16). This class of antimicrobial agents is characterized by their large lactone ring structure and contain one or more modified sugars, such as cladinose (1.17) (Figure 1.17). The mode of action of macrolide antibiotics is via binding to the 50S ribosomal subunit and thus inhibiting the biosynthesis of bacterial proteins. *S. aureus* was found to acquire mutations that change the macrolide binding site, which resulted in bacterial resistance. Other mechanisms of resistance to macrolides, including the activation of drug efflux proteins and the production of druginactivating enzymes, have emerged in some strains of bacteria.

**Figure 1.16** Structures of erythromycin (**1.15**) and clarithromycin (**1.16**), where the hydroxy group is changed to methoxy group.

**Figure 1.17** Structure of cladinose (1.17), which is an deoxysugar attached to the large macrocyclic lactone ring of the macrolides.

# 1.2.4.5 Vancomycin and VRSA

Vancomycin (1.18) (Figure 1.18), one of the glycopeptide antibiotics, is used as the last-line drug for the treatment of serious infections by Gram-positive pathogens, especially MRSA. It was first discovered in the 1950s. <sup>141</sup> However, due to the overuse of vancomycin, *S. aureus* has become resistant to vancomycin. The first report was found in 2002. Three more cases of vancomycin-resistant *S. aureus* (VRSA) infection were then reported in the U.S. in 2005. <sup>142,143</sup>

vancomycm (1.16)

Figure 1.18. Structure of vancomycin (1.18).

Vancomycin (1.18) prevents cell wall biosynthesis by targeting lipid II, the peptidoglycan precursor. The mode of action of vancomycin is found to be associated with the binding to the *C*-terminus (D-Ala-D-Ala) of the peptodoglycan and then blocking the addition of late precursors by transglycosylation and preventing subsequent cross-linking by transpeptidation. (Figure 1.19). From research into vancomycin resistance, analysis of the cell wall peptidoglycans from resistant *Staphylococci* has indicated the lack of altered cross-links compared to susceptible strains. It is also well-known that the outer membrane of Gramnegative bacteria is the main reason for the resistance to vancomycin due to their ability to prevent the permeation of large glycopeptide molecules. 146

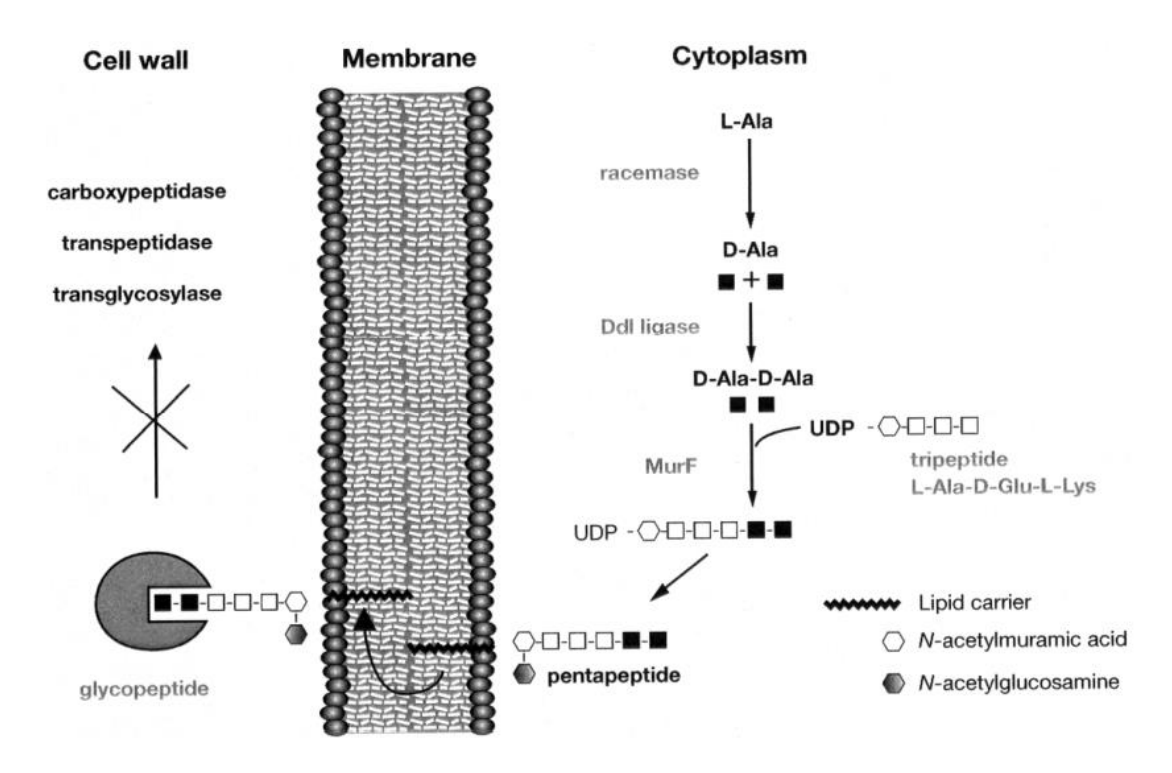


**Figure 1.19.** The diagram shows the biosynthesis of peptidoglycan and MoA of vancomycin. Antibiotics are able to bind to the *C*-terminus of peptidoglycan precursors and hence inhibit the catalytic reaction by enzymes (Figure obtained from Courvalin *et al.*). 144

# 1.3 Peptide medicines

# 1.3.1 Introduction of peptide medicines

During the past decade, studies have shown an increasing interest in peptides, especially in the applications of biotechnology and therapeutics. <sup>12</sup> Moreover, peptide therapeutics have already played a vital role in clinical treatments since the discovery and commercialization of insulin in the 1920s. <sup>147</sup> Insulin is a protein composed of two chains, an A chain (with 21 amino acids) and a B chain (with 30 amino acids), which are linked together by disulfide bonds (Figure 1.20). <sup>148</sup>

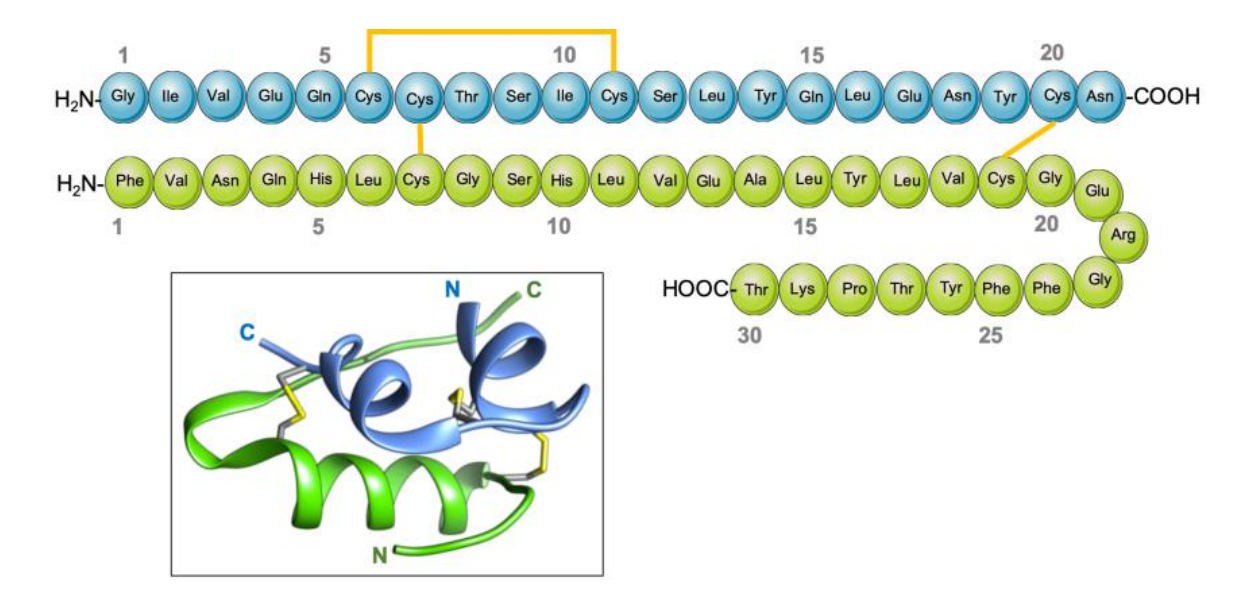


**Figure 1.20** Schematic drawing of human insulin and its 3D structure. The A-chain and the B-chain are shown in blue and green, respectively. The intra- and inter-chain disulfide bridges between cysteine residues are shown in yellow (Figure obtained from PDB-101).

With the undoubted benefits such as efficacy, good selectivity, safety, and tolerance, relative to traditional small molecule therapeutics, peptides are recognized as a potential source for pharmaceutical research and the development of novel medicines. Peptides represent a unique class of pharmaceutical compounds. Peptides have the advantage of filling a gap in molecular size space between small molecule therapeutics (<500 Da) and larger (>5000 Da) protein-based biologics. Biologics do have excellent specificity and potency but are typically not orally bioavailable like their small molecule counterparts and are more expensive than small molecule drugs. 152

Peptides are known as the intrinsic molecules for several physiological functions, and thus, offer a route of therapeutic intervention which is like natural pathways.<sup>147</sup> The utilization of peptides as therapeutics has evolved over time and continued to evolve with changes in the history of drug development over time.<sup>153</sup> In the 1950s, synthetic oxytocin and vasopressin

were introduced into clinical use due to the feasibility of sequence elucidation and chemical synthesis of peptides (Figure 1.21).<sup>154</sup> In the 20<sup>th</sup> century, peptides isolated from natural sources like insulin and adrenocorticotropic hormone (ACTH), were discovered as important clinical medicines.<sup>153</sup> Moreover, isolation of natural products from exotic sources became a popular strategy for identifying new potential therapeutics.<sup>147,155</sup> The genomic era allowed for the identification and molecular characterization of receptors for many important endogenous peptide hormones, which provided a good start to pursue novel peptidic ligands for these receptors, in industry and academia.<sup>156</sup>

The advantages of peptides are reflected in the market estimated for therapeutic peptides of more than 10 billion US dollars.<sup>12</sup> Still, there were more than 10 peptide-based drugs have entered the market since 2017.<sup>156</sup> So far, over 80 peptide drugs have been approved in the USA, Europe, and Japan, and additional hundreds more in preclinical or clinical trials. There is no doubt that peptides are having an impact in the pharmaceutical industry.<sup>147,150,152,157</sup>. Those peptides have been applied as medicines in several different therapeutic areas, such as cancer (abarelix and bleomycin), antifungal (anidulafungin and capsofungin), myeloma (carfilzomib and bortezomib), diabetes (exenatide and desmopressin), immunosuppressant (cyclosporine) and antibiotics (bacitracin, capreomycin, colistin, daptomycin and daptinomycin, as well as vancomycin which was discussed earlier).<sup>158</sup> Among them, there is more attention and interest in peptides as the source of antibiotics due to the increased resistance of bacteria and the difficulty in the development of novel antibiotics.

HO

$$NH$$
 $NH$ 
 $NH$ 

Figure 1.21 Chemical structures of oxytocin (left) and vasopressin (right).

## 1.3.2 Antimicrobial peptides

Naturally occurring antimicrobial peptides (AMPs) can be discovered in a wide range of sources from microorganisms to humans.<sup>159</sup> AMPs are also well known as the host defense peptides with the features of short and positively charged peptides.<sup>159</sup> As reported, most of the AMPs possess the ability to kill microbial pathogens, while some can only modulate the host defense systems.<sup>160</sup> Since 2000, due to the increasing resistance to current antimicrobial agents, efforts to bring AMPs as novel drug candidates into clinical use are accelerating and thus, the number of published articles on AMPs have also increased (Figure 1.22).<sup>161</sup>

AMPs can be found in all organisms, and they demonstrate several features such as remarkable structural and functional diversity, direct antimicrobial activity and immunomodulatory properties. With these advantages, AMPs are always regarded as a reliable source for the development of novel antimicrobial therapeutics. Figure 1.23 shows that more than 10% of the developing AMPs had already been introduced into the market, and around 30% of them are

also being tested in clinical trials. 146 It provides a positive aspect for the introduction of novel AMP-based medicines in different areas of disease. 160,163-165

In broad terms, many peptide antimicrobial agents have been discovered during the past 50 years. <sup>166</sup> They can be divided into two classes, the ribosomally synthesized peptides and non-ribosomally synthesized peptides. <sup>167</sup> Ribosomally synthesized are produced by all species of life as a major component of the natural host defense. <sup>167,168</sup> Non-ribosomally synthesized peptides are often drastically modified and produced by bacteria and will be discussed in more detail with emphasis on their clinical importance, similarities in function to the natural peptides and future prospects. <sup>169</sup>

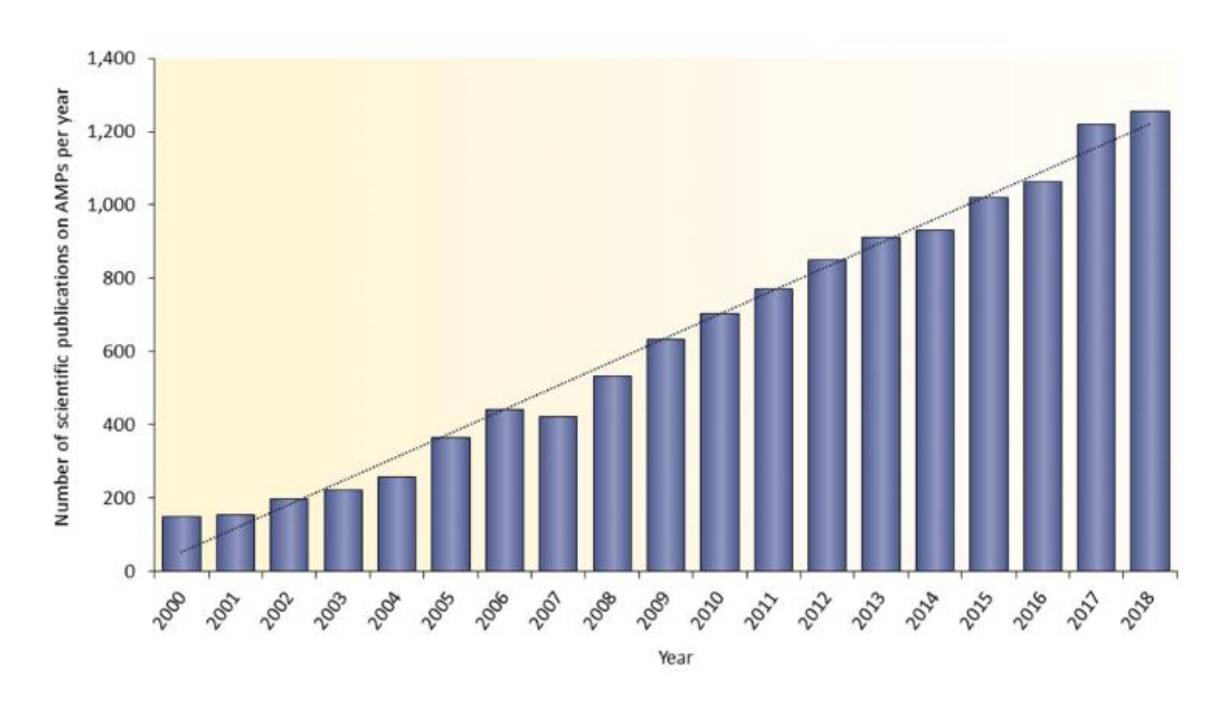


**Figure 1.22** Published research on AMPs identified from 2000 to 2018. From the figure, it is found that the number of published articles on AMPs is increasing stably (Figure obtained from Mahlapuu *et al.*).<sup>161</sup>

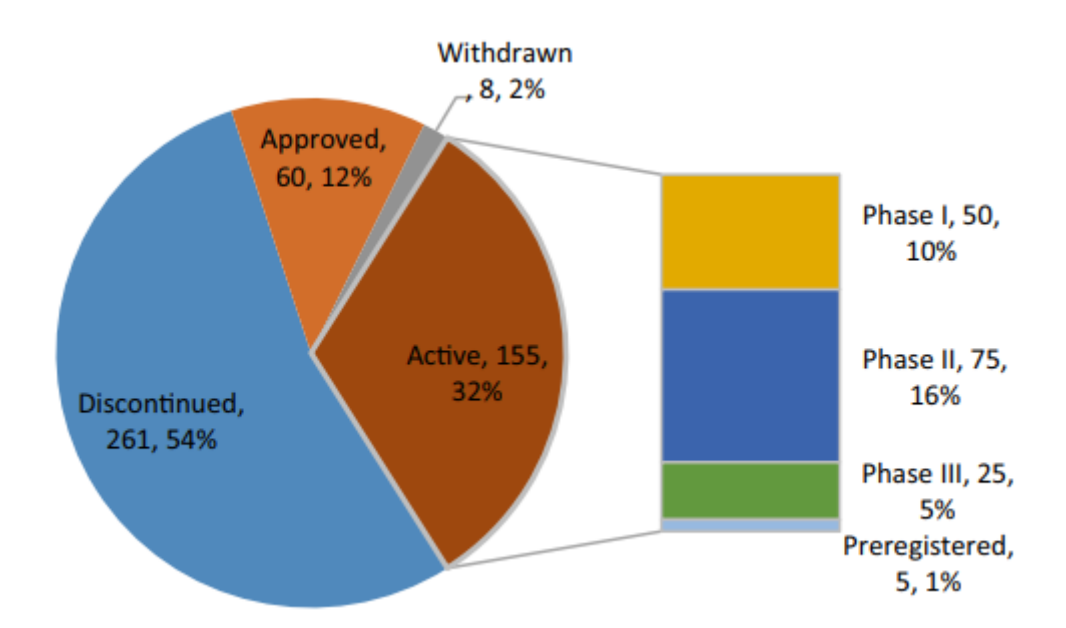


**Figure 1.23** Current development status of therapeutic AMPs in 2018, of which more than half of discovered drugs were discontinued and only 10-12 % were approved for clinical use. Moreover, most of the active drugs were still in the phase 1 or 2 stages (Figure obtained from Lau *et al.*). 146

## 1.3.3 Ribosomally synthesized peptides

#### 1.3.3.1 Ribosomally synthesized peptides from natural sources

Ribosomally synthesized peptides with antimicrobial properties can be produced by most organisms, including bacteria, plants and animals and represent crucial components of their defensive systems against microorganisms. <sup>170-173</sup> Structures of ribosomally synthesized AMPs encompass molecules ranging from 6 and up to 60 amino-acid residues, being linear, cyclic, or cross-linked by numerous internal disulfide bridges. <sup>166,174,175</sup> Despite the difference in structure, they are all cationic and very often amphiphilic, which reflects the fact that many of them attack their target cells by permeabilizing the cell membrane. The details of the mechanism will be further discussed in the later section.

Certain ribosomally synthesized compounds show an exceptionally broad spectrum of activity against fungi, viruses, parasites and both Gram-negative and -positive bacteria.<sup>173</sup> Thus,

ribosomally synthesized AMPs and their derivatives are thought to be potential new classes of antimicrobial agents.

#### 1.3.3.2 Mechanism of ribosomally synthesized AMPs

As mentioned before, most of the structures of ribosomally synthesized AMPs are cationic. Thus, their positive charge facilitates interactions with the negatively charged bacterial phospholipid-containing membranes and or acidic bacterial cell walls, whereas their amphiphilic character enables membrane permeabilization. Pepending on the peptide and the microbial species, two possible MoA of ribosomally synthesized peptides have been reported. The peptides can be membrane-disruptive or membrane-interactive. The former is known to result in cell lysis. The latter leads to the formation of transient pores and the transport of peptides inside the cell, which brings them into contact with intracellular targets. Models of peptide insertion and membrane permeabilization can be categorized into three types, one with a high content of a certain amino acid, most often proline, one with intramolecular disulfide bridges, and the one with an amphiphilic region if an  $\alpha$ -helical structure was assumed.

In mammals, ribosomally synthesized AMPs can be found in phagocytes and mucosal epithelial cells, which are regarded as crucial components of the innate immune system.<sup>170</sup> Amphibian skin is another rich source of AMPs, and these AMPs display potential microbiocidal activity against both Gram-positive and Gram-negative bacteria.<sup>178</sup> Thus, antimicrobial peptides in animals are thought to be significant effector molecules in innate immunity and therefore play a key role in early defense against the invasion of microorganism.<sup>179</sup> As reported by Bowman *et al.*, antimicrobial peptides can be considered as the ideal first line of defense due to their more rapid preparation than protein drugs.<sup>171,176,180</sup>

Moreover, it is found that small peptides diffuse faster than large protein molecules. <sup>176</sup> Furthermore, the production of ribosomally synthesized antimicrobial peptides by bacteria as a defense mechanism against other organisms had already been well reported. <sup>170,181</sup>

#### 1.3.3.3 Challenges in development of ribosomally synthesized AMPs

With several advantages such as the bioactivity against bacteria, effect on immune responses, stability at a wide range of temperature and pH values and different mode of actions from clinical antibiotics, ribosomally synthesized AMPs are regarded as a solution to the problem of increasing drug resistance. <sup>182</sup>

However, there are still challenges in the development of ribosomally synthesized AMPs. For example, their prominent level of chemical and biological diversity which lead to difficulty in identification in a specific screen. <sup>183,184</sup> Moreover, the production cost are not economically feasible and are 5-20 times higher than typical antibiotic drugs. <sup>173</sup> Still, the half-life of a peptide is particularly important and can be extended by modifications, such as glycosylation and conjugation. <sup>173</sup>

Although many challenges need to be addressed, the benefits of ribosomally synthesized AMPs are undeniable. Thus, ribosomally synthesized AMPs are still believed to be a good and important source in the development of new antimicrobial drugs.<sup>173</sup>

## 1.3.4 Non-ribosomally synthesized peptides

### 1.3.4.1 Introduction to non-ribosomally synthesized peptides

Non-ribosomal peptides (NRPs) are secondary metabolites synthesized by the non-ribosomal peptide synthetases (NRPSs), which are multi-modular enzyme complexes typically found in bacteria, cyanobacteria, and fungi. 185,186 Non-ribosomal peptide synthetase enzymes can be subdivided into modules, each module involved in the incorporation of one amino acid residue. Each module consists of three domains: adenylation (A) domain, peptidyl carrier protein (PCP) domain, and condensation (C) domain, which carry out the assembly of non-ribosomal peptides. 187 NRPs are formed from a series of enzymatic transformations employing a much more diverse set of precursors and biosynthetic reactions. Both proteinogenic and nonproteinogenic amino acids can be found as building blocks. 188,189 From antimicrobial to anticancer, NRPs exhibit a broad spectrum of biological activities because of their unique structural features. These secondary metabolite peptides contain either D-amino acids, Nterminally attached fatty acid chains, N- and C-methylated residues, N-formylated residues, heterocyclic elements, glycosylated amino acids, or phosphorylated residues. 190 Another common characteristic of non-ribosomally synthesized bioactive peptides is the macrocyclic structure, which is responsible for reduction in structural flexibility and results in a biologically active conformation.<sup>191</sup>

The discovery of NRPs began when tyrocidine, a cyclic decapeptide produced by *Bacillus brevis*, was first reported by Tatum and colleagues. Tyrocidine was biosynthesized by a mechanism which did not involve the ribosomal machinery for its synthesis. These observations also gave the first hint of an amino acid as a "carrier" being involved in NRPS enzymology. Considering the complexity and biological activities of NRPs, the relative biosynthetic research might be challenging. Each non-ribosomal peptide synthetase is

composed of distinct modular sections, each of which is responsible for the incorporation of one defined monomer into the final peptide product. <sup>195</sup> The potential of NRPs as therapeutic agents, especially with antimicrobial activity will be discussed in the next section.

#### 1.3.4.2 Non-ribosomally synthesized peptides as antimicrobial agents

Non-ribosomal antibacterial peptides (NRAPs) possess several features, such as versatile chemical scaffolds, potent antibacterial activity, and unique modes of action. In the past decade, a diverse range of NRAPs have been identified. Table 1.1 shows examples of several NRAPs including their sources, antibacterial activity, and targets. Research on NRAPs has been conducted for a long time since the initial discovery of penicillin in 1928. Subsequently, increasingly NRAPS from different bacteria sources have been discovered. Bacteria found in the soil are one of most important and the largest sources of NRAPs. Several NRAPs which are commonly used in the clinic, such as vancomycin and daptomycin were all discovered from soil bacteria. Other sources like marine, water, insect, mushroom, nematode, and even human are found to be useful sources of NRAPs. Due to the increasing problem of antimicrobial resistance, the need for novel antibiotics with different MoAs is urgent and necessary. Thus, NRAPs are highly regarded because of their unique range of bacterial targets, which contribute to different mechanisms in antimicrobial activity (Figure 1.24).

Although the interest in NRAPs as therapeutic agents is increasing, there are still several crucial obstacles: excessive cost of production or manufacture, poor protease stability and nonspecific toxicity in both in vivo and in vitro models. <sup>196</sup> Moreover, most NRAPs tend to be quite expensive drugs due to their unique structures with complicated modifications. <sup>196</sup>

Another problem in the development of NRAPs is the loss of activity due to protease-mediated proteolysis. 197

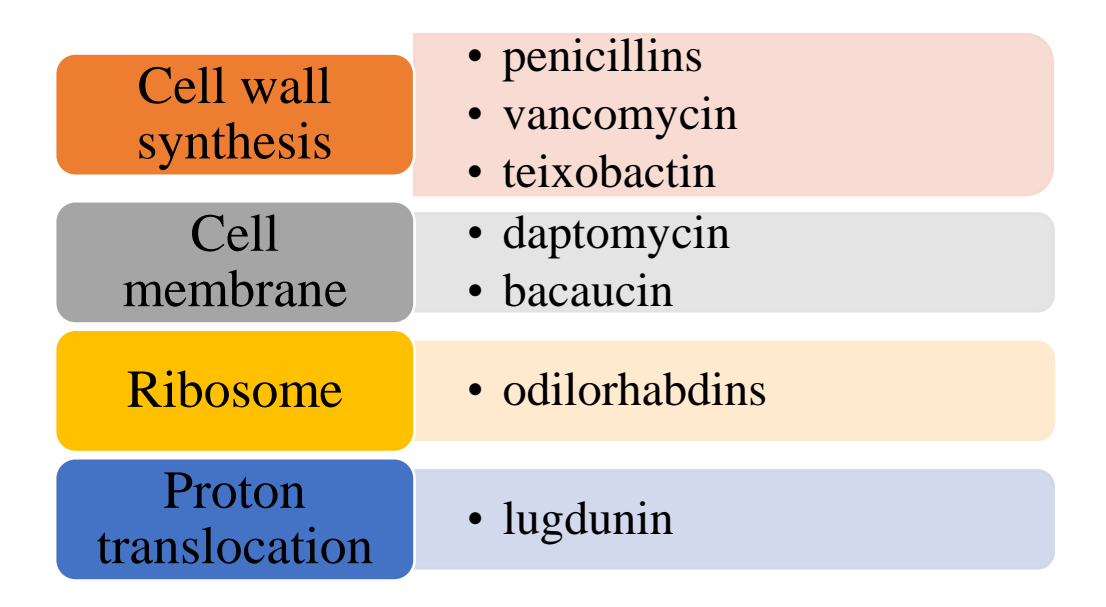


Figure 1.24 Examples of NRAPs with different MoAs and targets.

To improve the protease resistance of NRAPs, several approaches have been proposed. For example, the modification at *N*- and *C*-termini, such as acetylation and amidation, respectively. They are the most basic form to protect the *N*- and *C*- termini. They are the most basic form to protect the *N*- and *C*- termini. They are the most basic form to protect the *N*- and *C*- termini. They are the most basic form to protect the *N*- and *C*- termini. They are the most basic form to protect the *N*- and *C*- termini. They are the most basic form to protect the *N*- and *C*- termini. They are the most basic form to protect the *N*- and *C*- termini. They are the most basic form to protect the *N*- and *C*- termini. They are the most basic form to protect the *N*- and *C*- termini. They are the most basic form to protect the *N*- and *C*- termini. They are the most basic form to protect the *N*- and *C*- termini. They are the most basic form to protect the *N*- and *C*- termini. They are the most basic form to protect the *N*- and *C*- termini. They are the most basic form to protect the *N*- and *C*- termini. They are the most basic form to protect the *N*- and *C*- termini. They are the most basic form to protect the *N*- and *C*- termini. They are the most basic form to protect the *N*- and *C*- termini. They are the most basic form to protect the *N*- and *C*- termini. They are the most basic form to protect the *N*- and *C*- termini. They are the most basic form to protect the *N*- and *C*- termini. They are the most basic form to protect the *N*- and *C*- termini. They are the most basic form to protect the *N*- and *C*- termini. They are the most basic form to protect the *N*- and *C*- termini. They are the most basic form to protect the *N*- and *C*- termini. They are the most basic form to protect the *N*- and *C*- termini. They are the most basic form to protect the *N*- and *C*- termini. They are the most basic form to protect the *N*- and *C*- termini. They are the most basic form to protect the *N*-

While modification of peptide is helpful for the resistance to proteolytic degradation, it may also lead to the reduction of peptide affinity.<sup>204,205</sup> In contrast, cyclization may increase not only hydrolytic stability but also binding to the target protein.<sup>206</sup> Cyclic peptides often show improved biological activity compared with their linear counterparts since the active

conformation can be favored, thereby decreasing the entropic component in binding.<sup>207</sup> In addition, the constraint induced by cyclization decreases the probability of a good fit in the active site of endoproteases.<sup>208</sup> Amide bonds that are part of a hydrogen-bonding network, as in stapled peptides, are particularly poor enzymatic substrates.<sup>209</sup> Furthermore, most cyclizations are also designed to involve the terminal residues.<sup>210</sup> Thus, they also protect the peptide from exoproteases.<sup>210</sup> Depending on the peptide structural context, several cyclization strategies can be applied: head-to-tail, side chain-to-head, side chain-to-tail and side chain-to-side chain.<sup>208</sup>

In fact, due to the unfavorable pharmacokinetic properties or toxicity, synthesis of compounds with antibacterial activity is still difficult.<sup>211</sup> Some clinically used antibiotics have been criticized for their toxicity, including their ability to cause hemolysis, cytotoxicity, apoptosis, and degranulation of mast cells.<sup>211</sup> It leaves without doubt another huge obstacle and challenge in the development of NRAPs.

Multi drug-resistant pathogens are regarded as a severe threat to human health. The development of antibiotics from a diverse range of sources offers promising approaches to tackle antimicrobial resistance. Innovative approaches such as high-throughput screening in genome sequencing and bioinformatics tools have been applied to accelerate the discovery of new NRAPs. 196 Compared to conventional antibiotics, NRAPs are less prone to causing resistance due to their unique MoAs. Furthermore, the combination therapy containing NRAPs based antibiotic and other existing antibiotics could enhance antibacterial activity and reverse resistance. 212 With these benefits, NRAPs are valuable leads for developing next-generation antibiotics. Within those NRAPs, lugdunin (mentioned in Table 1.1) has awakened interest. First reported in 2016, lugdunin was thought to be a potent antimicrobial agent with a mode of

action different from other antibiotics.<sup>20</sup> Therefore, lugdunin and analogues thereof were synthesized, and their activity as antimicrobial agents were determined.<sup>20,213</sup> The details are discussed in the next section.

**Table 1.1** Examples of discovered NRAPs. From the table, it is found that NRAPs can be obtained from different sources like soil, marine and insect. Among them, lugdunin was specially found form human.

NRAPs	Years of discovery	Organism	Sources	Activity	Targets
Penicillin	1928	Penicillium	Soil	Gram (+)	PBP <sup>214</sup>
Polymycins	1947	Paenibacillus polymyxa	Soil	Gram (-)	LPS <sup>215</sup>
Vancomycin	1953	Amycolatopsis	Soil	Gram (+)	Lipid II <sup>216</sup>
Daptomycin	1987	Streptomyces roseosporus	Soil	Gram (+)	Cell membrane <sup>217-</sup> <sup>218</sup>
Bogorol A	2001	Bacillus sp.	Marine	MRSA, VRE	Unknown <sup>219</sup>
Bogorols B-E	2006	Brevibacillus laterosporus	Marine	MRSA, VRE,	Unknown <sup>220</sup>
				E. coli	
Sansanmycin	2007	Streptomyces sp. SS	Soil	M. tuberculosis	Translocase I <sup>221</sup>
Entolycin	2010	Pseudomonas entomophila	Soil	S. aureus	Unknown <sup>222</sup>
Pseudofctin	2010	Pseudomonas fluorescens	Water	Gram (+) and (-)	Unknown <sup>223</sup>
Sevadicin	2014	Paenibacillus larvae	Insect	B. megaterium	Unknown <sup>224</sup>
Teixobactin	2015	Eleftheria terrae	Soil	Gram (+)	Lipid II and lipid III <sup>225</sup>
Telomycin	2016	Streptomyces canus	Soil	S. aureus, B. subtilis	Cardiolipin <sup>226</sup>
Lugdunin	2016	Staphylococcus lugdunensis	Human	Gram (+)	DNA, RNA, protein and cell wall <sup>20</sup>
Paenipeptins	2017	Paenibacillus sp.	Mushroom	Gram (+) and (-)	Unknown <sup>227</sup>
Bacaucin	2017	Bacillus subtilis	Soil	Gram (+)	Cell membrane <sup>228</sup>
Odilorhabdins	2018	Xenorhabdus nematophila	Nematode	Gram (+) and (-)	Ribosome <sup>229</sup>

## 1.4 Lugdunin – an overview

## 1.4.1 Background of lugdunin

Since the host defence peptides from higher organisms, as well as organisms that colonise specific tissues/organs in mammals, are regarded as a powerful source of new anti-infective compounds, many researchers are focusing their efforts in this area. <sup>159,230</sup> In 2016 a novel and potent compound named lugdunin was isolated from *Staphylococcus lugdunensis*. <sup>20</sup>

Staphylococcus lugdunensis, a coagulase-negative staphylococcus (CoNS), is thought to cause several important infections, such as skin infections, endocephalitis, cardiovascular infections, osteomyelitis, central nervous infections, and urinary tract infections.<sup>231,232</sup> It is also part of the normal skin flora and is frequently found in the nasal cavity.<sup>233,234</sup> Moreover, unlike other CoNS, S. lugdunensis is sensitive to most antibiotics.<sup>234</sup>

The microbiota in humans, such as the nasal microbiota is a valuable resource for novel antibiotics, as opposed to screening soil microorganisms which has been exploited extensively over the decades and frequently the same compounds are found. Thus, in the study by Zipperer *et al.*, a collection of nasal staphylococcal isolates was tested for antimicrobial activity against *S. aureus*. Among those strains, an antimicrobial substrate produced by *S. lugdunensis* IVK28 was found to be highly active against *S. aureus*.<sup>20</sup>

Furthermore, in *S. lugdunensis* IVK28, an uncharacterized gene that encodes for several non-ribosomal peptide synthetases (NRPS) was found to be associated with the antibiotic biosynthesis. (Figure 1.25).<sup>20</sup> The operon consists of four NRPS genes encoding adenylation domains for five amino acids (Figure 1.25). The *lug* operon is comprised of all genes whose protein products are required for the biosynthesis of the non-ribosomally synthesized peptide,

lugdunin (Figure 1.26).

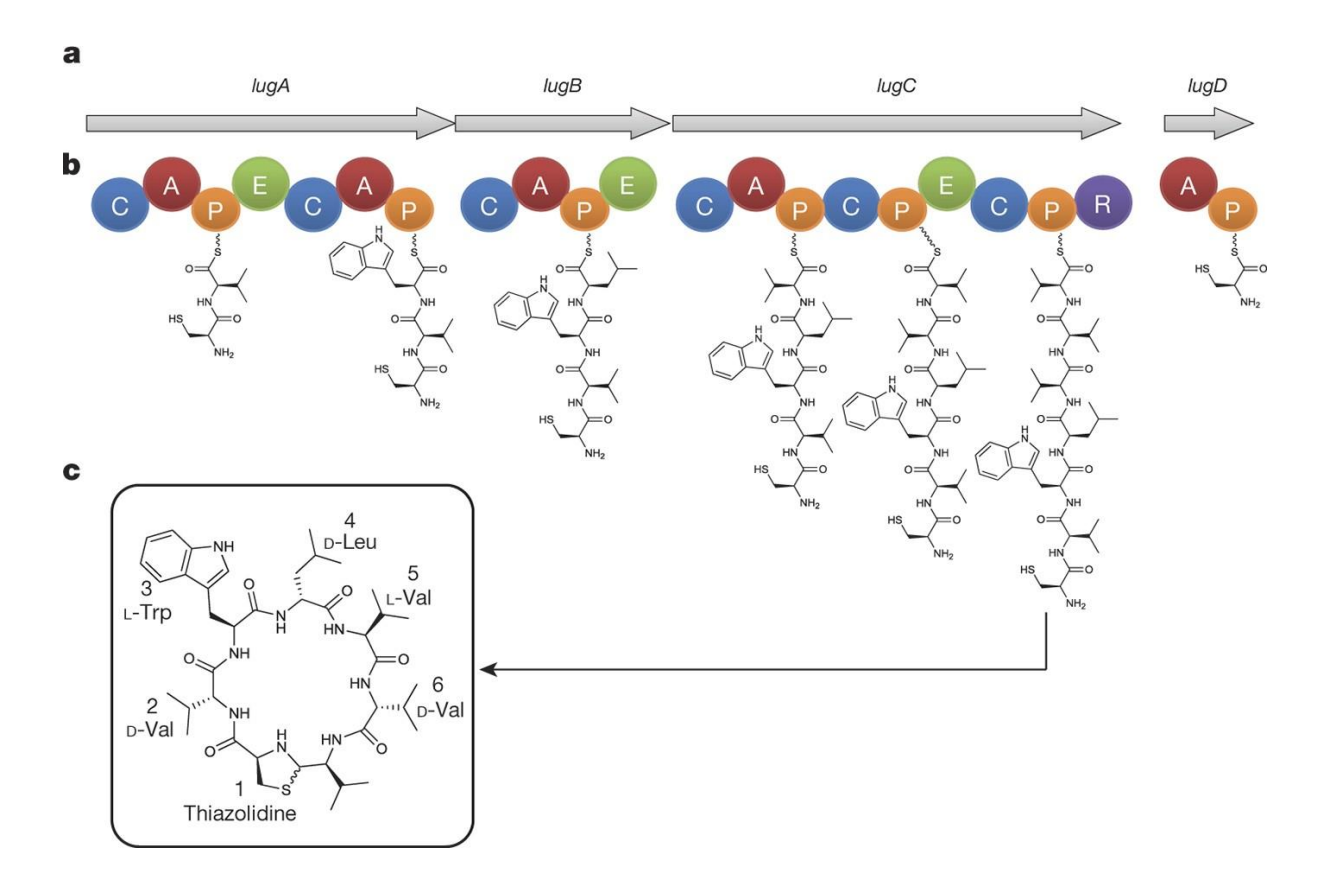


**Figure 1.25** The figure reveals the biosynthesis pathway of lugdunin. **a**, NRPS genes lugA, B, C, D. **b**, Modular organization of gene products. Functional domains: A, adenylation; P, peptidyl carrier protein; C, condensation; E, epimerization; R, reductase. The sequential biosynthesis of lugdunin starts presumably at the characteristic initiation module of LugD and continues with LugA-C (Figure obtained from Zipperer *et al.*).<sup>20</sup>

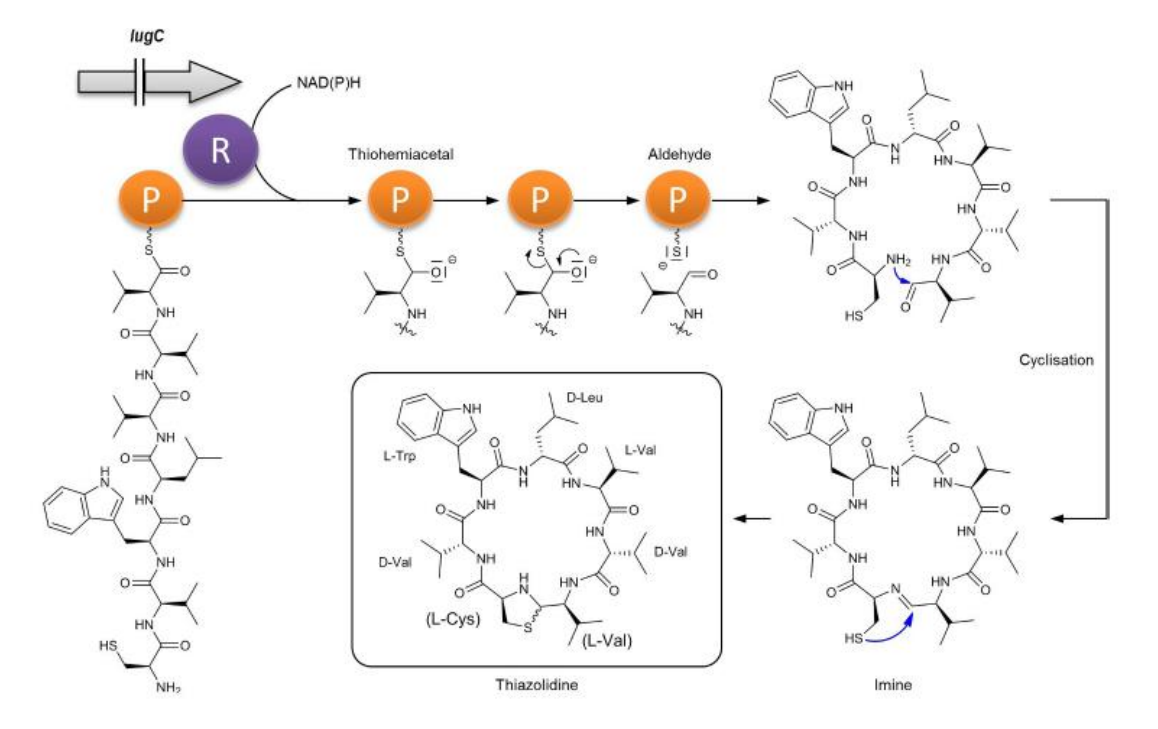


**Figure 1.26** The formation of thiazolidine ring through peptide cyclisation. The terminal reductase of LugC is proposed to initiate cleavage of the thioester-bound peptide chain with the aid of an NAD(P)H cofactor. The mature heptapeptide is liberated reductively from the NRPS multienzyme complex and cyclises via the *N*-terminal amine (L-Cys) and *C*-terminal aldehyde (L-Val) to form a macrocyclic imine/Schiff base. Subsequent nucleophilic attack of the cysteine thiol group generates the five-membered thiazolidine heterocycle (Figure obtained from Zipperer *et al.*).<sup>20</sup>

Structurally, although the thiazolidine moiety can also be found in certain linear NRPS products, such as watasemycin A and yersiniabactin (Figure 1.27) but it is unique to be reported in a macrocyclic peptide so far.<sup>20</sup> The thiazolidine ring is formed by condensation of an *N*-terminal L-cysteine with a *C*-terminal L-valine residue upon reductive release of a linear heptapeptide aldehyde from the NRPS mega-enzyme by the terminal reductase of LugC (Figure 1.26).<sup>20</sup>

It was unexpected that lugdunin would be obtained from a heptapeptide due to the limited adenylation domains on NRPS proteins. As known, the number of incorporated amino acids are determined by the number of central enzymatic domains, which indicates that it should be only restricted to 5 amino acids.<sup>20</sup> However, a new specificity for the second adenylation

domain of LugA was observed at position 3, where threonine was replaced by tryptophan.<sup>20</sup> Furthermore, LugC displayed an unusual modular organization with one adenylation (A) domain (valine), but two downstream peptide-bond-forming condensation (C) and three peptidyl carrier protein (P) domains required for amino acid transfer.<sup>20</sup> The result indicated that the single adenylation domain of LugC is responsible for activation of three subsequent valine residues, which are then incorporated in alternating L- and D-configurations.<sup>20</sup>

Figure 1.27 Structures of watasemycin A (1.21) and yersiniabactin (1.22).

# 1.4.2 Antimicrobial activity and MoA of lugdunin<sup>20,213</sup>

Lugdunin is known to possess potent antimicrobial activity against antibiotic-resistant Grampositive bacteria, such as methicillin-resistant S. aureus and vancomycin-resistant Enterococcus. The minimal inhibitory concentration (MIC) values for lugdunin tested on different strains of bacteria showed high potency (Table 1.2). It was also found that lugdunin is broadly inactive against Gram-negative bacteria (MIC value for S. aureus, MRSA and  $Pseudomonas\ aeruginosa$  was  $3\ \mu g/ml$ ,  $1.5\ \mu g/ml$  and  $>50\ \mu g/ml$ , respectively). Importantly, lugdunin was found not to cause lysis of primary human cells nor inhibit the metabolic activity of the human monocytic cell line, even at higher concentrations. In earlier studies, lugdunin was discovered to cause a rapid breakdown of bacterial energy resources, suggesting that the mode of action of lugdunin was to cause cessation of metabolic pathways in a manner similar to daptomycin (Figure 1.28).

**Table 1.2** Lugdunin spectrum of activity.<sup>20</sup>

Species and strain	Resistance	Lugdunin MIC
		(μg/ml)
S. aureus USA300 (LAC)	MRSA	1.5
+ 50% human serum		1.5
S. aureus USA300 (NRS384)	MRSA	1.5
S. aureus Mu50	Glycopeptide-intermediate Staphylococcus aureus	3
	(GISA)	
Enterococcus faecium BK463	VRE	3
Enterococcus faecium VRE366	VRE	12
Listeria monocytogenes ATCC19118		6
Streptococcus pneumonia ATCC49619		1.5
Bacillus subtilis 168 (trpC2)		4
Pseudomonas aeruginosa PAO1		> 50
Escherichia coli DH5a		> 50

Figure 1.28 Structure of daptomycin (1.23).

Daptomycin (1.23)

However, further investigation showed that the exact mode of action is thought to be proton translocation because of the observation of the dissipation of the membrane potential in *S. aureus*. Lugdunin and its analogues were found to disrupt the electrical potential of bacterial cell membranes, thereby leading to the bacteria death. Based on the structure-activity relationship (SAR) results by Schilling *et al.* it was suggested lugdunin modulated ion transport across the bacterial membrane, which results in the difference in voltage between the interior and exterior (Figure 1.29).<sup>213</sup>

**Figure 1.29** Proton translocation is thought to be the mode of action of lugdunin. Lugdunin causes proton leakage in synthetic, protein-free membrane vesicles, suggesting that it does not need to target a proteinaceous molecule to exert its antibacterial activity (Figure obtained from Schilling *et al.*).<sup>213</sup>

# 1.4.3 Research on lugdunin analogues and SAR study

Lugdunin is comprised of five kinds of amino acids (L-tryptophan, D-leucine, L-cysteine, L-valine and D-valine) and a unique thiazolidine ring which results from the condensation of L-cysteine and L-valine. To investigate the importance of each amino acid residue for the antimicrobial activity of lugdunin, the common method of alanine-scanning was performed.<sup>213</sup> Alanine is a commonly and useful tool for mutational scanning. Replacing the side chains with other larger, more constrained, more polar/non-polar substitutions may lead to changes in structures and conformation as well as the side-chain chemistry, and thus complicating analyses

of results. More details of alanine scanning will be discussed in Chapter 3. Figure 1.30 shows the structures of lugdunin and the analogues synthesized following alanine scanning. Their antimicrobial activities were also determined by the evaluation against USA 300 LAC.<sup>213</sup> In the antimicrobial activity test against *S. aureus* USA300, the results showed that all the alanine analogues were less active or inactive compared to lugdunin itself (Table 1.3).<sup>213</sup>

1.24

Figure 1.30 Structures of lugdunin (1.24) and its alanine scan analogues 1.25 to 1.30. All the amino

acids are replaced by alanine with the same stereo-configuration.<sup>213</sup>

**Table 1.3** Antimicrobial test (against MRSA USA300 LAC) of lugdunin and analogues from alanine scanning by *Schilling et al.*<sup>213</sup>

	MIC (μM)
Compound	(USA300 LAC)
Lugdunin (lug) ( <b>1.24</b> )	3.9
$(L-Ala)^7$ -lug (1.25)	33.1
$(D-Ala)^6$ -lug ( <b>1.26</b> )	33.1
(L-Ala) <sup>5</sup> -lug ( <b>1.27</b> )	16.6
(D-Ala <sup>4)</sup> -lug ( <b>1.28</b> )	≥ 100
(L-Ala <sup>3)</sup> -lug ( <b>1.29</b> )	≥ 100
$(D-Ala)^2$ -lug (1.30)	16.6

A further study on the effect of a change in the stereo-configuration of individual amino acid residues was then conducted by Schilling *et al.*<sup>213</sup> Compounds **1.31-1.37** were synthesized with each amino acid replaced by its enantiomer (Figure 1.31).<sup>213</sup> All the compounds were found to be inactive (Table 1.4).<sup>213</sup> The results indicate that the potency is affected by the inversion of a stereogenic centre. To understand the crucial impact of the absolute configuration of lugdunin on bioactivity, compound **1.38**, an enantiomer analogue of lugdunin was synthesized (Figure 1.31).<sup>213</sup> Interestingly, this analogue showed identical antibiotic activity to lugdunin (Table 1.4). The insignificance of the absolute configuration of lugdunin suggests that the mode of action is not relative to a stereospecific receptor-ligand interaction but could involve the recognition of achiral compounds.

**Figure 1.31** Structures of compounds **1.31-1.38**. Compounds **1.31-1.37** were synthesized as a stereoscan series of lugdunin while **1.38** was an enantiomer of lugdunin.

Table 1.4 Bioactivity test (against MRSA USA300 LAC) of compounds 1.8-1.15.213

		MIC (μM)
Compound		(USA300 LAC)
1.24	lugdunin (lug)	3.9
1.31	(D-Val) <sup>7</sup> -lug	≥ 100
1.32	(L-Val) <sup>6</sup> -lug	≥ 100
1.33	(D-Val) <sup>5</sup> -lug	≥ 100
1.34	(L-Leu) <sup>4</sup> -lug	≥ 100
1.35	(D-Trp) <sup>3</sup> -lug	≥ 100
1.36	(L-Val) <sup>2</sup> -lug	≥ 100
1.37	(D-Val) <sup>1</sup> -lug	≥ 100
1.38	enantio-lug	3.9

Then, compounds **1.39-1.45** were synthesized by Schilling *et al.* to determine the importance of the thiazolidine ring since it is thought to be the core structure.<sup>213</sup> Compounds **1.39** and **1.40** are both linear peptides without a thiazolidine ring (Figure 1.32). Compound **1.39** carries neither thiazolidine nor cyclic structure due to the lack of cysteine. Compound **1.40** was regarded as the linear peptide of lugdunin and the analogue **1.41**, in which the ring is composed exclusively of normal peptide bonds, was formed by the intramolecular cyclization of **1.40**. All compounds turned out to be inactive against *S. aureus* USA300 (Table 1.5).<sup>213</sup>

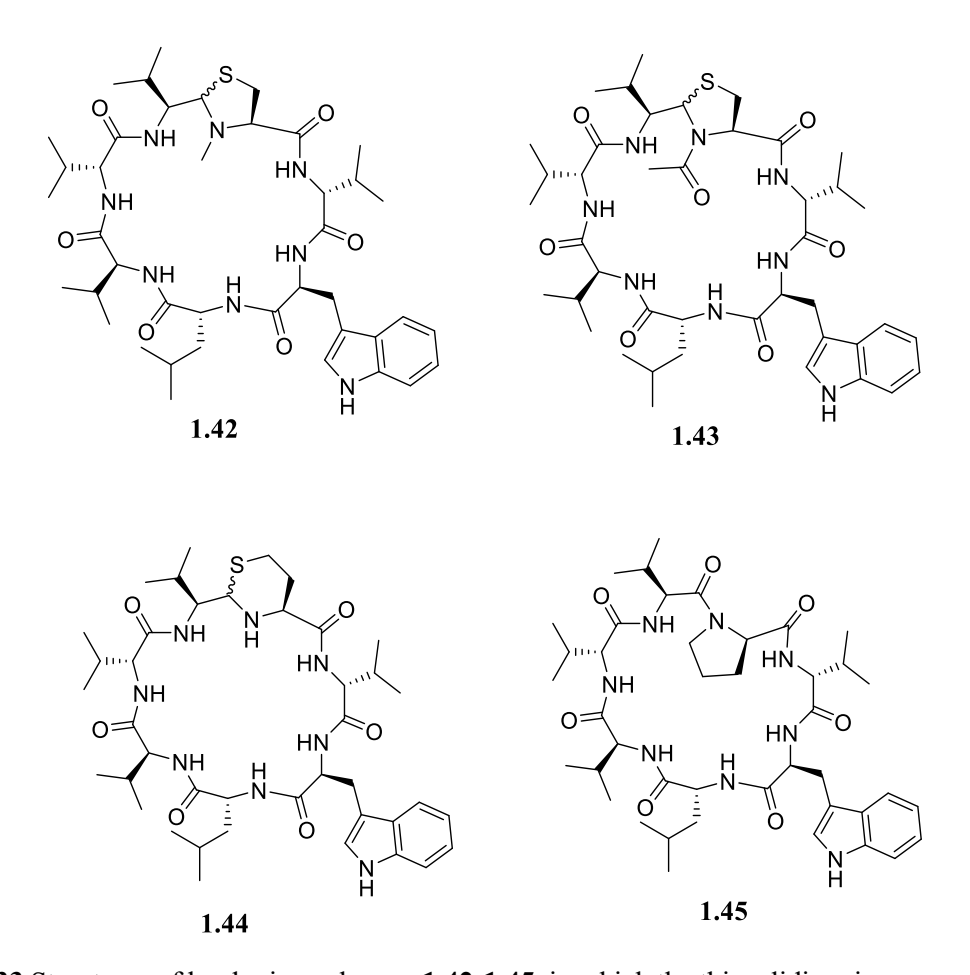
Figure 1.32 Structures of linear or cyclic lugdunin analogues 1.39-1.41 which lack the thiazolidine ring.<sup>213</sup>

Table 1.5 Bioactivity against MRSA USA 300 LAC of compounds 1.16-1.18.213

		MIC (μM)
Compound		(USA300 LAC)
1.24	Lugdunin (lug)	3.9
1.39	(Ala)¹-lug	≥ 100
1.40	Linear-lug (-COOH)	≥ 100
1.41	Cyclized homodemic-lug	≥ 100

In an experiment to demonstrate the importance of the thiazolidine NH functionality, compounds **1.42** and **1.43** were designed and synthesized.<sup>213</sup> Modifications in these analogues consist of *N*-methylation or *N*-acetylation in the thiazolidine ring (Figure 1.33). Consequently,

these analogues with a tertiary amine or amide were found to be inactive against *S. aureus* USA300, thus revealing the requirement of the secondary amine in the thiazolidine ring.<sup>213</sup> Investigations into the importance of the size of the five-member thiazolidine ring were then carried out. Compounds **1.44** and **1.45** (Figure 1.33), with an expanded heterocycle by an additional methylene group or a simplified proline-containing homodetic peptide were also found to be inactive (Table 1.6).<sup>213</sup> Therefore, to maintain the antimicrobial activity, the presence of both the thiazolidine ring and its secondary amine is required.



**Figure 1.33** Structures of lugdunin analogues **1.42-1.45**, in which the thiazolidine ring was modified or replaced with 1,3-thiazinane and L-proline homodemic. <sup>213</sup>

Table 1.6 Bioactivity against MRSA USA300 LAC of compounds 1.19-1.22. 213

		MIC (μM)
Compound		(USA300 LAC)
1.24	lugdunin (lug)	3.9
1.42	N-methylthiazolidine-lug	≥ 100
1.43	N-acetylthiazolidine-lug	≥ 100
1.44	1,3-thiazinane-lug	≥ 100
1.45	L-Pro homodetic-lug	≥ 100

Nevertheless, analogue **1.46** with two tryptophan residues in the structure was synthesized to strengthen the assumed interaction with the bacterial membrane (Figure 1.34).<sup>213</sup> Surprisingly, the analogue showed a two-fold increase in activity (Table 1.7).<sup>213</sup>

Figure 1.34 Structure of lugdunin analogue 1.46, in which another tryptophan is introduced.<sup>213</sup>

Table 1.7 Bioactivity test against MRSA USA300 LAC of compound 1.46.213

Compound		MIC (μM) (USA300 LAC)
1.24	lugdunin (lug)	3.9
1.46	(D-Trp) <sup>6</sup> -lug	1.8

In 2021, more lugdunin analogues were designed and synthesized by Saur *et al.*<sup>235</sup> In this latest published paper, the authors have focused on a different synthetic method for the preparation of lugdunin and the analogues with modifications at position 2, 3 and 4. The new synthetic route which was via the pre-synthesis of a thiazolidine dipeptide building block will be discussed more in detail in Chapter 2 and compared to our synthetic strategy.<sup>235</sup>

At position 2, compounds **1.47-1.52** were synthesized by the replacement of original D-Val residue with hydrophobic aliphatic amino acids, including D-*allo*-Ile, D-Leu, D-Hle, D-Nva, D-Ile and D-Phe (Figure 1.35). All the analogues were found to be less active or inactive compared to lugdunin (Table 1.8). Among them, compound **1.47**, with an incorporated D-*allo*-Ile residue, was found the most potent analogue which is only around 2-fold less active than lugdunin. In general, prolongation, extended branching, and increased bulkiness of substituents at D-Val<sup>2</sup> of lugdunin resulted in reduced biological activity.<sup>235</sup>

**Figure 1.35** Structures of lugdunin analogues **1.47-1.52**, in which the D-Val at position 2 was substituted with a set of hydrophobic aliphatic amino acids.<sup>235</sup>

Table 1.8 Bioactivity against MRSA USA 300 LAC of compounds 1.47-1.52.235

		MIC (μM)
Compound		(USA300 LAC)
1.24	lugdunin (lug)	3.9
1.47	(D- <i>allo</i> -Ile) <sup>2</sup> -lug	7.9
1.48	(D-Leu) <sup>2</sup> -lug	15.7
1.49	(D-Hle) <sup>2</sup> -lug	61.7
1.50	(D-Nva) <sup>2</sup> -lug	16
1.51	(D-Ile) <sup>2</sup> -lug	31.4
1.52	(D-Phe) <sup>2</sup> -lug	≥ 100

At position 3, the original L-Trp was substituted with (hetero)aromatic amino acids, and the

variants were evaluated in terms of their membrane interaction properties by *S. aureus* inhibition assays. Compound **1.53** (Figure 1.36), where the original L-Trp was replaced by L-Phe, was found to be 4-fold less active than lugdunin (Table 1.9). Then, a wider range of unusual, noncanonical, aromatic amino acids was set out to substitute L-Trp<sup>3</sup> and to get access to an attractive chemical diversity. Modified phenylalanine analogues **1.54** and **1.55** (Figure 1.36) were both found inactive (Table 1.9). These findings indicate that polarity or charges is not tolerated. Among all the analogues with the modifications at position 3, the hydrophobically enhanced amino acids with annelated benzene rings, such as naphthalene **1.56** and anthracene side chains **1.57** (Figure 1.36) were found only 2-fold less active than lugdunin (Table 1.9). It indicated the influence of hydrophobicity on the biological activity of lugdunin. The highly hydrophobic aromatic functionality ensures the fast association as well as insertion into the bacterial membrane, representing the initial step for membrane penetration as a protonophore.<sup>235</sup>

Figure 1.36 Structures of lugdunin analogues 1.53-1.57.<sup>235</sup>

Table 1.9 Bioactivity against MRSA USA 300 LAC of compounds 1.53-1.57.235

Compound		MIC (μM) (USA300 LAC)
1.24	lugdunin (lug)	3.9
1.53	(L-Phe) <sup>3</sup> -lug	16.8
1.54	L-Phe (4-chloro) <sup>3</sup> -lug	≥ 100
1.55	L-Phe (3-nitro) <sup>3</sup> -lug	≥ 100
1.56	L-Ala (1-naphthyl) <sup>3</sup> -lug	7.9
1.57	L-Ala (9-anthracenyl) <sup>3</sup> -lug	7.4

At position 4, D-Leu was proven as a critical residue for substitution in the research by Schilling *et al.*<sup>213</sup> To address the prominent importance in dynamic membrane interactions, compound **1.58** (Figure 1.37), in which the original D-Leu was replaced by D-Ile, was found to have an 8-fold reduced activity compared to lugdunin (Table 1.10). Then, based on the previous research on the most potent compound **1.46** at position 6 (where D-Val was replaced by D-Trp), several analogues with the combination of D-Trp<sup>6</sup> and modifications of D-Leu<sup>4</sup> were synthesized.<sup>235</sup> Among them, only compounds **1.59-1.61** (Figure 1.37), in which the residue at position 4 was substituted by D-*allo*-Ile, D-Tle and D-Nva, show weak antimicrobial activity (Table 1.10).<sup>235</sup>

Figure 1.37 Structures of lugdunin analogues 1.58-1.61.

Table 1.10 Bioactivity against MRSA USA 300 LAC of compounds 1.58-1.61.

		MIC (μM)
Compound		(USA300 LAC)
1.24	lugdunin (lug)	3.9
1.58	(L-Ile) <sup>4</sup> -lug	25
1.59	(L-allo-Ile) <sup>4</sup> -(D-Trp) <sup>6</sup> -lug	12.5
1.60	(L-Tle) <sup>4</sup> -(D-Trp) <sup>6</sup> -lug	25
1.61	$(L-Nva)^4-(D-Trp)^6-lug$	12.5

Moreover, as mentioned before, the synthetic enantiomer of lugdunin was found to display the same antimicrobial potency as lugdunin. Compound **1.62** was synthesized as a *retro*-sequence of lugdunin, where the amino acid residues at position 3, 4, 5 and 6 are in an opposite order compared to the original lugdunin (Figure 1.38) and it was found to be only 2-fold reduced activity compared to lugdunin (Table 1.11). It was thought that **1.62** resembles the lugdunin enantiomer due to its similarity to a mirror image of lugdunin.<sup>235</sup>

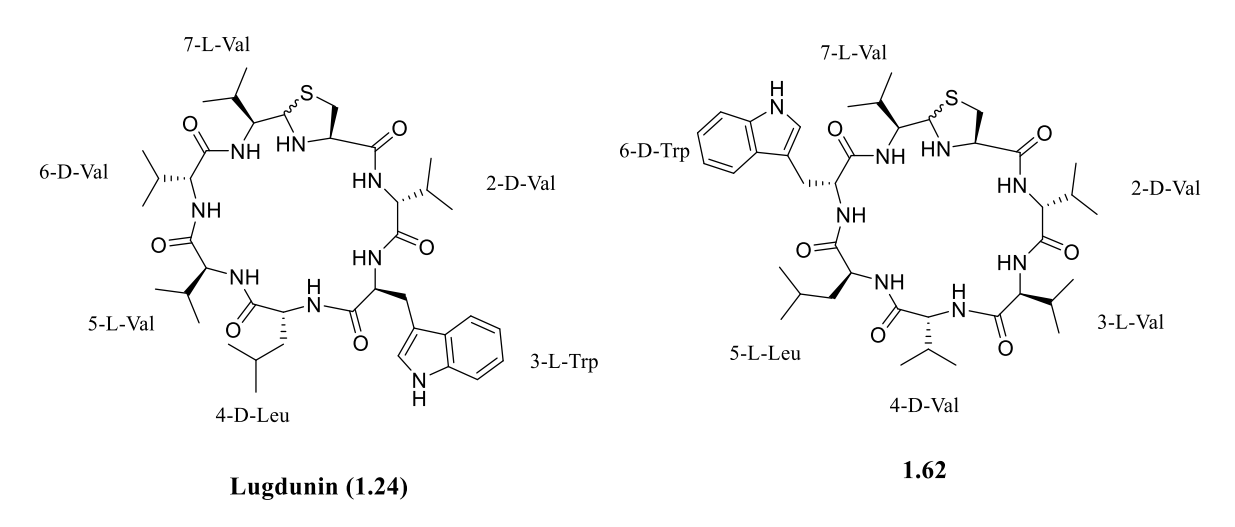


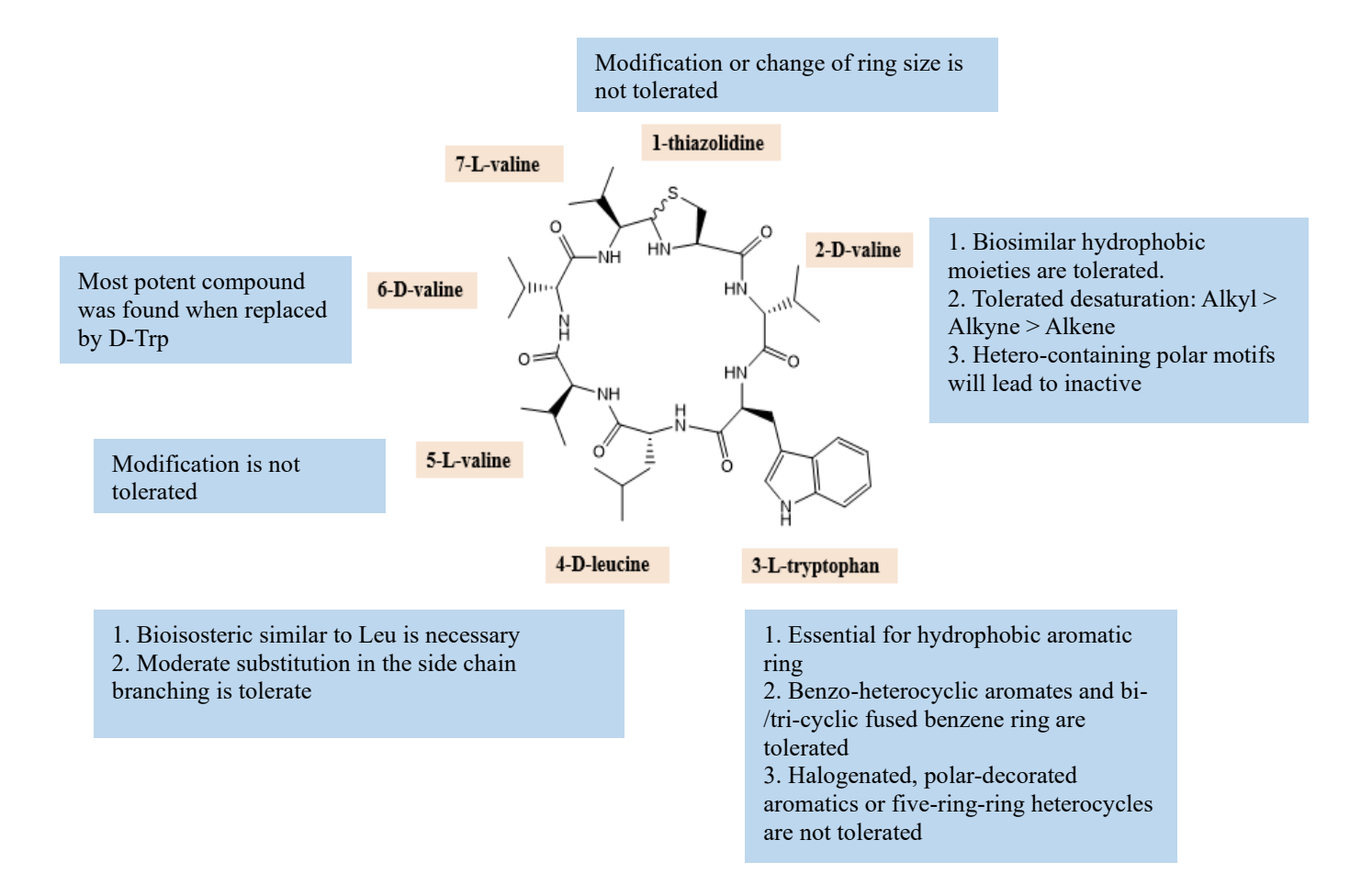
Figure 1.38 Structures of lugdunin and the *retro*-sequence analogue 1.62.

Table 1.11 Bioactivity against MRSA USA 300 LAC of compounds 1.62.

Compound		MIC (μM) (USA300 LAC)
1.24	lugdunin (lug)	3.9
1.62	$(L-Val)^3-(D-Val)^4-(L-Leu)^3-(D-Trp)^6-lug$	8.0

Thus, based on the SAR study performed by Schilling *et al.*, several factors are significant contributors to the antimicrobial activity of lugdunin.<sup>213,235</sup> For example, the *N*-unsubstituted thiazolidine ring at position 1 is required and any change of the ring size is not tolerable. At position 2, prolongation, extended branching, and increased bulkiness of substituents will lead

to the reduction of biological activity.<sup>235</sup> At position 3, hydrophobic aromaticity is thought to be necessary, and only the modifications with benzo-heterocyclic aromates or fused benzene rings are accepted. Position 4 is classified as essential in the comprehensive alanine scan. Therefore, it is thought the both residues at position 3 and 4 strictly tolerate only a small alteration of polarity and charge. Still, it was found that there is no benefit for the D-Trp<sup>6</sup> with simultaneous D-Val<sup>2</sup> and D-Leu<sup>4</sup> substitution. Moreover, the alternating D- and L- amino acids are also necessary (Figure 1.39).<sup>213</sup>



**Figure 1.39** An overall review of the structure of lugdunin and a summary of the importance of each residue in the structure. <sup>213,235</sup>

# 1.4.4 Interaction between lugdunin and bacterial membrane resulting in proton translocation

Whilst the work described in this thesis was ongoing, a SAR study of lugdunin was reported by Schilling *et al.* in 2019, which highlighted the importance of the unsubstituted thiazolidine ring, tryptophan, leucine and alternating stereo-configuration of amino acid residues as necessary elements of lugdunin.<sup>213</sup> It was hypothesized that, in the interactions of lugdunin with the bacterial membrane, both the leucine-4 and tryptophan-3 residues in lugdunin point towards the hydrophobic region of the bacterial membrane. As mentioned before, compound 1.38 which is the enantiomer analogue of lugdunin showed the identical activity to ludgunin (1.24).<sup>213</sup> The result suggested that the MoA of lugdunin might be related to the enhanced transfer of achiral molecules or ions through lipid membranes.

An experiment was then carried out by Schilling *et al.* to investigate the different effect of analogues on the transmembrane potential of *S. aureus* NCTC8325 (Figure 1.40).<sup>213</sup> Transmembrane potential is referred to the difference in electric potential between the interior and the exterior of a biological cell. 3,3'-Diethyloxacarbocyanine iodide (DiOC<sub>2</sub>(3)) was used as the dye in this study. DiOC<sub>2</sub>(3) is a membrane potential probe which is usually utilized to analyse bacterial viability by flow cytometry using fluorescence emission ratio detection.<sup>213</sup> Moreover, the phenomenon of partial membrane depolarization was also found when the active analogues were tested.<sup>213</sup> It was suggested that the MoA of lugdunin and other active analogues was related to the impairment of membrane integrity or ion leakage-transport.<sup>213</sup>

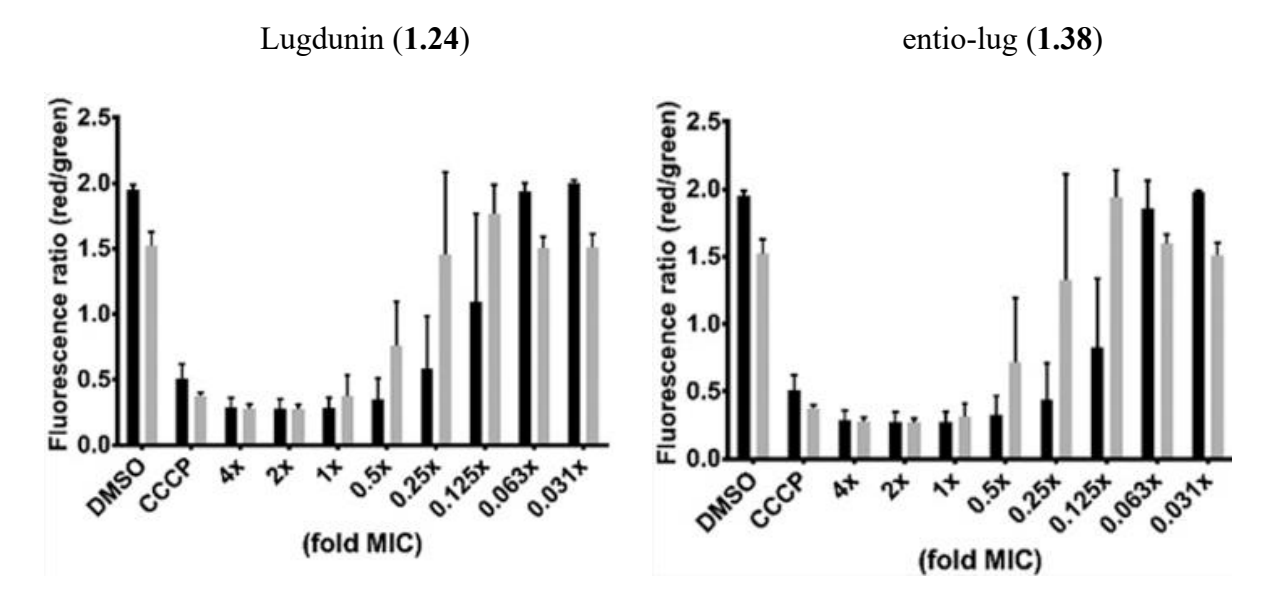


**Figure 1.40** Effect of lugdunin (**1.24**) and entio-lug (**1.38**) on the *S.aureus* NCTC8325 membrane potential after 0.5 (black bars) and 1 hour (gray bars) of treatment. The positive and negtive contol was protonophore CCCP (5mm) and DMSO repectively. Error bars represent the standard deviation (SD) of two biological replicates including two technical replicates each.

In a further study by Schilling *et al.*, *S. aureus* was treated with lugdunin and a mixture of dyes, Syto9 and propidium iodide (PI) to understand the influence on bacterial membranes.<sup>213</sup> Syto9 is a fluorescent nucleic acid stain which is commonly used in microbiology, especially in fluorescence microscopy and flow cytometry analyses, while PI is a popular red fluorescent intercalating agent that can be used to stain cells and nucleic acids.<sup>213</sup> The addition of these two reagents can be used as an indicator for pore formation. The result revealed that the MoA of lugdunin was not connected to the formation of pores.<sup>213</sup> The ability of lugdunin to impair vesicle integrity was then investigated.<sup>213</sup> In this experiment, unilamellar vesicles composed of 1-palmitoyl-2-oleoyl-*sn*-glycero-3-phosphocholine (POPC) was applied as a membrane model system in order to evaluate the bioactivity of 1.24.<sup>213</sup> An investigation whether 1.24 impairs vesicle integrity was first conducted by Schilling *et al.*<sup>213</sup> Lugdunin (1.24) was compared with the cyclic decapeptide gramicidin S for the ability to induce the release of the fluorescent dye carboxyfluorescein (CF), while the latter can lead to destabilization of membranes.<sup>213</sup> The dye

is entrapped in vesicles and an increase in fluorescence is caused by leakage. In contrast to gramicidin S, only a small smount of leakage was observed with lugdunin (1.24) even at higher concentrations. The outcome indicated that lugdunin might act by translocating ions since it would not destabilize the membrane.<sup>213</sup>

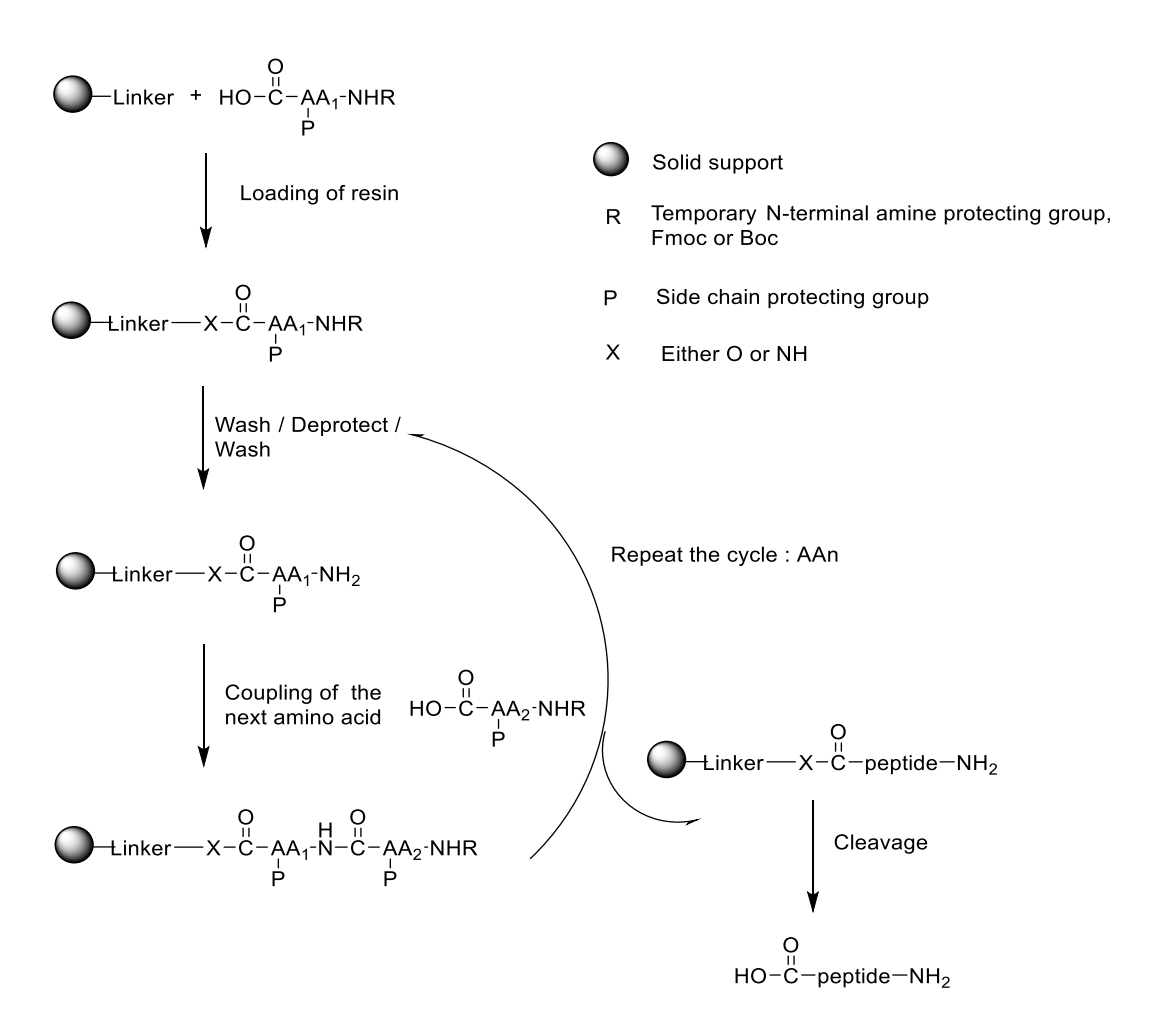
The ability of lugdunin to facilitate the translocation of protons was subsequently established by Schilling *et al.*<sup>213</sup> Vesicles filled with 8-hydroxypyrene-1,3,6-trisulfonic acid trisodium salt (HPTS) were used as the dye in the experiment.<sup>213</sup> HPTS is also known as a fluorescent membrane-impermeant pH indicator.<sup>213</sup> Lugdunin was found to cause a rapid increase in intracellular fluorescence, indicating an increase in intracellular proton concentration. Thus, the MoA of lugdunin was thought to be associated with enhanced proton translocation.<sup>213</sup>

## 1.5 Aims and objectives

As discussed in the previous section, lugdunin displayed potent antimicrobial activity against Gram-positive bacteria, including antibiotic-resistant strains, and hence was considered to be a promising lead compound. In this project, several lugdunin analogues were designed, synthesized and evaluated for their antimicrobial activity against *S. aureus*, in order to establish a structure-activity relationship (SAR).

The synthetic strategy for the preparation of lugdunin is first discussed. The formation of the thiazolidine ring was thought to be the key part in the total synthesis of lugdunin. Thus, several methods were investigated including the introduction of a dipeptide building block and the utilizing of various kinds of resins. Since the same synthetic method via the preparation of dipeptide building block had been reported by Saur *et al.* in 2021, differences will be discussed

as well in Chapter  $2.^{235}$  Due to the higher yields and simple operation, a method that utilized a modified Threonine-Glycine (TG) resin was adopted. The desired linear peptide chain will be assembled following general Fmoc-SPPS protocol (Scheme 1.3). Then, the linear peptide chain with C-terminal aldehyde will be afforded by acidolytic cleavage and the lugdunin (1.24) will be secured via a peptide cyclization. The detailed synthetic strategies and mechanisms will be discussed in Chapter 2.



**Scheme 1.3** General protocol of SPPS. The first  $N^{\alpha}$  -protected amino acid is attached to the linker-polymer support. Then, DMF was used to remove excess amino acids and coupling reagents. After deprotection, DMF was still used to remove the deprotecting reagent, which is followed by the coupling of the next amino acid residue. The linear peptide chain is thus assembled by coupling cycles. Finally, the free linear peptide may be obtained after an acidolytic cleavage from the resin.

In the method to prepare the modified TG resin, the reaction with Fmoc-amino aldehyde is the

most crucial step. Thus, different synthetic strategies will also be discussed in Chapter 2. A rapid and efficient one-pot synthetic protocol reported by Ivkovic *et al.* was adapted (Scheme 1.4).<sup>237</sup> The method was subsequently used for the total synthesis of lugdunin analogues, in which different Fmoc-amino aldehydes (at position 7) will be utilized.

**Scheme 1.4** Synthesis of Fmoc-amino aldehyde (**1.64**) by using CDI/DIBAH-H.<sup>237</sup> The Fmoc-protected carboxylic acid (**1.63**) will be converted to an activated amide via the reaction with CDI. Then the desired aldehyde product will be obtained after cleavage by DIBAL-H.

As the synthetic method was established, the first series of analogues was synthesized after the alanine-scan. Alanine-scan was considered as an effective method to investigate the significance of each amino acid residue. Analogues were prepared by the replacement of L- or D-alanine at each position without the change of its original stereo-configuration.

Following the SAR study from Schilling *et al.*<sup>213</sup> and the specific alanine-scan study carried out in this project, it was found that position 7 could be an important site for chemical modifications. Thus, several analogues with the modification at position 7 of lugdunin were then designed and synthesized. The L-leucine (1.65) and L-homoleucine (1.66) analogues were firstly used to investigate the importance of the hydrocarbon length in the side chain. Then, analogues with position 7 replacement by L-norvaline (1.67), L-norleucine (1.68), L-tryptophan (1.69), L-phenylalanine (1.70) and L-cyclopropyl alanine (1.71) were prepared to determine the influence of branched and (hetero)aromatic groups in the amino acid side chain. Figure 1.39 shows the structures of analogues 1.65-1.71.

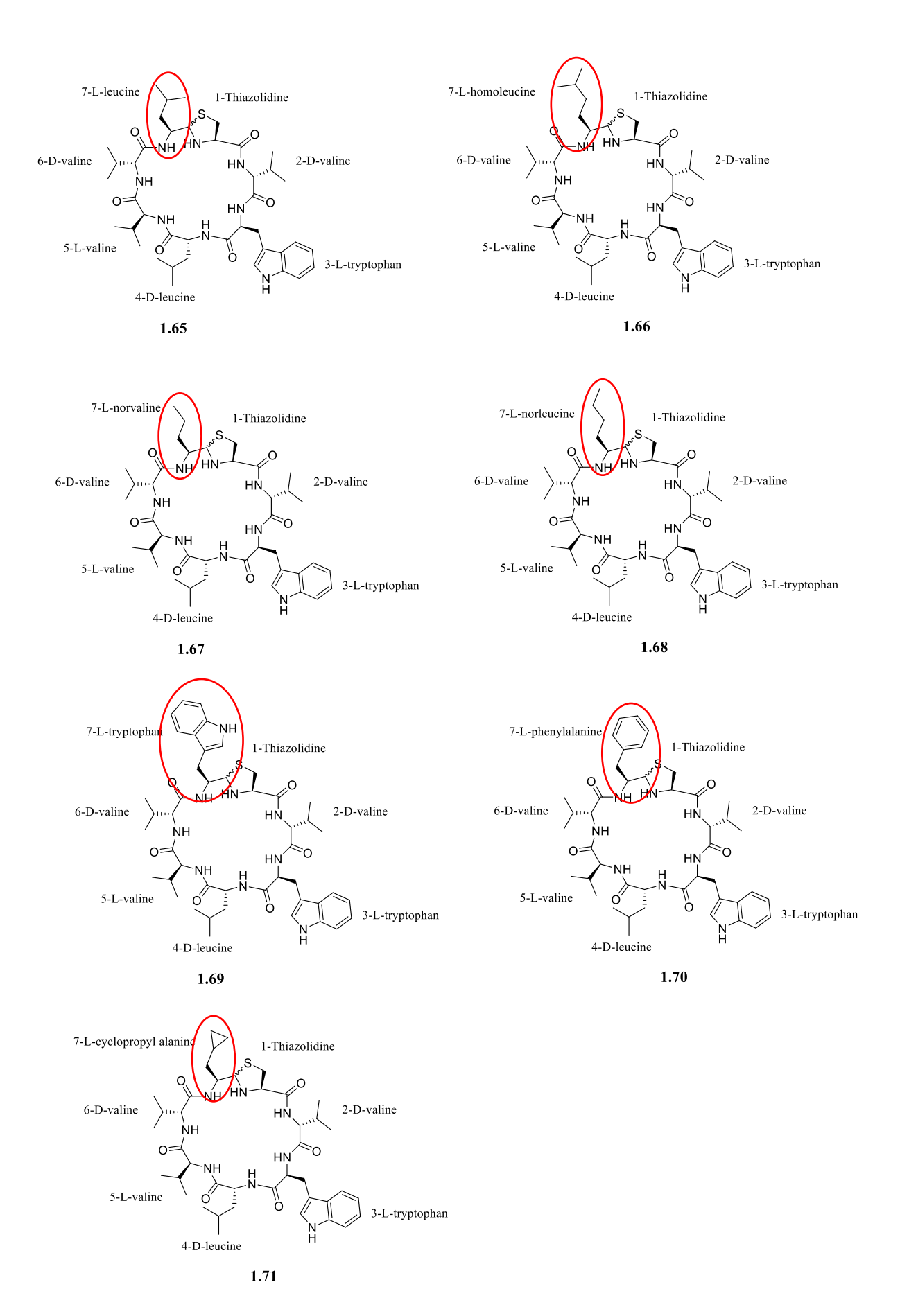


Figure 1.39 Structures of planned analogues 1.65-1.71.

Furthermore, analogues with *N*-methylated amino acids were synthesized to increase the hydrophobicity, while the introduction of L-threonine will make the structure more hydrophilic. In Chapter 4, synthetic strategies for the preparation Fmoc-*N*-methyl amino acids will be discussed in detail. The robust protocol shown in Scheme 1.5 was previously reported by Freidinger *et al.*<sup>238</sup>, which was adopted for the synthesis of the building blocks, Fmoc-*N*-methyl amino acids.

**Scheme 1.5** Protocol for the preparation of Fmoc-*N*-methylated amino acid. The oxazolidinone intermediated will be firstly formed from the amino acid. Then the desired *N*-methyl compound will be obtained after cleavage by TFA.

In the SAR study by Schilling *et al.*, several lugdunin with modification at position 6 were synthesized. Their results indicated that position 6 is also a site that tolerates modifications.<sup>213</sup> Therefore, to compare with position 7, three analogues with the modifications at position 6 were designed and synthesized. At this position, compounds with replacement by D-leucine (1.72), D-tryptophan (1.46) and D-phenylalanine (1.73) were prepared (Figure 1.40). Similar to the SAR study at position 7, the substitution with D-leucine was used to determine if the length of the hydrocarbon side-chain affects antimicrobial activity.

Figure 1.40 Structures of planned analogues 1.46, 1.72 and 1.73.

In order to establish an SAR, all synthesized analogues, including lugdunin, were tested for their antimicrobial activity against different strains of *S. aureus*. The *in vitro* antimicrobial potency of compounds were determined via growth inhibition assay and broth microdilution assay, and the IC<sub>50</sub> and MIC values will be obtained, respectively. The growth inhibition assay was generally performed using the Gram-positive strains, *S. sureus* SH1000 and USA300 JE2. MIC is determined as the lowest concentration (in µg/mL) of a tested compound that inhibits the growth of a given strain of bacteria. Herein, *S. aureus* SH1000 and USA300 JE2 were used as the strains for initial assessments. The most active compounds were then further tested against another three different strains of *S. aureus*, including Newman, PM64 and Mu50. The results of the in vitro antimicrobial assays and the SAR will be further discussed in detail.

# Chapter 2

# Total synthesis of lugdunin

## 2.1 Synthesis of lugdunin

As reported by Schilling *et al.*, total chemical synthesis of lugdunin could be achieved by a Fmoc solid-phase peptide synthesis strategy and using a H-Val-H NovaSyn TG resin (2.1) and HATU was used as the coupling reagent (Scheme 2.1). $^{213}$  After assembly of the peptide chain and deprotection of the side chains, the linear peptide aldehyde was released from the resin. $^{213}$  Subsequent intramolecular cyclization via the *C*-terminal aldehyde and the *N*-terminal cysteine afforded the macrocycle through in situ thiazolidine formation. $^{213}$  The thiazolidine exists in two interconverting and therefore, inseparable epimeric forms (Scheme 2.1). $^{213}$ 

Scheme 2.1 The reported solid-phase aldehyde peptide synthesis of lugdunin (1.24).<sup>213</sup>

In 2021, an apparently improved synthetic method was further published by Saur *et al.*, which was based on a dipeptide building block.<sup>235</sup> The required thiazolidine building block Fmoc-L-Thz(L-Val) (2.5) was achieved in three steps (Scheme 2.2). Firstly, reduction of the amino acid Fmoc-L-Val-OH (2.2) to the corresponding amino alcohol Fmoc-L-valinol (2.3) using sodium borohydride (NaBH<sub>4</sub>) following pre-activation of the carboxylic acid by carbonyl diimidazole (CDI).<sup>235</sup> The intermediate 2.3 was then re-oxidized to the corresponding aldehyde 2.4 by Dess-Martin periodinane (DMP).<sup>235</sup> Finally, condensation of the amino aldehyde 2.4 with L-cysteine gave the desired Fmoc-L-Thz(L-Val)-OH (2.5), which favorably precipitates during the reaction.<sup>235</sup>

Fmoc 
$$\stackrel{\text{H}}{\longrightarrow}$$
  $\stackrel{\text{O}}{\longrightarrow}$   $\stackrel{\text{O}}{\longrightarrow}$   $\stackrel{\text{H}}{\longrightarrow}$   $\stackrel{\text{O}}{\longrightarrow}$   $\stackrel{\text{H}}{\longrightarrow}$   $\stackrel{\text{O}}{\longrightarrow}$   $\stackrel{\text{H}}{\longrightarrow}$   $\stackrel{\text{O}}{\longrightarrow}$   $\stackrel{\text{H}}{\longrightarrow}$   $\stackrel{\text{C}}{\longrightarrow}$   $\stackrel{\text{C}}{\longrightarrow}$   $\stackrel{\text{H}}{\longrightarrow}$   $\stackrel{\text{C}}{\longrightarrow}$   $\stackrel{\text{H}}{\longrightarrow}$   $\stackrel{\text{C}}{\longrightarrow}$   $\stackrel{\text{C}}{\longrightarrow}$ 

<sup>a</sup>Reagents and conditions: (a) Fmoc-L-Val-OH, CDI, tetrahydrofuran (THF), room temperature (rt), 15 min; (b) NaBH<sub>4</sub> in H<sub>2</sub>O, 0 °C, 25 min; (c) Dess-Martin periodinane, 0 °C to rt, DCM, addition of 1.1 equiv. of H<sub>2</sub>O during the first hour of the reaction, O/N; (d) L-cysteine, MeOH/H<sub>2</sub>O (2:1), 24 h, 65 °C

Scheme 2.2 Synthesis of Fmoc-protected thiazolidine amino acid which was reported by Saur et al.<sup>235</sup>

The subsequent synthesis of lugdunin (1.24) was then achieved by the standard solid-phase peptide synthesis (SPPS) protocol (Scheme 2.3).<sup>235</sup> In their protocol, Fmoc removement was achieved by treatment of the resin with a mixture of 2,3,4,6,7,8,9,10-octahydropyrimido[1,2-a] azepine (DBU, 2%) and morpholine (10%) in DMF, resulting in a fast and efficient Fmoc removal.<sup>235</sup> A double coupling strategy, with the initial use of 1-[bis(dimethylamino)-

methylene]-1H-1,2,3-triazolo[4,5-b] pyridinium 3-oxide (HATU) followed by (benzotriazol-1yloxyo)tripyrrolidinophosphonium hexafluorophosphate (PyBOP) carboxyl-activating reagents was introduced to avoid truncation products.<sup>235</sup> Efforts to reduce the coupling reaction to only one reagent turned out to give truncated sequences. Furthermore, a capping step with  $Ac_2O/Pyr$  in DMF was included in the SPPS protocol after the consecutive  $Val^6 \rightarrow Val^5$ coupling to prevent truncated peptide byproducts.<sup>235</sup> Complete assembly of the lugdunin peptide sequence on-resin was followed by the removal of the terminal Fmoc group. The linear lugdunin heptapeptide 2.8 was cleaved off the resin under standardized conditions TFA/TIPS/H<sub>2</sub>O: 90/5/5). After lyophilization, the linear peptide was subjected to macrolactamization under high dilution conditions of 2.8 (2 mM) in DMF using HATU/3hydroxytriazolo[4,5-b] pyridine (HOAt)/DIPEA as coupling reagents.<sup>236</sup> Due to the high hydrophobicity of 1.24, all byproducts after the SPPS and macrolactamization can be extracted by polar solvents (DMF), whereas lugdunin remains in the lipophilic CHCl<sub>3</sub>/n-BuOH phase.<sup>235</sup>

a Reagents and conditions: (a) Fmoc deprotection: 2% DBU/10% morpholine (v/v) in DMF, rt, 3 and 12 min; (b) double coupling: Fmoc-D/L-AA-OH, (1.) HATU, HOBt, 4-methylmorpholine (NMM), DMF, rt, 30-45 min, (2.) PyBOP, HOBt, NMM, DMF, rt, 30-45 min; (c) capping after Val <sup>6</sup>-Val <sup>5</sup> coupling: DMF/Ac<sub>2</sub>O/Pyr (6:3:1, v/v); (d) cleavage: TFA/TIPS/H<sub>2</sub>O (90:5:5, v/v); (e) macrolactamization: **2.8**, HATU, HOAt, DIPEA, DMF (conc. of **2.8** = 2 mM), rt, 24 h.

Scheme 2.3 Synthesis of lugdunin (1.24) with the use of a thiazolidine dipeptide building block which was reported by Saur  $et\ al.^{235}$ 

## 2.2 An overview of synthetic strategies

The structure of lugdunin (1.24) contains several important parts. First, there are seven amino acids residues in total, comprising of two L-alanine, two D-alanine, one D-leucine, one L-tryptophan, and one L-cysteine. Secondly, the structure is a cyclic peptide with a core thiazolidine ring, which is partly derived from the cysteine residue, and a configuration of alternating D- and L-amino acids (Figure 2.1). The formation of the thiazolidine ring is thought to be a key part in the synthesis of lugdunin.

Herein, in our consideration of synthetic methods for the total synthesis of lugdunin, two contrasting synthetic strategies were envisaged (Figure 2.2). The first method was via the

condensation of an aldehyde-containing building block with L-Cys-OH to form a thiazolidine dipeptide. Then the thiazolidine dipeptide was used as a new building block in the synthesis of lugdunin following general Fmoc solid-phase peptide synthesis (Fmoc-SPPS) protocol. This approach is similar to that reported by Saur *et al.* in 2021.<sup>235</sup> However, the work reported in this thesis was completed by early 2019, which was approximately 1-2 years prior to the publication by Saur *et al.* An overview of the basic principles of Fmoc-SPPS will be further discussed in the next section. The final cyclisation step would be achieved via an amide-bond formation at a strategic location.

The other method was based on the use of different kinds of modified polymer or solid support, in which a peptidyl aldehyde is generated. This approach is like that reported by Schilling *et al.* in 2019.<sup>213</sup> In this approach, the expected linear peptide would be assembled following the general Fmoc-SPPS strategy, and then a chemical reagent-mediated cleavage or release will trun the *C*-terminal carbonyl ester of the peptide into an aldehyde functionality. Subsequently, cyclization will be performed to form the thiazolidine ring via condensation of the *C*-terminal aldehyde with a *N*-terminus located L-cysteine residue. These two different methods were investigated and discussed in the next section.

**Figure 2.1** Structure of lugdunin. The core structure is a thiazolidine ring which is derived from the condensation of L-Val-H with L-Cys-OH.

**Figure 2.2** The two strategies for the total chemical synthesis of lugdunin: (a) *N*-protected modified L-Val-OH (where PG is Fmoc or Boc) was condensed with L-Cys-OH to form the thiazolidine building block, PG- L-Thz(L-Val)-OH and then used in the synthesis of lugdunin via assembly of the linear sequence followed by a cyclisation step, and (b) the linear peptide sequence with L-cysteine and L-Val amino aldehyde as the head and tail was synthesized first, and then the desired lugdunin compound is obtained via a cyclisation step.

## 2.3 Solid-phase peptide synthesis (SPPS)

## 2.3.1 An overview of peptide synthesis

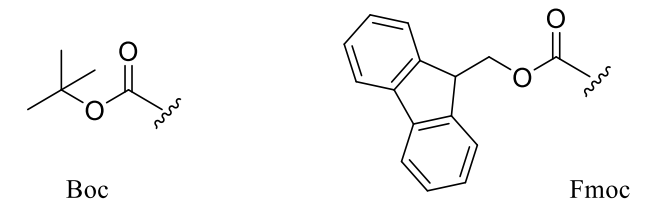
It has been over a hundred years since a peptide was first assembled from amino acids by Fischer and Fourneau in 1906.<sup>239</sup> The key conception in peptide assembly is the coupling reaction between amino acids and the removal of  $N^{\alpha}$ -protecting groups.<sup>240</sup> In 1932, the first reversible  $N^{\alpha}$  -protecting group-carboxybenzyl (Cbz) was established by Bergmann and Zervas<sup>241</sup> and then was applied to peptide synthesis by Vigneaud *et al* in 1953<sup>242</sup> (Figure 2.3). Although the classical solution-phase method is still usable for large-scale or laboratory preparation, it is the use of solid-phase techniques that makes peptide synthesis more practical in current scientific research.<sup>243</sup>

Figure 2.3 Structure of carboxybenzyl group.

### 2.3.2 Introduction of solid-phase peptide synthesis (SPPS)

The concept of SPPS is to elongate the peptide chain that is attached to polymeric support such as resin by a repetitive acylation reaction.<sup>240</sup> Although excess reagents will be used in the reaction, their removal can be achieved easily through washing and filtration steps. After the linear peptide sequence is obtained, different reagents or conditions can be used to cleave the crude peptide product from the resin.<sup>243,244</sup>

Peptides can be assembled by amino acids (typically 2 to 50) and the amino acids are usually combined through the amide coupling reaction. Following the carboxybenzyl group (Cbz), another protecting group t-butyloxycarbonyl (Boc) (Figure 2.4) was introduced for the peptide synthesis reaction. In the Cbz methodology, strong acids like anhydrous hydrofluoric acid (HF) or trifluoromethanesulfonic acid (TFMS) are required to cleave the protecting groups. In contrast, the removal of the  $N^{\alpha}$ -Boc group can be achieved by trifluoroacetic acid (TFA) in DCM (25-50%). However, the above methods have several disadvantages. For example, with strong acids, there are established side reactions and limitations to the use of some acidabile amino acids, such as tryptophan. Thus, an alternative  $N^{\alpha}$ -protecting group was introduced: 9-fluorenylmethyloxycarbonyl (Fmoc) (Figure 2.4).



**Figure 2.4** Structures of *t*-butyloxycarbonyl group (Boc) and 9-fluorenylmethoxycarbonyl group (Fmoc).

#### 2.3.3 Introduction of Fmoc-SPPS

The 9-fluorenylmethoxycarbonyl (Fmoc) was first introduced for peptide synthesis in 1972. In contrast to acid-labile Boc/benzyl (Bzl) methodology, the Fmoc-based strategy relies on an orthogonal scheme which utilizes base to remove the  $N^{\alpha}$ -protecting group. Fmoc-deprotection is usually accomplished with 20% piperidine in dimethylformamide (DMF). The Fmoc cleavage mechanism is an E1cB elimination reaction (Scheme 2.4). The electron-withdrawing fluorene ring system makes the hydrogen on the  $\beta$ -carbon highly acidic, which is readily removed/abstracted by a weak or mild base. Subsequently, migration of the anionic charge triggers the release of CO<sub>2</sub> and dibenzofulvene (DBF). Finally, the base, typically an amine used for Fmoc cleavage 'neutralizes' the reactive dibenzofulvene (DBF). An important stage in Fmoc cleavage is dibenzofulvene (DBF) scavenging. DBF is a highly reactive molecule which can cause the peptide alkylation side reaction(s). Consequently, the base used for deprotection should be present in excess to scavenge the reactive DBF.

In Fmoc SPPS, removal of the side-chain protecting groups and release/cleavage of the peptide chain from resin is always mediated by an acidic reagent. Scavengers such as water and triisopropylsilane (TIPS) are added during the final cleavage step to prevent side-chain deprotection due to the release of reactive cationic species.<sup>253</sup>

Due to the employment of the Fmoc protecting group, some problems in peptide synthesis have been solved. For instance, tryptophan (Trp) is challenging to use and is readily modified when using Boc-based peptide synthesis strategy because of the reactivity of the indole ring.<sup>254</sup> In Boc-based SPPS chemistry, tryptophan is usually protected with a formyl group on the indole nitrogen.<sup>255</sup> The formyl group can be removed with the use of hydrogen fluoride (HF). However, this step must be prior to other cleavage reagents. In Fmoc chemistry, the tryptophan side chain is usually protected with a Boc group and can be easily removed with TFA, which is also the reagent used for the cleavage of the resin.<sup>256</sup> In this context, using Boc/Bzl-based chemistry, the yield of a pentadecapeptide gramicidin A is poor (5% to 24%) due to the presence of four tryptophan residues, but improvement was observed (up to 87% in some cases) after the introduction of Fmoc-SPPS.<sup>257</sup> Indolicidin, another peptide that contains multiple tryptophan residues, is also successfully synthesized in high yield by Fmoc-SPPS. 258,259 Following the general method of SPPS, the required linear peptide sequence in the preparation of lugdunin could be synthesized. Thus, it is important to consider the most appropriate solid support (resin) for the preparation of linear peptide and the coupling reagent(s) for peptide cyclization.

Scheme 2.4 Mechanism of Fmoc-deprotection reaction in peptide synthesis. Fmoc group removal in

solid phase peptide synthesis (SPPS) proceeds through a two-step mechanism: the removal of the acidic proton at the 9-position of the fluorenyl ring system by piperidine, and the subsequent  $\beta$ -elimination gives the deprotection product and a highly reactive dibenzofulvene (DBF) intermediate which is immediately trapped by the piperidine to form stable adducts.

#### 2.3.4 Solid supports (resin) for Fmoc-SPPS

For the solid supports (resin) in the SPPS reaction, several characteristics are required. First, it should be stable and allow the successful attachment of the first amino acid. Second, it must allow rapid filtration of reagents and will not generate any side reactions with solvents or reagents. <sup>259</sup> Initially, different kinds of resins were evaluated for the synthesis of lugdunin and its analogues, including 2-chlorotrityl chloride resin, Weinreb AM resin and modified TG resin (derived from Rink amide AM resin) (Figure 2.5). For example, following peptide assembly, the peptidyl moiety tethered to 2-chlorotrityl chloride resin can be cleaved under extremely mild acid conditions that leave Boc/tBu based protecting groups in place and give a peptide acid (COOH). <sup>260</sup> Thus, it is used to prepare protected peptide fragments. Amino acids can be attached to 2-Cl-Trt chloride resin with very little or no racemization. The steric bulk of 2-chlorotrityl chloride resin inhibits diketopiperazine formation, which can be a major side reaction in the synthesis of peptides with *C*-terminal proline. <sup>261</sup> In contrast to the 2-Cl-Trt chloride resin, the product of the Weinreb AM resin and the Rink amide AM resin will finally give a peptide aldehyde and a peptide amide respectively (CONH<sub>2</sub>).

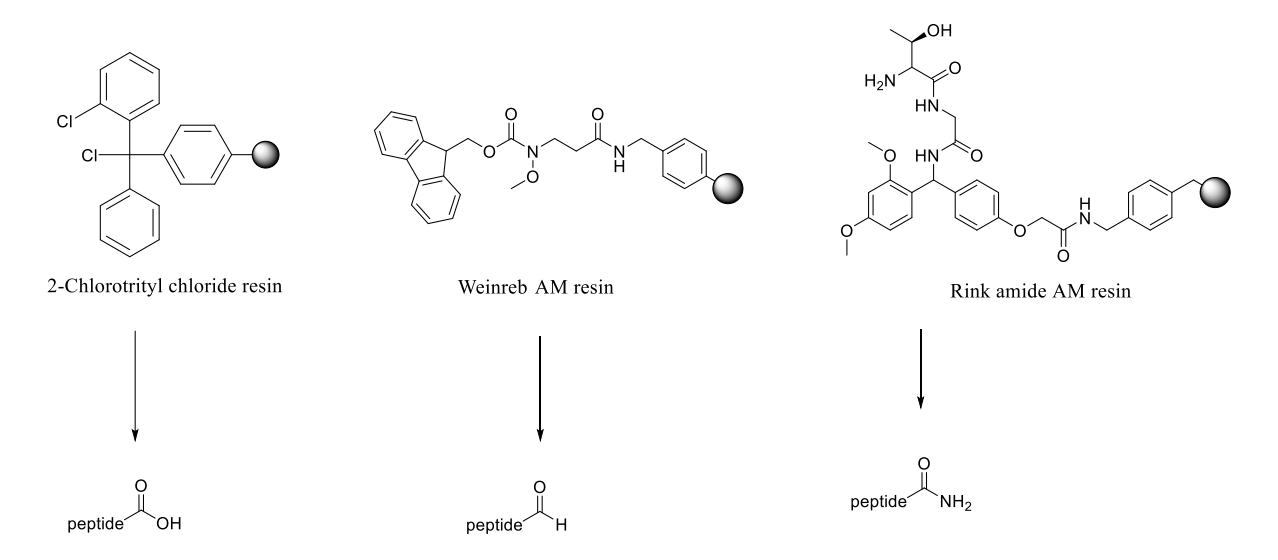


**Figure 2.5** Structures of 2-Chlorotrityl chloride resin, Weinreb AM resin and TG resin and their peptide products after cleavage from the resins.

## 2.3.5 Introduction of peptide macrocyclization

Lugdunin and its analogues all possess a macrocyclic scaffold. As discussed previously, cyclic peptides are known as an important source of therapeutic agents and hence the development of various cyclization strategies were considerd.

Generally, the most common methods to cyclize a linear peptide are macrolactonization (via ester bond formation), macrolactamization (via amide bond formation), and disulfide bridge formation (Figure 2.6). <sup>262,264</sup> With the advantage that the amine group is a better nucleophile, macrolactamization is the more frequently used method. <sup>265</sup> In the macrocyclization reaction, a highly diluted condition is always used to avoid unwanted intermolecular reactions such as oligomerization and polymerization. <sup>262</sup> Besides that, the linear peptide can be cyclized before the cleavage from the resin (on resin) or after (in solution). Alternatively, the cleavage and the cyclization reaction can also be combined in one step which is known as cyclative cleavage. Cyclative cleavage is a very effective methodology for the synthesis of amide-containing heterocycles in the solid phase. <sup>266</sup>

An important factor for successful macrocyclization is the ring size. Cyclization of several naturally occurring tetrapeptides and pentapeptides have been attempted, and the results were largely negative.<sup>267</sup> In fact, it was found that cyclization of smaller peptides that contain less than seven amino acids is thought to be difficult and troublesome.<sup>262</sup> Apart from that, the composition of the linear peptide sequence is also regarded as a significant reason. Due to the tendency to adopt an extended conformation, peptides with amino acids in only one configuration such as all L- or all D-residues are more difficult to cyclize.<sup>262, 268</sup>

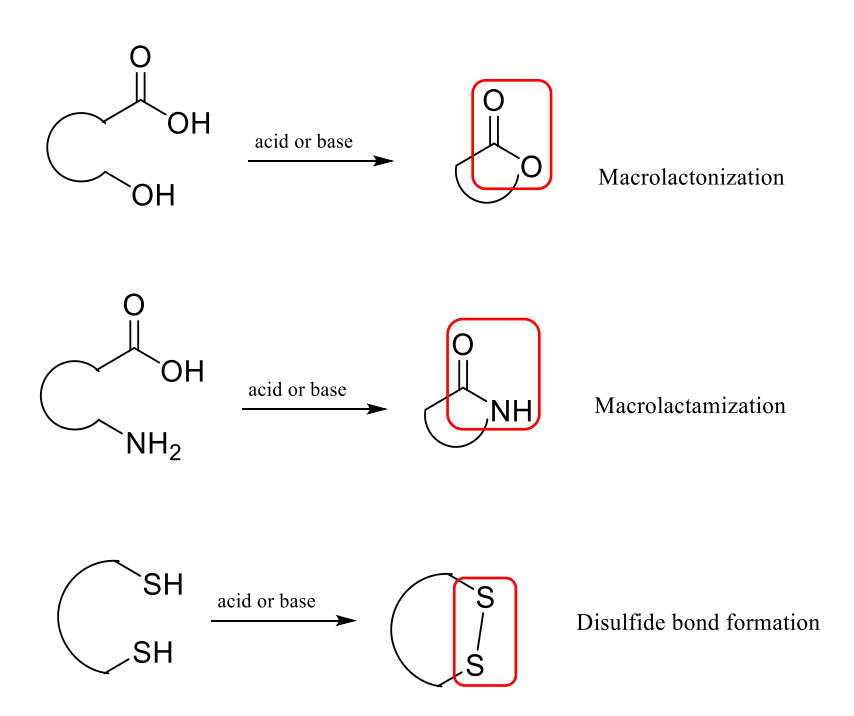


**Figure 2.6** Common cyclization strategies. The cyclic peptides are usually formed by macrolactonization, macrolactamization and disulfide bond linkage.

# 2.3.6 Peptide coupling reagents

The coupling step is an important feature to ensure high yields in Fmoc-SPPS.<sup>269</sup> Therefore, optimized amide bond formation conditions are important and necessary.<sup>269</sup> This involves activation of the carboxyl group of an amino acid, which plays a vital role in increasing the reaction efficiency. It is often activated to a more reactive 'active ester'.<sup>269</sup> In this context,

several peptide coupling reagents have been developed and can be generally divided into three categories: the carbodiimides, aminium/uronium salts and phosphonium salts.

#### 2.3.6.1 Carbodiimides

The carbodiimides, including dicyclohexylcarbodiimide (DCC), diisopropylcarbodiimide (DIC) and 1-ethyl-3-(3-dimethylaminopropyl) carbodiimide (EDC) have been used as activators in peptide synthesis (Table 2.1). <sup>270</sup> They are also commonly used for the preparation of carboxylic acid derivatives such as esters. These reagents are also useful in the chemical reaction for the synthesis of nitriles from primary amides. <sup>271</sup> Moreover, DCC is advantageous in solution phase reactions since its byproduct, dicyclohexylurea, is almost insoluble in most organic solvents and will therefore precipitate from the reaction mixture. <sup>272</sup> However, it is not appropriate for reactions on resin. Thus, DIC is alternatively used in solid phase synthesis due to the better solubility of its urea byproduct. <sup>273</sup> EDC is more often utilized in certain reactions, such as modifying proteins. The byproduct formed from EDC and excess coupling reagent can be easily removed by aqueous extraction since both of them are water soluble. <sup>274</sup> However, there are disadvantages to their use such as the problem of racemization. To overcome this problem, benzotriazole-based additives such as 1-hydroxy-7-aza-benzotriazole (HOAt) and 1-hydroxy-benzotriazole (HOBt) are often added into the reaction (Figure 2.7). Scheme 2.5 shows the mechanism of DIC-mediated carboxylic acid activation with the addition of HOBt.

Figure 2.7 Structures of HOAt and HOBt.

**Table 2.1.** Carbodiimide coupling reagents.

Carbodiimides <sup>275-280</sup>				
DCC	DIC	EDC		
N=C=N	\textstyle	N=C=N\N		
Lower racemization or epimerization when combined with HOAt or HOBt.	Lower racemization or epimerization when combined with HOAt or HOBt.	<ol> <li>Water-soluble reagent.</li> <li>Water-soluble byproduct.</li> <li>Suitable for the conjugation of small molecules or peptides to</li> </ol>		
2. Due to its insoluble by- product (DCU), it is more favorable in solution reaction.	<ul><li>2. It is more useful in SPPS because the urea byproduct has better solubility in most organic solvents.</li><li>3. Ideal for base free condition</li></ul>	proteins.		

#### 2.3.6.2 Aminium/uronium salts

Examples of aminium/uronium reagents include 1-[bis(dimethylamino)methylene]-1*H*-1,2,3-triazolo[4,5-*b*] pyridinium 3-oxide hexafluorophosphate (HATU) and 3-[bis(dimethylamino)methyliumyl]-3*H*-benzotriazol-1-oxide hexafluorophosphate (HBTU) (Table 2.2). They are derived from HOAt and HOBt respectively, so they similarly form a benzotriazole-based active ester.<sup>281-282</sup> However, aminium/uronium reagents are capable of reacting with the peptide *N*-terminus to yield an inactive guanidino byproduct which terminates peptide elongation.<sup>283</sup>

The 1-[1-(cyano-2-ethoxy-2-oxoethylideneaminooxy)-dimethylamino-morpholino]-uronium hexafluorophosphate (COMU) (Table 2.2) is known as a coupling reagent with better efficiencies and higher safety compared to HATU and HBTU.<sup>284</sup>

**Table 2.2** Aminium/Uronium salts coupling reagents.

	Aminium/Uronium <sup>285-290</sup>				
	HATU	HBTU	COMU		
	$ \begin{array}{c} \bigcirc \\ PF_{6} \\ -N \\ \nearrow \\ N \\ \nearrow \\ N \end{array} $	© PF <sub>6</sub> N, N, ⊕ N, N, ⊕ O O	O O O O O O O O O O O O O O O O O O O		
1. 2.	Highly efficient coupling reagent for solid- and solution-phase reactions Faster coupling rates than	1. Widely applied in both solid- phase reactions and in solution because of water- soluble byproduct.	<ol> <li>Safer and better solubility than HBTU and HATU</li> <li>Especially suitable for microwave accelerated SPPS.</li> </ol>		
	HBTU.	2. Possibility of allergic reactions.	3. It is better to use for ester formation.		

#### 2.3.6.3 Phosphonium salts

The phosphonium reagents, including 7-azabenzotriazol-1-yloxy) trispyrrolidinophosphonium hexafluorophosphate (PyAOP) and benzotriazol-1-yloxy)-trispyrrolidinophosphonium hexafluorophosphate (PyBOP), have the similar function to aminium/uranium salts, but these reagents will not cause the side reaction of guanidinylation (Table 2.3). 286, 291,292

Due to the potential explosive properties of HOAt and HOBt, making them hazardous for use, [ethylcyano(hydroxyimino)acetato- $O^2$ ] tri-1-pyrrolidinylphosphoniumhexafluorphosphate (PyOxim) is used alternatively to improve safety (Table 2.3). The use of PyOxim is limited due to its side product tris-pyrrolidinophosphoramide (Figure 2.8), which leads to difficulty of separation in solution phase peptide synthesis.  $^{294,295}$ 

$$\begin{bmatrix}
N \\
N \\
P = 0
\end{bmatrix}$$

Figure 2.8 Structure of tris-pyrrolidinophosphoramide.

Table 2.3 Phosphonium salts coupling reagents.

Phosphonium <sup>292,293,296,297</sup>				
PyAOP	РуВОР	PyOxim		
N N N N N N N N N N N N N N N N N N N	N N N N N PF <sub>6</sub>	$ \begin{array}{c c}  & N \\  & N \\$		
HOAt-analogue to PyBOP.     Fast coupling rates than PyBOP.	<ol> <li>Safer to use.</li> <li>Fast coupling rates</li> </ol>	<ol> <li>Safety is improved because of the different core structure.</li> <li>Good choice for SPPS, but removal of by-product remains a problem.</li> </ol>		

## 2.4 Synthesis of thiazolidine dipeptide

# 2.4.1 Synthesis of amino aldehyde

As mentioned earlier in section 2.1 for the total synthesis of lugdunin, one approach is to use the pre-assembled thiazolidine dipeptide, which could be formed through the condensation of L-Cys-OH with an appropriate amino aldehyde. Hence, the preparation of the suitable amino aldehyde was first considered. To prepare the aldehyde compounds from a carboxylic acid, two distinct routes were typically followed (Scheme 2.5). In the first route, the *N*-protected amino

acid is reduced to the corresponding amino alcohol and then the desired *N*-protected amino aldehyde is obtained via oxidation. In the second route, the amino acid is initially converted into an activated carboxylic acid derivative, such as activated ester or amide and then reduced to the corresponding aldehyde.

**Scheme 2.5** Two distinct routes for the synthesis of *N*-protected amino aldehydes. PG can be Boc/Fmoc/Cbz. R group was varied when different amino acids were used. Group X was varied when different reagents were used, such as an imidazole if CDI was used.

The reduction-oxidation route was first attempted, and Fmoc-L-Ala-OH (2.9) was used (Scheme 2.6). In this step, sodium borohydride (NaBH<sub>4</sub>) was used as a reducing reagent since it is safer compared to lithium tetrahydridoaluminate. However, NaBH<sub>4</sub> is not reactive enough to reduce carboxylic acids. Thus, 2.9 was first converted to succinimide ester by reacting an EDC-activated intermediate with *N*-hydroxysuccinimide (NHS) to form an activated carboxylic acid derivative 2.10, and NaBH<sub>4</sub> was used subsequently to reduce 2.10 to the corresponding amino alcohol 2.11. Then, the oxidation reaction to the desired amino aldehyde 2.12 was achieved by the use of Dess-Martin periodinane (DMP) as oxidant. DMP is a hypervalent iodine compound which offers selective and very mild oxidation of alcohols to aldehydes or ketone.<sup>298</sup> The oxidation is usually performed in dichloromethane or chloroform at room temperature and is usually complete within 0.5-2 hours. DMP was chosen as the oxidant because of its advantages over chromium- and DMSO-based oxidants that include milder conditions, rapid reaction, better yields, simplified workups, and good chemoselectivity.

Products are easily separated from the iodo-compound by-product after basic work-up. Herein, Fmoc-L-Ala-OH was used in the trial reaction and due to the poor solubility of the intermediate compound **2.11**, a mixture solvent of DCM and DMSO was used as solvent. The total yield by this method was about 70%.

In contrast, Saur *et al.* reported the method for preparing Fmoc-L-Val-H by using CDI, NaBH<sub>4</sub> and Dess-Martin periodinane.<sup>235</sup> Their overall yields of the Fmoc-L-Val aldehyde were typically 90%, which is more efficient than our results. The most different step was found to be the use of Dess-Martin perodinane (71% yield and 90% yield respectively). It is thought that the operation of this step might be a key point and should be further improved.

<sup>a</sup>Reagents and conditions: (a) *N*-hydroxysuccinimide, 1-ethyl-3-(3-dimethylaminopropyl)carbodiimide hydrochloride, dry dichloromethane, rt, 3 h. (b) NaBH<sub>4</sub>,  $-10^{\circ}$ C, 1 h, then H<sub>2</sub>O, rt, 30 mins. (c) Dess-Martin perodinane, rt, 3 h

**Scheme 2.6** Method A: synthesis of amino aldehyde by reduction-oxidation.

In the second approach, the reduction of carboxylic acid to aldehyde can be achieved via the formation of carboxylic acid derivatives such as activated esters or amides. It is often a challenge because stronger reducing agents, such as lithium aluminium hydride (LiAlH<sub>4</sub>) further reduce the formed aldehyde to an alcohol. Alternatively, diisobutylaluminium hydride (DIBAL-H) is often used as a reduction reagent in organic synthesis, including converting carboxylic acids to the corresponding aldehydes.

The use of N-methoxy-N-methylamides has rapidly become popular in organic synthesis since

it was first reported by Nahm and Weinreb.<sup>299</sup> This functional group had advantages such as the ease of preparation, the lack of side reactions during nucleophilic addition, and the selective reduction, e.g., with DIBAL-H to aldehydes (Scheme 2.7). The aldehyde compound would not be formed until aqueous workup because of a stable intermediate, and therefore, over-reduction was prevented. Overall, the efficiency of this method was poor, with a yield of 48% when applied to the reaction with *N*-protected amino acid. Thus, a rapid and efficient one-pot synthetic protocol reported by Ivkovic *et al.* was adapted (Scheme 2.8)<sup>237</sup>.

<sup>a</sup>Reagents and conditions: (a) THF, NMM CDI, *N,O*-dimethylhydroxylamine hydrochloride, DCM, rt, 2-3 h. (b) DIBAL-H (1.0 M in toluene), dry DCM, -78 °C, 2 h

Scheme 2.7 Method B: synthesis of amino aldehyde by the forming of Weinreb amide.

2.11: 
$$R_1 = CH_3$$
,  $R_2 = Fmoc$   
2.14:  $R_1 = CH_3$ ,  $R_2 = Boc$   
2.16:  $R_1 = CH(CH_3)_2$ ,  $R_2 = Fmoc$   
2.17:  $R_1 = CH(CH_3)_2$ ,  $R_2 = Fmoc$   
2.18:  $R_1 = CH(CH_3)_2$ ,  $R_2 = Fmoc$   
2.19:  $R_1 = CH(CH_3)_2$ ,  $R_2 = Boc$   
2.19:  $R_1 = CH(CH_3)_2$ ,  $R_2 = Boc$ 

<sup>a</sup>Reagents and conditions: (a) Carbonyldiimidazole (CDI), dry DCM, 0°C, 1 h, then (b) DIBAL-H (1.0M in toluene), -78°C, 1.5 h

Scheme 2.8 Method C: synthesis of amino aldehyde by using CDI/DIBAL-H.

In this method, N-protected amino acids were converted to the N-protected  $\alpha$ -amino aldehydes by in

situ activation with 1,1'-carbonyldiimidazole (CDI) to form the activated amide and facilitates the diisobutylaluminium hydride (DIBAL-H) reduction reaction. Scheme 2.8 shows the activation by CDI. With the advantages of the convenient one-step reaction, simple extractive workup and short overall reaction time (commonly less than 4 hours), compound 2.12 was obtained in a high yield of 85% and confirming the good efficiency of the method. Following this evaluation, the method was successfully applied to prepare *N*-protected amino aldehyde compounds 2.4, 2.12, 2.16 and 2.17, and the yields were between 75% to 85%. The purified aldehyde compounds 2.4, 2.12, 2.16 and 2.17 were then used into the next step for the preparation of dipeptide. Moreover, an optical rotation study was carried out to determine if there are any differences between the three methods.

#### 2.4.2 Optical rotation study

To check the stereo-integrity of the synthesized compounds, optical rotation was measured. Optical rotation, also known as polarization rotation or circular birefringence, is the rotation of the orientation of the plane of polarization about the optical axis of linearly polarized light as it travels through certain materials.<sup>300</sup> For a pure substance in solution, if the wavelength and path length are fixed and the specific rotation is known, the observed rotation can be used to calculate the concentration.<sup>301</sup>

Due to the different reported values, an optical rotation study of compounds **2.4**, **2.12**, **2.16** and **2.17** and in either DCM or MeOH was investigated (Table 2.4) and a comparison with all reported values was considered. In the first instance, tested compounds were all synthesized by the same method which was via CDI/DIBAL-H. From Table 2.4, it was found that the same amino aldehyde with different protecting groups was quite similar in the solvent DCM, but

slightly different in MeOH. The value was always observed positive in DCM but negative in MeOH which indicated that the value is influenced by the solvents.

Then, compound **2.12** prepared by different synthetic methods was used to evaluate the effect of synthetic method on optical purity (Table 2.5). From Table 2.5, it was found that though the optical rotation of compound **2.12** was almost the same when obtained by different synthetic methods, the yield was the highest in the method via CDI/DIBAL-H. As a conclusion, the observed specific rotation angles and optical rotatory dispersion (ORD) spectra are strongly influenced by solvent-solute interactions.<sup>302</sup> The opposite measuring value of the same compound was observed when different solvents were used. Still, it was observed that the same compound **2.12** prepared by different methods (methods A to C) showed no significant difference. Hence, CDI/DIBAL-H approach (method C) was used in the preparation of all other *N*-protected amino aldehydes, which were subsequently used for synthesis of lugdunin analogues.

Table 2.4: optical rotation of compounds 2.4, 2.12, 2.16 and 2.17 in different solvents.

	Optical rotation [α] <sub>D</sub> <sup>23.4</sup> , DCM	Optical rotation [α] <sub>D</sub> <sup>23.4</sup> , MeOH	Value reported
Fmoc-L-Ala-H (2.12)	+30.9 ( $c = 0.69$ )	-8.5 ( $c = 0.5$ )	$[\alpha]_D^{20} = +43.4 \ (c = 1.00 \text{ in CHCl}_3)^{303}$ $[\alpha]_D^{20} = +13.0 \ (c = 1.00 \text{ in CHCl}_3)^{304}$
Boc-L-Ala-H (2.16)	+29.4 ( $c = 0.58$ )	-30.5 ( $c = 0.98$ )	$[\alpha]_{D}^{23} = +14.2 \ (c = 1.07 \text{ in DCM})^{305}$ $[\alpha]_{D}^{20} = +33.9 \ (c = 1.00 \text{ in DCM})^{306}$ $[\alpha]_{D}^{20} = -25.5 \ (c = 1.00 \text{ in MeOH})^{307}$ $[\alpha]_{D}^{18} = -33.3 \ (c = 1.01 \text{ in MeOH})^{308}$ $[\alpha]_{D}^{25} = +23.4 \ (c = 2.30 \text{ in CHCl}_{3})^{309}$
Fmoc-L-Val-H (2.4)	+61.8 ( $c = 0.58$ )	+22.1 ( $c = 0.58$ )	$[\alpha]_D^{20} = -10.9 \ (c = 0.22 \text{ in MeOH})^{310}$ $[\alpha]_D^{20} = +16.6 \ (c = 1.00 \text{ in MeOH})^{311}$
Boc-L-Val-H (2.17)	+77.8 ( $c = 0.76$ )	-12.4 ( $c = 0.76$ )	$[\alpha]_D^{23} = +78.6 \ (c = 1.07 \text{ in DCM})^{238}$ $[\alpha]_D^{20} = -11.6 \ (c = 1.00 \text{ in MeOH})^{312}$ $[\alpha]_D^{23} = +80.4 \ (c = 1.00 \text{ in DCM})^{306}$ $[\alpha]_D^{23} = -19.0 \ (c = 1.00 \text{ in MeOH})^{313}$

Compounds were all prepared by the method of using CDI/DIBAL-H.

**Table 2.5:** yield and optical rotation of compound **2.12** by different methods.

	Yields (%)	Optical rotation [α] <sub>D</sub> <sup>23.4</sup> , DCM	Optical rotation [α] <sub>D</sub> <sup>23.4</sup> , MeOH
Method A	70	+23.6 (c=0.7)	-7.4 (c = 0.7)
Method B	48	+25.2 (c = 0.7)	-5.9 (c = 0.7)
Method C	85	+30.9 (c = 0.69)	-8.5 (c = 0.5)

A: synthesis by oxidation from alcohol

B: synthesis by reduction from Weinreb amide

C: synthesis by CDI/DIBAL-H

# 2.4.3 Synthesis of thiazolidine dipeptide

As mentioned in the previous section, the thiazolidine ring can be formed by the condensation of an amino aldehyde and L-cysteine (2.18) (Scheme 2.9). Hence, *N*-protected amino aldehyde compounds 2.4, 2.12, 2.16 and 2.17 were reacted with L-cysteine in a mixture of methanol and

water and stirred for 18 hours to afford their corresponding thiazolidine dipeptide compounds **2.5** and **2.19-2.21** (Scheme 2.9).

However, in our hands, compounds **2.5**, **2.20** and **2.21** were found to have extremely poor solubility in most of the common solvents, including dichloromethane, chloroform, methanol, water, DMF or even a mixture with DMSO. Only compound **2.19** was found to be slightly dissolved in DMF. Therefore, compounds **2.5**, **2.20** and **2.21** being insoluble in a wide range of solvents were considered unsuitable for application in SPPS. Compound **2.19** was able to be applied to the next step to prepare (L-Ala)<sup>7</sup>-lugdunin (**1.25**) as one of the lugdunin analogues by the use of 2-chlorotrityl chloride resin in Chapter 3. Moreover, alternative methods to synthesize lugdunin were evaluated, which do not require the use of pre-assembled thiazolidine building blocks.

Scheme 2.9 Condensation of amino aldehyde and L-Cys-OH (2.18) to form the desired thiazolidine.

#### 2.5 Synthesis of lugdunin

#### 2.5.1 Synthesis of lugdunin by Weinreb AM resin

<sup>a</sup>Reagents and conditions: (a) MeOH/H<sub>2</sub>O, RT, 18 h

Since the poor solubility of thiazolidine dipeptide compounds make it difficult for them to be used as a building block in the method by 2-Cl-Trt chloride resin, another strategy was

evaluated. Thus, L-Val-OH and L-Cys-OH were designed to be the head and tail, respectively, of the linear peptide sequence (Figure 2.9). Importantly, when the peptide is cleaved from the resin, the carboxylic acid group will be converted to an aldehyde group. As a result, the thiazolidine ring will be formed spontaneously via the condensation of the head and tail moieties (Figure 2.9). The synthetic approach is like that reported by Schilling *et al.* in 2019.<sup>213</sup> Thus, Weinreb AM resin was firstly evaluated (Figure 2.13).

**Figure 2.9** Structure of linear peptide sequence of lugdunin and the linear lugdunin with the *C*-terminal aldehyde.

Weinreb AM resin can be used for the peptide sequence directly without a pre-loading step. Likewise, L-Val-OH and L-Cys-OH were designed as the head and tail in the sequence and all the amino acids (L-Val-OH, D-Val-OH, L-Val-OH, D-Leu-OH, L-Trp-OH, D-Val-OH, L-Cys(Trt)-OH) were attached stepwise and all double coupled. Following the general Fmoc-SPPS protocol, the desired linear peptide sequence **2.24** was obtained.

After the sequence was completed, DIBAL-H (1.0 M in THF) was used to cleave the peptide from the resin and compound 2.25 was afforded as a linear peptide with the side-chain protected L-cysteine as the *N*-terminus and L-valine amino aldehyde as *C*-terminus (Scheme 2.10). Here, three different conditions were tested to find the best solvent system for the cleavage reaction. These were DCM, THF and 1:1 mixture of DCM and THF; anhydrous solvents were used in all cases. The results showed no differences between these three conditions. Thus, for the convenience of work up, the co-solvent containing anhydrous DCM-THF (1:1) was chosen. Then, the desired lugdunin (1.24) was obtained after treatment with TFA – it was anticipated that thiazolidine formation. i.e., head-to-tail cyclisation, would occur under acid conditions. The TFA mixture, TFA-TIPS-H<sub>2</sub>O (90:5:5) was used to cleave the protecting groups and the subsequently cyclized crude peptide product 1.24 was obtained. The scale was based on 0.1 mmol of Weinreb AM resin. Only 0.22 mg of the crude product 1.24 was obtained (overall yield less than 1%) as pure compound after purification by RP-HPLC. Due to the low yield of this method, an alternative method to improve the yield was evaluated.

Scheme 2.10 Protocol to prepare lugdunin (1.24) by using Weinreb AM resin.

# 2.5.2 Synthesis of lugdunin by Thr-Gly functionalized Rink TG resin

Threonyl-glycyl functionalized Rink amide resin (TG resin) was recently exploited for the total synthesis of lugdunin.<sup>235</sup> The TG resin, first reported by Ede and Bray, relies on a reversible oxazolidine formation between an aldehyde building block and the threonine 1,2-amino alcohol motif.<sup>314</sup> The oxazolidine tether is stable to the reaction conditions employed in standard Fmoc-SPPS but is readily hydrolyzed upon treatment with aqueous acid to afford a *C*-terminal peptide aldehyde. Herein, a method following the approach reported by Malins *et al.* in 2017 was adopted.<sup>236</sup>

Thus, Fmoc-Gly-OH and Fmoc-Thr-OH were used for derivatisation of the Rink amide AM resin to form the TG resin 2.28 (Scheme 2.11). Subsequently, a loaded resin 2.29 with an oxazolidine ring was obtained after the condensation of the amino aldehyde, Fmoc-L-Val-H with the TG resin. Next, Boc<sub>2</sub>O was utilized to protect the NH group in the oxazolidine ring to afford the product 2.30, and then used to assemble the peptide sequence following general Fmoc-SPPS protocol.

**Scheme 2.11** Chemical preparation of modified TG resin. The rink amide AM resin (2.26) is commercial available. 2.26 was first attached by glycine and threonine. Then, the thiazolidine ring was formed after the reaction with Fmoc-L-valine aldehyde. The final product 2.30 was then obtained after the protection reaction by Boc.<sup>236</sup>

Although the resin **2.30** is commercially available, it is prepared manually due to the higher loading capacity (0.21 g/mmol in the commercial resin, but 0.36 g/mmol in the in-house prepared) and lower cost. As indicated earlier, the linear sequence was assembled by following

the general Fmoc SPPS protocol (Scheme 2.12). As the adjacent valine residues in the sequence may sterically impede coupling efficiency, all the amino acids were double coupled at room temperature for 24 h. The mixture TFA-TIPS-H<sub>2</sub>O (90:5:5) was used to cleave the resin, trityl protecting group on the L-cysteine and the Boc protecting group on the oxazolidine ring. The linear peptide with L-Val-H as the *C*-terminal was obtained, which should participate in the condensation reaction of the head (amino acid aldehyde) and the tail (L-cysteine) to form the thiazolidine ring, and to afford the desired lugdunin (1.24) as a crude product. The crude lugdunin (1.24) was then purified by RP-HPLC.

In this method, crude product **1.24** was obtained of 30 mg under 0.1 mmol scale, and the 1.5 mg (1.9 % overall yield) was recovered as pure compound following purification by RP-HPLC. Due to the better yield and more convenient to operate, all lugdunin analogues were synthesized using this method.

Scheme 2.12 Protocol to prepare lugdunin by using modified TG resin.

#### 2.5.3 Purification by RP-HPLC

Herein, RP-HPLC was used to purify the crude compound **1.24**. Several peaks were found by semi-preparative column under the condition: 45 to 61% B over 17 min, at 4 mL/min (Figure 2.10). When checked by LC/MS/MS, the peak at a retention time of 14.9 min was considered to be the desired compound **1.24**. High-resolution mass spectrometry (HRMS) also showed the expected molecular ion (Figure 2.11). The overall yield of **1.24** was 1.9 % based on the original Rink amide AM resin (0.1 mmole was used, with its loading capacity as 0.66 mmol/g).

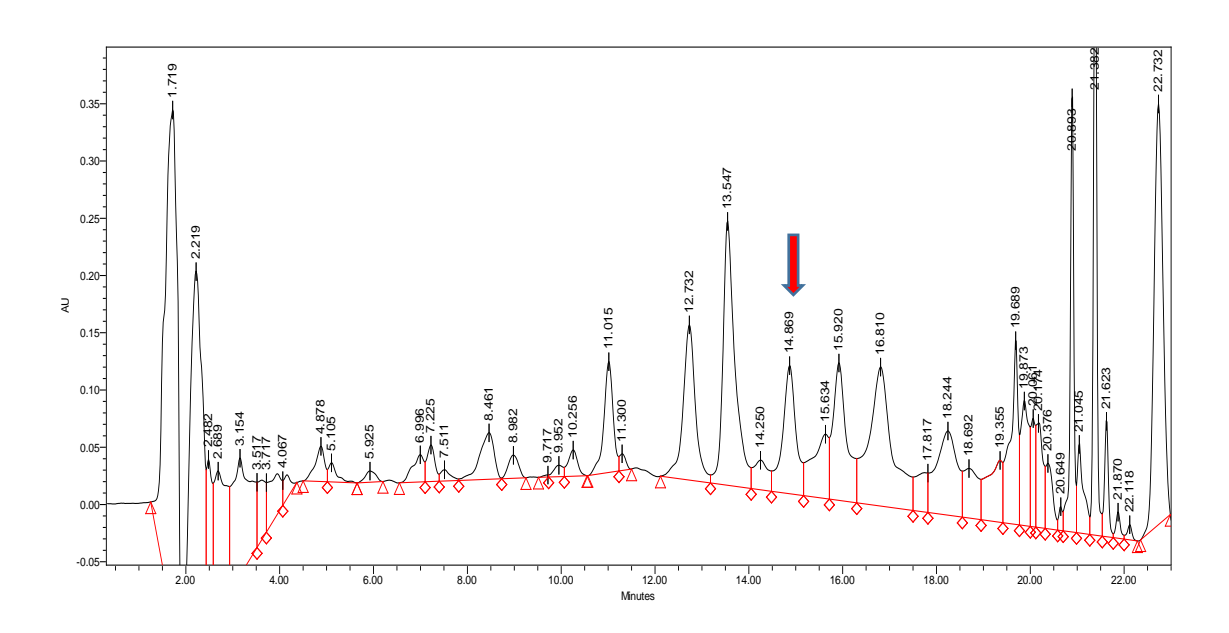


Figure 2.10 RP-HPLC trace of compound 1.24.

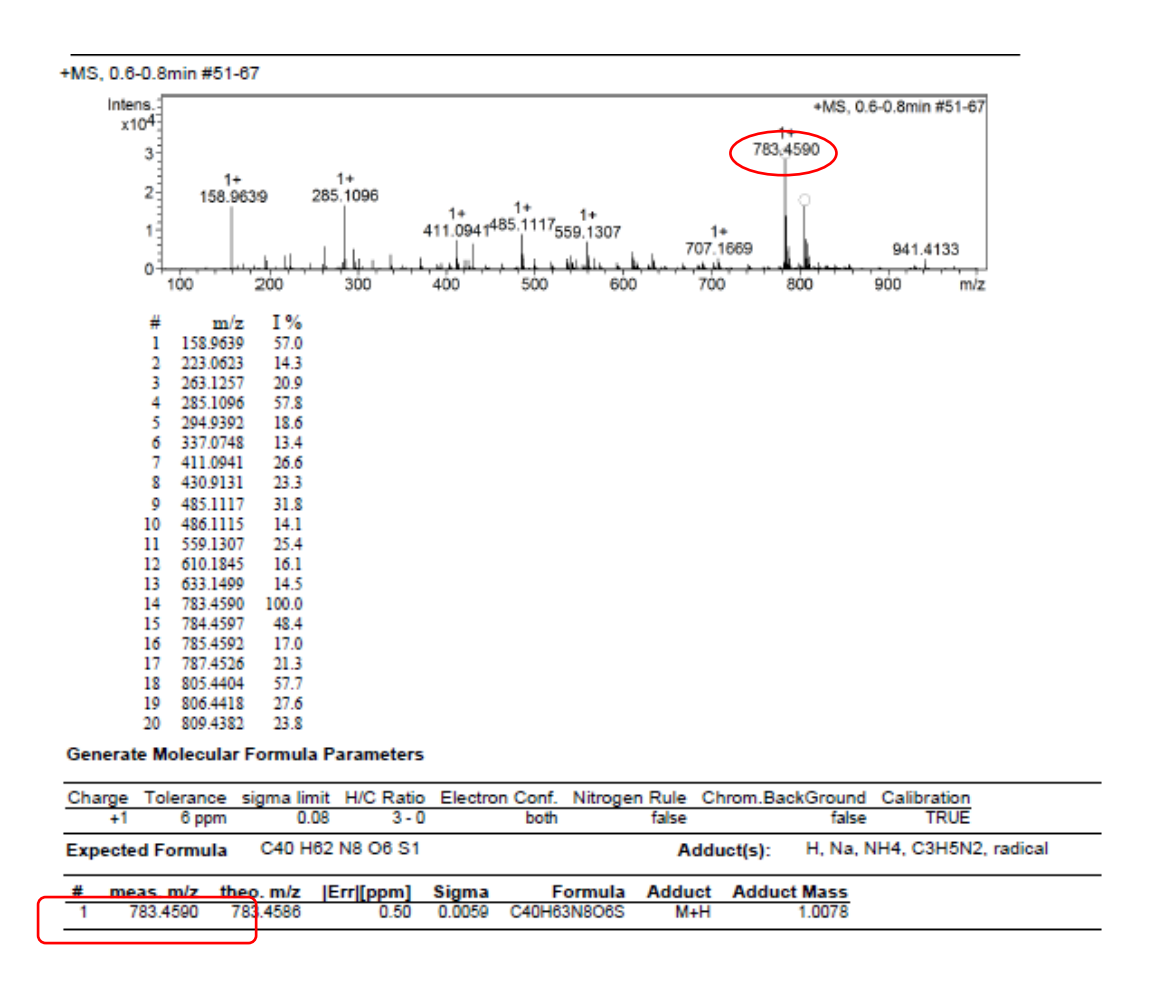


Figure 2.11 HRMS result of the sample with retention time of 14.9 min.

#### 2.6 Conclusions

In summary, this Chapter outlined an overview of the synthetic strategies toward the preparation of lugdunin (1.24). As discussed in section 2.2, the key part of the synthesis was the formation of thiazolidine. Thus, different methods including the preparation of thiazolidine dipeptide building block and the use of various resins were evaluated.

The first method was via the synthesis of the thiazolidine building block. The thiazolidine ring can be formed by the condensation reaction between an amino aldehyde and the L-cysteine. Thus, *N*-Fmoc-L-valine, *N*-Boc-L-valine, *N*-Fmoc-L-alanine and *N*-Boc-L-alanine were used and converted to corresponding amino aldehyde compounds **2.4**, **2.12**, **2.16** and **2.17** using CDI/DIBAL-H. Subsequently, the desired thiazolidine dipeptide compounds **2.5** and **2.19-2.21** were obtained through the condensation reaction. However, due to the poor solubility in a wide range of solvents, Fmoc-L-Thz(L-Ala) (**2.19**) was the only one that could be used for the next step. Thus, **2.19** will be introduced to prepare lugdunin analogue in Chapter 3.

An alternative method utilizing aldehyde-generated resin was then considered. Two resins were introduced in this Chapter, which were Weinreb AM resin and the TG resin. The *C*-terminal aldehyde was obtained by Weinreb AM resin when DIBAL-H was treated for the resin cleavage. Different from Weinreb AM resin, the *C*-terminal aldehyde was obtained when treated with TFA to cleave both the linear peptide from the Rink TG resin support and the oxazolidine ring. The method with the use of TG resin was then adopted for the synthesis of all lugdunin analogues due to its higher yield and simpler operation.

The optical rotation of synthesized Fmoc-amino aldehydes was then further measured to check their stereo-integrity and compared with the reported values. The results indicated that the optical rotation value will be strongly influenced by solvent-solute interactions. Moreover, it was found that the optical rotation value of the same Fmoc-amino aldehyde synthesized by different methods (methods A to C, which showed in section 2.3.1) showed no significant difference.

Due to the different reported values, an optical rotation study of compounds **2.4**, **2.12**, **2.16** and **2.17** and in either DCM or MeOH was investigated (Table 2.4) and a comparison with all reported values was considered. It was observed that the compound **2.12** prepared by different methods (methods A to C) showed no significant difference.

Subsequently, the desired linear peptide sequence of lugdunin was assembled following general Fmoc-SPPS protocols. For this method, the step to deprotect the Fmoc was accomplished with 20% piperidine in DMF. Then coupling reaction between each amino acid was accomplished via the the use of HATU and DIPEA. Different types of coupling reagents were also discussed in section 2.3.6. The method of Fmoc-SSPS was thus applied to all synthesized lugdunin analogues in this project.

# Chapter 3

# Synthesis and alanine-scanning of (Ala)<sup>7</sup>-lugdunin

## 3.1 Synthesis of (Ala)<sup>7</sup>-lugdunin

## 3.1.1 Synthesis of (Ala)<sup>7</sup>-lugdunin by using 2-Cl-Trt chloride resin

To investigate the effect of the 7-Val in lugdunin on the antimicrobial bioactivity, the first modification was to make the side-chain simpler. Thus, (Ala)<sup>7</sup>-lugdunin was synthesized. Whilst the work was ongoing, Schilling *et al.* in 2019 reported the synthesis and antimicrobial evaluation of (Ala)<sup>7</sup>-lugdunin, which was observed to be approximately 8-fold less potent than the native lugdunin against *S. aureus* USA300 LAC.<sup>213</sup>

As discussed in Chapter 2, the thiazolidine dipeptide Fmoc-L-Thz(L-Ala) (2.19), which was obtained by condensation of Fmoc-L-Ala-OH and L-Cys-OH, is fortuitously the only building block with acceptable and usable solubility. Hence, the method utilizing 2-Cl-Trt chloride resin was first attempted (Scheme 3.1). The desired peptide sequence was prepared following general Fmoc-SPPS protocol, in which the Fmoc-D-valine was the pre-loaded amino acid and Fmoc-L-Thz(L-Ala) (2.19) was the last coupled building block. The carboxyl-activating reagent, COMU was chosen since it is reported to display better efficiency, higher safety and comparable to HATU/HBTU. However, the assembly of the linear sequence was found to be incomplete, leading to a mixture of the linear five-mer 3.5 and seven-mer 3.4 after cleavage from the resin using 2% of TFA in DCM. Unexpectedly, though peptides under seven amino acids are thought to be difficult in undergoing intramolecular ring closing reactions, it was observed that both linear five-mer 3.5 and seven-mer 3.4 were cyclized to form cyclic peptides 3.6 and 1.25 respectively. When monitored by LC/MS, the molecular ions 754.42 and 596.37 were both observed, accounting for 1.25 and 3.6 respectively. Since both compounds 1.25 and

**3.6** showed nearly identical retention time, they were difficult to separate by RP-HPLC. Thus, an alternative method to prepare the peptide compounds by using TG resin which was had been described in Chapter 2 was applied.

<sup>a</sup>Reagents and conditions: (a) Coupling cycle: Fmoc-amino acid, HATU, DIPEA, DMF, RT, 4-6 hr; deprotection cycle: 20% piperidine in DMF, RT, 15 minutes. (b) 2% TFA:1% TIPS:97% DCM, RT, 30 minutes. (c)COMU, DIPEA, DCM/DMF, RT, 2 h

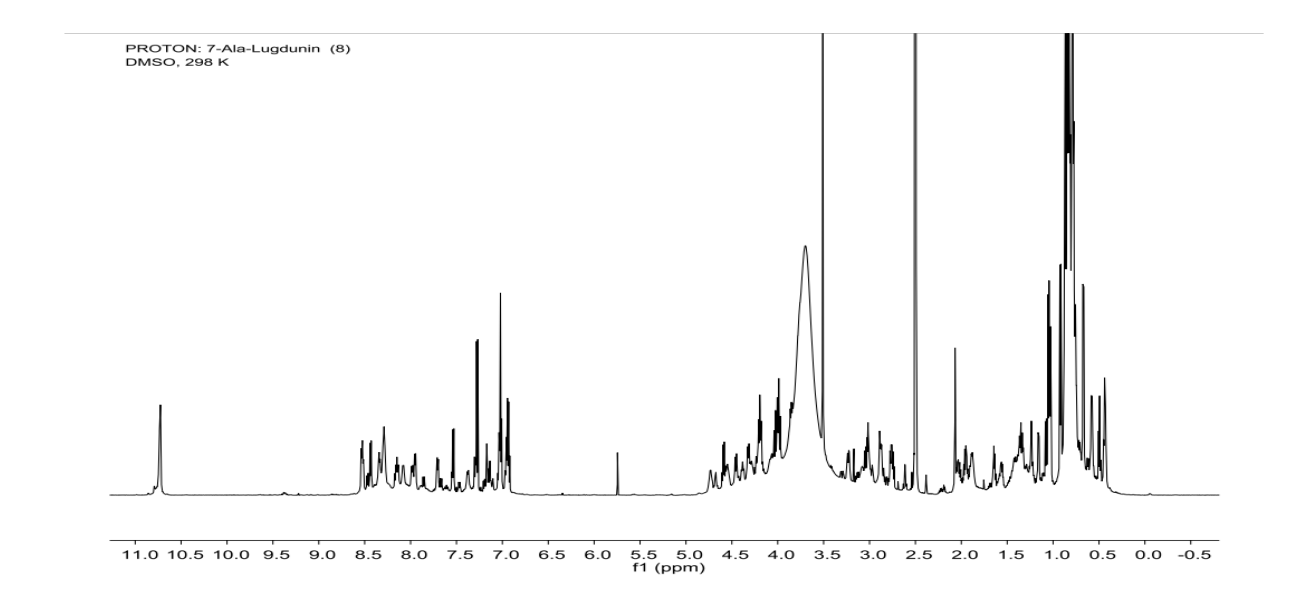
Scheme 3.1 Synthesis of (Ala<sup>7</sup>)-lugdunin 1.25 by using dipeptide and 2-chlorotrityl chloride resin.

#### 3.1.2 Synthesis of (Ala<sup>7</sup>)-lugdunin by TG resin

The preparation and utilization of the TG resin had been previously discussed, in section 2.5.5. Herein, to synthesize (Ala)<sup>7</sup>-lugdunin (1.25), a modified TG resin with the pre-loading of Fmoc-L-Ala-H was needed. The protocol to prepare the desired modified TG resin is outlined in Scheme 3.2. Then, the desired (Ala)<sup>7</sup>-lugdunin (1.25) was obtained by applying the general Fmoc-SPPS protocol.

Following purification by RP-HPLC, the overall yield of (Ala)<sup>7</sup>-lugdunin (1.25) was 3.7 %.

The unexpected low yield might due to the lower loading capacity (0.47 mmol/g) of the modified resin (modified TG resin pre-loaded with L-Ala which was prepared from rink amide AM resin (0.79 mmol/g). Still, the purification method by RP-HPLC might be another reason. The crude product was usually purified by semi-prep column and then further purified by analytical column to obtain an acceptable ratio (> 95 %). Hence, the loss of the product would increase after each injection into the RP-HPLC.



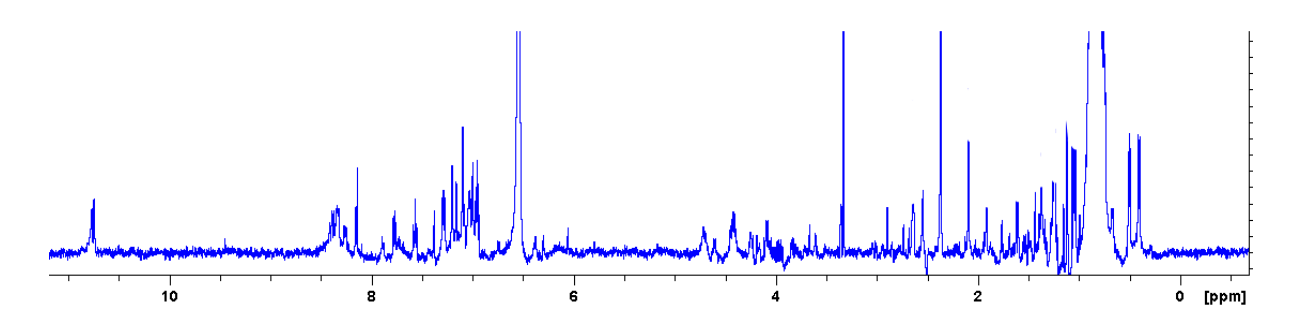


**Figure 3.1** <sup>1</sup>H-NMR spectra of (Ala)<sup>7</sup>-lugdunin (**1.25**) reported in literature (upper one) and this project (lower one).<sup>213</sup>

The structure of the purified compound was then analysized by <sup>1</sup>H-NMR and compared with the literature. Figure 3.1 shows the NMR spectra from the literature and synthesis in this project

and several key signals were also found.<sup>213</sup> For examples, the CH<sub>3</sub> on L-Ala-OH at position 7 was found at 0.8 (in this project) and 0.87 (in the literature); the NH on L-Trp-OH at position 3 was found at 10.62-10.71 (in this project) and 10.69-10.77 (in the literature)<sup>213</sup>.

<sup>a</sup>Reagents and conditions: (a) 1.Fmoc-Gly-OH; 2.Fmoc-Thr-OH, folloeing general Fmoc-SPPS protocol (b) Fmoc-L-Ala-H, DIPEA, MeOH, 5h, 60°C (c) Boc<sub>2</sub>O, NMM, THF, 5h, 50°C

Scheme 3.2 Preparation of pre-loaded (Fmoc-L-Ala-H) TG resin from Rink amide AM resin.

1.25

Scheme 3.3 Synthesis of (Ala)<sup>7</sup>-lugdunin (1.25) by using modified TG resin.

# 3.2 Alanine-scanning of (Ala<sup>7</sup>)-lugdunin

## 3.2.1 Introduction of alanine-scanning

The alanine-scanning is a common and useful method to determine the contribution of a specific residue to the stability and/or function of a peptide or protein.<sup>315</sup> For example, the noncovalent binding between the receptors and ligand molecules is determined by the residues present in the receptor and the ligand.<sup>316</sup> The binding contacts could be revealed by biophysical techniques such as X-ray crystallography and NMR.<sup>317</sup> A majority of the binding interactions is mediated by a subset of residues through hydrogen bonds, salt bridges, dipole-dipole interactions and hydrophobic interactions.<sup>318</sup> Identification of these amino acid residues that

partake in the interactions helps to understand the protein function. Residues are also responsible for the folding of the protein, which contributes to the stability of the protein. Alanine-scanning is ideally suited for identifying these residues. In fact, the alanine residue with a beta carbon but without any other side-chain functionality is commonly regarded as the first choice for mutational scanning.

In medicinal chemistry, alanine-scanning is one of the useful tools for understanding peptide activity and for determining structure-activity relationships (SARs). This approach establishes the contribution of each amino acid residue to specific peptide pharmacology/activity and helps to rationalize further modifications. As an example, alanine scan was applied in the research of aurein 1.2 by Migoń *et al.*<sup>320</sup> Aurein 1.2 is an antimicrobial peptide with 13 residues. In their study, the alanine scan of aurein was performed to investigate the effect of each amino acid residue on its biological and physico-chemical properties, including the determination of MIC, activity against biofilm, inhibitory effect on its formation, hemolytic activity and serum stability. The results not only provided information on the SAR study of aurein but also gave insights into design of novel analogs of AMPs in the future.<sup>320</sup> Thus, the alanine residue, as the smallest chiral amino acid, was exploited in a similar manner as outlined above to establish an initial SAR.

Furthermore, it was anticipated that the bulky structure due to continuous valine residues in lugdunin leads to lower yields and difficulties in purification. Therefore, (Ala)<sup>7</sup>-lugdunin (1.25), with a less bulky structure, has used as the reference compound for initial SAR study. Moreover, Schilling *et al.* previously had reported that Ala-scanning of the native lugdunin afforded analogues that are 4- to 8-fold less potent ((Ala)<sup>2</sup>-lugdunin; (Ala)<sup>5</sup>-lugdunin; (Ala)<sup>6</sup>-lugdunin and (Ala)<sup>7</sup>-lugdunin) or inactive analogues ((Ala)<sup>3</sup>-lugdunin and (Ala)<sup>4</sup>-lugdunin).<sup>213</sup> Uniquely,

the study reported herein would determine the importance of individual amino acid residues by an alanine-scanning of (Ala)<sup>7</sup>-lugdunin (1.25) to yield compounds 3.11-3.15 (Figure 3.2). Here, the effects of combining two changes, i.e., Ala-OH at position 7 and Ala-scanning at the other positions, were systematically evaluated. Thus, each amino acid residue of compound (Ala)<sup>7</sup>-lugdunin (1.25) was replaced by alanine with the same stereo-configuration.

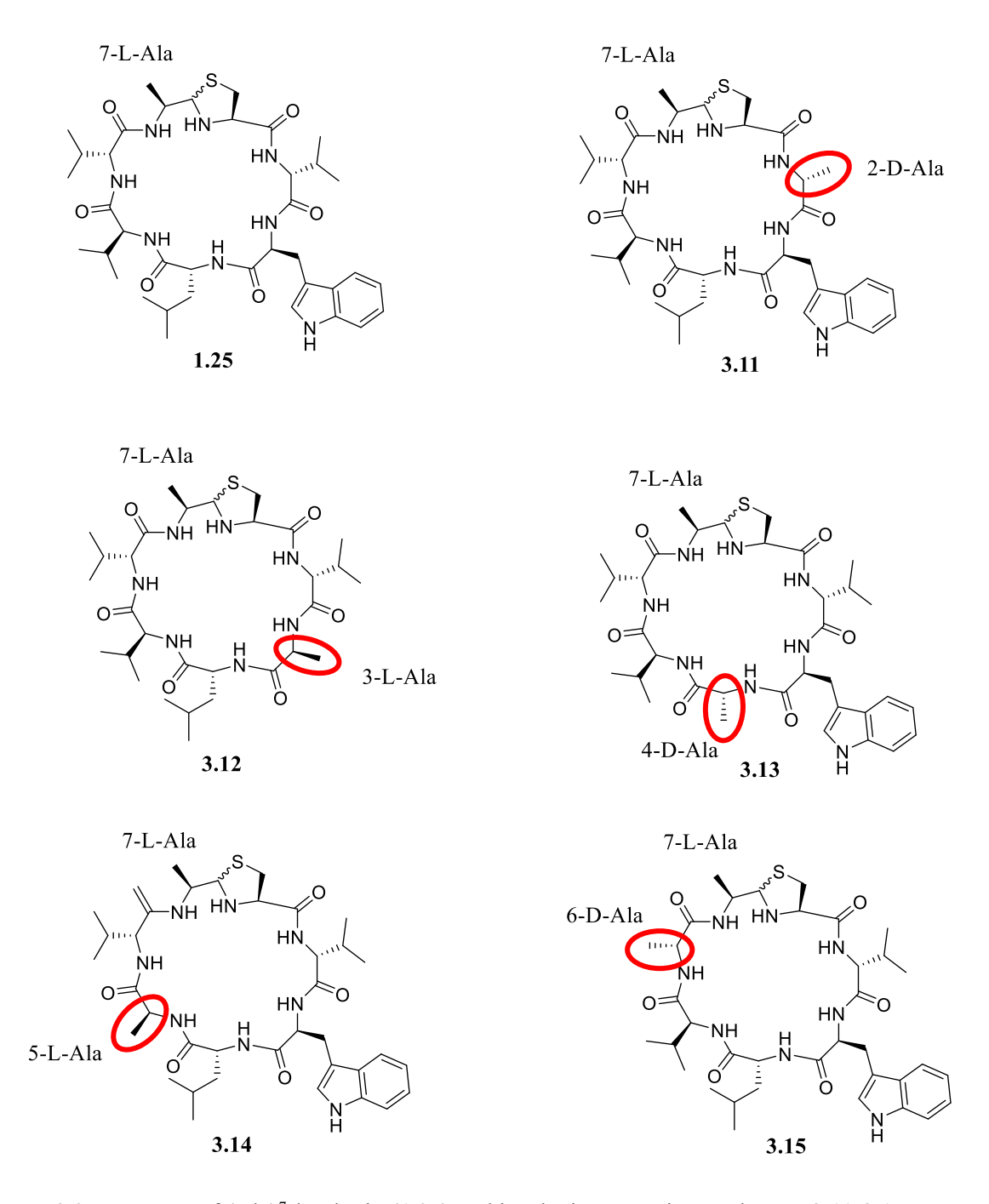


Figure 3.2 Structures of (Ala)<sup>7</sup>-lugdunin (1.25) and its alanine-scanning analogues 3.11-3.15.

#### 3.2.2 Synthesis of compounds 3.11-3.15

To synthesize the alanine-scanning analogues **3.11-3.15**, the method that utilizes a TG resin was deployed. Since the position 7 on all compounds is L-alanine, the modified TG resin **3.8** with the pre-loaded Fmoc-L-Ala-H was prepared on a larger scale following Scheme 3.2. No significant difference in the loading capacity was found when the reaction was scaled up (at 0.4 mmol scale) – the loading capacity was 0.39 mmol/g compared to 0.35 mmol/g when the reaction was carried out at 0.1 mmol scale. After the preparation of resin **3.8**, compounds **3.11-3.15** were then synthesized following general Fmoc-SPPS protocol (Scheme 3.4). The crude products were purified by RP-HPLC and also evaluated for their antimicrobial activity against *S. aureus*. Typically, the yields were 1.5-2.5% (based on the loading scale of Rink amide AM resin), with purity in excess of 95%.

```
a: AA^7 = L-AIa, AA^6 = D-AIa, AA^5 = L-VaI, AA^4 = D-Leu, AA^3 = L-Trp, AA^2 = D-VaI
b: AA^7 = L-AIa, AA^6 = D-VaI, AA^5 = L-AIa, AA^4 = D-Leu, AA^3 = L-Trp, AA^2 = D-VaI
c: AA^7 = L-AIa, AA^6 = D-VaI, AA^5 = L-VaI, AA^4 = D-AIa, AA^3 = L-Trp, AA^2 = D-VaI
d: AA^7 = L-AIa, AA^6 = D-VaI, AA^5 = L-VaI, AA^4 = D-Leu, AA^3 = L-AIa, AA^2 = D-VaI
e: AA^7 = L-AIa, AA^6 = D-VaI, AA^5 = L-VaI, AA^4 = D-Leu, AA^3 = L-Trp, AA^2 = D-AIa
```

```
 \begin{array}{l} \textbf{3.11:} \ AA^7 = \textbf{L-Ala,} \ AA^6 = \textbf{D-Ala,} \ AA^5 = \textbf{L-Val,} \ AA^4 = \textbf{D-Leu,} \ AA^3 = \textbf{L-Trp,} \ AA^2 = \textbf{D-Val} \ (4.2\%) \\ \textbf{3.12:} \ AA^7 = \textbf{L-Ala,} \ AA^6 = \textbf{D-Val,} \ AA^5 = \textbf{L-Ala,} \ AA^4 = \textbf{D-Leu,} \ AA^3 = \textbf{L-Trp,} \ AA^2 = \textbf{D-Val} \ (4.1\%) \\ \textbf{3.13:} \ AA^7 = \textbf{L-Ala,} \ AA^6 = \textbf{D-Val,} \ AA^5 = \textbf{L-Val,} \ AA^4 = \textbf{D-Ala,} \ AA^3 = \textbf{L-Trp,} \ AA^2 = \textbf{D-Val} \ (3.2\%) \\ \textbf{3.14:} \ AA^7 = \textbf{L-Ala,} \ AA^6 = \textbf{D-Val,} \ AA^5 = \textbf{L-Val,} \ AA^4 = \textbf{D-Leu,} \ AA^3 = \textbf{L-Ala,} \ AA^2 = \textbf{D-Val} \ (3.4\%) \\ \textbf{3.15:} \ AA^7 = \textbf{L-Ala,} \ AA^6 = \textbf{D-Val,} \ AA^5 = \textbf{L-Val,} \ AA^4 = \textbf{D-Leu,} \ AA^3 = \textbf{L-Trp,} \ AA^2 = \textbf{D-Ala} \ (3.0\%) \\ \end{array}
```

<sup>a</sup>Reagents and conditions: (a) Coupling cycle: Fmoc-amino acid, HATU, DIPEA, DMF, RT, 4-6 hr; deprotection cycle:20% piperidine in DMF, RT, 15 minutes. (b) 90% TFA:5% TIPS:5% H<sub>2</sub>O, RT, 3 h

**Scheme 3.4** Chemical synthesis of compounds **3.11-3.15**.

#### 3.3 Conclusions

In summary, this Chapter outlined the synthesis of (Ala)<sup>7</sup>-lugdunin (1.25) by the use of two different resins and the alanine-scanning analogues 3.11-3.15 (Figure 3.3) which were prepared using specifically the modified TG resin.

	Position 1	Position 2	Position 3	Position 4	Position 5	Position 6	Position 7
1.25	thiazolidine	D-Val	L-Trp	D-Leu	L-Val	D-Val	L-Ala
3.11	thiazolidine	D-Ala	L-Trp	D-Leu	L-Val	D-Val	L-Ala
3.12	thiazolidine	D-Val	L-Ala	D-Leu	L-Val	D-Val	L-Ala
3.13	thiazolidine	D-Val	L-Trp	D-Ala	L-Val	D-Val	L-Ala
3.14	thiazolidine	D-Val	L-Trp	D-Leu	L-Ala	D-Val	L-Ala
3.15	thiazolidine	D-Val	L-Trp	D-Leu	L-Val	D-Ala	L-Ala

**Figure 3.3** A highlight of the structural differences of (Ala)<sup>7</sup>-lugdunin **1.25** and its alanine-scanning analogues **3.11-3.15**.

In the method that utilized a pre-prepared building block Fmoc-L-Thz(L-Ala) (2.19) and 2-Cl-Trt resin, D-valine was first pre-loaded to the resin. Then the linear peptide sequence was assembled following general Fmoc-SPPS protocol through the coupling with amino acids in the order of L-valine, D-leucine, L-tryptophan and D-valine. The synthesized thiazolidine dipeptide 2.19 was coupled as the last building block. Subsequently, (Ala)<sup>7</sup>-lugdunin (1.25) was obtained after resin cleavage. However, when monitored by LCMS, an unexpected cyclic

five-mer **3.6** due to the incomplete coupling of **2.19** was also found. It was difficult to purify the mixture of **1.25** and **3.6** by RP-HPLC since their retention times are nearly identical. Thus, the alternative method that utilized TG resin was applied.

The method to prepare TG resin has previously been described in Chapter 2. To synthesize (Ala)<sup>7</sup>-lugdunin (1.25), the modified TG resin 3.8 with the pre-loaded Fmoc-L-Ala-H was first prepared, and the desired compound 1.25 was obtained by following a general Fmoc-SPPS protocol.

In order to determine the importance of each amino acid residue to specific peptide pharmacology, alanine-scanning was applied to establish an initial SAR. Thus, analogues 3.11-3.15, obtained from the alanine-scanning of (Ala)<sup>7</sup>-lugdunin (1.25) were synthesized using modified TG resin 3.8 and following a general Fmoc-SPPS protocol. Figure 3.3 shows the structure of (Ala)<sup>7</sup>-lugdunin (1.25) and its five alanine-scanning analogues. In contrast to the study reported by Schilling *et al.* in which Ala scan was carried out on the native lugdunin,<sup>213</sup> the analogues 3.11-3.15 will determine the effects combining two changes, i.e. Ala at position 7 and Ala-scanning at the other positions. All compounds reported in this Chapter 3 were tested for their antimicrobial activity against *S. aureus* and the results are reported in Chapter 6.

# **Chapter 4**

# Synthesis of Fmoc-N-methyl amino acids and

## Fmoc-L-homoleucine

#### 4.1 Introduction of N-methyl amino acids

*N*-Methylated amino acids are frequently discovered in naturally occurring compounds. As previously reported, *N*-methylation of amino acids is known to improve pharmacokinetic properties of peptide drugs.<sup>321</sup> Moreover, several unique features are found in *N*-methylated amino acids, such as enhanced proteolytic stability and higher lipophilicity.<sup>322</sup> Thus, interest in the research and study of *N*-methylated amino acids is increasing, especially by the pharmaceutical industry.<sup>323</sup>

Many peptides are readily degraded by exo- and endo-proteolytic enzymes resulting in a short half-life in vivo.<sup>324</sup> Since *N*-methyl amino acid residues are poorly recognized as substrate domains, the incorporation of *N*-methyl amino acids generally increases the stability of peptides to proteolysis, and thus extends their in vivo half-life.<sup>325</sup> Moreover, most peptides have poor oral bioavailability due to the hydrolysis reaction by digestive enzymes and/or have poor absorption through the intestine. *N*-methylation, as a chemical modification, could also be utilized in the design of peptides to improve their drug-like properties<sup>326</sup>. Several investigations have been reported about the influences of backbone *N*-methylation on the permeability of cyclic peptides. For example, Sanguinamide A, which is isolated as a novel thiazole-containing macrocyclic heptapeptide (cyclo- [Ile(Thz)-Ala-Phe-Pro-Ile-Pro]), has been regarded as a good molecular template for the study of relationships between *N*-methylation on its backbone amides and the changes of conformation and permeability. In the study by Bockus *et al.*, a new *N*-methylated analogue of Sanguinamide A with a Leu substitution at position 2 exhibited

solvent-dependent flexibility and improved permeability over that of the natural product.<sup>327</sup> A report published in 2010 had also highlighted that peptides rich in *N*-methyl phenylalanine residues can be used as blood-brain barrier shuttles due to its ability to passively penetrate the barrier.<sup>328</sup> These changes usually resulted from the reduced flexibility of the backbone structure due to the introduction of the *N*-methyl group.

## 4.2 Reported synthetic strategies to N-methyl amino acids

### 4.2.1 N-methylation via α-bromo acids

In 1915, the first protocol for the *N*-methylation of amino acids was established by Fischer and Mechel.<sup>329</sup> In this method, *N*-tosyl amino acids and  $\alpha$ -bromo acids were used as intermediates. In their study, several *N*-methyl amino acids, such as alanine, leucine and phenylalanine were synthesized by nucleophilic displacement of  $\alpha$ -bromo acids (Scheme 4.1).<sup>330</sup> However, due to the disadvantages of low yields and racemization, the technique is rarely used now.

**Scheme 4.1** Synthesis of *N*-methyl amino acids via  $\alpha$ -bromo acids.

To prepare the  $\alpha$ -bromo acids used in the reaction, diazotization of the parent amino acid was required (Scheme 4.2). The reaction results in a Walden inversion, with the diazonium ion as the intermediate. Subsequently, via a  $S_N2$  pathway, the diazonium ion is intramolecularly attacked by the neighbouring carboxylate group to form the highly reactive cyclic lactone (4.5). Then, the optically active  $\alpha$ -bromo acids (4.6) will be afforded via a second  $S_N2$ 

nucleophilic addition by a bromide ion. Consequently, exposure of the intermediate **4.6** to an excess of methylamine provides *N*-methyl amino acid with an opposite configuration to the parent amino acid.

**Scheme 4.2** Mechanism for preparing  $\alpha$ -bromo acids.

#### 4.2.2 N-methylation via a Mitsunobu reaction

Typically, the Mitsunobu reaction has been applied in the conversion of primary and secondary alcohols to esters, phenyl ethers, and thioethers. The nucleophile employed should be acidic, since one of the reagents diethylazodicarboxylate (DEAD) must be protonated during the course of the reaction. The first step, a betaine intermediate is afforded via the nucleophilic attack. Then the carboxylic acid is deprotonated and the alcohol is subsequently deprotonated by DEAD to form the key oxyphosphonium ion. The attack of the carboxylate anion upon intermediate is the only productive pathway to afford the desired methylated product.

In the method reported by Papaioannou *et al.* (Scheme 4.3), *N*-tosyl amino acid esters (4.7) and (4.8) were alkylated through a Mitsunobu reaction,<sup>335</sup> in which the tosylamide moiety is considered as the acidic component of the reaction. The secured *N*-methyl-*N*-tosyl-L-valine methyl ester (4.9) was then evaluated for the degree of epimerization via a saponification reaction.<sup>336</sup> It was found that saponifying with NaOH in methanol at room temperature produced up to 44% of the D-enantiomer. Alternatively, removal of the methyl ester via the

deprotection with iodotrimethylsilane was observed as an effective method without epimerization.<sup>337</sup>

However, the application of iodotrimethylsilane is limited due to its non-selectivity against other protecting groups. Thus, the benzyl esters were introduced as an alternative. They are readily removed under hydrogenolytic conditions, in which the epimerization of the *N*-methyl amino acids was not observed and was therefore the preferred choice for carboxyl protection.<sup>338</sup> Finally, the tosyl group was cleaved with the treatment of sodium in liquid ammonia to afford optically active *N*-methyl amino acids.

Scheme 4.3 N-methylation method reported by Papaioannou et al. 335

#### 4.2.3 N-methylation via base-mediated alkylation

Scheme 4.4 shows the N-methylation method reported by Fischer and Lipschitz.<sup>329</sup> In their study, N-tosyl  $\alpha$ -amino acids were reacted with NaOH at a temperature of 65-70 °C and methyl iodide was used as the alkylating agent. An advantage of N-tosyl protection is the high degree of crystallinity of the product, but a vigorous condition is usually required to remove the tosyl group. The free N-methyl amino acids were then obtained via the acid hydrolysis with concentrated HCl at 100 °C. However, epimerization was observed in the methylation step which involved treatment with NaOH at a high temperature. The problem was reported by Quitt

Subsequently, in a method reported by Hlavacek *et al.*, no epimerization was observed when the alkylation reaction was performed at 0°C.<sup>340</sup> Furthermore, since the method used was recognised as a biphasic reaction, a detergent was included to improve phase mixing. The free acids could then be obtained by treatment with trifluoroacetic acid (TFA) or 4 M HCl. Subsequent tosyl group removal was accomplished with the use of calcium metal in liquid ammonia or HBr at reflux in the presence of phenol.

**Scheme 4.4** *N*-methylation method reported by Fischer and Lipschitz.

#### 4.2.4 N-Methylation via an oxazolidinone intermediate

Herein, another method for the synthesis of *N*-methyl amino acids was introduced. The method involved the formation of an oxazolidinone intermediate which is especially designed to prepare unusual *N*-methyl amino acids. As reported by Ben-Ishai, the synthesis of oxazolidin-5-ones (**4.15**) (Scheme 4.5) was achieved via the refluxing of *N*-protected amino acids with paraformaldehyde and an acid catalyst.<sup>341</sup> The oxazolidin-5-one ring is then susceptible to nucleophilic attack, in which amines and alcohols as nucleophiles would afford the amides and esters, respectively.<sup>342-345</sup> Hence, treatment of compound **4.15** with an equivalent amount of benzylamine in alcohol afforded the *N*-hydroxymethyl amide (**4.16**). The desired product *N*-methylglycine derivative (**4.17**) was then obtained via the hydrogenation by 10% Pd-C/H<sub>2</sub>.

Bn O N COOH 
$$\frac{(CH_2O)_n, C_6H_6}{TsOH (cat.)}$$
 Bn O N BnNH<sub>2</sub> Bn O N BnNH<sub>2</sub> Bn O N Bn O N BnNH<sub>2</sub> Bn O N Bn O N

**Scheme 4.5** N-methylation method reported by Ben-Ishai et al. 341

Chemists had thus recognized the efficacy of 5-oxazolidinones, and improvements were made to their preparation and utility in conversion to other synthetically useful intermediates.

Freidinger *et al.* extended the range of substrates that can be converted to 5-oxazolidinones through the use of 9-fluorenylmethoxycarbonyl (Fmoc) protected amino acids and alkanals including paraformaldehyde.<sup>238</sup> This sequence was applied to Fmoc-alanine, valine, methionine, phenylalanine, lysine, serine, and histidine.<sup>346</sup> In their study, the oxazolidinone intermediates were formed with the addition of paraformaldehyde. Then the desired *N*-Fmoc-*N*-methyl amino acids compounds were subsequently obtained with the treatment of triethylsilane/TFA (Scheme 4.6). Moreover, the method was also applied to the *N*-Cbz-protected amino acids and further extended to *N*-Boc-protected amino acids by Reddy *et al.*<sup>345,346</sup>

Fmoc 
$$N$$
 OH  $C_6H_6$   $C_6H_6$ 

**Scheme 4.6** N-methylation method reported by Freidinger et al.<sup>238</sup>

Due to the several advantages, such as the tolerance for Fmoc-protected amino acids, simple and convenient to operate, less side reactions and freedom from racemization, the method in

scheme 4.6 was chosen for the synthesis of Fmoc-L-*N*-methyl-valine (4.24) and Fmoc-L-*N*-methyl-leucine (4.25). Scheme 4.8 shows the protocol used for the synthesis of compounds 4.24 and 4.25. The oxazolidinone compounds 4.22 and 4.23 were first obtained from commercial Fmoc-L-valine (2.2) and Fmoc-L-leucine (4.21), respectively. The addition of paraformaldehyde was separated into four batches and the *p*-toluenesulfonic acid (PTSA) was used as the acid catalyst. Then the oxazolidinone ring was reductively cleaved using the mixture Et<sub>3</sub>SiH/TFA to give the desired *N*-methylated compounds 4.24 and 4.25, and then used in the preparation of lugdunin analogues.

Fmoc 
$$N$$
 OH  $C_6H_6$  Fmoc  $N$   $C_6H_6$   $C_6H_6$ 

Scheme 4.7 Synthesis of Fmoc-L-*N*-Me-Val-OH (4.24) and Fmoc-L-*N*-Me-Leu-OH (4.25).

Following the method established by Freidinger *et al.*, the oxazolidinone intermediate compounds **4.22** and **4.23** were obtained in a yield of 92% and 85%, respectively. Finally, the desired compounds Fmoc-L-*N*-Me-Val-OH (**4.24**) and Fmoc-L-*N*-Me-Leu-OH (**4.25**) were obtained in high yields (92% and 86%, respectively). In the study by Freidinger *et al.*,<sup>238</sup> **4.22** was afforded in a yield of 96% and **4.24** in 100%. For comparison, the results are similar and therefore indicated the reproducibility of this method.

Furthermore, different concentrations of TFA were used to investigate the efficiency of the ring cleavage. 40% of TFA in DCM with one equivalent of TES was first tried. When monitoring by the TLC and LCMS, it was found that around 50% of starting material had reacted over 24

h. However, no further change was observed after a further 24 h under the same conditions. Thus, additional TFA was used and the concentration was up to 50% and stirred for a further 24 h. It was found that more products (around 60%) were obtained but the reaction was still incomplete. Then, one extra equivalent of TES was added, and the reaction was found to be near 100% complete. In another trial with a starting concentration of 50% TFA and one equivalent of TES, the conversion reaction was observed to be around 50% after 24 h. Then, with a 55% of TFA and two equivalents of TES, the reaction was found to be complete. However, more by-products were also observed. Hence, the addition of fresh TES was thought to be a key point to reduce the reaction time. Thus, to prevent the unexpected side-reaction due to higher concentration of TFA, a protocol was devised which involved treatment with 40% TFA in DCM with one equivalent of TES for 24 h followed by an additional one equivalent of TES with the final concentration of 50% of TFA for another 24 h.

### 4.3 Synthesis of Fmoc-L-homoleucine via Ni (II)-Gly-BPB complex

## 4.3.1 Chiral glycine equivalent approach

To prepare various unnatural amino acids, asymmetric synthesis of  $\alpha$ -amino acids through homologation of chiral equivalents of glycine is methodologically the most practical and reliable approach. <sup>238,347-349</sup> However, glycine is not chiral and thus a racemic mixture might be generated. Thus, a chiral glycine equivalent comprising of a chiral auxiliary moiety is needed to control the stereo-chemical result of the alkylation reaction. Several studies of chiral glycine equivalents have been reported and the majority are cyclic structures that are sterically hindered on one face, directing the alkylating agent to the opposite face of the molecule. <sup>350-351</sup>

So far, several chiral equivalents of glycine have been reported. However, the Ni (II) complex of glycine Schiff base (Ni (II)-Gly-BPB), which was introduced by Belokon *et al.* was one of

the most frequently used (Scheme 4.8).<sup>352</sup> The details of this synthetic route will be discussed in the next section. The Ni (II) complex is the chiral equivalent of glycine, and it offers a stereochemically reliable and efficient (>95% de) homologation via alkyl halide-mediated alkylation, aldol and Michael addition reactions. These reactions are generally under simple and convenient conditions, i.e., without the need for inert atmosphere, dried and degassed solvents, or low temperature.<sup>353</sup>

Scheme 4.8 Synthesis of the Ni (II)-glycine Schiff's base complex (4.29) from (S)-proline (4.26) and the desired  $\alpha$ -amino acid (4.31) is obtained via the alkylation of the Ni (II)-glycine Schiff's base complex (4.29) with an alkyl halide. 352.353

To synthesize the desired  $\alpha$ -amino acid (4.31), compound 4.30 was first prepared via the alkylation reaction of 4.29 with the corresponding alkyl halide. Then, 4.31 would be afforded by the disassembly of 4.30 under acidic (HCl) conditions (Scheme 4.8).

## 4.3.2 Total synthesis of Ni (II)-Gly-BPB complex

#### 4.3.2.1 Synthesis of N-benzyl-(S)-proline

To prepare the unnatural amino acid, Fmoc-L-homoleucine (4.37), a synthetic route using the

Ni (II)-Gly-BPB complex was applied. Scheme 4.9 shows the overall synthetic route to the Fmoc-L-homoleucine (4.37).

Reagent: (a) benzel chloride, KOH, iPrOH.  $45^{\circ}$ C; (b) 1. PCl5, chlorobenzene,  $0^{\circ}$ C; 2.2-aminobenzophenone; (C) 1. glycine, Ni(NO<sub>3</sub>)<sub>2</sub> 6H<sub>2</sub>O, MeOH,  $50^{\circ}$ C. 2. K<sub>2</sub>CO<sub>3</sub>  $65^{\circ}$ C; (d). 1. **4.33**, DMF, NaOH. 2. K<sub>2</sub>CO<sub>3</sub>, MeOH,  $60^{\circ}$ C; (e) 1. 2 M HCl, MeOH, microwave  $75^{\circ}$ C 50W 30 min; 2. **4.35**, Na<sub>2</sub>CO<sub>3</sub>, THF/H<sub>2</sub>O

4.37

Scheme 4.9 Synthesis of Fmoc-L-homoleucine (4.37) via Ni (II)-Gly-BPB complex.

The first step in this method is the *N*-benzylation of (*S*)-proline (**4.26**) to give *N*-benzyl-(*S*)-proline (**4.27**). Following the protocol reported by Belokon *et al.*, **4.26** was reacted with benzyl chloride (**4.32**) under basic conditions (KOH).<sup>352</sup> For work up, concentrated HCl was used added to quench the reaction and the pH was adjusted to 5-6. The KCl was then precipitated and was filtered off after the adding chloroform. The resulting residual material was subsequently triturated with acetone to afford compound **4.27**. This reaction was carried out on a large scale, starting with 20 g of **4.26**, and gave a reproducible high yield of 94%. This is like the yield (89%) obtained by Belokon *et al.*, from which this procedure was taken.<sup>352</sup> The product was then used in the next step without further purification.

# 4.3.2.2 Synthesis of chiral ligand (S)-2- [N'- (N benzylprolyl)amino]benzophenone (BPB) (4.28)

The chiral ligand (*S*)-2- [*N*'- (*N*-benzylprolyl)amino]benzophenone (BPB) **4.28** was obtained via the formation of an amide bond in a reaction between *N*-benzyl-(*S*)-proline **4.27** and 2-aminobenzophenone **4.32**. The method involved the use of phosphorus (V) pentachloride (PCl<sub>5</sub>) was previously reported by Romoff *et al.*<sup>354</sup> Compound **4.28** was obtained as off-white solids and the yield was 54%. The purity of the product was confirmed by <sup>1</sup>H NMR, optical rotation and melting point analysis, and further used directly for the next step.

#### 4.3.2.3 Synthesis of Ni (II)-Gly-BPB complex (4.29)

For the synthesis of Ni (II)-Gly-BPB complex **4.29**, the protocol reported by Ng *et al.*<sup>355</sup> was adopted. The mixture of (*S*)-BPB ligand, glycine and Ni (NO<sub>3</sub>)<sub>2</sub>•6H<sub>2</sub>O was refluxed in MeOH and then K<sub>2</sub>CO<sub>3</sub> was added. It was observed that the color of the reaction suspension would quickly turn from green to dark red. The reaction proceeded via imine formation between BPB and glycine and the chelation of Ni <sup>2+</sup> ions to form the complex. Additional K<sub>2</sub>CO<sub>3</sub> was added

after stirring for 1 h and refluxed for a further 2 h until the reaction completed. For workup, the reaction mixture was quenched with AcOH before being filtrated. Then the filtrate had H<sub>2</sub>O added and the suspension was stirred for a couple of hours to precipitate out and be collected as a red amorphous solid, which was dried in an oven to give pure product **4.29**. Then Ni (II)-Glycine-BPB complex **4.29** was afforded in a reproducible yield of 82%, which is similar to the results reported by Ng *et al.* (88%) and Belokon *et al.* (91%).<sup>352,355</sup>

#### 4.3.2.4 Alkylation of Ni (II)-Glycine-BPB complex

Compound **4.35** was obtained by the alkylation reaction of Ni (II)-Glycine-BPB complex (**4.29**) with isopentyl iodide (**4.34**). The reaction can be conducted under either a homogeneous condition or a heterogeneous phase-transfer (PTC) condition. Homogeneous reactions are chemical reactions in which the reactants and products are in the same phase, while heterogeneous reactions have reactants in two or more phases. Herein, due to the reasons of better diastereoselectivity and the poor solubility of **4.29** in solvents commonly used in PTC, a homogeneous condition was applied.

Thus, to a solution of Ni (II)-Gly-BPB complex (**4.29**) in anhydrous DMF was added 5 equivalents of NaOH. Subsequently, **4.34** in anhydrous DMF was added dropwise and stirred for a further 1 h. Studies have shown that the equilibrium could be driven towards the thermodynamically favored (*S*, *S*)-diastereomer in basic conditions, which is the thermodynamically favourable product when the proline chiral centre is in the (*S*) configuration.<sup>357</sup> Thus, to improve the stereochemical outcome, a second base treatment (3 equivalents of K<sub>2</sub>CO<sub>3</sub>) was subsequently added to the previous reaction mixture and refluxed for another 2 h.<sup>355</sup> An analysis by RP-HPLC showed the diastereomeric ratio was improved from 95:5 (90 % de) to an acceptable level (97:3, 94 % de).

# 4.3.2.5 Disassembly of the alkylated Ni (II)-Glycine-BPB complex and N-Fmoc-protection reaction

The final step of the whole procedure is the disassembly of the C-alkylated Ni (II)-Gly-BPB complex and followed by an N-Fmoc-protection reaction. The disassembly of the C-alkylated complex was achieved by acid-mediated hydrolysis. The alkylated Ni complex compound 4.35 was dissolved in a mixture of MeOH and 2 M HCl (3:1), and heated in a microwave under the condition of 50 W and 75°C. It was observed that the color changed from red to light green after the microwave heating which indicated the high efficiency of the hydrolysis reaction to give the desired amino acid analogue, and the by-products (S)-BPB and NiCl<sub>2</sub>. After solvent removal in vacuo, the residue was re-dissolved in H<sub>2</sub>O. Adjustment to pH 9 was achieved using saturated aqueous Na<sub>2</sub>CO<sub>3</sub> and the mixture was extracted with DCM. Addition of ethylenediaminetetraacetic acid (EDTA) disodium salt dihydrate is a necessary step to form a stable chelate with NiCl<sub>2</sub>. Fmoc-oxyma is selected as the introduction of Fmoc protecting group due to the relatively simple workup and negligible formation of impurities.<sup>281</sup> Scheme 4.10 shows the mechanism of Fmoc-protection to L-Hle using Fmoc-Oxyma. The by-product (oxyma impurity) can be easily removed by column chromatography. Following THF removal in vacuo, the aqueous suspension was extracted with Et<sub>2</sub>O. Acidification of the aqueous layer was carried out using KHSO<sub>4</sub> until pH 1-2. This was subsequently extracted with EtOAc, the combined organic extracts dried over MgSO<sub>4</sub> and concentrated in vacuo to give the desired product Fmoc-L-homoleucine 4.37.

Scheme 4.10 Mechanism of Fmoc-protection by Fmoc-oxyma.

#### 4.4 Conclusions

In summary, this chapter outlined the synthetic strategies for the preparation of Fmoc-*N*-methyl amino acids and Fmoc-L-homoleucine. Several routes to synthesize *N*-methylated amino acids have been reported, such as via α-bromo acid, Mitsunobu reaction, base-mediated alkylation and the unique method that involves the formation of a 5-oxazolidinone ring (Scheme 4.11). <sup>322,329,334,343,346</sup> The 5-oxazolidinone route was evaluated. The overall yields of the 5-oxazolidinone intermediates **4.22** and **4.23** were high (85-92%), and the desired products **4.24** and **4.25** were then afforded also in an excellent yield of 82-94% after the cleavage of the 5-oxazolidinone ring.

**Scheme 4.11** Different methods for the synthesis of *N*-methylated Fmoc-Hle-OH (**4.37**). Among them, the route via the formation of 5-oxazolidinone was adopted in the thesis.

Furthermore, different concentrations of TFA were used to investigate the best condition for the ring-cleavage step. It was found that the reaction would be completed under the condition of 50% TFA, while more by-products were also observed when the concentration was increased. Moreover, the addition of fresh TES was deemed necessary. Thus, a protocol was established, in which the 5-oxazolidinone intermediates were treated with 40% TFA in DCM and one equivalent of TES for the first 24 h, and then with an additional one equivalent of TES in a final concentration of 50% of TFA for a further 24 h.

With the advantages of high yields (overall > 80%), convenient to operate and a simple work-up, this method was selected as the protocol for the chemical synthesis of Fmoc-L-*N*-Me-Val-OH and Fmoc-L-*N*-Me-Leu-OH; these building blocks were then used for the preparation of the lugdunin analogues, (*N*-Me-Val<sup>7</sup>)-lugdunin and (*N*-Me-Leu<sup>7</sup>)-lugdunin, respectively.

For the preparation of unnatural amino acid, the method via Ni (II)-Gly-BPB complex was

used.<sup>352,355</sup> The protocol involved *N*-benzylation, amidation, Schiff base formation, alkylation, hydrolysis and the final Fmoc-protection to give the desired unnatural Fmoc-protected amino acids. This synthetic approach had been introduced due to its high diastereoselectivity of the optimized alkylation reaction and milder reaction condition due to the high reactivity of Schiff's.

Moreover, in the step of the alkylation of Ni (II)-Glycine-BPB complex **4.29**, it was observed that an additional base treatment improved the ratio between the diastereoisomers (S, S) and (S, R) to an acceptable level of 97:3 (94% de).

Thus, the method was used to synthesize L-homoleucine. Subsequent *N*-protection reaction involved the use of Fmoc-Oxyma. The secured Fmoc-L-homoleucine was subsequently used for the synthesis of the lugdunin analogue, (*N*-L-homoleucine<sup>7</sup>)-lugdunin.

# Chapter 5

## Lugdunin analogues with modifications at position 6 and 7

#### 5.1 Synthesis of lugdunin analogues with modification at position 7

#### 5.1.1 Strategy for the design of lugdunin analogues

In Chapter 2, a study of alanine-scanning of (Ala)<sup>7</sup>-lugdunin (**1.25**) was established. Hence, more analogues were designed to investigate the systematic replacement of different amino acids at different positions. As reported by Schilling *et al.*, modification at position 1 including the ring opened analogue and the change of the ring size resulted in compounds that are less active or inactive as antimicrobial agents.<sup>213</sup> Modifications at position 3, 4 and 5 also resulted in inactive compounds. In contrast, modifications or changes at position 2, 6 and 7 displayed the same or even better activity than the natural product lugdunin.<sup>213</sup> In the most recent study that involved changes at positions 2, 3 and 4, it is found that all the analogues are inactive compared to lugdunin.<sup>235</sup>

Since there is still no systematic study on the modification at position 7 of lugdunin, an extensive SAR study at this position was carried out (Figure 5.1). As mentioned in Chapter 1, the antibacterial activity strongly correlates with dissipation of the membrane potential in *S. aureus*. Lugdunin equalizes pH gradients in artificial membrane vesicles, thereby maintaining membrane integrity, which demonstrates that proton translocation is the mode of action. The overall polarity and hydrophobicity of lugdunin and analogues thereof could potentially modulate antimicrobial activity. Thus, several analogues were designed and synthesized with the modification at position 7 for the SAR study including the importance of the length of linear carbon chain, importance of branched chain, and the replacement of associated heterocyclic structures.

1-thiazolidine 7-L-Val 7-L-Valine was substituted by: 1. Linear/branched side chain: L-Leu, L-Hle, L-Nva, L-Nle. 2-D-Val 6-D-Val ΗŃ 2. Aromatic side chain: L-CPA, HN L-Phe, L-Trp. 3-L-Trp 3. Others: L-N-Me-Val, L-N-5-L-Val Me-Leu. 4-D-Leu

Figure 5.1 Structure of natural product lugdunin (1.24) and the modifications at position 7.

#### 5.1.2 Synthesis of the lugdunin analogues with linear/branched side chain

To first investigate the effect of the length of the side chain, (L-Leu)<sup>7</sup>-lugdunin and (L-Hle)<sup>7</sup>-lugdunin were synthesized (Figure 5.2). Compared to the L-valine residue at position 7 at lugdunin, its replacements L-leucine and L-homoleucine are comprised of one and two more methylene moieties, respectively. The Fmoc-L-leucine (4.21) is commercially available while the Fmoc-L-homoleucine (4.37) was synthesized following the method previously discussed in Chapter 4. Thus, Fmoc-L-Leu-H (5.1) and Fmoc-L-Hle-H (5.2) were synthesized by the CDI/DIBAL-H method, previously outlined in Chapter 2, and then used in the preparation of modified TG resin (Scheme 5.1).

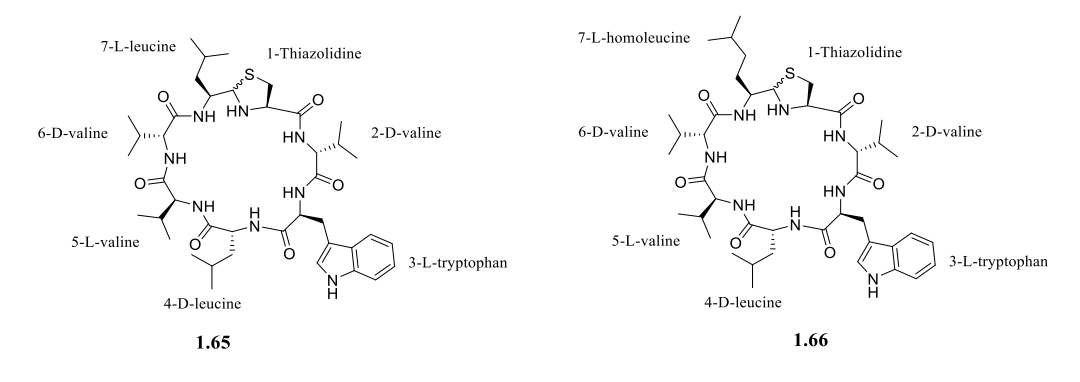


Figure 5.2 Structures of (L-Leu)<sup>7</sup>-lugdunin 1.65 and (L-Hle)<sup>7</sup>-lugdunin 1.66.

<sup>a</sup>Reagents and conditions: (a) CDI, dry DCM, 0°C, 1 h, then (b) DIBAL-H (1.0M in toluene), -78°C, 1.5 h

Scheme 5.1 Synthesis of Fmoc-L-Leu-H (5.1) and Fmoc-L-Hle-H (5.2).

After the respective Fmoc-amino aldehydes were obtained, the modified TG resin was prepared by the pre-loading of compounds **5.1** and **5.2** on TG resin (Scheme 5.2). Subsequently, the desired cyclic peptide (L-Leu)<sup>7</sup>-lugdunin (**1.65**) and (L-Hle)<sup>7</sup>-lugdunin (**1.66**) were synthesized following general Fmoc-SPPS protocol (Scheme 5.3). Synthesized compounds were then tested for their antimicrobial activity against different strains of *S. aureus*. The details of the antimicrobial results will be discussed in Chapter 6.

<sup>a</sup>Reagents and conditions: (a) 1.Fmoc-Gly-OH; 2.Fmoc-Thr-OH, following general Fmoc-SPPS protocol (b) Fmoc-L-Ala-CHO, DIPEA, MeOH, 5h, 60°C (c) Boc<sub>2</sub>O, NMM, THF, 5h, 50°C

Scheme 5.2 Preparation of modified rink TG resin 5.5 and 5.6.

HN Finot 
$$AA^7$$
 O  $AA^{2-6} - AA^7$  O  $AA^{3-6} - AA^7$  O  $AA^{3-6} - AA^7$  S  $AA^{4-6} - AA^{3-6} - AA^7$  S  $AA^{5-6} - AA^7$ 

**5.7**:  $AA^6 = D\text{-Val}$ ,  $AA^5 = L\text{-Val}$ ,  $AA^4 = D\text{-Leu}$ ,  $AA^3 = L\text{-Trp}$ ,  $AA^2 = D\text{-Val}$ **5.8**:  $AA^6 = D\text{-Val}$ ,  $AA^5 = L\text{-Val}$ ,  $AA^4 = D\text{-Leu}$ ,  $AA^3 = L\text{-Trp}$ ,  $AA^2 = D\text{-Val}$ 

**1.65**:  $AA^6 = D\text{-Val}$ ,  $AA^5 = L\text{-Val}$ ,  $AA^4 = D\text{-Leu}$ ,  $AA^3 = L\text{-Trp}$ ,  $AA^2 = D\text{-Val}$ **1.66**:  $AA^6 = D\text{-Val}$ ,  $AA^5 = L\text{-Val}$ ,  $AA^4 = D\text{-Leu}$ ,  $AA^3 = L\text{-Trp}$ ,  $AA^2 = D\text{-Val}$ 

<sup>a</sup>Reagents and conditions: (a) Coupling cycle: Fmoc-amino acid, HATU, DIPEA, DMF, RT, 4-6 hr; deprotection cycle:20% piperidine in DMF, RT, 15 minutes. (b) 90% TFA:5% TIPs:5% H<sub>2</sub>O, RT, 3 h

Scheme 5.3 Synthesis of lugdunin analogues (L-Leu)<sup>7</sup>-lugdunin (1.65) and (L-Hle)<sup>7</sup>-lugdunin (1.66).

Then, to investigate the effect of amino acids with linear side-chain compared to branched side chain, L-norvaline and L-norleucine were installed. Fmoc-L-norvaline has the same number of carbons as Fmoc-L-valine but arranged as a linear carbon chain. Similarly, L-norleucine is the linear chain equivalent of L-leucine. Thus, a SAR study between linear and branched side chain could be established. Both Fmoc-L-norvaline and Fmoc-L-norleucine were commercially available. Using the method mentioned before, the first step was the conversion of the Fmoc-amino acids to Fmoc-amino aldehyde. Therefore, Fmoc-L-Nva-H and Fmoc-L-Nle-H were synthesized by the CDI/DIBAL-H route (Scheme 5.4). Then, modified TG resin with pre-loaded 5.11 and 5.12 were prepared (Scheme 5.5). Following the general Fmoc-SPPS protocol, (L-Nva)<sup>7</sup>-lugdunin (1.67) and (L-Nle)<sup>7</sup>-lugdunin (1.68) were subsequently synthesized (Scheme 5.6). Figure 5.3 shows the chemical structures of lugdinin analogues 1.67 and 1.68.

<sup>a</sup>Reagents and conditions: (a) CDI, dry DCM, 0°C, 1 h, then (b) DIBAL-H (1.0M in toluene), -78°C, 1.5 h

#### Scheme 5.4 Synthesis Fmoc-L-Nva-H (5.11) and Fmoc-L-Nle-H (5.12).

Find 
$$AM$$
 resin (simplified)

5.13:  $AA = AB$ 

Find  $AB$ 

Find  $AB$ 

Find  $AB$ 
 $AB$ 

<sup>a</sup>Reagents and conditions: (a) 1.Fmoc-Gly-OH; 2.Fmoc-Thr-OH, following general Fmoc-SPPS protocol (b) Fmoc-L-Ala-CHO, DIPEA, MeOH, 5h, 60°C (c) Boc<sub>2</sub>O, NMM, THF, 5h, 50°C

#### Scheme 5.5 Preparation of modified TG resin 5.13 and 5.14.

deprotection cycle:20% piperidine in DMF, RT, 15 minutes. (b) 90% TFA:5% TIPs:97%  $\rm H_2O$ , RT, 3 h

<sup>a</sup>Reagents and conditions: (a) Coupling cycle: Fmoc-amino acid, HATU, DIPEA, DMF, RT, 4-6 hr;

Scheme 5.6 Synthesis of lugdunin analogues (L-Nva)<sup>7</sup>-lugdunin (1.67) and (L-Nle)<sup>7</sup>-lugdunin (1.68).

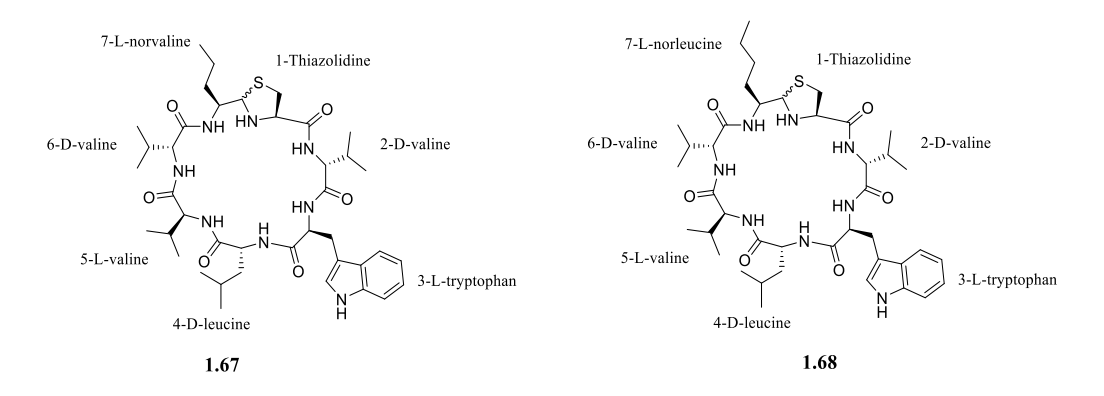


Figure 5.3 Structures of (L-Nva)<sup>7</sup>-lugdunin (1.67) and (L-Nle)<sup>7</sup>-lugdunin (1.68).

#### 5.1.3 Synthesis of the lugdunin analogues with cyclic/aromatic side chain

Since analogues with hydrophobic side-chain structure might lead to retention or possibly an increased antimicrobial activity, L-cyclopropyl alanine (CPA), L-phenylalanine and L-tryptophan were installed at position 7 to afford the lugdunin analogues (L-Trp)<sup>7</sup>-lugdunin (1.69), (L-Phe)<sup>7</sup>-lugdunin (1.70) and (L-CPA)<sup>7</sup>-lugdunin (1.71) (Figure 5.4). Fmoc-L-tryptophan (5.17), Fmoc-L-phenylalanine (5.18) and Fmoc-L-cyclopropyl alanine (5.19) were first converted to Fmoc-amino aldehyde compounds 5.20 to 5.22 (Scheme 5.7). Next, the desired modified TG resin 5.23 to 5.25 were obtained following the protocol in Scheme 5.8. Following peptide assembly and cyclisation (Scheme 5.9), and purification by semi-preparative RP-HPLC, the analogues 1.69, 1.70 and 1.71 were obtained in acceptable yields.

Figure 5.4 Structures of (L-Trp)<sup>7</sup>-lugdunin (1.69), (L-Phe)<sup>7</sup>-lugdunin (1.70) and (L-CPA)<sup>7</sup>-lugdunin (1.71).

<sup>a</sup>Reagents and conditions: (a) CDI, dry DCM, 0°C, 1 h, then (b) DIBAL-H (1.0M in toluene), -78°C, 1.5 h

Scheme 5.7 Synthesis of Fmoc-L-Trp-H (5.20), Fmoc-L-Phe-H (5.21) and Fmoc-L-CPA-H (5.22).

Rink amide AM resin (simplified)

5.23: 
$$aa = L$$
-Trp
5.24:  $aa = L$ -Phe
5.25:  $aa = L$ -CPA

<sup>a</sup>Reagents and conditions: (a) 1.Fmoc-Gly-OH; 2.Fmoc-Thr-OH, following general Fmoc-SPPS protocol (b) Fmoc-L-Ala-CHO, DIPEA, MeOH, 5h,  $60^{\circ}$ C (c) Boc<sub>2</sub>O, NMM, THF, 5h,  $50^{\circ}$ C

Scheme 5.8 Preparation of modified TG resin 5.23-5.25.

<sup>a</sup>Reagents and conditions: (a) Coupling cycle: Fmoc-amino acid, HATU, DIPEA, DMF, RT, 4-6 hr; deprotection cycle:20% piperidine in DMF, RT, 15 minutes. (b) 90% TFA:5% TIPs:97% H<sub>2</sub>O, RT, 3 h

Scheme 5.9 Synthesize lugdunin analogues (L-Trp)<sup>7</sup>-lugdunin (1.69), (L-Phe)<sup>7</sup>-lugdunin (1.70) and (L-CPA)<sup>7</sup>-lugdunin (1.71).

#### 5.1.4 Synthesis of the lugdunin analogues with N-methylated amino acids

The *N*-alkyl amino acids are valuable building blocks because their incorporation into peptides can modify their conformation by decreasing the number of hydrogen bonds and increasing backbone steric hindrance, and therefore, modulate their biological properties, such as potency,

selectivity, and bioavailability.<sup>321</sup> Furthermore, *N*-alkyl amino acids increase peptide resistance to proteases and their cell permeability. In the earlier section, it was established that the residue at position 7 is more tolerant to an amino acid with branched hydrocarbon side chain and especially with three carbon (L-valine) and four carbon (L-leucine). Hence, lugdunin analogues with the *N*-methylation of L-valine and L-leucine residues were synthesized for further SAR study. Figure 5.5 shows the structures of the designed analogues.

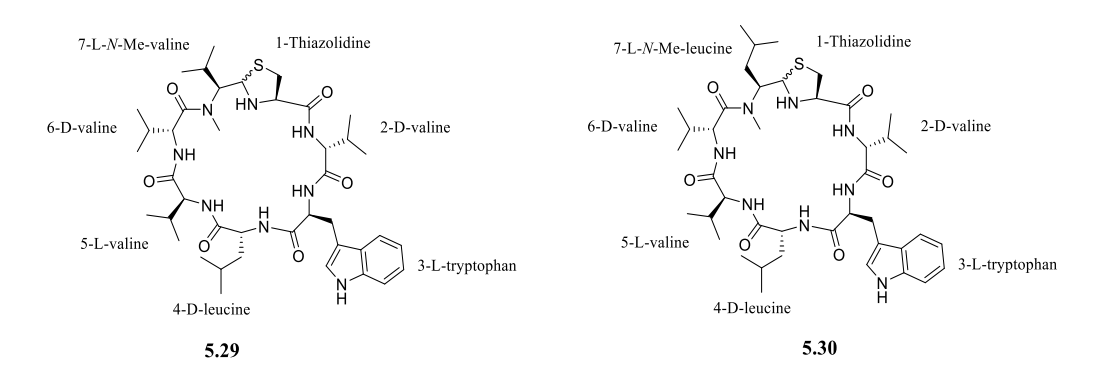


Figure 5.5 Structures of (L-*N*-Me-Val)<sup>7</sup>-lugdunin (5.29) and (L-*N*-Me-Leu)<sup>7</sup>-lugdunin (5.30).

The preparation of Fmoc-*N*-methyl amino acids was following the synthetic method which had been discussed in Chapter 4 and the compounds Fmoc-L-*N*-Me-Val-OH (**4.24**) and Fmoc-L-*N*-Me-Leu-OH (**4.25**) were subsequently applied to the preparation of analogues **5.29** and **5.30**.

Thus, Fmoc-L-*N*-Me-Val-OH (**4.24**) and Fmoc-L-*N*-Me-Leu-OH (**4.25**) were converted to their corresponding amino aldehyde compounds, Fmoc-L-*N*-Me-Val-H (**5.31**) and Fmoc-L-*N*-Me-Leu-H (**5.32**), respectively (Scheme 5.10). The desired modified TG resin **5.33** and **5.34** were then prepared by the procedure shown in Scheme 5.11. With modified TG resin **5.33** and **5.34**, the peptide sequences were then assembled using general Fmoc-SPPS protocol and the desired lugdunin analogues **5.29** and **5.30** were afforded after resin cleavage and peptide cyclization (Scheme 5.12).

<sup>a</sup>Reagents and conditions: (a) CDI, dry DCM, 0°C, 1 h, then (b) DIBAL-H (1.0M in toluene), -78°C, 1.5 h

#### Scheme 5.10 Synthesis of Fmoc-L-N-Me-Val-H (5.31) and Fmoc-L-N-Me-Leu-H (5.32).

Rink amide AM resin (simplified)

**5.33:** aa = L-*N*-Me-valine **5.34:** aa = L-*N*-Me-leucine

<sup>a</sup>Reagents and conditions: (a) 1.Fmoc-Gly-OH; 2.Fmoc-Thr-OH, following general Fmoc-SPPS protocol (b) Fmoc-L-Ala-CHO, DIPEA, MeOH, 5h, 60°C (c) Boc<sub>2</sub>O, NMM, THF, 5h, 50°C

#### Scheme 5.11 Preparation of modified TG resin 5.33 and 5.34.

<sup>a</sup>Reagents and conditions: (a) Coupling cycle: Fmoc-amino acid, HATU, DIPEA, DMF, RT, 4-6 hr; deprotection cycle: 20% piperidine in DMF, RT, 15 minutes. (b) 90% TFA: 5% TIPs: 97% H<sub>2</sub>O, RT, 3 h

**Scheme 5.12** Synthesis of lugdunin analogues (L-*N*-Me-Val)<sup>7</sup>-lugdunin (**5.29**) and (L-*N*-Me-Leu)<sup>7</sup>-lugdunin (**5.30**).

### 5.1.5 Synthesis of the lugdunin analogue (L-Thr)<sup>7</sup>-lugdunin

In the previous section, position 7 analogues with more hydrophobic residues, such as hydrocarbon side chain, aromatic side chain or *N*-methylated amino acids were designed and tested for antimicrobial activity. Several analogues showed activity while most of them were inactive against *S. aureus*. To fully investigate the SAR for the modification at position 7, Fmoc-L-threonine was installed to give (L-Thr)<sup>7</sup>-lugdunin (**5.37**) (Figure 5.6). Given the apparent preference for hydrophobic side chain, it was anticipated that the L-Thr<sup>7</sup>-analogue would be inactive and hence could be a useful negative control compound.

**Figure 5.6** Structures of (L-Thr)<sup>7</sup>-lugdunin **5.37**.

Threonine is an amino acid which comprises a side chain with a hydroxyl group, making it a polar and uncharged and thus could be used to compare with the hydrophobic moieties. Scheme 5.13 shows the protocol for the preparation of Fmoc-L-Thr-H. The modified TG resin **5.40** was prepared following Scheme 5.14. (L-Thr)<sup>7</sup>-lugdunin **5.37** was then obtained following Fmoc-SPPS procedure (Scheme 5.15).

<sup>a</sup>Reagents and conditions: (a) CDI, dry DCM, 0°C, 1 h, then (b) DIBAL-H (1.0M in toluene), -78°C, 1.5 h

# Scheme 5.13 Synthesis of Fmoc-L-Thr-H 5.39

<sup>a</sup>Reagents and conditions: (a) 1.Fmoc-Gly-OH; 2.Fmoc-Thr-OH, following general Fmoc-SPPS protocol (b) Fmoc-L-Ala-CHO, DIPEA, MeOH, 5h, 60°C (c) Boc<sub>2</sub>O, NMM, THF, 5h, 50°C

#### Scheme 5.14 Preparation of modified TG resin 5.40.

**5.41**:  $AA^6 = D\text{-Val}$ ,  $AA^5 = L\text{-Val}$ ,  $AA^4 = D\text{-Leu}$ ,  $AA^3 = L\text{-Trp}$ ,  $AA^2 = D\text{-Val}$ 

**5.37**:  $AA^6 = D\text{-Val}$ ,  $AA^5 = L\text{-Val}$ ,  $AA^4 = D\text{-Leu}$ ,  $AA^3 = L\text{-Trp}$ ,  $AA^2 = D\text{-Val}$ 

<sup>a</sup>Reagents and conditions: (a) Coupling cycle: Fmoc-amino acid, HATU, DIPEA, DMF, RT, 4-6 hr; deprotection cycle:20% piperidine in DMF, RT, 15 minutes. (b) 90% TFA:5% TIPs:5% H<sub>2</sub>O, RT, 3 h

#### **Scheme 5.15** Synthesis of lugdunin analogue (L-Thr)<sup>7</sup>-lugdunin **5.37**.

# 5.2 Synthesis of lugdunin analogues with modification at position 6

As mentioned in the previous section 1.4 analogues with the modification at position 6 might still display antimicrobial activity. Three lugdunin analogues, including (D-Leu)<sup>6</sup>-lugdunin (1.72), (D-Trp)<sup>6</sup>-lugdunin (1.46) and (D-Phe)<sup>6</sup>-lugdunin (1.73) (figure 5.7) were designed and synthesized to investigate the SAR. Since (L-Leu)<sup>7</sup>-lugdunin was found to be the most active compound, the substitution of D-valine to D-leucine at position 6 was designed. Besides, D-tryptophan and D-phenylalanine were also introduced for further SAR study. Moreover, the (D-Trp)<sup>6</sup>-lugdunin was recently reported by Schilling *et al.* to be active against *S. aureus*, hence the preparation of this compound could confirm their results.<sup>213</sup>

The first step was the conversion of an Fmoc-amino acid to the corresponding Fmoc-amino aldehyde (Scheme 5.16). Since position 7 is fixed as L-valine, only Fmoc-L-Val-H was needed for the preparation of modified TG resin. The protocol for the preparation of Fmoc-L-Val-H and relative modified TG resin has been discussed before. The desired analogues (D-Leu)<sup>6</sup>-lugdunin (1.72), (D-Trp)<sup>6</sup>-lugdunin (1.46) and (D-Phe)<sup>6</sup>-lugdunin (1.73) were subsequently obtained following a general Fmoc-SPPS procedure (Scheme 5.16).

Figure 5.7 Structures of (D-Leu)<sup>6</sup>-lugdunin (1.72), (D-Trp)<sup>6</sup>-lugdunin (1.46) and (D-Phe)<sup>6</sup>-lugdunin (1.73).

**5.42**:  $AA^6 = D$ -Leu,  $AA^5 = L$ -Val,  $AA^4 = D$ -Leu,  $AA^3 = L$ -Trp,  $AA^2 = D$ -Val **5.43**:  $AA^6 = D$ -Trp,  $AA^5 = L$ -Val,  $AA^4 = D$ -Leu,  $AA^3 = L$ -Trp,  $AA^2 = D$ -Val **5.44**:  $AA^6 = D$ -Phe,  $AA^5 = L$ -Val,  $AA^4 = D$ -Leu,  $AA^3 = L$ -Trp,  $AA^2 = D$ -Val **1.72**:  $AA^6 = D$ -Leu,  $AA^5 = L$ -Val,  $AA^4 = D$ -Leu,  $AA^3 = L$ -Trp,  $AA^2 = D$ -Val **1.46**:  $AA^6 = D$ -Trp,  $AA^5 = L$ -Val,  $AA^4 = D$ -Leu,  $AA^3 = L$ -Trp,  $AA^2 = D$ -Val

**1.73**:  $AA^6 = D$ -Phe,  $AA^5 = L$ -Val,  $AA^4 = D$ -Leu,  $AA^3 = L$ -Trp,  $AA^2 = D$ -Val

<sup>a</sup>Reagents and conditions: (a) Coupling cycle: Fmoc-amino acid, HATU, DIPEA, DMF, RT, 4-6 hr; deprotection cycle:20% piperidine in DMF, RT, 15 minutes. (b) 90% TFA:5% TIPs:5% H<sub>2</sub>O, RT, 3 h

Scheme 5.16 Synthesis of lugdunin analogues (D-Leu)<sup>6</sup>-lugdunin (1.72), (D-Trp)<sup>6</sup>-lugdunin (1.46) and (D-Phe)<sup>6</sup>-lugdunin (1.73).

# 5.3 Synthesis of lugdunin analogues with combined modification at position6 and 7

Among the analogues modified at position 7, (L-Leu)<sup>7</sup>-lugdunin was found to be the most active compound while (D-Trp)<sup>6</sup>-lugdunin was the most active one when modified at position-6. Therefore, an analogue (D-Trp)<sup>6</sup>-(L-Leu)<sup>7</sup>-lugdunin (**5.45**) (Figure 5.8) with the combination of the two features was synthesized. Since the residue at position 7 is L-leucine, the modified TG resin with pre-loaded Fmoc-L-Leu-H was first synthesized. The protocol to prepare Fmoc-L-Leu-H and relative modified TG resin has been shown in the previous section (Scheme 5.1 and 5.2). Subsequently, following the general Fmoc-SPPS procedure, the desired compound **5.45** was afforded (Scheme 5.17).

**Figure 5.8** Structure of (D-Trp)<sup>6</sup>-(L-Leu)<sup>7</sup>-lugdunin (**5.45**).

**5.46**:  $AA^7 = L-Leu$ ,  $AA^6 = D-Trp$ ,  $AA^5 = L-Val$ ,  $AA^4 = D-Leu$ ,  $AA^3 = L-Trp$ ,  $AA^2 = D-Val$ 

**5.45**:  $AA^7 = L-Leu$ ,  $AA^6 = D-Trp$ ,  $AA^5 = L-Val$ ,  $AA^4 = D-Leu$ ,  $AA^3 = L-Trp$ ,  $AA^2 = D-Val$ 

<sup>a</sup>Reagents and conditions: (a) Coupling cycle: Fmoc-amino acid, HATU, DIPEA, DMF, RT, 4-6 hr; deprotection cycle:20% piperidine in DMF, RT, 15 minutes. (b) 90% TFA:5% TIPs:5% H<sub>2</sub>O, RT, 3 h

Scheme 5.17 Synthesis of lugdunin analogue (D-Trp)<sup>6</sup>-(L-Leu)<sup>7</sup>-lugdunin (5.45).

### **5.4 Conclusions**

In summary, this chapter outlined the design and total synthesis of a focused library of lugdunin analogues. These compounds are designed to facilitate early SAR study. Whilst the work was in-progress, Schilling *et al.* reported their results on a number of lugdunin analogues, which indicated tolerance to modifications at position 2, 6 and 7.<sup>213</sup> Herein, an in-depth SAR study of modifications at position 6 and 7 is reported.

Compounds **1.65** and **1.66** were first designed to investigate the importance of the length of the hydrocarbon side chain in residue 7. Then compounds **1.67** and **1.68** were synthesized as the residue was changed to a linear side chain. It was found that structure with a branched side chain and the length of four carbons gave the most active compound (see Chapter 6 for the antimicrobial activity). Subsequently, the effect of hydrophobicity on antimicrobial activity was considered. Hence, amino acids with non-polar and (hetero) aromatic side chain were installed. Thus, the compounds **1.69**, **1.70** and **1.71** were designed in which L-valine residue is replaced with L-tryptophan, L-phenylalanine and L-cyclopropyl alanine, respectively.

Since *N*-methylated amino acids possess several advantages including conformational changes and improved proteolytic stability and/or higher lipophilicity, they have been shown to improve pharmacokinetic properties of peptide drugs. Therefore, due to the potency of lugdunin (1.24) (in which position 7 is L-valine) and (L-Leu)<sup>7</sup>-lugdunin (1.65), Fmoc-L-*N*-Me-Val and Fmoc-L-*N*-Me-Leu were introduced as the alternative amino acids at position 7. The results showed that the antimicrobial activity of (L-*N*-Me-Val)<sup>7</sup>-lugdunin 5.29 is quite similar to lugdunin while (L-*N*-Me-Leu)<sup>7</sup>-lugdunin (5.30) was found to be less active than (L-Leu)<sup>7</sup>-lugdunin (1.65). The last analogue with modification at position 7 is (L-Thr)<sup>7</sup>-lugdunin (5.37). Due to a hydroxyl group in the side chain of Thr residue, it was anticipated that 5.37 would be more

hydrophilic. Indeed, the compound **5.37** was found to be inactive.

A further SAR study on position 6 was established by the synthesized analogues **1.72**, **1.46**, and **1.73**. Among these compounds, (D-Trp)<sup>6</sup>-lugdunin (**1.46**) had been reported by Schilling *et al.* and the result of bioactivity was the compared in chapter 6 to confirm the observation of reported data.<sup>213</sup>

Finally, (D-Trp)<sup>6</sup>-(L-Leu)<sup>7</sup>-lugdunin (**5.44**) with the modifications at both position 6 and 7 was synthesized. However, compound **5.44** was found to be inactive against *S. aureus*. Figure 5.9 shows the structure of lugdunin and the modification strategy. Table 5.1 shows all the analogues synthesized in this chapter. Detailed results of the antimicrobial activity will be discussed in Chapter 6.

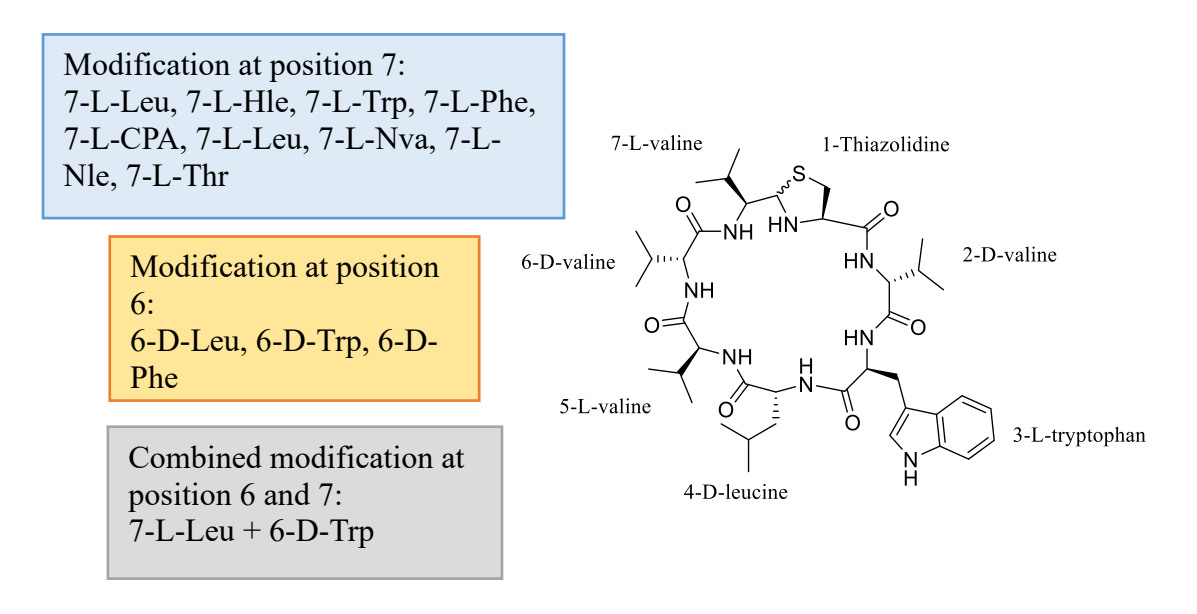


Figure 5.9 Structure of lugdunin and modifications at position 6 and 7.

**Table 5.1** Synthesized analogues with modifications at position 6 or 7. The difference in amino acid residue is highlighted in red.

Compounds	Position 1	Position 2	Position 3	Position 4	Position 5	Position 6	Position 7
Lugdunin	thiazolidine	D-Val	L-Trp	D-Leu	L-Val	D-Val	L-Val
1.24							
1.25	thiazolidine	D-Val	L-Trp	D-Leu	L-Val	D-Val	L-Ala
1.65	thiazolidine	D-Val	L-Trp	D-Leu	L-Val	D-Val	L-Leu
1.66	thiazolidine	D-Val	L-Trp	D-Leu	L-Val	D-Val	L-Hle
1.67	thiazolidine	D-Val	L-Trp	D-Leu	L-Val	D-Val	L-Nva
1.68	thiazolidine	D-Val	L-Trp	D-Leu	L-Val	D-Val	L-Nle
1.69	thiazolidine	D-Val	L-Trp	D-Leu	L-Val	D-Val	L-Trp
1.70	thiazolidine	D-Val	L-Trp	D-Leu	L-Val	D-Val	L-Phe
1.71	thiazolidine	D-Val	L-Trp	D-Leu	L-Val	D-Val	L-CPA
5.29	thiazolidine	D-Val	L-Trp	D-Leu	L-Val	D-Val	L-N-Me-Val
5.30	thiazolidine	D-Val	L-Trp	D-Leu	L-Val	D-Val	L-N-Me-Leu
5.37	thiazolidine	D-Val	L-Trp	D-Leu	L-Val	D-Val	L-Thr
1.72	thiazolidine	D-Val	L-Trp	D-Leu	L-Val	D-Leu	L-Val
1.46	thiazolidine	D-Val	L-Trp	D-Leu	L-Val	D-Trp	L-Val
1.73	thiazolidine	D-Val	L-Trp	D-Leu	L-Val	D-Phe	L-Val
5.44	thiazolidine	D-Val	L-Trp	D-Leu	L-Val	D-Trp	L-Leu

# Chapter 6

# Antibacterial assessment of lugdunin and analogues thereof

#### 6.1 Introduction

The total synthesis of lugdunin and 20 analogues thereof have already been described in the previous Chapters 2, 3 and 5. All the compounds were evaluated for their antibacterial activity against several different strains of the Gram-positive bacterium *S. aureus*.

Lugdunin is a natural product which was isolated from the human nasal bacterium *Staphylococcus lugdunensis*.<sup>20</sup> Lugdunin was discovered to be a novel thiazolidine-containing cyclic peptide antibiotic and the first antibiotic to come from a bacterium that lives primarily in humans.<sup>20</sup> Lugdunin was found to be active against both methicillin-resistant *Staphylococcus aureus* and vancomycin-resistant *E. coli* in cell culture tests.<sup>20</sup> Moreover, lugdunin is also effective in treating skin infections caused by *S. aureus*.<sup>20</sup> In this chapter, a detailed account of the MoA will be first discussed, and subsequently the antibacterial results and the SAR study of all synthesized compounds.

Based on th proposed mode of action reported by Schilling *et al.*, proton translocation is thought to be the mechanism and thus, the polarity of the compounds may be taken into important consideration when designing analogues for SAR studies. Initially, all the lugdunin analogues including alanine scanning and the modifications at positions 6 and 7 were tested in antimicrobial assays against multiple strains of *S. aureus*.

# 6.2 Antimicrobial activity of lugdunin and its analogues against S. aureus

# 6.2.1 Growth inhibition and broth microdilution assays

The growth inhibition assay was performed using the Gram-positive strains, *S. aureus* SH1000 and USA300 JE2. To this end, a growth inhibition assay was performed which followed changes in optical density of the bacterial culture over time, at various concentrations of the tested compounds. The normalised percentage growth at 13 h was used to generate doseresponse curves and from these, the concentration at which 50 % of the bacterial growth was inhibited (IC<sub>50</sub>) was calculated.

Thus, an overnight culture of a single SH1000 colony in Luria-Bertani (LB) media was adjusted to an OD600 of 0.01, giving approximately 106 colony forming units per mL (CFU/mL). A 10 mM stock solution of the tested compound in DMSO was added to the culture and serially diluted to obtain various concentrations in a 96-well plate, with the DMSO concentration adjusted to 1 % in all test compound wells. In addition, vancomycin treated culture was used as a positive control and LB media, untreated culture and culture with 1 % DMSO were used as negative controls. The plate was then incubated at 37°C for 20 h and OD600 measurements were taken every 15 min using a TECAN microplate reader. The growth curves and the corresponding dose-response curves for lugdunin and analogues thereof were obtained, such as the one shown in Figure 6.1 (a) that was obtained with (Leu)<sup>7</sup>-lug (1.65). The normalised percentage growth of the bacteria at 13 h was calculated for each concentration of the test compound and visualised in a dose-response curve (Figure 6.1 (b)). Finally, the IC50 value was calculated from the dose-response curve and was found to be  $6.47 \pm 0.14 \,\mu\text{M}$  for 1.65. Growth curves and does-response curves of both *S. aureus* SH1000 and USA300 JE2 for all synthesized compounds are shown in appendix 1 and 2.

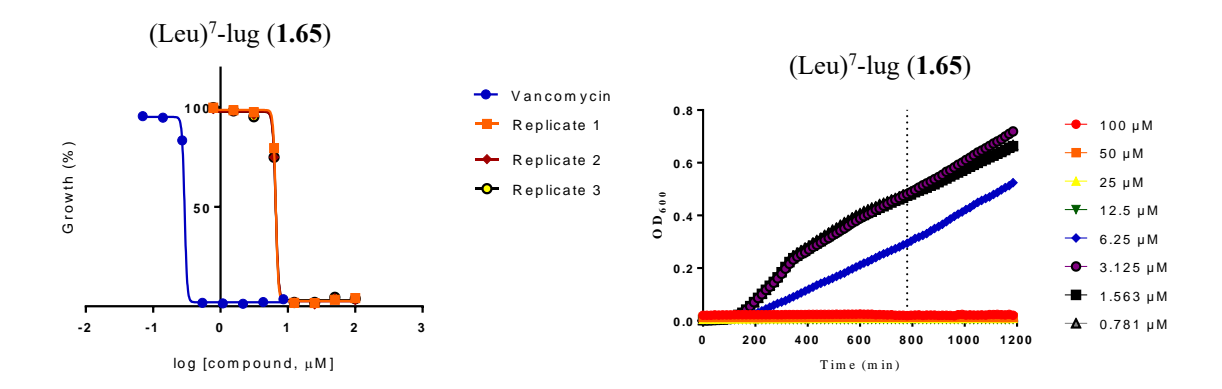


**Figure 6.1** (a) A growth curve of *S. aureus* SH1000 in various concentrations of (Leu)<sup>7</sup>-lug (**1.65**). (b) A dose-response curve generated from the percentage growth at 13 h. Three independent experiments were conducted, with vancomycin as a positive control.

The growth inhibition assay is useful for SAR studies as it allows for subtle differences in the potencies of different analogues to be determined. However, a complementary assay was performed to obtain MICs against a range of *S. aureus* strains. Additionally, a general broth microdilution method was adopted to obtain the minimum inhibitory concentration (MIC) values. MIC is determined as the lowest concentration (in µg/mL) of a tested compound that inhibits the growth of a given strain of bacteria. The broth microdilution assay is convenient to screen antimicrobial compounds against many different strains of the same species or different microorganisms. However, the results are taken at the endpoint of the assay and therefore lack any information on how the bacterial growth is affected over time at the different test compound concentrations. On the other hand, the growth inhibition assay does supply this information and allows subtle differences between the activities of analogues to be seen. Hence, the growth inhibition assay was used to inform decisions on where to make changes in the chemical structures to improve activity, whereas the broth microdilution assay was useful to compare activities between strains. The IC<sub>50</sub> and MIC data against the five *S. aureus* strains mentioned above is discussed in the following sections for all the analogues.

Herein, *S. aureus* SH1000 and USA300 JE2 were used as the tested strains for the initial assay. The most active compounds **1.24**, **1.46**, **1.65** and **5.29** were tested, and their activity will be determined against another three different strains of *S. aureus*, Newman, PM64 and Mu50. Table 6.1 outlines the phenotypic features of all five strains of *S. aureus*. Among these 5 different strains of *S. aureus*, SH1000 and Newman are methicillin-sensitive, while USA300 JE2, PM64 and Mu50 are all methicillin-resistant, especially the Mu50 is also vancomycin-intermediate-resistant. *S. aureus* SH1000 is known to harbour 15 single-nucleotide polymorphisms. Sensitive USA300 JE2 is the strain responsible for the community-acquired skin infection. Sensitive aureus strain Newman, which was also isolated from a human infection, displays robust virulence properties in animal models of disease. As reported, the complete genome sequence of *S. aureus* Newman, which carries four integrated prophages, as well as two large pathogenicity islands. Sensitive Mu50 was used as the only strain with resistance to vancomycin. Sensitive will be a sensitive and their activity will be determined against another three different strains of *S. aureus* SH1000 and Sensitive strains of *S. aureus* and SH1000 and Newman are methicillin-sensitive, while USA300 sensitive, while USA300 sensitive, while USA300 and SH1000 and Newman are methicillin-sensitive, while USA300 sensitive, while USA300 sensitive,

Table 6.2 shows the IC<sub>50</sub> and MIC values of synthesized analogues against *S. sureus* SH1000 and *S. aureus* USA300 JE2. A SAR study of the compounds using both broth microdilution and growth inhibition assays was established and will be further discussed in the following section.

Table 6.1 Features of different strains of S. aureus used in antimicrobial tests

Strain of S. aureus	Features
SH1000 <sup>371</sup>	Methicillin–sensitive, derivative of RN6390 with the rsbU gene
	restored
USA 300 JE2 <sup>367</sup>	Methicillin–resistant, associated with unusually invasive diseases
Newman <sup>368</sup>	Methicillin–sensitive, isolated from a human infection, robust
	virulence phenotypes
PM64 <sup>369</sup>	Methicillin-resistant
Mu50 <sup>370</sup>	Vancomycin-resistant MRSA, isolated in Japan in 1997, possess a
	thickened cell wall

**Table 6.2** *In vitro* potency of lugdunin analogues and vancomycin against *S. aureus* SH1000 and USA300 JE2.

Compounds	IC50 (	$(\mu \mathbf{M})^a$	$\mathbf{MIC}\;(\mathbf{\mu g/ml})^b$		
	S. aureus		S. aureus		
	SH1000	USA300 JE2	SH1000	USA300 JE2	
Vancomycin	$1.31 \pm 0.28 \ (n=3)$	$0.62 \pm 0.01 \ (n=3)$	1	2	
Lugdunin ( <b>1.24</b> )	$25.42 \pm 0.45 \; (n=3)$	$27.58 \pm 0.62  (n=3)$	32	32	
(Ala) <sup>7</sup> -Lug ( <b>1.25</b> )	$95.25 \pm 1.05 \ (n=3)$	$97.05 \pm 2.08 \ (n=3)$	> 32	> 32	
$(Ala)^7$ - $(Ala^2)$ -Lug ( <b>3.11</b> )	>100 (n = 2)	>100 (n = 2)	> 32	> 32	
$(Ala)^7$ - $(Ala^3)$ -Lug ( <b>3.12</b> )	>100 (n = 2)	>100 (n = 2)	> 32	> 32	
(Ala) <sup>7</sup> -(Ala <sup>4</sup> )-Lug	>100 (n = 2)	>100 (n = 2)	> 32	> 32	
(3.13)					
$(Ala)^7$ - $(Ala^5)$ -Lug	>100 (n = 2)	>100 (n = 2)	> 32	> 32	
(3.14)					
$(Ala)^7$ - $(Ala^6)$ -Lug	>100 (n = 2)	>100 (n = 2)	> 32	> 32	
(3.15)	(45 : 0.14 ( 2)	( 00 ) 0 77 ( 2)	0	0	
(Leu) <sup>7</sup> -Lug ( <b>1.65</b> )	$6.47 \pm 0.14  (n=3)$	$6.88 \pm 0.75  (n=3)$	8	8	
(Hle) <sup>7</sup> -Lug ( <b>1.66</b> )	>100 (n = 2)	>100 (n = 2)	> 32	> 32	
$(\text{Nva})^7$ -Lug ( <b>1.67</b> )	$35.7 \pm 0.21 \ (n = 3)$	$34.0 \pm 0.33 \; (n=3)$	> 32	> 32	
$(Nle)^7$ -Lug ( <b>1.68</b> )	$39.77 \pm 0.28 \ (n=3)$	$38.5 \pm 0.41 \ (n=3)$	> 32	> 32	
$(Trp)^7$ -Lug ( <b>1.69</b> )	>100 (n = 2)	>100 (n = 2)	> 32	> 32	
$(Phe)^7$ -Lug ( <b>1.70</b> )	>100 (n = 2)	>100 (n = 2)	> 32	> 32	
(L-cyclopropyl-Ala) <sup>7</sup> -	>100 (n = 2)	>100 (n = 2)	> 32	> 32	
Lug (1.71)					
$(L-N-Me-Val)^7-Lug$	$27.32 \pm 0.48 \ (n=3)$	$25.49 \pm 0.18  (n=3)$	32	32	
(5.29)					
(L-N-Me-Leu) <sup>7</sup> -Lug	$60.25 \pm 0.27 $ (n = 3)	$47.58 \pm 1.16  (n=3)$	> 32	> 32	
(5.30)					
$(Thr)^7$ -Lug ( <b>5.37</b> )	>100 (n = 2)	>100 (n = 2)	> 32	> 32	
(D-Leu) <sup>6</sup> -Lug ( <b>1.72</b> )	>100 (n = 2)	>100 (n = 2)	> 32	> 32	
(DTrp) <sup>6</sup> -Lug ( <b>1.46</b> )	$36.45 \pm 0.33 \; (n=3)$	$19.74 \pm 0.27 \ (n=3)$	32	32	
$(D-Phe)^6$ -Lug (1.73)	$50.29 \pm 0.29 \; (n=3)$	$68.06 \pm 1.16  (n=3)$	> 32	> 32	
(Leu) <sup>7</sup> -(Trp) <sup>6</sup> -Lug ( <b>5.44</b> )	>100 (n = 2)	>100 (n = 2)	> 32	> 32	

 $<sup>^</sup>a$  IC<sub>50</sub> values are given as the mean  $\pm$  standard deviation of three independent growth inhibition assays.

<sup>&</sup>lt;sup>b</sup> MIC determined using the broth microdilution assay, performed in triplicates according to CLSI guidelines.

# 6.2.2 Structure-activity relationships study of lugdunin and the analogues against *S. aureus*

#### 6.2.2.1 SAR study of alanine-scanning

Alanine-scanning as discussed in the previous chapter 3 is a useful tool to determine the importance of each residue on bioactivity. The amino acid at each position were replaced by the alanine without the change of stereo-configuration. In this project, (L-Ala)<sup>7</sup>-lugdunin (1.25) was used as the starting point for the design and synthesis of the alanine-scanning analogues, 3.11-3.15. Using the growth inhibition assay, the antimicrobial activity of the synthesized compounds was determined against both *S. aureus* SH1000 and USA300 JE2; the IC<sub>50</sub> values are recorded in Table 6.1. The acquired MIC values against both *S. aureus* SH1000 and USA300 JE2 are also reported in Table 6.1.

It was found that, compared to lugdunin (1.24) (IC<sub>50</sub> =  $25.42 \pm 0.45 \,\mu\text{M}$  against against *S. aureus* SH1000), only (Ala)<sup>7</sup>-Lug (1.25) (IC<sub>50</sub> =  $95.25 \pm 1.05 \,\mu\text{M}$  against against *S. aureus* SH1000) displayed potent antimicrobial activity but is *ca.* 4-fold less potent compared to lugdunin. Moreover, the alanine-scanning analogues 3.11-3.15 were all found to be inactive against both *S. aureus* SH1000 and USA300. The results indicate that substitution or modification at position 7 is tolerated but not with double substitutions. Hence, a further SAR study of analogues with modification at position 7 was carried out and the results are discussed in the next section.

# 6.2.2.2 SAR study of analogues modified at position 7

To establish SAR at position 7, several analogues were designed and synthesized. To determine the effect of the length of the hydrocarbon side chain, (Leu)<sup>7</sup>-Lug (1.65) and (Hle)<sup>7</sup>-Lug (1.66) were first introduced. The results showed that the (Leu)<sup>7</sup>-Lug (1.65) was the most potent

analogue among all the synthesized compounds (IC<sub>50</sub> = 6.47  $\pm$  0.14  $\mu$ M against *S. aureus* SH 1000 and 6.88  $\pm$  0.75  $\mu$ M against USA300 JE2). In fact, (Leu)<sup>7</sup>-Lug (**1.65**) is four-fold more active than lugdunin (**1.24**). However, (Hle)<sup>7</sup>-Lug (**1.66**) was found to be inactive, thus indicating a further lengthening of the hydrocarbon chain (by one methylene group) is detrimental. Moreover, to investigate the effect of linear versus branched side chains, (Nva)<sup>7</sup>-Lug (**1.67**) and (Nle)<sup>7</sup>-Lug (**1.68**) were then installed. With the same number of carbons in the side chain, norvaline and norleucine are the linear side-chain variants of valine and leucine, respectively. The antimicrobial activity of (Nva)<sup>7</sup>-Lug (**1.67**) (IC<sub>50</sub> = 35.7  $\pm$  0.21  $\mu$ M against SH1000 and 34.0  $\pm$  0.33  $\mu$ M against USA300 JE2) shows 1.5-fold less potent than lugdunin, while (Nle)<sup>7</sup>-Lug (**1.68**) is substantially less active, by approximately 6-fold, compared to the corresponding branched hydrocarbon variant, (Leu)<sup>7</sup>-Lug (**1.65**).

Subsequently, replacement of the hydrocarbon amino acid residue at position 7 with (hetero)aromatic or cyclic side chain was investigated, and thus (Trp)<sup>7</sup>-Lug (1.69), (Phe)<sup>7</sup>-Lug (1.70) and (L-cyclopropyl-Ala)<sup>7</sup>-Lug (1.71) were synthesized. These three analogues were found to be inactive. It is hypothesized that the (hetero)aromatic ring at position 7 might be too bulky to the neighbouring thiazolidine ring. Hence, amino acids with bulky side chains should be avoided at position 7. Unexpectedly, the analogue (L-cyclopropyl-Ala)<sup>7</sup>-Lug (1.71), essentially a cyclic variant of valine, was also found to be inactive.

As discussed in the previous chapter, the hydrophobicity of the structure might be an important factor for antimicrobial activity. Thus, *N*-methylated amino acid was then considered as the substitution at position 7. The (L-*N*-Me-Val)<sup>7</sup>-Lug (**5.29**) and (L-*N*-Me-Leu)<sup>7</sup>-Lug (**5.30**) were introduced for the SAR study. As the result shown in Table 6.1, replacement with *N*-methyl

amino acid led to similar or less active compounds, thus indicating that tertiary amide bond is tolerated here. The effect on the overall structural conformation will be investigated in the future. Finally, (Thr)<sup>7</sup>-Lug (5.37), with a hydroxyl group in the hydrocarbon side chain was prepared and found to be inactive, thus indicating that a hydrophilic moiety within the hydrocarbon side chain is not tolerated.

#### 6.2.2.3 SAR study of analogues modified at position 6

To also establish a focused SAR at position 6, three analogues were synthesized and evaluated. The amino acid at this position in lugdunin is D-valine. Since replacement at position 7 with Leu significantly increases the antimicrobial activity, (D-Leu)<sup>6</sup>-Lug (1.72) was first synthesized. However, the result showed an inactive analogue (Table 6.1). Furthermore, to investigate the effect of substitution by (hetero)aromatic amino acids, (D-Trp)<sup>6</sup>-Lug (1.46) and (D-Phe)<sup>6</sup>-Lug (1.73), in which the D-valine was replaced by D-tryptophan and D-phenylalanine were prepared. Besides, (D-Trp)<sup>6</sup>-Lug (1.46) was previously reported by Schilling *et al.*, so the preparation of the compound could be regarded as a control. Among the three analogues, (D-Trp)<sup>6</sup>-Lug (1.46) and (D-Phe)<sup>6</sup>-Lug (1.73) were found to be active against both *S. aureus* strains (IC<sub>50</sub> = 36.45 ± 0.33  $\mu$ M against SH1000 and 19.74 ± 0.27 against USA300  $\mu$ M for 1.46; IC<sub>50</sub> = 50.29 ± 0.29  $\mu$ M against SH1000 and 68.06 ± 1.16  $\mu$ M against USA300 for 1.73) while (D-Leu)<sup>6</sup>-Lug (1.73) was found to be inactive. Thus, although a branched hydrocarbon side chain, i.e., leucine residue, was favourable at position 7, substitution with a (hetero)aromatic side chain, i.e., Trp residue, is preferred at position 6.

Following the SAR assessment at position 6 and 7, the analogue (Trp)<sup>6</sup>-(Leu)<sup>7</sup>-Lug (**5.44**), with the combination of D-tryptophan at position 6 and L-leucine at position 7 was synthesized as the last analogue in this project. Unexpectedly, this combination analogue showed a complete

lack of antimicrobial activity.

# 6.2.3 Broth microdilution antimicrobial assessment of selected analogues

Among all the synthesized compounds, the analogues (L-Leu)<sup>7</sup>-Lug (1.65), (L-*N*-Me-Val)<sup>7</sup>-Lug (5.29), (D-Trp)<sup>6</sup>-Lug (1.46), as well as lugdunin (1.24) were further tested in different strains of *S. aureus*, including Mu50, Newman and PM64. The description of these strains was outlined earlier in section 6.3. The highest concentration applied in this assay was 64 μg/mL. Vancomycin was used as a positive control. The antimicrobial assessment results showed no significant difference between the five *S. aureus* strains. From Table 6.3, it was observed that the MIC value of vancomycin and analogues including (L-Leu)<sup>7</sup>-Lug (1.65) and (L-*N*-Me-Val)<sup>7</sup>-Lug (5.30) against Mu50 was higher than other strains because Mu50 is a VRSA strain with changes in the membrane thickness/composition. Moreover, the MIC values for each of the four compounds were identical against the other SH1000, USA300 JE2 and PM64. Gratifyingly, 1.65 is typically 4-fold more potent than lugdunin and the other two analogues, which included the most active analogue, 1.46 reported by Schilling *et al.*<sup>213</sup>

**Table 6.3** MIC values of the most potent analogues against different strains of *S. aureus*. MIC determined using the broth microdilution assay, performed in duplicate.

Compounds	MIC (μg/mL)					
	SH1000	USA300 JE2	Mu50	Newman	PM64	
Vancomycin	1 (n = 2)	2 (n = 2)	4 (n = 2)	2 (n = 2)	2 (n = 2)	
Lugdunin ( <b>1.24</b> )	32 (n = 2)	32 (n = 2)	32 (n = 2)	32 (n = 2)	32 (n = 2)	
$(L-Leu)^7-Lug (1.65)$	8 (n = 2)	8 (n = 2)	16 (n = 2)	16 (n = 2)	8 (n = 2)	
(L- <i>N</i> -Me-Val) <sup>7</sup> -Lug ( <b>5.29</b> )	32 (n = 2)	32 (n = 2)	64 (n = 2)	32 (n = 2)	32 (n = 2)	
(D-Trp) <sup>6</sup> -Lug ( <b>1.46</b> )	32 (n = 2)	32 (n = 2)	32 (n = 2)	32 (n = 2)	32 (n = 2)	

#### **6.3 Conclusions**

In summary, this chapter described the antimicrobial evaluation of lugdunin and analogues thereof which were synthesized in this project against different strains of *S. aureus*. The SAR study had been established with the results from the growth inhibition assay and broth microdilution assay.

The growth inhibition assay was performed by the use of *S. aureus* SH1000 and USA300 JE2. Vancomycin was used as the positive control in the assay. Percentage (%) growth of bacteria at 13 h was calculated and the IC<sub>50</sub> was then determined using GraphPad Prism. For the broth microdilution assay, a general broth microdilution method was established, and the minimum inhibitory concentration (MIC) values of all tested compounds was then obtained. Moreover, five different strains of *S. aureus* including SH1000, USA300 JE2, Newman, Mu50 and PM64 were used in the assay. Among them, SH1000 and Newman are methicillin-sensitive strains, USA300 JE2 and PM64 are methicillin-resistant strains, and Mu50 is a vancomycin-resistant MRSA.

For the compound (Ala)<sup>7</sup>-Lug (1.25) and its alanine-scanning analogues 3.11-3.15 (Figure 6.2), the antimicrobial activity were determined against both *S. aureus* SH1000 and USA300 JE2 using the growth inhibition assay. It was found that only (Ala)<sup>7</sup>-Lug (1.25) showed potent antimicrobial activity but was four-fold less active than lugdunin (1.24). In contrast, the alanine-scanning analogues 3.11-3.15 were all tested inactive against both *S. aureus* strains. The results indicate that substitution or modification at position 7 is tolerated but not simultaneous changes at two positions.

**Figure 6.2** Chemical structures of  $(Ala)^7$ -Lug (1.25) and its alanine-scanning analogues 3.11-3.15. Among them, 1.25 was the only active compound against *S. aureus*. The structural differences relative to lugdunin (1.24) are shown in highlight.

For the analogues in which replacement occurred at position 6, amino acid with branched side chain like leucine was found inactive while (hetero)aromatic side chain, such as tryptophan and phenylalanine were tested active (Figure 6.3), especially (D-Trp)<sup>6</sup>-lugdunin (1.46) showed similar activity as lugdunin. The analogue 1.46 was previously reported by Schilling *et al.*<sup>213</sup>

Thus, the analogue **1.46** was further tested against different strains of *S. aureus*. It was proposed that a hydrophobic heterocyclic ring might be more favourable for the future analogues design.

**Figure 6.3** Chemical structures of lugdunin analogues with the modifications at position-6. Analogues with substitution of D-leucine **1.72** and D-phenylalanine **1.73** were tested inactive and less active against *S. aureus* respectively, while (D-Trp)<sup>6</sup>-lugdunin (**1.46**), was found the most potent analogue of the modification at position 6. The structural differences relative to lugdunin (**1.24**) are shown in highlight

For the lugdunin analogues with replacement at the position 7, amino acid residues with branched hydrocarbon side chain was generally found to be more potent than those with (hetero)aromatic side chain. Moreover, *N*-methylated amino acid substitution were all found to be less active or inactive (Figure 6.4). Gratifyingly, (L-Leu)<sup>7</sup>-lugdunin (1.65), which is fourfold more active than lugdunin, was found to be the most active analogue among all synthesized compounds. However, all other analogues showed less active or inactive against *S*.

aureus. The SAR study at position 7 indicated that modification at this position might also be restricted due to the neighbouring thiazolidine ring. Therefore, the future work, including the design of new analogues and time-kill assay will be discussed in the next chapter.

**Figure 6.4** Chemical structures of lugdunin analogues with the modifications at position 7. R group was varied when different amino acid residues were used. Among them, (L-Leu)<sup>7</sup>-lugdunin (**1.65**) was found to be the most potent analogue within all synthesized analogues.

Furthermore, when tested against *S. aureus* SH1000, Figure 7.5 shows illustrative examples of the dose-response curves for lugdunin (**1.24**), (Ala)<sup>7</sup>-lugdunin (**1.25**), (Leu)<sup>7</sup>-Lug (**1.65**) and (D-Trp)<sup>6</sup>-Lug (**1.46**), from which the IC<sub>50</sub> values were calculated.

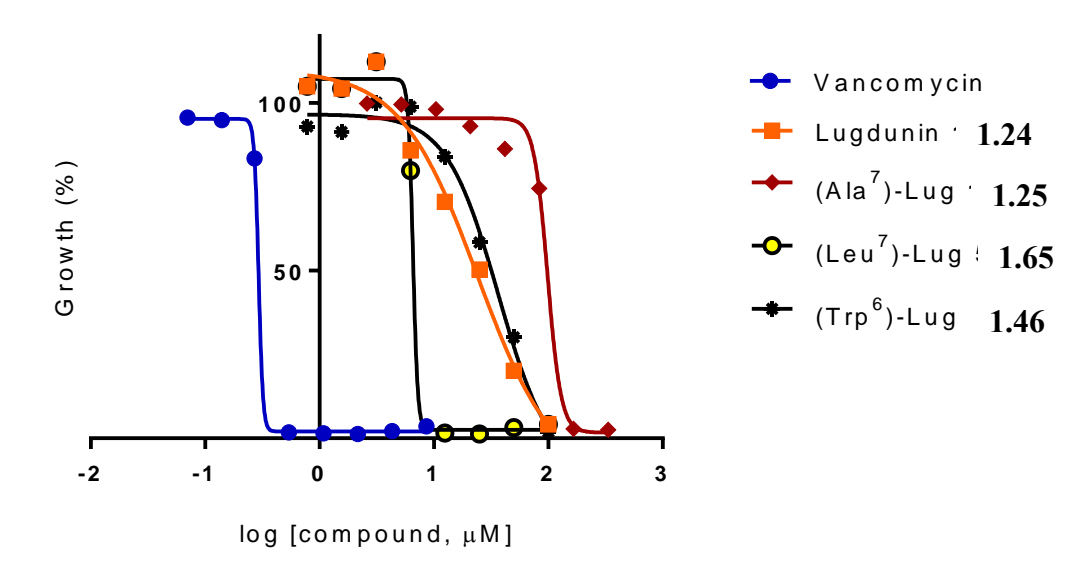


**Figure 7.5** Dose-response curve of lugdunin (1.24), (Ala)<sup>7</sup>-lugdunin (1.25), (Leu)<sup>7</sup>-Lug (1.65) and (D-Trp)<sup>6</sup>-Lug (1.46) against *S. aureus* SH 1000. The experiment was carried out with vancomycin as the positive control.

# Chapter 7

# General conclusions and future work

# 7.1 General conclusions

**Figure 7.1** Chemical structure of lugdunin (1.24) with the unique thiazolidine ring. The SAR study was focused on the modifications at position 6 and 7.

Lugdunin (1.24) is a novel non-ribosomally synthesized cyclic peptide which was first discovered and reported by Zipperer *et al.* in 2016 (Figure 7.1).<sup>20</sup> The structure of lugdunin contains an unique thiazolidine ring and the amino acids are with alternating D- and L-configuration.<sup>20</sup> Lugdunin is also the first antibiotic isolated from a bacterium *Staphylococcus lugdunensis* which resides primarily in the nasal cavity of humans. The MoA of lugdunin is broadly different to all antibiotics currently in clinical use. In a recent study, lugdunin was found to cause rapid and efficient translocation of protons across bacterial membrane, whilst maintaining membrane integrity.<sup>213</sup>

In the SAR study reported by and Schilling *et al.* in 2019, it was found that an unsubstituted thiazolidine, tryptophan, leucine, and the alternating D- and L-amino acid backbone were found to be essential (Figure 7.2).<sup>213</sup> Moreover, change of macrocyclic ring size were also found to be not permitted. A further SAR study had then been reported by Saur *et al.* in 2021.<sup>235</sup> It was

concluded that at position 2, hetero-containing polar motifs will lead to inactive in antimicrobial activity. At position 3, it was found that a hydrophobic aromatic ring was essential. At position 4, modest modifications such as D-IIe and D-Nva were tolerated while the bioisosteric similarity to leucine was necessary. At position 6, analogue with the replacement of D-Trp was the found to be the most potent compound, which displayed typically 2-fold higher potency than native lugdunin (Fofure 7.1).<sup>213</sup>

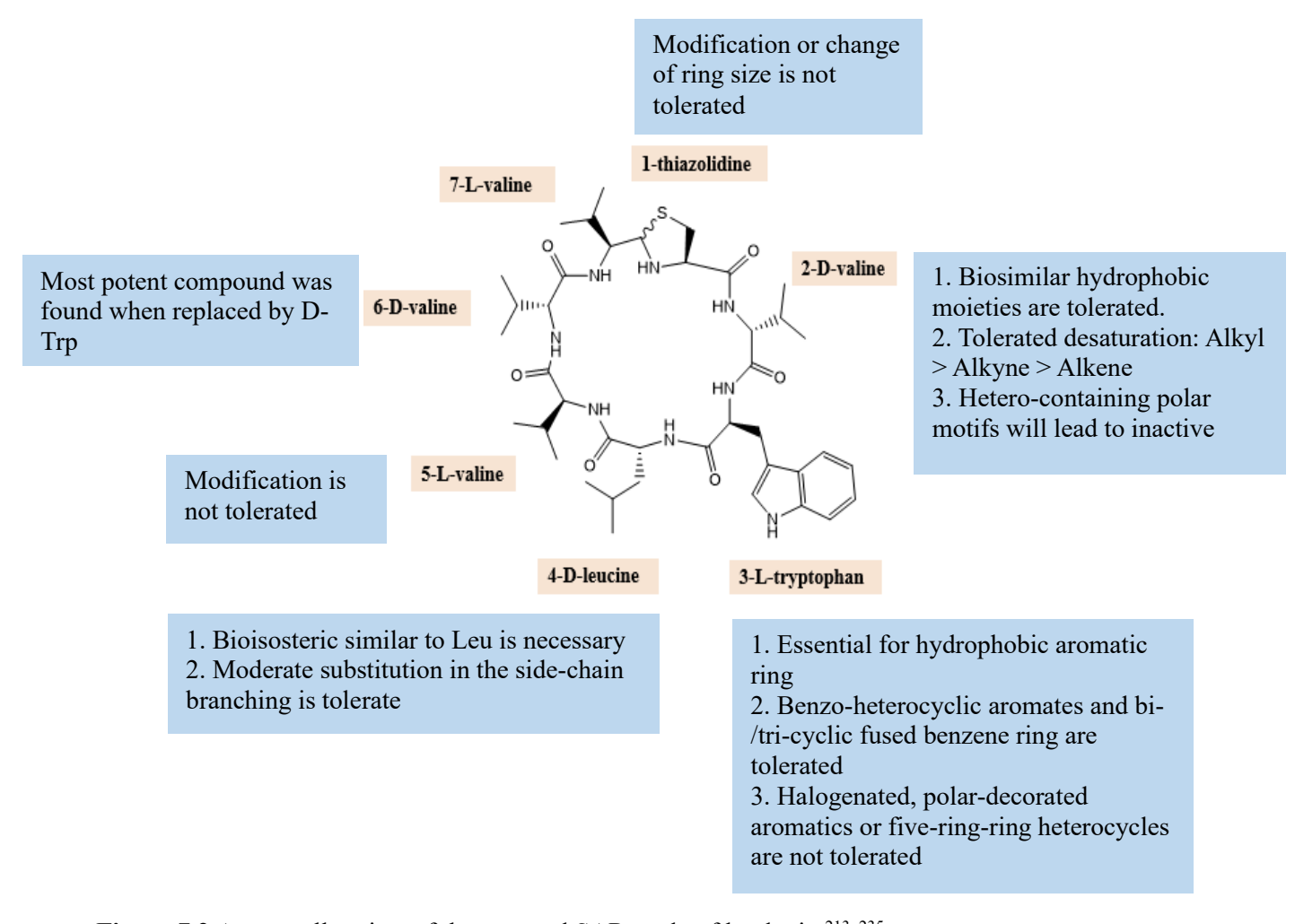


Figure 7.2 An overall review of the reported SAR study of lugdunin. 213, 235

Given the potential antimicrobial application of lugdunin, the design and synthesis of lugdunin analogues to develop more potent antimicrobials and to establish the SAR are thus the primary aims of the project outlined in this thesis. Since the lugdunin analogues with the modification

or substitution at position 6 have been extensively explored by Schilling *et al*, new analogues reported in this project will be focused on the modification at position 7, including the alanine-scanning. Moreover, different synthetic strategies for the total chemical synthesis of lugdunin and analogues thereof, as well as unique/modified amino acid building blocks are fully discussed. Subsequently, the SAR study obtained from the microbiological assessment of all synthesized compounds against different strains of *S. aureus* are outlined.

In this project, different methods for the synthesis of lugdunin and its analogues were investigated. Since the thiazolidine moiety was thought to be the key point of the structure, strategies were focused on the formation of the thiazolidine ring. several synthetic routes and various of resins were tried. Among them, the method via the preparation of the modified TG resin was adopted. The procedure to synthesize the modified TG resin was through the reaction between threonine and the different Fmoc-protected amino aldehydes. The amino aldehyde compounds were all synthesized via the DIBAL-H/CDI method. Then the expected linear peptide chains were assembled following the general Fmoc-SPPS protocol. The desired pure products were obtained after the resin cleavage, cyclization and the purification by HPLC. All synthesized compounds were tested their antimicrobial activities against different strains of *S. aureus* to obtain the IC<sub>50</sub> and MIC values (see Chapter 6). As the result, (L-Leu)<sup>7</sup>-lug (1.65) was found to be the most potent compound in this project.

To establish a full SAR study, several analogues with the modifications at position 7 were designed and synthesized. The original L-Val at this position was substituted with various L-amino acids such as Hle, Nva, Nle, Trp, Phe, cyclopropylanaline, Thr, N-Me-Val and N-Me-Leu. The result showed that a linear/branched side chain might be more tolerated than a cyclic/aromatic one. However, the SAR study at position 6 showed the oppisite result, which a

cyclic/aromatic side chain was found to be more potent.

### 7.1.1 Synthesis of Fmoc-N-methyl amino acids

Cyclic peptides with *N*-methylated amino acid residue(s) have been associated with their improved permeability across the epithelial membrane and good stability against enzymatic degradation.<sup>372</sup> The replacement of natural amino acids led to analogues with enhanced pharmacological properties, such as enzymatic stability, receptor selectivity, potency and bioavailability.<sup>372</sup> Thus, structural modification of the peptide backbone via *N*-methylation is a powerful tool to modulate pharmacokinetic and also the pharmacodynamic profile of peptides. The ability of *N*-methylated amide bonds to interact with complementary hydrophobic pocket(s) can result in an enhancement of membrane permeability.<sup>373</sup> Therefore, Fmoc-*N*-methyl-L-valine **4.24** and Fmoc-*N*-methyl-L-leucine **4.25** were synthesized to replace the original L-valine at position 7 of lugdunin.

Various synthetic routes for the preparing of N-methylated amino acids were described in Chapter 4, including the methods via  $\alpha$ -bromo acids, the Mitsunobu reaction, base-mediated alkylation and a unique protocol involving the formation of an 5-oxazolidinone intermediate. Among the various methods, the protocol reported by Freidinger  $et\ al.$  was adopted. Thus, a two-step reaction was established for the synthesis of N-Fmoc-protected N-methyl amino acids (Scheme 7.1).

Fmoc N OH 
$$C_6H_6$$
  $C_6H_6$   $C_6H_6$ 

Scheme 7.1 Synthesis of Fmoc-L-N-Me-Val-OH 4.24 and Fmoc-L-N-Me-Leu-OH 4.25.

# 7.1.2 Synthesis of Fmoc-L-homoleucine

To synthesize Fmoc-L-homoleucine for the preparation of lugdunin analogue (L-Hle)<sup>7</sup>-lug (**5.2**), a method via the use of a Ni (II)-Gly-BPB complex was established (Scheme 7.2). The chiral glycine equivalent Ni(II)-glycine Schiff's base complex **4.29**, originally reported by Belokon *et al.*<sup>352</sup>, was synthesised as a key intermediate to control the stereochemistry of the amino acids. The benzylation of (*S*)-proline (**4.26**) was followed by the conversion of **4.27** into the BPB-HCl salt **4.28**. Finally, the alkylated complexes **4.35** were disassembled in a microwave-assisted reactor under acidic conditions and the released amino acids were Fmocprotected with Fmoc-Oxyma, to afford the desired product **4.37**. The yields of each reaction step was found to be within the range of 47-94 %, and the final product, Fmoc-L-Hle-OH (**4.37**) was obtained in an overall yield of 13 %.

Scheme 7.2 An overall synthetic route for the preparation of Fmoc-L-homoleucine.

# 7.1.3 Total synthesis of lugdunin and analogues thereof

As outlined in Chapter 2, the formation of the thiazolidine ring is the key part in the synthetic strategy. Thus, several methods were discussed in Chapter 2, including the construction of the thiazolidine dipeptide building blocks and the utilization of different resins or polymer supports.

In the first method, the thiazolidine dipeptide was prepared as a building block (Scheme 7.3). Moreover, a rapid and efficient one-pot synthetic protocol established by Jakov *et al.* was

adopted for the synthesis of amino aldehydes (Scheme 7.3). Herein, Fmoc/Boc-L-valine and Fmoc/Boc-L-alanine were used as the initial building blocks. As outlined in Chapter 2, the synthesized compounds **2.4**, **2.12 and 2.16-2.17** were subsequently used for the preparation of thiazolidine building blocks **2.5 and 2.19-2.21** (Scheme 7.3). However, due to the poor solubility of compounds **2.5 and 2.19-2.21** in all evaluated solvents, including those commonly used in Fmoc-SPPS, an alternative method via the use of aldehyde-generating resin was evaluated.

2.9: 
$$R_1 = CH_3$$
,  $R_2 = Fmoc$  2.12:  $R_1 = CH_3$ ,  $R_2 = Fmoc$  (85 %) 2.19:  $R_1 = CH_3$ ,  $R_2 = Fmoc$  (72 %) 2.14:  $R_1 = CH_3$ ,  $R_2 = Fmoc$  2.16:  $R_1 = CH_3$ ,  $R_2 = Fmoc$  (83 %) 2.20:  $R_1 = CH_3$ ,  $R_2 = Fmoc$  (75 %) 2.2:  $R_1 = CH(CH_3)_2$ ,  $R_2 = Fmoc$  2.4:  $R_1 = CH(CH_3)_2$ ,  $R_2 = Fmoc$  (83 %) 2.5:  $R_1 = CH(CH_3)_2$ ,  $R_2 = Fmoc$  (78 %) 2.15:  $R_1 = CH(CH_3)_2$ ,  $R_2 = Fmoc$  (72 %) 2.21:  $R_1 = CH(CH_3)_2$ ,  $R_2 = Fmoc$  (72 %) 2.22:  $R_1 = CH(CH_3)_2$ ,  $R_2 = Fmoc$  (73 %) 2.23:  $R_1 = CH(CH_3)_2$ ,  $R_2 = Fmoc$  (73 %) 2.24:  $R_1 = CH(CH_3)_2$ ,  $R_2 = Fmoc$  (73 %) 2.25:  $R_1 = CH(CH_3)_2$ ,  $R_2 = Fmoc$  (73 %) 2.21:  $R_1 = CH(CH_3)_2$ ,  $R_2 = Fmoc$  (73 %) 2.21:  $R_1 = CH(CH_3)_2$ ,  $R_2 = Fmoc$  (73 %)

**Scheme 7.3** Synthesis of Fmoc-protected amino aldehydes and relative thiazolidine dipeptide building blocks. The amino aldehydes were prepared via the CDI/DIBAL-H method.

As alternative methods, two linker-resins, Weinreb AM resin and the TG resin were investigated. Based on better yields and simpler operation, the application of the TG resin was found to be most efficient and therefore adopted for the synthesis of lugdunin and all analogues thereof. Scheme 7.4 shows the synthetic protocol to prepare the general and modified TG resin, where different Fmoc-amino aldehydes were pre-loaded. All Fmoc-amino aldehydes were synthesized following the protocol showed in the above Scheme 7.3. Subsequently, the desired peptidic compounds, including lugdunin and its analogues were assembled following the general Fmoc-SPPS procedures. All synthesized compounds were started at a 0.1 mmol of Rink amide AM resin, and the DMF-wash and Fmoc-deprotection reaction were carried out using a manual peptide synthesizer.

1.64, 3.8, 5.5-5.6, 5.13-5.14, 5.23-5.25, 5.33-5.34, 5.45

$$R_1 = H, R_2 =$$
 $R_1 = H, R_2 =$ 
 $R_1 = CH_3, R$ 

**Scheme 7.4** Synthesis of the modified TG resins with different pre-loaded Fmoc-amino aldehydes. R<sub>1</sub> and R<sub>2</sub> refer to the amino acid side chains used in this project including L-Val, L-Ala, L-Leu, L-Hle, L-Nva, L-Nle, L-Trp, L-Phe, L-CPA, L-N-Me-Val, L-N-Me-Leu and L-Thr.

To investigate the importance of each amino residue on the bioactivity, alanine-scanning was first introduced. Hence, the (L-Ala)<sup>7</sup>-lugdunin (1.25), which the L-valine at position 7 in lugdunin was replaced by L-alanine was first synthesized. Due to the less steric hindrance and better yields of (L-Ala)<sup>7</sup>-lugdunin compared to lugdunin, (L-Ala)<sup>7</sup>-lugdunin (1.25) was used as the starting point for the alanine-scanning study. Thus, the alanine scanning analogues 3.11-3.15 were subsequently prepared.

A further SAR study on the modifications at position 6 and 7 was then carried out. Figure 7.3

shows the structure of lugdunin and all the analogues with the modification at position 6 or 7. Given the limited assessment of the modification at position 7, a SAR study that focused on this position was carried out in this project and outlined in detail in Chapters 5 and 6. To first understand the effect of the length of the side chain, (L-Leu)<sup>7</sup>-lugdunin (1.65) and (L-Hle)<sup>7</sup>-lugdunin (1.66) were synthesized. Then (L-Nva)<sup>7</sup>-lugdunin (1.67) and (L-Nle)<sup>7</sup>-lugdunin (1.68) were prepared to compare the effects of a linear and branched side chain. Next, (L-Trp)<sup>7</sup>-lugdunin (1.69), (L-Phe)<sup>7</sup>-lugdunin (1.70), and (L-CPA)<sup>7</sup>-lugdunin (1.71) were synthesized to evaluate the effects of cyclic/aromatic ring substitutions.

To further investigate the effect of polarity on the antimicrobial activity, (L-*N*-Me-Val)<sup>7</sup>-lugdunin (**5.29**), (L-*N*-Me-Leu)<sup>7</sup>-lugdunin (**5.30**) and (L-Thr)<sup>7</sup>-lugdunin (**5.37**) were designed and synthesized. *N*-methylated amino acids were introduced due to the advantages including conformational changes, improved proteolytic stability, higher lipophilicity, and improved pharmacokinetic properties in peptide drugs. The synthetic method of Fmoc-*N*-methyl amino acids had been discussed in Chapter 4.

Modification at position 7: 7-L-Leu, 7-L-Hle, 7-L-Nva, 7-L-Nle, 7-L-Trp, 7-L-Phe, 7-L-CPA, N-Me-7-Val, N-Me-7-Leu, 7-L-Thr 7-L-valine 1-Thiazolidine Combined modification at position 6 and 7: 2-D-valine 6-D-valine 6-D-Trp-7-L-Leu HN Modification at position 6: 5-L-valine 3-L-tryptophan 6-D-Leu, 6-D-Trp, 6-D-Phe 4-D-leucine

**Figure 7.3** Structure of lugdunin and all modifications at position 6 or/and 7.

#### 7.1.4 Antimicrobial assessment of lugdunin and analogues thereof

The growth inhibitory assay was used to obtain the IC<sub>50</sub> values of the analogues against S. aureus SH1000 and USA300 JE2. Table 7.1 shows the IC<sub>50</sub> and MIC values for the key compounds including lugdunin (1.24), (L-Leu)<sup>7</sup>-lugdunin (1.65), (L-N-Me-Val)<sup>7</sup>-lugdunin (5.29) and (D-Trp)<sup>6</sup>-lugdunin (1.46) against different strains of S. aureus. It was found that (L-Leu)<sup>7</sup>-lugdunin (1.65) was the most potent analogue with an activity of four-fold higher than the natural product lugdunin (1.24). The analogues with shorter or linear hydrocarbon side chains were observed to be inactive or of lower antimicrobial activity. Moreover, alteration with amino acids comprising cyclic/aromatic and a 3-membered hydrocarbon ring, i.e. tryptophan, phenylalanine and cyclopropyl alanine, respectively, were also not tolerated. Furthermore, the compounds 5.29 and 5.30, comprising of N-methylated amino acids, were both tested less active than ludunin when against S. aureus. The results might indicate that the modification at position 7 is also quite restricted, since only a substitution with a branched and

adequate length of side-chain gave a more potent compound.

Unlike modification at position 7, analogues (Trp)<sup>6</sup>-Lug (**1.46**) was found more active than the leucine substituted analogue (Leu)<sup>6</sup>-Lug (**1.72**). The results indicated that the alteration with a cyclic/aromatic structure is more tolerated than a branched structure at position 6. In fact, Schilling *et al.* have previously reported the marginally improved potency of (Trp)<sup>6</sup>-Lug (**1.46**). Unexpectedly, the analogue (D-Trp)<sup>6</sup>-(Leu)<sup>7</sup>-Lug (**5.44**), which is a combination of the features **1.46** and **1.65**, were tested inactive against *S. aureus*.

All the analogues were also tested of their MIC values against clinically important strains of *S. aureus* (SH1000 and USA300 JE2) by using CLSI broth microdilution method. Then a further investigation of the MIC values against different strains of *S. aureus* (Mu50, Newman and PM64) for the four most potent analogues including lugdunin (1.24), (Leu)<sup>7</sup>-Lug (1.65), (L-*N*-Me-Val)<sup>7</sup>-Lug (5.29), and (D-Trp)<sup>6</sup>-Lug (1.46) were determined. The result showed no significantly difference on the MIC values against various strains of *S. aureus*.

**Table 7.1** *In vitro* antimicrobial activity of lugdunin and analogues thereof and vancomycin against *S. aureus* SH1000 and USA300 JE2.

Compounds	IC <sub>50</sub> (μM)		MIC (μg/ml)				
	S. aureus		S. aureus				
	SH1000	USA300 JE2	SH1000	USA300 JE2	Mu 50	Newman	PM64
Vancomycin	$1.31 \pm 0.28$	$0.62 \pm 0.01$	1	2	4	2	2
	(n=3)	(n=3)	(n=2)	(n=2)	(n=2)	(n=2)	(n=2)
Lugdunin (1.24)	$25.42 \pm 0.45$	$27.58 \pm 0.62$	32	32	32	32	32
	(n = 3)	(n=3)	(n=2)	(n = 2)	(n = 2)	(n = 2)	(n = 2)
(Leu) <sup>7</sup> -Lug	$6.47 \pm 0.14$	$6.88 \pm 0.75$	8	8	16	16	8
(1.65)	(n=3)	(n=3)	(n=2)	(n=2)	(n = 2)	(n=2)	(n=2)
$(L-N-Me-Val)^7-$	$27.32 \pm 0.48$	$25.49 \pm 0.18$	32	32	64	32	32
<b>Lug</b> (5.29)	(n = 3)	(n=3)	(n = 2)	(n=2)	(n = 2)	(n = 2)	(n = 2)
(D-Trp) <sup>6</sup> -Lug	$36.45 \pm 0.33$	$19.74 \pm 0.27$	32	32	32	32	32
(1.46)	(n = 3)	(n = 3)	(n = 2)	(n = 2)	(n=2)	(n = 2)	(n=2)

Among all the synthesized compounds, analogues (L-Leu)<sup>7</sup>-Lug (1.65), (*N*-Me-L-Val<sup>7</sup>)-Lug 5.30, (D-Trp<sup>6</sup>)-Lug 1.46, as well as lugdunin 1.24 were further tested against different strains of *S. aureus*, including Mu50, Newman and PM64. The phenotypic features of these strains were described earlier in Chapter 6. Vancomycin was used as a positive control. The results showed no significant difference between the five *S. aureus* strains. From Table 7.2, it was observed that the MIC value of vancomycin and the analogues (L-Leu<sup>7</sup>)-Lug 1.65 and (*N*-Me-L-Val<sup>7</sup>)-Lug 5.30 against Mu50 was higher than other strains because Mu50 is a VRSA strain with changes in the membrane thickness/composition. Moreover, the MIC values for each of the four compounds were identical against the other SH1000, USA300 JE2 and PM64. Gratifyingly, (L-Leu<sup>7</sup>)-Lug 1.65 is typically 4-fold more potent than lugdunin and the other two analogues, which included the most active analogue, (D-Trp<sup>6</sup>)-Lug 1.46 reported by Schilling *et al.*<sup>213</sup>

# 7.1.5 A brief overview on SAR study

From the published literature, the MoA of lugdunin and SAR studies on analogues with modifications at position 2, 3, 4 and 6 had been reported.<sup>20, 231, 235</sup> Since the SAR study on position 7 had not been established, this project is focused on the designed and synthesis of analogues with modifications at this position.

To invstigate the effect of the length of the hydrocarbon side chain, analogues including (Ala)<sup>7</sup>-Lug (1.25), (Leu)<sup>7</sup>-Lug (1.65), (Hle)<sup>7</sup>-Lug (1.66), (Nva)<sup>7</sup>-Lug (1.67) and (Nle)<sup>7</sup>-Lug (1.68) were synthesized. It was found that the antimicrobial activity generally increased as the length of the hydrocarbon side chain increased. However, the potency was decreased when the amount of carbon was more than four. (Leu)<sup>7</sup>-Lug (1.65) was found the most potent analogue among all the synthesized compounds (IC<sub>50</sub> =  $6.47 \pm 0.14 \mu M$  against and  $6.88 \pm 0.75$  against USA300 JE2), which is four-fold more active than lugdunin. Moreover, the antimicrobial results of (Nva)<sup>7</sup>-Lug (1.67) and (Nle)<sup>7</sup>-Lug (1.68) showed that a branched side chain is more tolerate compared to a linear side chain.

Subsequently, analogues with cyclic/aromatic side chains were investigated, and thus (Trp)<sup>7</sup>-Lug (1.69), (Phe)<sup>7</sup>-Lug (1.70) and (L-cyclopropyl-Ala)<sup>7</sup>-Lug (1.71) were synthesized. The three analogues were all found to be inactive. It is hypothesized that the cyclic/aromatic ring at position 7 might be too bulky to the neighbouring thiazolidine ring and hence lead to inactive.

As discussed in the previous chapter, the hydrophobicity of the structure might be a key factor for antimicrobial activity. Thus, *N*-methylated amino acids were then considered. The (L-*N*-Me-Val)<sup>7</sup>-Lug (**5.29**) and (L-*N*-Me-Leu)<sup>7</sup>-Lug (**5.30**) were synthesized for the SAR study. As a result, replacement with *N*-methyl amino acid led to similar or less active compounds, thus

indicating that tertiary amide bond is tolerated here.

At position 6, a brief SAR study were also established. (D-Leu)<sup>6</sup>-Lug (1.72), (D-Trp)<sup>6</sup>-Lug (1.46) and (D-Phe)<sup>6</sup>-Lug (1.73) were designed and synthesized. The result indicated that substitution with a cyclic/aromatic side chain is preferred at this position.

From the antimicrobial test of all synthesized compounds, it is thought that modifications at position 6 and 7 are tolerated but might be still restricted. At position 7, a branched and suitable length of side chain is preferred. At position 6, it was found that a cyclic/aromatic side chain is more favourable.

#### 7.2 Future work

# 7.2.1 Further investigation into the residue at position 7

Although the modification at the position 7 of lugdunin is known to be limited, the discovery of the potent analogue (Leu)<sup>7</sup>-Lug (1.65) indicated the possibility to develop analogues with more potent antimicrobial activity. Thus, based on the discusion before, the design strategy will be focused on the substitution of amio acids with different side chains. Figure 7.4 shows the design of several modified Fmoc-amino acids for replacement at position 7. Compound 7.1 with the substitution of isolecine was first considered due to its same chemical composition as leucine but with a different branch configuration. Then based on the leucine structure, analogues 7.2 is designed as unsaturated side chain with the expectation to increase the hydrophobicity. With the synthetic method via the use of Ni(II)-Gly-BPB complex, Fmoc-protected unnatural amino acid 7.2 could be obtained following the method reported by Belokon *et al.*<sup>352</sup>

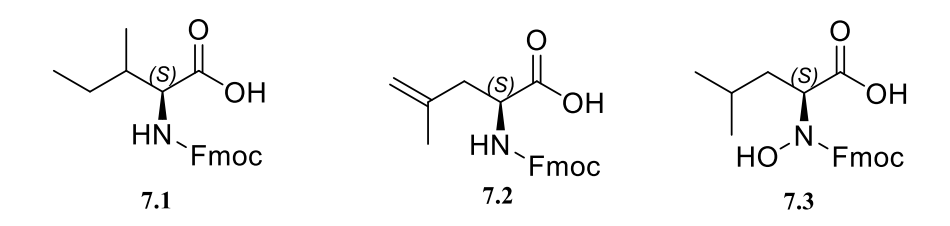


**Figure 7.4** Proposed Fmoc-amino acids used for substitution at the position 7.

Compounds **7.3** is designed as a *N*-hydroxy amino acid. Although uncommon relative to *N*-alkyl substituents, peptides harboring main-chain *N*-hydroxy groups exhibit unique conformational preferences and biological activities.<sup>373</sup> The *N*-hydroxy amino acid residue is encountered in several natural metabolites and is biosynthetic precursors to structurally complex non-ribosomal peptides.<sup>373</sup> Several *N*-hydroxy peptide (NHP) natural products exhibit potent antibacterial properties, cancer cell cytotoxicity, or activity against endogenous hormone receptors.<sup>373</sup> To synthesis Fmoc-*N*-hydroxy-L-leucine (**7.3**), a proposed synthetic route reported by Antonia and Ruggero will be attempted (Scheme **7.5**).<sup>374</sup>

**Scheme 7.5** Proposed protocol for the synthesis of Fmoc-*N*-hydroxy-L-leucine.

The new approach involved the direct oxyfunctionalization of a readily available primary amino acid to the corresponding *N*-hydroxy amino acid by the use of dioxirane via an oxidation reaction. With the advantages of high activity and selectivity, neutral pH and ease of product isolation, dioxirane is used as an efficient oxidants.<sup>375</sup>

Moreover, to prevent the deprotection of the Fmoc protection group during the hydrolysis of the methyl ester, a selective condition will be considered. Therefore, a synthetic route reported by Nicolaou *et al.* will be attempted.<sup>375</sup> It is a selective method under mild conditions involving the use of trimethyltin hydroxide (Me<sub>3</sub>SnOH).<sup>375</sup> In their study, Fmoc-D-Ala-OMe was hydrolysed to its corresponding carboxylic acid with complete retention of the Fmoc protecting group in a yield of 75%.<sup>376</sup> Overall, three new lugdunin analogues have been proposed for the future investigation and a further SAR study (Figure 7.5).

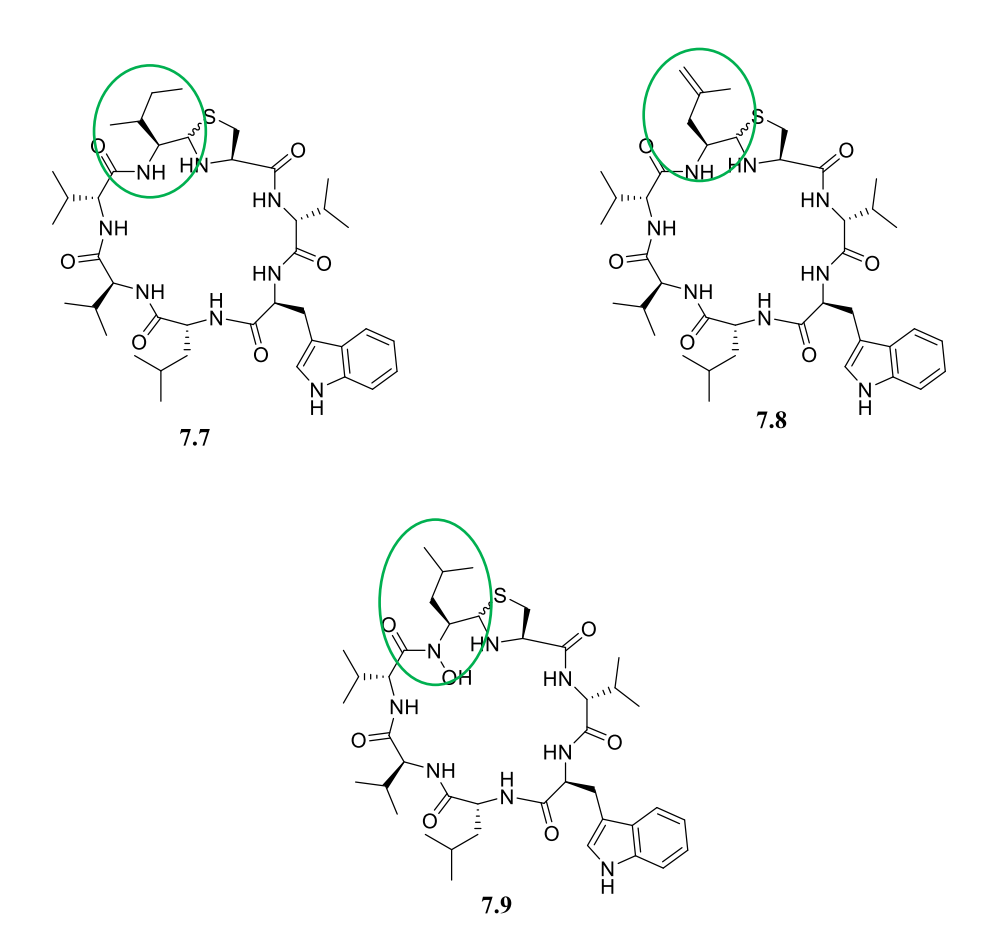
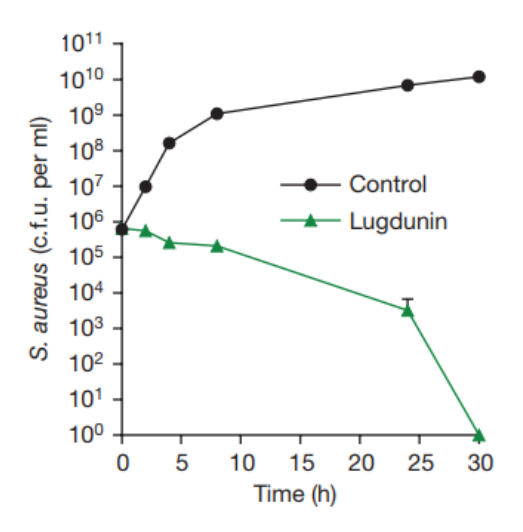


Figure 7.5 Proposed new lugdunin analogues 7.7-7.9 for the future investigation.

# 7.2.2 Evaluation of lugdunin analogues by time-kill assay

The difference between bactericidal and bacteriostatic is that the former is referred to antibacterial agents which kill bacteria while the later could only prevent or suspend bacterial growth. In the previous section, the MIC and IC<sub>50</sub> values had indicated the *in vitro* potency of the lugdunin and its analogues against various *S. aureus* strains. From the growth curves, the growth of the bacteria in the presence of the tested compounds at different concentrations are observed. In fact, Zipperer *et al.* reported that lugdunin was bactericidal against methicillin-resistant *S. aureus* with complete killing at  $10 \times \text{MIC}$  (Figure 7.6).<sup>20</sup>



**Figure 7.6** The time-killing curve of lugdunin against *S. aureus* reported by Zipperer *et al.* Incubation of *S. aureus* with a  $10 \times MIC$  of lugdunin leads to complete killing of the inoculum after 30 h.<sup>20</sup>

For a further investigation into whether the analogues reported in this thesis exert a bacteriostatic or bactericidal effect, a time-kill assay will be utilised to investigate the killing kinetics of the tested compounds. The killing kinetics of the analogues will be assessed using the two strains, *S. aureus* SH1000 and USA300 JE2, and using 4x MIC of the test compound or 4x MIC of vancomycin. Viable counts, i.e. CFU/mL will be determined at 0, 1, 2, 4, 6, 8 and 24 h. Consequently, a compound is considered bactericidal if there is a  $\geq$ 3 log<sub>10</sub> reduction in CFU/mL relative to the starting inoculum.

# 7.2.3 Determination of logP values for synthesized compounds

Since it had been mentioned earlier that the mechanism of action of lugdunin is due to the proton translocation, it is thought that the hydrophobic property might affect the antimicrobial activity. Thus, the measurement of logP could be a further proof for our SAR study. LogP is an important molecular physical property that impacts a wide range of systems. Using prediction of logP before a substance is even synthesized offers a means to guide scientists toward more fruitful research an development.

Lipophilicity can help scientists predict and understand the transport and impact of chemicals in physiological and ecological systems.<sup>377</sup> LogP values are important to many industries and areas of research in determining how to deliver or eliminate chemical substances to/from specific sites, as well as limiting unwanted dispersal of chemicals through the environment.<sup>378</sup>

The partition coefficient of a compound can be experimentally measured by a variety of methods. The two most common methods are Shake Flask and HPLC.<sup>379</sup> The Shake Flask Method, suitable for the broadest range of solutes, is rather time-consuming, though generally thought to be the most accurate. High performance liquid chromatography (HPLC) is a faster method that can be used when the chemical structure of the solute is known.<sup>379</sup>

Prediction of logP is another method to obtain the information. Software, such as ACD/logP, uses algorithms to calculate the logP of a compound by the sum of its fragments.<sup>380</sup> Prediction is an useful resource because it can be done without the presence of a compound sample. It is used, even by groups that carry out measurements of logP, to plan experiments and verify results. Table 7.2 shows the predicted ClogP obtained from chemdraw of all synthesized compounds in this project.

 Table 7.2 Predicted ClogP obtained from chemdraw.

Compounds	ClogP		
Lugdunin 1.24	6.74		
(Ala) <sup>7</sup> -Lug (1.25)	5.81		
(Ala) <sup>7</sup> -(Ala <sup>2</sup> )-Lug (3.11)	4.88		
(Ala) <sup>7</sup> -(Ala <sup>3</sup> )-Lug (3.12)	4.40		
(Ala) <sup>7</sup> -(Ala <sup>4</sup> )-Lug (3.13)	4.35		
(Ala) <sup>7</sup> -(Ala <sup>5</sup> )-Lug (3.14)	4.88		
(Ala) <sup>7</sup> -(Ala <sup>6</sup> )-Lug (3.15)	4.88		
(Leu) <sup>7</sup> -Lug (1.65)	7.26		
(Hle) <sup>7</sup> -Lug (1.66)	7.79		
(Nva) <sup>7</sup> -Lug (1.67)	6.87		
(Nle) <sup>7</sup> -Lug (1.68)	7.39		
(Trp) <sup>7</sup> -Lug (1.69)	7.37		
(Phe) <sup>7</sup> -Lug (1.70)	7.38		
(L-cyclopropyl-Ala) <sup>7</sup> -Lug (1.71)	6.78		
(L-N-Me-Val) <sup>7</sup> -Lug (5.29)	7.28		
(L-N-Me-Leu) <sup>7</sup> -Lug (5.30)	7.81		

(Thr) <sup>7</sup> -Lug (5.37)	5.78
(D-Leu) <sup>6</sup> -Lug (1.72)	7.81
(DTrp) <sup>6</sup> -Lug (1.46)	7.76
(D-Phe) <sup>6</sup> -Lug (1.73)	7.77
(Leu) <sup>7</sup> -(Trp) <sup>6</sup> -Lug (5.44)	8.29

For the future work, efforts will be focusing on more analogues at position 7 and the measurement of LogP will be attempted to establish a more detail SAR study. Moreover, to investigate whether the synthesized analogues exert a bacteriostatic or bactericidal effect, a time-kill assay will also be utilised.

# 7.3 Summary

Lugdunin (1.24) was reported as a potent antimicrobial agent by Zipperer *et al.*<sup>20</sup> Researches of lugdunin on its mode of action and SAR study were also pulished by schilling *et al.* and Saur *et al.* respectively.<sup>213,235</sup> This project is focused on the SAR study at position 6 and 7, and the antimicrobial activity against various strains of *S. aureus*.

For the chemical synthesis of analogues, the method via the preparation of modified TG resin was adopted in the project. The Fmoc-protected amino aldehydes were all synthesized through the reaction with DIBAL-H/CDI.

Among all the synthesized compounds, 3.11-3.15 were designed as the alanine-scanning

analogues of (L-Ala)<sup>7</sup>-lug (1.25). 1.65-1.71, 5.30-5.31 and 5.41 were designed as the analogues with modifications at position 7. 1.46, 1.72-1.73 and 5.48 were synthesized for the SAR study at position 6. For the bioactivity test, all compounds were tested for against *S. aureus* SH1000 and USA300 JE2 and the IC<sub>50</sub> and MIC values were then obtained. A further antimicrobial test against more strains of *S. aureus* incliding Mu50, Newman and PM64 were subsquently taken for lugdunin (1.24), (L-Leu)<sup>7</sup>-lug (1.65), (L-*N*-Me-Val)<sup>7</sup>-lug (5.30) and (D-Trp)<sup>6</sup>-lug (1.46). Among all analogues, (L-Leu)<sup>7</sup>-lug (1.65) was found to be the most poten compound and showed 4-fold more active than lugdunin (1.24). Figure 7.7 shows a brief overview of the SAR study form literatures and this project.

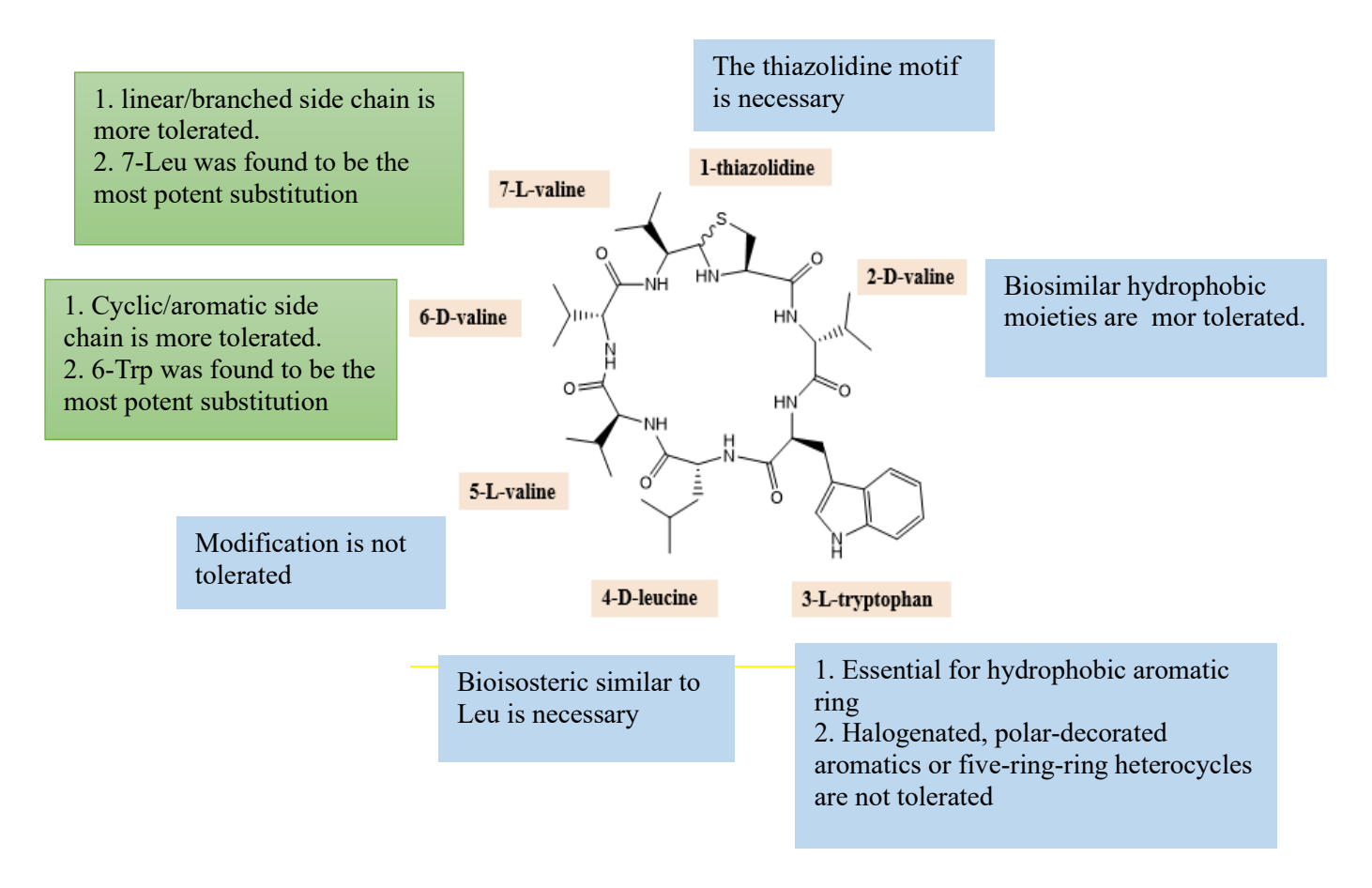


**Figure 7.7** An outline of the SAR study of lugdunin.<sup>213, 235</sup> The key findings showed in blue and green are from literatures and this project respectively.

# **Chapter 8**

# **Experimental**

#### 8.1 Methods and materials

Chemicals were purchased from Sigma Aldrich, Acros Organic. Silica gel for column chromatography was purchased from Acros Organic. Thin-layer chromatography (TLC, Silica gel 60 F<sub>254</sub>, aluminum silica plates) was purchased from Merck

All general solvents were either reagent or high performance liquid chromatography (HPLC) grade and were purchased from Fisher Scientific. For some dry reactions, the anhydrous grade solvents were purchased from Acros Organic and used directly. Solvents for NMR such as deuterated chloroform (CDCl<sub>3</sub>), deuterated dimethylformamide (d<sub>7</sub>-DMF), Deuterated dimethyl sulfoxide (d<sub>6</sub>-DMSO) and deuterated water (D<sub>2</sub>O) were purchased from Cambridge Isotope Laboratories Inc.

Melting points (°C) were determined with an electrical melting point apparatus (Gallenkamp 3A 3790) and are uncorrected. LCMS were recorded on a Shimadzu UFLCXR HPLC system combined with an Applied Biosystems MDS SCIEX API2000 electrospray ionisation mass spectrometer. The column used was a Gemini 3 μm C<sub>18</sub> 110Å, LC column (50 x 2 mm) and the solvent system was an increasing gradient (5 to 95% over 5 minutes) of acetonitrile in water containing 0.1% formic acid, flowing at 0.5 mL/min. A Bruker MicroTOF II mass spectrometer operating in positive-ion mode was employed to obtain high resolution mass spectra (HRMS). Optical rotation was measured in a 0.25 dm polarimeter cell with a Bellingham & Stanley ADP-220 polarimeter and concentration (c) of the compound was given in g/100 mL.

 $^{1}$ H NMR spectra were recorded with a Bruker AVANCE 400 spectrometer or Bruker AVANCE (III) 500 spectrometer, operating at 400.13 MHz and 500.23 MHz, respectively.  $^{13}$ C NMR were recorded with a Bruker AVANCE 400 spectrometer operating at 100.62 MHz. Unless stated otherwise, all spectra were obtained at 298 K. Chemical shifts (δ) are expressed in parts per million (ppm) relative to the residual proton signals of specified deuterated solvents. Coupling constants (J) are given in Hertz (Hz) and the multiplicity of a signal is indicated as br (broad), s (singlet), d (doublet), t (triplet), q (quartet), m (multiplet), etc. 2D spectra ( $^{1}$ H- $^{1}$ H COSY and

<sup>1</sup>H-<sup>13</sup>C HSQC) were used to facilitate <sup>1</sup>H-NMR assignments where necessary.

Solid-phase peptide synthesis (SPPS) was performed with a NovaSyn® GEM manual peptide synthesizer (Novabiochem) coupled to a Gilson 115 UV detector. All acylation reactions were carried out in an Omnifit<sup>TM</sup> Benchmark column assembly (150 x 10 mm). Peptide synthesis grade DMF and anhydrous solvents were utilised in all peptide synthesis steps. NovaSyn® GEM manual peptide synthesizer (Novabiochem) with Gilson 115 UV detector and an OmnifitTM Benchmark column assembly (150 x 10 mm) were used in general SPPS protocol. The resin, amino acids and reagents for peptide synthesis were purchased from Sigma Aldrich, Novabiochem and kept in the refrigerator if needed.

Analytical reverse-phase high performance liquid chromatography was carried out with a Waters 510 twin pump using a Phenomenex Onyx Monolithic C18 column (100 x 4.6 mm, 2 µm, 130 Å) at a flow rate of 3.0 mL min-1 and Crude peptides were purified using Hichrom Kromasil 100-5C8 column (150 x 10 mm) at a flow rate of 4.0 mL/min. Eluent detection was by ultra violet (UV) absorbance using a Waters 486 Tunable Absorbance Detector at 214 and 254 nm. The two solvent are A=0.06% trifluoroacetic acid (TFA) in distilled deionized *water* and B=0.06% aqueous TFA in 90% acetonitrile.

Analytical RP-HPLC (Method 1): 30 to 80% solvents B over 17 mins, 3.0 mL/min

Reactions were monitored by TLC (Merck 60 F254) and observed under UV radiation at 254 nm or by KMnO<sub>4</sub> staining.

To purify compounds, column chromatography was carried out using silica gel (230–400 mesh, 60 Å, 40–63  $\mu$ m).

The use of DIBAL-H solution (1.0 M in toluene) was under a dry condition with continuous flow of nitrogen gas. Moreover, the reaction was prepared in acetone/dry ice bath to keep the temperature at -78°C.

# 8.2 Experimental for Chapter 2

#### (9H-Fluoren-9-yl)methyl (S)-(3-methyl-1-oxobutan-2-yl)carbamate (2.4)

Fmoc-L-Val-OH (2.0 g, 5.90 mmol, 1.0 equiv.) was dissolved in dry DCM (40.0 mL). The solution was cooled to 0°C and CDI (1.1 g, 6.50 mmol, 1.1 equiv.) was added. After stirring for 1 h at 0 °C, the reaction solution was cooled to -78°C (acetone/CO<sub>2</sub> bath) for 15 min. The DIBAL-H solution (1.0 M in toluene) (12.4 ml, 12.40 mmol, 2.1 equiv.) was added dropwise over 10 min under N<sub>2</sub> gas. The reaction mixture was stirred at -78°C for 1.5 h and monitored by TLC (Hexane: EtOAc 2: 1). Upon completion, the reaction mixture diluted in EtOAc (40.0 mL) and quenched with the addition of tartaric acid solution (25% in H<sub>2</sub>O) (30.0 mL) with vigorous stirring. The mixture was warmed to room temperature and stirred at ambient temperature for 15 min. The organic phase was extracted with EtOAc (1×40.0 mL), and the combined organic layers were washed with sat. KHSO<sub>4</sub> aq (1×30.0 mL), 0.8M NaHCO<sub>3</sub> aq (1×30.0 mL), sat. NaCl aq (1×30.0 mL), dried over MgSO<sub>4</sub> and concentrated in vacuo. Purification was achieved by column chromatography (hexane/ethyl acetate, 3:1) to give 2.4 as white powder (1.61 g, 83% yield); M.p. 80-82 °C;  $R_f = 0.20$  (hexane/EtOAc = 2:1); <sup>1</sup>H NMR (CDCl<sub>3</sub>, 400 MHz)  $\delta$  9.67 (s, 1H, CHO), 7.77 (d, J = 7.5 Hz, 2H, Ar-H), 7.61 (d, J = 7.3 Hz, 2H, Ar-H), 7.41 (t, J = 7.5 Hz, 2H, Ar-H), 7.32 (t, J = 7.5 Hz, 2H, Ar-H), 5.35 (brs, 1H, NH), 4.42 (d, J = 6.8 Hz, 2H, COOC $H_2$ ), 4.32-4.38 (m, 1H, NHCH), 4.24 (t, J = 6.8 Hz, 1H, COOCH<sub>2</sub>CH), 2.30 (m, 1H, CH(CH<sub>3</sub>)<sub>2</sub>), 1.04 (d, J = 6.8 Hz, 3H, CH(CH<sub>3</sub>)<sub>2</sub>), 0.97 (d, J = 6.8Hz, 3H, CH(CH<sub>3</sub>)<sub>2</sub>); 13C NMR (CDCl<sub>3</sub>, 400 MHz) δ 199.8, 156.4, 143.8, 141.3, 127.8, 127.1, 125.1, 120.0, 67.1, 65.1, 47.3, 29.1, 17.6; LCMS: calcd. for C<sub>20</sub>H<sub>21</sub>NO<sub>3</sub> + 324.4, found 324.4  $[MH^+].$ 

# (R)-2-(1-((((9H-Fluoren-9-yl)methoxy)carbonyl)amino)-2-methylpropyl)thiazolidine-4-carboxylic acid (2.5)

(9*H*-Fluoren-9-yl)methyl (*S*)-(3-methyl-1-oxobutan-2-yl)carbamate (**2.4**) (646.8 mg, 2.00 mmol, 1.0 equiv.) was dissolved in MeOH (10.0 mL) and L-cysteine (218.0 mg, 1.80 mmol, 0.9 equiv.) in H<sub>2</sub>O (5.0 mL) were added and then stirred at room temperature for 18 h. The solvent was removed and the crystalline precipitate was filtered off, then washed with Et<sub>2</sub>O and dried by desiccator to afford crude product as white powder (665.4 mg, 78% yield); M.p. 149-151°C; <sup>1</sup>H NMR (d<sub>6</sub>-DMSO, 400 MHz)  $\delta$  7.88 (d, J = 7.4 Hz, 2H, Ar-H), 7.70 (d, J = 7.8 Hz, 2H, Ar-H), 7.30-7.45 (m, 4H, Ar-H), 4.95 (d, J = 7.1 Hz, 2H, COOC*H*<sub>2</sub>), 4.30-4.35 (m, 1H, C*H*CH (CH<sub>3</sub>)<sub>2</sub>), 4.22 (t, J = 6.8 Hz, 1H, COOCH<sub>2</sub>C*H*), 4.19 (d, J = 7.0 Hz, 1H, NHC*H*S), 4.08 (t, J = 6.4 Hz, 1H, NHC*H*COOH), 3.31-3.45 (m, 1H, SC*H*<sub>2</sub>), 3.18-3.25 (m, 1H, SC*H*<sub>2</sub>), 2.35 (m, 1H, C*H*(CH<sub>3</sub>)<sub>2</sub>), 0.88 (d, J = 6.9 Hz, 3H, CH(C*H*<sub>3</sub>)<sub>2</sub>), 0.75 (d, J = 6.8 Hz, 3H, CH(C*H*<sub>3</sub>)<sub>2</sub>); <sup>13</sup>C NMR (d<sub>6</sub>-DMSO, 400 MHz) 168.2, 157.2, 144.3, 141.2, 128.0, 127.4, 125.7, 120.4, 66.3, 66.2, 63.0, 57.3, 47.2, 35.2, 30.2, 20.0, 17.4, 14.5 ; LCMS: calcd. for C<sub>23</sub>H<sub>26</sub>N<sub>2</sub>O<sub>4</sub>S + 427.2, found 427.2 [MH<sup>+</sup>].

# (9H-Fluoren-9-yl)methyl (S)-(1-oxopropan-2-yl)carbamate (2.12)<sup>304</sup>

#### Method A:

Fmoc-L-Ala-OH (2.9) (200.0 mg, 0.64 mmol, 1.0 equiv.) was dissolved in a DCM solution (3.0 mL) containing EDC HCl (92.0 mg, 0.48 mmol, 0.75 equiv.) and followed by addition of

NHS (72.0 mg, 0.48 mmol, 0.75 equiv.) to allow reaction at rt while stirring for 3 h. Then NaBH<sub>4</sub> (6.8 g, 180.09 mmol) was added portionwise at -10°C and stirred for 1 h. H<sub>2</sub>O (50.0 mL) was added cautiously to the reaction mixture and stirring was continued for another hour at rt under N<sub>2</sub> for 30 minutes. The mixture was neutralized with sat. KHSO<sub>4</sub> aq and then was extracted with EtOAc. The org layer was dried (MgSO<sub>4</sub>) and concentrated. The residue was purified by silica gel chromatography to provide the intermediate compound **2.11**. Then Dess-Martin periodinane (170.0 mg, 0.4 mmol) was added under argon to a stirred solution of the **2.11** (153.7 mg, 0.41 mmol) in dry DCM. The reaction mixture was stirred at rt for 3 h. The mixture was concentrated in vacuo and the residue purified by flash chromatography to provide product **2.12** as white powder (124.1 mg, 71% yield)

#### Method B:

To a stirred solution of Fmoc-L-Ala-OH (2.9) (200.0 mg, 0.64 mmol, 1.0 equiv.) in THF, NMM (200.0 mg, 0.96 mmol, 1.5 equiv.) and CDI (200.0 mg, 0.96 mmol, 1.5 equiv.) was added at 0°C, followed by the addition of N, O-dimethylhydroxylamine hydrochloride (200.0 mg, 0.71 mmol, 1.1 equiv.) in dry DCM (5.0 mL), neutralized with NMM. The reaction mixture was stirred till the completion of reaction. THF was removed and the product was extracted into ethyl acetate and the organic layer was washed with sat. KHSO<sub>4</sub> aq (10.0 mL), sodium carbonate solution (2 x 15.0 mL), water (15.0 mL) and brine (15.0 mL). Then it was dried over anhydrous sodium sulfate and concentrated to give the intermediate 2.13. Then 2.13 was dissolved in dry DCM (8.0 mL). The solution was cooled to 0°C and CDI (114.0 mg, 0.7 mmol, 1.1 equiv.) was added. After stirring for 1 h at 0°C, the reaction solution was cooled to -78°C (acetone/CO<sub>2</sub> bath) for 15 min. The DIBAL-H solution (1.0 M in toluene) (1.3 ml, 1.3 mmol, 2.0 equiv.) was added dropwise over 10 min under N<sub>2</sub> gas. The reaction mixture was stirred at -78°C for 2 h and monitored by TLC (Hexane: EtOAc 2:1). Upon completion, the reaction mixture diluted in EtOAc (8.0 mL) and quenched with the addition of tartaric acid solution (25 % in H<sub>2</sub>O) (5.0 mL) with vigorous stirring. The mixture was warmed to room temperature and stirred at ambient temperature for 15 min. The organic phase was extracted with EtOAc (1×8.0 mL), and the combined organic layers were washed with sat. KHSO<sub>4</sub> aq (1×5.0 mL), sat. NaHCO<sub>3</sub> aq (1×5.0 mL), sat. NaCl aq (1×5.0 mL), dried over MgSO<sub>4</sub> and concentrated *in vacuo*. to afford the product as white powder (42.8 mg, 22.7% yield)

#### Method C:

Fmoc-L-Ala-OH (2.0 g, 6.40 mmol, 1.0 equiv.) was dissolved in dry DCM (80.0 mL). The solution was cooled to 0°C and CDI (1.1 g, 7.04 mmol, 1.1 equiv.) was added. After stirring for 1 h at 0°C, the reaction solution was cooled to -78°C (acetone/CO<sub>2</sub> bath) for 15 min. The DIBAL-H solution (1.0 M in toluene) (13.4 ml, 13.40 mmol, 2.1 equiv.) was added dropwise over 10 min under N<sub>2</sub> gas. The reaction mixture was stirred at -78°C for 1.5 h and monitored by TLC (Hexane: EtOAc 2:1). Upon completion, the reaction mixture diluted in EtOAc (80.0 mL) and quenched with the addition of tartaric acid solution (25% in H<sub>2</sub>O) (50.0 mL) with vigorous stirring. The mixture was warmed to room temperature and stirred at ambient temperature for 15 min. The organic phase was extracted with EtOAc (1×80.0 mL), and the combined organic layers were washed with sat. KHSO<sub>4</sub> aq (1×50.0 mL), sat. NaHCO<sub>3</sub> aq (1×50.0 mL), sat. NaCl aq (1×50.0 mL), dried over MgSO<sub>4</sub> and concentrated in vacuo. Purification was achieved by column chromatography (hexane/ethyl acetate, 3:1) to give 2.12 as white powder (1.75 g, 85% yield); M.p. 158-160 °C;  $R_f = 0.25$  (hexane/EtOAc = 2:1); <sup>1</sup>H NMR (CDCl<sub>3</sub>, 400 MHz)  $\delta$  9.57 (s, 1H, CHO), 7.77 (d, J = 7.5 Hz, 2H, Ar-H), 7.60 (d, J = 7.5Hz, 2H, Ar-H), 7.41 (t, J = 7.5 Hz, 2H, Ar-H), 7.32 (t, J = 7.5 Hz, 2H, Ar-H), 5.37 (brs, 1H, NH), 4.43 (d, J = 4.3 Hz, 2H, COOC $H_2$ ), 4.28-4.37 (m, 1H, NHCH), 4.23 (t, J = 6.8 Hz, 1H,  $COOCH_2CH$ ), 1.39 (d, J = 7.3 Hz, 3H,  $CHCH_3$ ), 0.97 (d, J = 6.8 Hz, 3H,  $CH(CH_3)_2$ ); <sup>13</sup>C NMR (CDCl<sub>3</sub>, 100 MHz) δ 199.0, 155.8, 143.8, 143.7, 141.4, 127.8, 127.1, 125.0, 120.0, 67.0, 56.0, 47.2, 14.9. LCMS: calcd. for C<sub>18</sub>H<sub>17</sub>NO<sub>3</sub> + 296.1, found 296.1 [MH<sup>+</sup>].

# tert-Butyl (S)-(1-oxopropan-2-yl)carbamate (2.16)<sup>304</sup>

Boc-L-Ala-OH (2.0 g, 10.60 mmol, 1.0 equiv.) was dissolved in dry DCM (60.0 mL). The solution was cooled to 0°C and CDI (1.9 g, 11.60 mmol, 1.1 equiv.) was added. After stirring for 1 h at 0 °C, the reaction solution was cooled to -78°C (acetone/CO<sub>2</sub> bath) for 15 min. The DIBAL-H solution (1.0 M in toluene) (22.2 ml, 22.21 mmol, 2.1 equiv.) was added dropwise over 10 min under N<sub>2</sub> gas. The reaction mixture was stirred at -78°C for 1.5 h and monitored by TLC (Hexane: EtOAc 2:1). Upon completion, the reaction mixture diluted in EtOAc (70.0

mL) and quenched with the addition of tartaric acid solution (25% in H<sub>2</sub>O) (50.0 mL) with vigorous stirring. The mixture was warmed to room temperature and stirred at ambient temperature for 15 min. The organic phase was extracted with EtOAc (1×70.0 mL), and the combined organic layers were washed with sat. KHSO<sub>4</sub> aq (1×50.0 mL), 0.8M NaHCO<sub>3</sub> aq (1×50.0 mL), sat. NaCl aq (1×50.0 mL), dried over MgSO<sub>4</sub> and concentrated *in vacuo*. Purification was achieved by column chromatography (hexane/ethyl acetate, 3:1) to give **2.16** as white powder (1.40 g, 77% yield); M.p. 82-84 °C;  $R_f$ = 0.23 (hexane/EtOAc = 2:1, KMNO<sub>4</sub> staining); <sup>1</sup>H NMR (CDCl<sub>3</sub>, 400 MHz)  $\delta$  9.72 (s, 1H, CHO), 5.08 (brs, 1H, NH), 4.23 (t, J = 7.0 Hz, 1H, NHCH), 1.45 (s, 9H, C(CH<sub>3</sub>)<sub>3</sub>), 1.34 (d, J = 7.4 Hz, 3H, CHCH<sub>3</sub>); <sup>13</sup>C NMR (CDCl<sub>3</sub>, 400 MHz)  $\delta$  199.7, 155.3, 80.1, 55.5, 28.3, 14.9. LCMS: calcd. for C<sub>8</sub>H<sub>15</sub>NO<sub>3</sub> + 174.2, found 174.2 [MH<sup>+</sup>].

#### tert-Butyl (S)-(3-methyl-1-oxobutan-2-yl)carbamate (2.17)

Boc-L-Val-OH (2.0 g, 9.21 mmol, 1.0 equiv.) was dissolved in dry DCM (60.0 mL). The solution was cooled to 0°C and CDI (1.6 g, 10.13 mmol, 1.1 equiv.) was added. After stirring for 1 h at 0°C, the reaction solution was cooled to -78°C (acetone/CO<sub>2</sub> bath) for 15 min. The DIBAL-H solution (1.0 M in toluene) (19.3 ml, 19.30 mmol, 2.1 equiv.) was added dropwise over 10 min under N<sub>2</sub> gas. The reaction mixture was stirred at -78°C for 1.5 h and monitored by TLC (Hexane : EtOAc 2 : 1). Upon completion, the reaction mixture diluted in EtOAc (70.0 mL) and quenched with the addition of tartaric acid solution (25% in H<sub>2</sub>O) (40.0 mL) with vigorous stirring. The mixture was warmed to room temperature and stirred at ambient temperature for 15 min. The organic phase was extracted with EtOAc (1×70.0 mL), and the combined organic layers were washed with sat. KHSO<sub>4</sub> aq (1×40.0 mL), 0.8M NaHCO<sub>3</sub> aq (1×40.0 mL), sat. NaCl aq (1×40.0 mL), dried over MgSO<sub>4</sub> and concentrated *in vacuo*. Purification was achieved by column chromatography (hexane/ethyl acetate, 3:1) to give **2.4** as colorless oil (1.50 g, 81% yield);  $R_f = 0.48$  (hexane/EtOAc = 2:1, KMNO<sub>4</sub> staining); <sup>1</sup>H NMR (CDCl<sub>3</sub>, 400 MHz)  $\delta$  9.63 (d, J = 1.2 Hz ,1H, CHO), 4.19-4.28 (m, 1H, NHCH), 2.15-2.17 (m, 1H, CH(CH<sub>3</sub>)<sub>2</sub>), 1.43-1.45 (m, 9H, C(CH<sub>3</sub>)<sub>3</sub>), 1.02 (d, J = 6.8 Hz, 3H, CH(CH<sub>3</sub>)<sub>2</sub>),

0.93 (d, J = 6.8 Hz, 3H, CH(C $H_3$ )<sub>2</sub>); 13C NMR (CDCl<sub>3</sub>, 400 MHz)  $\delta$  199.7, 155.3, 80.1, 55.5, 28.3, 18.7, 14.9; LCMS: calcd. for C<sub>10</sub>H<sub>9</sub>NO<sub>3</sub> + 202.3, found 202.3 [MH<sup>+</sup>].

# (R)-2-(1-((((9H-Fluoren-9-yl)methoxy)carbonyl)amino)ethyl)thiazolidine-4-carboxylic acid (2.19)

(9*H*-Fluoren-9-yl)methyl (*S*)-(1-oxopropan-2-yl)carbamate (**2.12**) (590.7 mg, 2.01 mmol, 1.0 equiv.) was dissolved in MeOH (10.0 mL) and L-cysteine (218.0 mg, 1.81 mmol, 0.9 equiv.) in H<sub>2</sub>O (5.0 mL) were added and then stirred at room temperature for 18 h. The solvent was removed and the crystalline precipitate was filtered off, then washed with Et<sub>2</sub>O and dried by desiccator to afford the product as white powder (573.8 mg, 72% yield); M.p. 138-140 °C; <sup>1</sup>H NMR (d<sub>6</sub>-DMSO, 400 MHz)  $\delta$  7.86 (d, J = 7.35 Hz, 2H, Ar-H), 7.73 (d, J = 7.8 Hz, 2H, Ar-H), 7.30-7.45 (m, 4H, Ar-H), 4.92 (d, J = 7.1 Hz, 2H, COOC*H*<sub>2</sub>), 4.31-4.36 (m, 1H, C*H*CH (CH<sub>3</sub>)<sub>2</sub>), 4.25 (t, J = 6.8 Hz, 1H, COOCH<sub>2</sub>C*H*), 4.21 (d, J = 7.0 Hz, 1H, NHC*H*S), 4.05 (t, J = 6.4 Hz, 1H, NHC*H*COOH), 3.32-3.44 (m, 1H, SC*H*<sub>2</sub>), 3.15-3.29 (m, 1H, SC*H*<sub>2</sub>), 2.32 (m, 1H, C*H*(CH<sub>3</sub>)<sub>2</sub>), 0.82 (d, J = 6.9 Hz, 3H, CH(C*H*<sub>3</sub>)<sub>2</sub>); <sup>13</sup>C NMR (d<sub>6</sub>-DMSO, 400 MHz) 168.3, 157.4, 145.3, 140.2, 128.5, 127.7, 125.7, 121.4, 67.3, 66.2, 63.0, 57.5, 48.2, 35.2, 33.2; LCMS: calcd. for C<sub>21</sub>H<sub>22</sub>N<sub>2</sub>O<sub>4</sub>S + 399.1, found 399.1 [MH<sup>+</sup>].

#### (R)-2-(1-((tert-butoxycarbonyl)amino)ethyl)thiazolidine-4-carboxylic acid (2.20)

tert-Butyl (S)-(1-oxopropan-2-yl)carbamate (2.16) (346.4 mg, 2.00 mmol, 1.0 equiv.) was dissolved in MeOH (10.0 mL) and L-cysteine (218.0 mg, 1.80 mmol, 0.9 equiv.) in H<sub>2</sub>O (5.0 mL) were added and then stirred at room temperature for 18 h. The solvent was removed and

the crystalline precipitate was filtered off, then washed with Et<sub>2</sub>O and dried by desiccator to afford the product as white powder (414.5 mg, 75% yield); M.p. 125-127 °C; <sup>1</sup>H NMR (d<sub>6</sub>-DMSO, 400 MHz)  $\delta$  4.95 (d, J = 7.1 Hz, 2H, COOC $H_2$ ), 4.28-4.35 (m, 1H, CHCH (CH<sub>3</sub>)<sub>2</sub>), 4.31 (t, J = 6.8 Hz, 1H, COOCH<sub>2</sub>CH), 4.20 (d, J = 7.0 Hz, 1H, NHCHS), 4.07 (t, J = 6.4 Hz, 1H, NHCHCOOH), 3.30-3.42 (m, 1H, SC $H_2$ ), 3.14-3.18 (m, 1H, SC $H_2$ ), 1.15 (s, 9H, C(C $H_3$ )<sub>3</sub>), 0.82 (d, J = 6.9 Hz, 3H, CHC $H_3$ ); <sup>13</sup>C NMR (d<sub>6</sub>-DMSO, 400 MHz) 168.3, 157.4, 77.4, 66.2, 63.0, 57.5, 35.2, 28.3, 14.9; LCMS: calcd. for C<sub>11</sub>H<sub>20</sub>N<sub>2</sub>O<sub>4</sub>S + 277.1, found 277.1 [MH<sup>+</sup>].

# (R)-2-(1-((tert-butoxycarbonyl)amino)-2-methylpropyl)thiazolidine-4-carboxylic acid (2.21)

tert-Butyl (*S*)-(3-methyl-1-oxobutan-2-yl)carbamate (**2.17**) (400.0 mg, 2.02 mmol, 1.0 equiv.) was dissolved in MeOH (10.0 mL) and L-cysteine (218.0 mg, 1.82 mmol, 0.9 equiv.) in H<sub>2</sub>O (5.0 mL) were added and then stirred at room temperature for 18 h. The solvent was removed and the crystalline precipitate was filtered off, then washed with Et<sub>2</sub>O and dried by desiccator to afford the product as white powder (396.5 mg, 72% yield); M.p. 146-148°C; <sup>1</sup>H NMR (d<sub>6</sub>-DMSO, 400 MHz) δ 6.62 (d, J = 4.9 Hz, 1H, NH), 4.55-4.67 (m, 1H, NHCHS), 3.66-3.74 (m, 2H, CHCH(CH<sub>3</sub>)<sub>2</sub>, NHCHCH<sub>2</sub>), 3.15 (dd, J = 9.9, 6.8 Hz, 1H, CHCH<sub>2</sub>S), 2.68 (t, J = 9.4 Hz, 1H, CHCH<sub>2</sub>S), 1.76-1.84 (m, 1H, CH(CH<sub>3</sub>)<sub>2</sub>), 1.39 (d, J = 3.0 Hz, 9H, C(CH<sub>3</sub>)<sub>3</sub>), 0.76-0.84 (m, 6H, CH(CH<sub>3</sub>)<sub>2</sub>); <sup>13</sup>C NMR (d<sub>6</sub>-DMSO, 400 MHz) δ 172.8, 157.0, 78.2, 73.4, 65.7, 58.5, 37.0, 28.7, 20.3, 18.4, 14.7; LCMS: calcd. for C<sub>13</sub>H<sub>20</sub>N<sub>2</sub>O<sub>3</sub>S + 305.2, found 305.2 [MH<sup>+</sup>].

#### Synthesis of lugdunin via TG resin

#### **TG** resin (2.28)

The dried Rink amide AM resin (Novagel) (1.0 equiv, loading = 0.7 mmol/g) was swollen in DMF (2.0 mL) for 15 h in a reaction column followed by washing with DMF (3.0 mL min<sup>-1</sup>) for 5-10 min. Then the resin was attached by Fmoc-Gly-OH and Fmoc-Thr-OH via general Fmoc SPPS protocol. The washing and Fmoc-deprotection cycles were carried out using the manual peptide synthesiser NOVASYN® GEM with a post-column UV monitoring at 355 nM. The peptide chains were assembled by stepwise coupling of Nα-Fmoc-amino acid (4.0 eq) in DMF (0.6 mL) in the presence of carboxyl activating agent 1-[bis(dimethylamino)methylene]-1H-1,2,3-triazolo[4,5-b]pyridinium 3-oxid hexafluorophosphate (HATU; 3.9 eq) and DIPEA (8.0 eq). Each acylation reaction was carried out in the reaction column for 4 h at room temperature and was followed by the wash and deprotection steps. Following the assembly of the desired sequence, the resin washed with DMF (3.0 mL min<sup>-1</sup>) for 15 min. The modified TG resin is used for peptide synthesis without further checking.

#### Preloaded L-Val TG resin (2.9)

A solution of Fmoc-L-Val-H (4.0 equiv) and DIPEA (1% with respect to MeOH) in MeOH (final concentration of 0.1 M) was added to the TG resin and the resulting mixture was agitated at 60°C for 5 h. the resin was then washed with MeOH (5x3.0 mL), DMF (5x3.0 mL), DCM (5x3.0 mL), and THF (5x3.0 mL). The preloading TG resin was used for next step directly.

#### NH-Boc preloaded L-Val TG resin (2.30)

A solution of Boc<sub>2</sub>O (5.0 equiv) and NMM (5.0 equiv) in THF was added to the preloaded TG resin and agitated at 50°C for 5 h. the resulting resin was washed with THF and DMF.

The loading efficiency was then evaluated. New loading capacity = 0.5 mmol/g % yield = 88%

#### General procedure to evaluate a preloaded resin

20% of piperidine in DMF (3.0 mL) was added to an accurately weighed amount of preloaded resin (5-10 mg) and the suspension was left for 2 h with occasional agitation. 300  $\mu$ L of the suspension was then diluted 10 folds with fresh 20% of piperidine in DMF (2.7 mL). The UV absorbance at 290 nm was measured. The amino acid loading and % loading efficiency were determined using the equation below:

Loading (mmol/g) = (absorbance sample) / (mg of sample x1.75) % loading efficiency = (calculated loading / theoretical loading) x 100%

#### Lugdunin (1.24)

Peptide chain with resin was filtered and washed with DMF, DCM and hexane. The resin was transferred into a round-bottom flask and dried in vacuo overnight. The dried resin was then suspended in TFA/H<sub>2</sub>O/TIPS (90:5:5) (10.0 mL) for 3 h. The suspension was then filtered by gravity and washed with TFA and DCM. The filtrate collected in a clean round-bottom flask was evaporated to dryness (DCM was added several times). The residue was triturated with cold diethyl ether (x3) to afford the crude product as white powder (71.3 mg, 91%). The peptide product was analysed using LCMS and found [MH<sup>+</sup>]: 783.6 at  $t_R$  of 2.89 min. Compound was then purified by RP-HPLC and obtained 2.1 mg as pure product (4.2% recovery). <sup>1</sup>H NMR (500 MHz, DMSO-d<sub>6</sub>)  $\delta$  10.69-10.77 (m, 1H, L-Trp<sup>3</sup>-CCHN*H*), 8.53 (d, J = 8.5, 1H, L-Trp<sup>3</sup>-N*H*), 8.52 (d, J = 8.5, 1H, D-Val<sup>2</sup>-N*H*), 8.44 (d, J = 8.5, 1H, D-Leu<sup>4</sup>-N*H*), 8.32-8.36 (m, 1H, L-Val<sup>5</sup>-N*H*), 8.27-8.31 (m, 1H, D-Val<sup>6</sup>-N*H*), 8.16-8.18 (m, 1H, L-Val<sup>7</sup>-N*H*), 7.98 (d, J = 7.8,

1H, L-Trp<sup>3</sup>-Ar-H), 7.95 (dd, J = 8.1, 3.7, 1H, L-Trp<sup>3</sup>-Ar-H), 7.86 (d, J = 7.9, 1H, L-Trp<sup>3</sup>-Ar-H), 7.71 (dd, J = 8.0, 1.3, 1H, L-Trp<sup>3</sup>-Ar-H), 7.52 (d, J = 2.0, 1H, L-Trp<sup>3</sup>-NHCHC), 4.59 (dd,  $J = 8.8, 4.5, 1H D-Val^6-NHCHCH$ ), 4.38 (t,  $J = 8.3, 1H, D-Leu^4-NHCHCH_2$ ), 4.03 (d, J = 9.0, 1H, D-Val<sup>2</sup>-NHCHCH), 3.95-4.02 (m, 1H, thiazolidine<sup>1</sup>-NHCHCH<sub>2</sub>S), 3.85 (dd, J = 9.0, 6.6, 1H, L-Val<sup>7</sup>-NHCHCH), 3.23 (dd, J = 10.5, 6.5, 1H, thiazolidine<sup>1</sup>-NHCHCH<sub>2</sub>S), 3.13 (dd, J =10.5, 6.5, 1H, thiazolidine<sup>1</sup>-NHCHC $H_2$ S), 3.05 (d, J = 7.8, 1H, L-Trp<sup>3</sup>-NHCHC $H_2$ ), 3.01 (dd,  $J = 13.5, 5.4, 1H, L-Trp^3-NHCHCH_2), 2.85-2.91$  (m, 1H, thiazolidine<sup>1</sup>- NHCHCH<sub>2</sub>S), 2.15-2.26 (m, 1H, L-Val<sup>7</sup>-CH(CH<sub>3</sub>)<sub>2</sub>), 2.00-2.06 (m, 1H, D-Val<sup>6</sup>-CH(CH<sub>3</sub>)<sub>2</sub>), 1.92-1.99 (m, 1H, L-Val<sup>5</sup>-CH(CH<sub>3</sub>)<sub>2</sub>), 1.66-1.72 (m, 1H, D-Val<sup>2</sup>-CH(CH<sub>3</sub>)<sub>2</sub>), 1.52-1.61 (m, 1H, D-Leu<sup>4</sup>-CHCH<sub>2</sub>CH), 1.27-1.42 (m, 1H, D-Leu<sup>4</sup>-CHC $H_2$ CH), 1.16 (d, J = 6.4, 3H, D-Val<sup>6</sup>-CH(C $H_3$ )<sub>2</sub>), 1.08 (d, J =6.7, 3H, D-Leu<sup>4</sup>-CH(C $H_3$ )<sub>2</sub>), 1.05 (d, J = 6.7, 3H, D-Leu<sup>4</sup>-CH(C $H_3$ )<sub>2</sub>), 1.03 (d, J = 6.5, 3H, D- $Val^6$ -CH(CH<sub>3</sub>)<sub>2</sub>), 0.92 (d, J = 6.8, 3H, L-Val<sup>5</sup>-CH(CH<sub>3</sub>)<sub>2</sub>), 0.87 (d, J = 6.4, 3H, L-Val<sup>5</sup>- $CH(CH_3)_2$ ), 0.84 (d, J = 8.5, 3H, L- $Val^7$ - $CH(CH_3)_2$ ), 0.82 (d, J = 6.4, 3H, L- $Val^7$ - $CH(CH_3)_2$ ), 0.78 (d, J = 6.5, 3H, D-Val<sup>2</sup>-CH(CH<sub>3</sub>)<sub>2</sub>), 0.67 (d, J = 6.4, 3H, D-Val<sup>2</sup>-CH(CH<sub>3</sub>)<sub>2</sub>); HRMS: calculated for C<sub>40</sub>H<sub>62</sub>N<sub>8</sub>O<sub>6</sub>S<sub>1</sub><sup>+</sup> 784.4513, found 784.4593 [MH<sup>+</sup>]; Analytical RP-HPLC (**Method 1**)  $t_R = 4.52 \text{ min.}$ 

# Synthesis of lugdunin via Weinreb AM resin

#### Compound 2.24

The dried Weinreb AM resin (1.0 equiv.) was swollen with DMF/DCM mixture (1 : 1 v/v) (4.0 mL) for 15 h in a reaction column followed by washing with DMF (3.0 mL min<sup>-1</sup>) for 6 min. Fmoc-cleavae was achieved through the continuous flow of 20% piperidine in DMF (3.0 mL min<sup>-1</sup>) for 6 min. Following deprotection, the resin was washed again with DMF (3.0 mL min<sup>-1</sup>) for 6 min. The washing and Fmoc-deprotection cycles were carried out using the manual peptide synthesiser NOVASYN® GEM with a post-column UV monitoring at 355 nM. The peptide chains were assembled by stepwise coupling of Nα-Fmoc-amino acid (4.0 eq) in DMF

(0.6 mL) in the presence of carboxyl activating agent 1-[bis(dimethylamino)methylene]-1H-1,2,3-triazolo[4,5-b]pyridinium 3-oxid hexafluorophosphate (HATU; 3.9 eq) and DIPEA (8.0 eq). Each acylation reaction was carried out in the reaction column for 4 hr at room temperature and was followed by the wash and deprotection steps. Following the assembly of the desired sequence, the resin washed with DMF (3.0 mL min<sup>-1</sup>) for 15 min. Finally, the resin was filtered and washed sequentially with DMF, DCM and hexane respectively before drying it in vacuo.

#### (L-Cys(Trt))-(D-Val)-(L-Trp)-(D-Leu)-(L-Val)-(D-Val)-(L-Val)-H (2.25)

The following reaction were carried out under an atmosphere of nitrogen. Compound **2.24** (1.0 equiv.) was suspended in dry THF/DCM (1:1) (20.0 mL) and the organometallic reagent DIBAL-H (1.0 M in THF) (5.0 equiv) were added, and the reaction mixture was stirred for 2 h. Next, 1 M HCl: THF (1:1, v/v, 5.0 mL) was carefully added to the vessel, and the mixture was stirred for another 15 min. The resin was washed with THF (2x20.0 mL), and DCM (3x20.0 mL). the combined filtrates were washed with water (1x60.0 mL), dried over MgSO<sub>4</sub> and filtered. Then the solvent was removed in vacuo to give the crude product (21.2 mg, 20% yield).

# Mini cleavage of compound 2.24 by three different solvent systems Condition 1:

# A small amount of compound (1.0 equiv.) was suspended in dry DCM (2.0 mL) and the organometallic reagent DIBAL-H (1.0 M in THF) (5.0 equiv) was added, and the reaction mixture was stirred for 2 h. Next, 1 M HCl: THF (1:1, v/v, 0.5 mL) was carefully added to the vessel, and the mixture was stirred for another 15 min. The resin was washed with THF

(2x2.0 mL), and DCM (3x2.0 mL). the combined filtrates were washed with water (1x6.0 mL), dried over MgSO<sub>4</sub> and filtered. Then the solvent was removed in vacuo to give the crude product.

#### **Condition 2:**

A small amount of compound (1.0 equiv.) was suspended in dry DCM/THF (1:1) (2.0 mL) and the organometallic reagent DIBAL-H (1.0 M in THF) (5.0 equiv) were added, and the reaction mixture was stirred for 2 h. Next, 1 M HCl: THF (1:1, v/v, 0.5 mL) was carefully added to the vessel, and the mixture was stirred for another 15 min. The resin was washed with THF (2x2.0 mL), and DCM (3x2.0 mL). the combined filtrates were washed with water (1x6.0 mL), dried over MgSO<sub>4</sub> and filtered. Then the solvent was removed in vacuo to give the crude product.

#### **Condition 3:**

A small amount of compound (1.0 equiv.) was suspended in dry THF (1:1) (2.0 mL) and the organometallic reagent DIBAL-H (1.0 M in THF) (5.0 equiv) were added, and the reaction mixture was stirred for 2 h. Next, 1 M HCl: THF (1:1, v/v, 0.5 mL) was carefully added to the vessel, and the mixture was stirred for another 15 min. The resin was washed with THF (2x2.0 mL), and DCM (3x2.0 mL). the combined filtrates were washed with water (1x6.0 mL), dried over MgSO<sub>4</sub> and filtered. Then the solvent was removed in vacuo to give the crude product.

#### **Conclusions:**

According to the trace of LCMS, the results show no difference between these three conditions. Thus, for the convenience to work up, solvent containing dry DCM and dry THF (1:1) was used in the large scale cleavage reaction.

#### 8.3 Experimental for Chapter 3

Preloaded L-Ala TG resin (3.7)

A solution of Fmoc-L-Ala-H (4.0 equiv) and DIPEA (1% with respect to MeOH) in MeOH (final concentration of 0.1 M) was added to the TG resin and the resulting mixture was agitated at 60°C for 5 h. the resin was then washed with MeOH (5x3.0 mL), DMF (5x3.0 mL), DCM (5x3.0 mL), and THF (5x3.0 mL). The preloading TG resin was used for next step directly.

#### NH-Boc preloaded L-Ala TG resin (3.8)

A solution of Boc<sub>2</sub>O (5.0 equiv) and NMM (5.0 equiv) in THF was added to the preloaded TG resin and agitated at 50°C for 5 h. the resulting resin was washed with THF and DMF.

The loading efficiency was then evaluated.

New loading capacity = 0.47 mmol/g

% yield = 83%

#### $(Ala)^7$ -lug (1.25)

Peptide chain with resin was filtered and washed with DMF, DCM and hexane. The resin was transferred into a round-bottom flask and dried in vacuo overnight. The dried resin was then suspended in TFA/H<sub>2</sub>O/TIPS (90:5:5) (10.0 mL) for 3 h. The suspension was then filtered by gravity and washed with TFA and DCM. The filtrate collected in a clean round-bottom flask was evaporated to dryness (DCM was added several times). The residue was triturated with cold diethyl ether (x3) to afford the crude product as white powder (56.6 mg, 75%). The peptide product was analysed by using LCMS and found [MH<sup>+</sup>]: 755.6 at  $t_R$  of 2.86 min. Compound was then purified by RP-HPLC and obtained 1.5 mg as pure product (3.7% recovery). <sup>1</sup>H NMR (500 MHz, DMSO-d<sub>6</sub>)  $\delta$  10.62-10.71 (m, 1H, L-Trp<sup>3</sup>-CCHN*H*), 8.55 (d, J = 8.5, 1H, L-Trp<sup>3</sup>-N*H*), 8.50 (d, J = 8.5, 1H, D-Val<sup>2</sup>-N*H*), 8.42 (d, J = 8.5, 1H, D-Leu<sup>4</sup>-N*H*), 8.30-8.35 (m, 1H, L-Val<sup>5</sup>-N*H*), 8.25-8.30 (m, 1H, D-Val<sup>6</sup>-N*H*), 8.15-8.17 (m, 1H, L-Ala<sup>7</sup>-N*H*), 7.96 (d, J = 7.8, 1H, L-Trp<sup>3</sup>-Ar-*H*), 7.94 (dd, J = 8.1, 3.7, 1H, L-Trp<sup>3</sup>-Ar-*H*), 7.83 (d, J = 7.9, 1H, L-Trp<sup>3</sup>-Ar-*H*), 7.72 (dd, J = 8.0, 1.3, 1H, L-Trp<sup>3</sup>-Ar-*H*), 7.51 (d, J = 2.0, 1H, L-Trp<sup>3</sup>-NHC*H*C), 4.59 (dd, J = 8.8, 4.5, 1H D-Val<sup>6</sup>-NHC*H*CH), 4.35 (t, J = 8.3, 1H, D-Leu<sup>4</sup>-NHC*H*CH<sub>2</sub>), 4.03 (d, J = 9.0, 1H, D-Val<sup>2</sup>-NHC*H*CH), 3.96-4.00 (m, 1H, thiazolidine<sup>1</sup>-NHC*H*CH<sub>2</sub>S), 3.86 (dd, J = 9.0, 6.6,

1H, L-Ala<sup>7</sup>-NHC*H*CH), 3.25 (dd, J = 10.5, 6.5, 1H, thiazolidine<sup>1</sup>-NHCHC*H*<sub>2</sub>S), 3.13 (dd, J = 10.5, 6.5, 1H, thiazolidine<sup>1</sup>-NHCHC*H*<sub>2</sub>S), 3.05 (d, J = 7.8, 1H, L-Trp<sup>3</sup>-NHCHC*H*<sub>2</sub>), 3.01 (dd, J = 13.5, 5.4, 1H, L-Trp<sup>3</sup>-NHCHC*H*<sub>2</sub>), 2.85-2.91 (m, 1H, thiazolidine<sup>1</sup>- N*H*CHC*H*<sub>2</sub>S), 2.19-2.30 (m, 1H, L-Ala<sup>7</sup>-C*H*(CH<sub>3</sub>)<sub>2</sub>), 2.00-2.06 (m, 1H, D-Val<sup>6</sup>-C*H*(CH<sub>3</sub>)<sub>2</sub>), 1.92-1.99 (m, 1H, L-Val<sup>5</sup>-C*H*(CH<sub>3</sub>)<sub>2</sub>), 1.66-1.72 (m, 1H, D-Val<sup>2</sup>-C*H*(CH<sub>3</sub>)<sub>2</sub>), 1.52-1.61 (m, 1H, D-Leu<sup>4</sup>-CHC*H*<sub>2</sub>CH), 1.27-1.42 (m, 1H, D-Leu<sup>4</sup>-CHC*H*<sub>2</sub>CH), 1.16 (d, J = 6.4, 3H, D-Val<sup>6</sup>-CH(C*H*<sub>3</sub>)<sub>2</sub>), 1.08 (d, J = 6.7, 3H, D-Leu<sup>4</sup>-CH(C*H*<sub>3</sub>)<sub>2</sub>), 1.05 (d, J = 6.7, 3H, D-Leu<sup>4</sup>-CH(C*H*<sub>3</sub>)<sub>2</sub>), 1.03 (d, J = 6.5, 3H, D-Val<sup>6</sup>-CH(C*H*<sub>3</sub>)<sub>2</sub>), 0.92 (d, J = 6.8, 3H, L-Val<sup>5</sup>-CH(C*H*<sub>3</sub>)<sub>2</sub>), 0.87 (d, J = 6.4, 3H, L-Val<sup>5</sup>-CH(C*H*<sub>3</sub>)<sub>2</sub>), 0.80 (d, J = 6.4, 3H, L-Ala<sup>7</sup>-CHC*H*<sub>3</sub>), 0.78 (d, J = 6.5, 3H, D-Val<sup>2</sup>-CH(C*H*<sub>3</sub>)<sub>2</sub>), 0.67 (d, J = 6.4, 3H, D-Val<sup>2</sup>-CH(C*H*<sub>3</sub>)<sub>2</sub>); HRMS: calculated for C<sub>38</sub>H<sub>58</sub>N<sub>8</sub>O<sub>6</sub>S<sub>1</sub><sup>+</sup>755.4200, found 755.4185 [MH<sup>+</sup>]; Analytical RP-HPLC (**Method 1**)  $I_R = 4.42$  min.

# $(Ala)^2$ - $(Ala)^7$ -lug (3.11)

Peptide chain with resin was filtered and washed with DMF, DCM and hexane. The resin was transferred into a round-bottom flask and dried in vacuo overnight. The dried resin was then suspended in TFA/H<sub>2</sub>O/TIPS (90:5:5) (10.0 mL) for 3 h. The suspension was then filtered by gravity and washed with TFA and DCM. The filtrate collected in a clean round-bottom flask was evaporated to dryness (DCM was added several times). The residue was triturated with cold diethyl ether (x3) to afford the crude product as white powder (53.7 mg, 74%). The peptide product was analysed by using LCMS and found [MH<sup>+</sup>]: 783.6 at  $t_R$  of 2.89 min. Compound was then purified by RP-HPLC and obtained 2.1 mg as pure product (4.2% recovery). <sup>1</sup>H NMR (500 MHz, DMSO-d<sub>6</sub>)  $\delta$  10.61-10.75 (m, 1H, L-Trp<sup>3</sup>-CCHN*H*), 8.57 (d, J = 8.5, 1H, L-Trp<sup>3</sup>-N*H*), 8.48 (d, J = 8.6, 1H, D-Ala<sup>2</sup>-N*H*), 8.42 (d, J = 8.5, 1H, D-Leu<sup>4</sup>-N*H*), 8.30-8.35 (m, 1H, L-Val<sup>5</sup>-N*H*), 8.25-8.30 (m, 1H, D-Val<sup>6</sup>-N*H*), 8.15-8.17 (m, 1H, L-Ala<sup>7</sup>-N*H*), 7.96 (d, J = 7.8, 1H, L-Trp<sup>3</sup>-Ar-*H*), 7.94 (dd, J = 8.1, 3.7, 1H, L-Trp<sup>3</sup>-Ar-*H*), 7.83 (d, J = 7.9, 1H, L-Trp<sup>3</sup>-Ar-*H*), 7.72 (dd, J = 8.1, 1.3, 1H, L-Trp<sup>3</sup>-Ar-*H*), 7.55 (d, J = 2.2, 1H, L-Trp<sup>3</sup>-NHC*H*C), 4.60 (dd, J = 8.8, 4.5, 1H D-Val<sup>6</sup>-NHC*H*CH), 4.36 (t, J = 8.3, 1H, D-Leu<sup>4</sup>-NHC*H*CH<sub>2</sub>), 4.03 (d, J = 9.0,

1H, D-Ala²-NHCHCH), 3.96-4.00 (m, 1H, thiazolidine¹-NHCHCH2S), 3.86 (dd, J = 9.0, 6.6, 1H, L-Ala²-NHCHCH), 3.26 (dd, J = 10.5, 6.5, 1H, thiazolidine¹-NHCHCH2S), 3.13 (dd, J = 10.5, 6.5, 1H, thiazolidine¹-NHCHCH2S), 3.05 (dd, J = 7.8, 1H, L-Trp³-NHCHCH2), 3.05 (dd, J = 13.5, 5.4, 1H, L-Trp³-NHCHCH2), 2.86-2.92 (m, 1H, thiazolidine¹- NHCHCH2S), 2.19-2.30 (m, 1H, L-Ala²-CH(CH3)2), 2.00-2.06 (m, 1H, D-Val⁶-CH(CH3)2), 1.92-1.99 (m, 1H, L-Val⁶-CH(CH3)2), 1.66-1.72 (m, 1H, D-Ala²-CH(CH3)2), 1.52-1.61 (m, 1H, D-Leu⁴-CHCH2CH), 1.27-1.42 (m, 1H, D-Leu⁴-CHCH2CH), 1.16 (d, J = 6.4, 3H, D-Val⁶-CH(CH3)2), 1.08 (d, J = 6.7, 3H, D-Leu⁴-CH(CH3)2), 1.03 (d, J = 6.5, 3H, D-Val⁶-CH(CH3)2), 0.92 (d, J = 6.8, 3H, L-Val⁶-CH(CH3)2), 0.89 (d, J = 6.4, 3H, L-Val⁶-CH(CH3)2), 0.82 (d, J = 6.5, 3H, D-Ala²-CHCH3), 0.80 (d, J = 6.4, 3H, L-Ala²-CHCH3); HRMS: calculated for C<sub>36</sub>H<sub>54</sub>N<sub>8</sub>O<sub>6</sub>S₁<sup>+</sup> 727.3887, found 727.3930 [MH<sup>+</sup>]; Analytical RP-HPLC (**Method 1**)  $t_R = 4.46$  min.

# $(Ala)^3$ - $(Ala)^7$ -lug (3.12)

Peptide chain with resin was filtered and washed with DMF, DCM and hexane. The resin was transferred into a round-bottom flask and dried in vacuo overnight. The dried resin was then suspended in TFA/H<sub>2</sub>O/TIPS (90:5:5) (10.0 mL) for 3 h. The suspension was then filtered by gravity and washed with TFA and DCM. The filtrate collected in a clean round-bottom flask was evaporated to dryness (DCM was added several times). The residue was triturated with cold diethyl ether (x3) to afford the crude product as powder (52.6 mg, 68%). The peptide product was analysed by using LCMS and found [MH<sup>+</sup>]: 640.6 at  $t_R$  of 2.92 min. Compound was then purified by RP-HPLC and obtained 1.3 mg as pure product (4.1% recovery). <sup>1</sup>H NMR (500 MHz, DMSO-d<sub>6</sub>)  $\delta$  8.52 (d, J = 8.5, 1H, L-Ala<sup>3</sup>-NH), 8.47 (d, J = 8.4, 1H, D-Val<sup>2</sup>-NH), 8.38 (d, J = 8.5, 1H, D-Leu<sup>4</sup>-NH), 8.32-8.35 (m, 1H, L-Val<sup>5</sup>-NH), 8.22-8.27 (m, 1H, D-Val<sup>6</sup>-NH), 8.15-8.19 (m, 1H, L-Ala<sup>7</sup>-NH), 7.51 (d, J = 2.0, 1H, L-Trp<sup>3</sup>-NHCHC), 4.75-4.78 (m, 1H, L-Ala<sup>3</sup>-NHCHCH<sub>3</sub>), 4.62 (dd, J = 8.8, 4.5, 1H D-Val<sup>6</sup>-NHCHCH<sub>3</sub>), 4.35 (t, J = 8.3, 1H, D-Leu<sup>4</sup>-NHCHCH<sub>2</sub>), 4.03 (d, J = 9.0, 1H, D-Val<sup>2</sup>-NHCHCH), 3.96-4.00 (m, 1H, thiazolidine<sup>1</sup>-

NHCHCH<sub>2</sub>S), 3.86 (dd, J = 9.0, 6.6, 1H, L-Ala<sup>7</sup>-NHCHCH), 3.25 (dd, J = 10.5, 6.5, 1H, thiazolidine<sup>1</sup>-NHCHCH<sub>2</sub>S), 3.13 (dd, J = 10.5, 6.5, 1H, thiazolidine<sup>1</sup>-NHCHCH<sub>2</sub>S), 2.87-2.94 (m, 1H, thiazolidine<sup>1</sup>- NHCHCH<sub>2</sub>S), 2.25-2.32 (m, 1H, L-Ala<sup>7</sup>-CH(CH<sub>3</sub>)<sub>2</sub>), 2.03-2.07 (m, 1H, D-Val<sup>6</sup>-CH(CH<sub>3</sub>)<sub>2</sub>), 1.92-1.95 (m, 1H, L-Val<sup>5</sup>-CH(CH<sub>3</sub>)<sub>2</sub>), 1.66-1.72 (m, 1H, D-Val<sup>2</sup>-CH(CH<sub>3</sub>)<sub>2</sub>), 1.57-1.65 (m, 1H, D-Leu<sup>4</sup>-CHCH<sub>2</sub>CH), 1.35-1.42 (m, 1H, D-Leu<sup>4</sup>-CHCH<sub>2</sub>CH), 1.18 (d, J = 6.4, 3H, D-Val<sup>6</sup>-CH(CH<sub>3</sub>)<sub>2</sub>), 1.08 (d, J = 6.7, 3H, D-Leu<sup>4</sup>-CH(CH<sub>3</sub>)<sub>2</sub>), 1.07 (d, J = 6.7, 3H, D-Leu<sup>4</sup>-CH(CH<sub>3</sub>)<sub>2</sub>), 1.03 (d, J = 6.5, 3H, D-Val<sup>6</sup>-CH(CH<sub>3</sub>)<sub>2</sub>), 0.92 (d, J = 6.8, 3H, L-Val<sup>5</sup>-CH(CH<sub>3</sub>)<sub>2</sub>), 0.87 (d, J = 6.4, 3H, L-Val<sup>5</sup>-CH(CH<sub>3</sub>)<sub>2</sub>), 0.80 (d, J = 6.4, 3H, L-Ala<sup>7</sup>-CH(CH<sub>3</sub>)<sub>2</sub>), 0.78 (d, J = 6.5, 3H, D-Val<sup>2</sup>-CH(CH<sub>3</sub>)<sub>2</sub>), 0.75 (d, J = 6.7, 3H, L-Ala<sup>3</sup>-CHCH<sub>3</sub>), 0.65 (d, J = 6.4, 3H, D-Val<sup>2</sup>-CH(CH<sub>3</sub>)<sub>2</sub>); HRMS: calculated for C<sub>30</sub>H<sub>53</sub>N<sub>7</sub>O<sub>6</sub>S<sub>1</sub><sup>+</sup> 640.3778, found 640.3792 [MH<sup>+</sup>]; Analytical RP-HPLC (**Method 1**)  $t_R = 4.50$  min.

#### $(Ala)^4$ - $(Ala)^7$ -lug (3.13)

Peptide chain with resin was filtered and washed with DMF, DCM and hexane. The resin was transferred into a round-bottom flask and dried in vacuo overnight. The dried resin was then suspended in TFA/H<sub>2</sub>O/TIPS (90:5:5) (10.0 mL) for 3 h. The suspension was then filtered by gravity and washed with TFA and DCM. The filtrate collected in a clean round-bottom flask was evaporated to dryness (DCM was added several times). The residue was triturated with cold diethyl ether (x3) to afford the crude product as white powder (55.4 mg, 81%). The peptide product was analysed by using LCMS and found [MH<sup>+</sup>]: 685.4 at  $t_R$  of 2.88 min. Compound was then purified by RP-HPLC and obtained 0.9 mg as pure product (3.2% recovery). <sup>1</sup>H NMR (500 MHz, DMSO-d<sub>6</sub>)  $\delta$  10.60-10.65 (m, 1H, L-Trp<sup>3</sup>-CCHN*H*), 8.52 (d, J = 8.5, 1H, L-Trp<sup>3</sup>-N*H*), 8.45 (d, J = 8.5, 1H, D-Val<sup>2</sup>-N*H*), 8.38 (d, J = 8.5, 1H, D-Ala<sup>4</sup>-N*H*), 8.27-8.32 (m, 1H, L-Val<sup>5</sup>-N*H*), 8.21-8.25 (m, 1H, D-Val<sup>6</sup>-N*H*), 8.11-8.15 (m, 1H, L-Ala<sup>7</sup>-N*H*), 7.94 (d, J = 7.9, 1H, L-Trp<sup>3</sup>-Ar-*H*), 7.95 (dd, J = 8.0, 1.3, 1H, L-Trp<sup>3</sup>-Ar-*H*), 7.53 (d, J = 2.0, 1H, L-Trp<sup>3</sup>-NHC*H*C), 4.56 (dd, J = 8.8, 4.5, 1H D-Val<sup>6</sup>-NHC*H*CH), 4.34 (t, J = 8.5, 1H, D-Ala<sup>4</sup>-NHC*H*CH<sub>3</sub>), 4.03 (d, J = 9.0,

1H, D-Val<sup>2</sup>-NHC*H*CH), 3.96-4.00 (m, 1H, thiazolidine<sup>1</sup>-NHC*H*CH<sub>2</sub>S), 3.86 (dd, J = 9.0, 6.6, 1H, L-Ala<sup>7</sup>-NHC*H*CH), 3.25 (dd, J = 10.5, 6.5, 1H, thiazolidine<sup>1</sup>-NHCHC*H*<sub>2</sub>S), 3.13 (dd, J = 10.5, 6.5, 1H, thiazolidine<sup>1</sup>-NHCHC*H*<sub>2</sub>S), 3.05 (d, J = 7.8, 1H, L-Trp<sup>3</sup>-NHCHC*H*<sub>2</sub>), 3.01 (dd, J = 13.5, 5.4, 1H, L-Trp<sup>3</sup>-NHCHC*H*<sub>2</sub>), 2.85-2.91 (m, 1H, thiazolidine<sup>1</sup>- N*H*CHC*H*<sub>2</sub>S), 2.19-2.30 (m, 1H, L-Ala<sup>7</sup>-C*H*(CH<sub>3</sub>)<sub>2</sub>), 2.00-2.06 (m, 1H, D-Val<sup>6</sup>-C*H*(CH<sub>3</sub>)<sub>2</sub>), 1.92-1.99 (m, 1H, L-Val<sup>5</sup>-C*H*(CH<sub>3</sub>)<sub>2</sub>), 1.66-1.72 (m, 1H, D-Val<sup>2</sup>-C*H*(CH<sub>3</sub>)<sub>2</sub>), 1.18 (d, J = 6.4, 3H, D-Val<sup>6</sup>-CH(C*H*<sub>3</sub>)<sub>2</sub>), 1.15 (d, J = 6.7, 3H, D-Ala<sup>4</sup>-CHC*H*<sub>3</sub>), 1.03 (d, J = 6.5, 3H, D-Val<sup>6</sup>-CH(C*H*<sub>3</sub>)<sub>2</sub>), 0.92 (d, J = 6.8, 3H, L-Val<sup>5</sup>-CH(C*H*<sub>3</sub>)<sub>2</sub>), 0.87 (d, J = 6.4, 3H, L-Val<sup>5</sup>-CH(C*H*<sub>3</sub>)<sub>2</sub>), 0.80 (d, J = 6.4, 3H, L-Ala<sup>7</sup>-CHC*H*<sub>3</sub>), 0.78 (d, J = 6.5, 3H, D-Val<sup>2</sup>-CH(C*H*<sub>3</sub>)<sub>2</sub>), 0.67 (d, J = 6.4, 3H, D-Val<sup>2</sup>-CH(C*H*<sub>3</sub>)<sub>2</sub>); HRMS: calculated for C<sub>33</sub>H<sub>48</sub>N<sub>8</sub>O<sub>6</sub>S<sub>1</sub><sup>+</sup> 685.3418, found 685.3422 [MH<sup>+</sup>]; Analytical RP-HPLC (**Method 1**)  $I_R = 4.52$  min.

## $(Ala)^5$ - $(Ala)^7$ -lug (3.14)

Peptide chain with resin was filtered and washed with DMF, DCM and hexane. The resin was transferred into a round-bottom flask and dried in vacuo overnight. The dried resin was then suspended in TFA/H<sub>2</sub>O/TIPS (90:5:5) (10.0 mL) for 3 h. The suspension was then filtered by gravity and washed with TFA and DCM. The filtrate collected in a clean round-bottom flask was evaporated to dryness (DCM was added several times). The residue was triturated with cold diethyl ether (x3) to afford the crude product as white powder (54.5 mg, 78%). The peptide product was analysed by using LCMS and found [MH<sup>+</sup>]: 699.4 at  $t_R$  of 2.89 min. Compound was then purified by RP-HPLC and obtained 0.62 mg as pure product (3.4% recovery); HRMS: calculated for  $C_{34}H_{50}N_8O_6S_1^+$  699.3574, found 699.3593 [MH<sup>+</sup>]; Analytical RP-HPLC (**Method 1**)  $t_R$  = 4.25 min.

 $(Ala)^6$ - $(Ala)^7$ -lug (3.15)

Peptide chain with resin was filtered and washed with DMF, DCM and hexane. The resin was transferred into a round-bottom flask and dried in vacuo overnight. The dried resin was then suspended in TFA/H<sub>2</sub>O/TIPS (90:5:5) (10.0 mL) for 3 h. The suspension was then filtered by gravity and washed with TFA and DCM. The filtrate collected in a clean round-bottom flask was evaporated to dryness (DCM was added several times). The residue was triturated with cold diethyl ether (x3) to afford the crude product as white powder (51.7 mg, 74%). The peptide product was analysed by using LCMS and found [MH<sup>+</sup>]: 699.4 at  $t_R$  of 2.89 min. Compound was then purified by RP-HPLC and obtained 0.51 mg as pure product (3.0% recovery); HRMS: calculated for  $C_{34}H_{50}N_8O_6S_1^+$  699.3574, found 699.3594 [MH<sup>+</sup>]; Analytical RP-HPLC (**Method 1**)  $t_R$  = 4.48 min.

## 8.4 Experimental for Chapter 4

Synthesis of Fmoc-N-methyl amino acids

(9H-Fluoren-9-yl)methyl (S)-4-isopropyl-5-oxooxazolidine-3-carboxylate (4.22)

Fmoc-L-Val-OH (1.6 g, 5.10 mmol) was suspended in toluene (100.0 mL), and paraformaldehyde (1.0 g) and p-toluenesulfonic acid (100.0 mg) were added. The mixture was refluxed for 30 min with azeotropic water removal. The solution was cooled, washed with 1 N aqueous NaHCO<sub>3</sub> (2x25.0 mL) and dried over Na<sub>2</sub>SO<sub>4</sub>. Concentration in vacuo gave 1.42 g (92%) of product:  $[\alpha]_D^{23} = -27.5$  (c 1.0, DCM); <sup>1</sup>H NMR (400 MHz, CD<sub>3</sub>OD)  $\delta$  7.77 (d, J = 7.5 Hz, 2H, Ar-H), 7.62 (d, J = 7.5 Hz, 2H, Ar-H), 7.42 (t, J = 7.5 Hz, 2H, Ar-H), 7.30 (t, J = 7.5 Hz, 2H, Ar-H), 5.77 (s, 1H, COOC $H_2$ N), 5.75 (s, 1H, COOC $H_2$ N), 4.43 (d, J = 4.3 Hz, 2H, COOC $H_2$ ), 4.23 (t, J = 6.8 Hz, 1H, COOC $H_2$ CH), 4.05 (d, J = 4.3 Hz, 1H, NCHCOOC $H_2$ ),

2.30 (m, 1H,  $CH(CH_3)_2$ ), 1.04 (d, J = 6.8 Hz, 3H,  $CH(CH_3)_2$ ), 0.97 (d, J = 6.8 Hz, 3H,  $CH(CH_3)_2$ ); <sup>13</sup>C NMR (100 MHz,  $CD_3OD$ )  $\delta$ 178.2, 155.6, 142.6, 126.7, 126.2, 125.2, 120.5, 95.6, 78.9, 67.3, 47.0, 27.9, 18.9; LCMS: calculated for  $C_{21}H_{21}NO_4^+$  352.1, found 352.1 [MH<sup>+</sup>]

#### N-(((9H-Fluoren-9-yl)methoxy)carbonyl)-N-methyl-L-valine (4.24)

(9*H*-Fluoren-9-yl)methyl (*S*)-4-isopropyl-5-oxooxazolidine-3-carboxylate (**4.22**) (1.0 g, 2.81 mmol, 1.0 equiv.) was dissolved in CHC1<sub>3</sub> (15.0 mL), and trifluoroacetic acid (15.0 mL) and triethylsilane (1.4 mL, 1.0 g, 9.01 mmol, 3.2 equiv.) were added. The solution was stirred at room temperature for 24 h. Then additional fresh TFA (up to 50%) and one equivalent of TES was added and stirred for another 24 h followed by concentration in vacuo to an oil. The oil was dissolved in CH<sub>2</sub>C1<sub>2</sub> and re-concentrated three times. The resultant oil crystallized on standing. The crystals were dissolved in ether and concentrated to a crystalline solid which was washed with 5% ether in hexane and dried to give the product: yield (0.96 g, 94%); M.p. 142-144 °C; [α]<sub>D</sub><sup>23</sup> = -25.4° (c 1.0, CH<sub>2</sub>C1<sub>2</sub>); <sup>1</sup>H NMR (400 MHz, CD<sub>3</sub>OD) δ 7.79 (d, *J* = 7.5 Hz, 2H, Ar-H), 7.60 (d, *J* = 7.5 Hz, 2H, Ar-H), 7.44 (t, *J* = 7.5 Hz, 2H, Ar-H), 7.33 (t, *J* = 7.5 Hz, 2H, Ar-H), 4.23 (t, *J* = 6.8 Hz, 1H, COOCH<sub>2</sub>CH), 4.05 (d, *J* = 4.3 Hz, 1H, NCHCOOCH<sub>2</sub>), 3.56 (s, 3H, NCH<sub>3</sub>), 2.30 (m, 1H, CH(CH<sub>3</sub>)<sub>2</sub>), 1.05 (d, *J* = 6.8 Hz, 3H, CH(CH<sub>3</sub>)<sub>2</sub>), 0.95 (d, *J* = 6.8 Hz, 3H, CH(CH<sub>3</sub>)<sub>2</sub>); <sup>13</sup>C NMR (100 MHz, CD<sub>3</sub>OD) δ178.3, 155.6, 142.8, 126.9, 126.0, 125.2, 120.5, 95.6, 73.5, 67.3, 47.0, 33.1, 27.7, 19.1; LCMS: calculated for C<sub>21</sub>H<sub>23</sub>NO<sub>4</sub><sup>+</sup> 354.2, found 354.2 [MH<sup>+</sup>]

#### (9H-Fluoren-9-yl)methyl (S)-4-isobutyl-5-oxooxazolidine-3-carboxylate (4.23)

Fmoc-L-Leu-OH (1.0 g, 2.83 mmol) was suspended in toluene (100.0 mL), and paraformaldehyde (0.5 g) and p-toluenesulfonic acid (50.0 mg) were added. The mixture was refluxed for 30 min with azeotropic water removal. The solution was cooled, washed with 1 N aqueous NaHCO<sub>3</sub> (2x25.0 mL) and dried over Na<sub>2</sub>SO<sub>4</sub>. Concentration in vacuo gave 1.12 g

(85%) of product: M.p. 140-142 °C;  $[\alpha]_D^{23} = -30.5$  (c 1.0, DCM); <sup>1</sup>H NMR (400 MHz, CD<sub>3</sub>OD)  $\delta$  7.78 (d, J = 7.5 Hz, 2H, Ar-H), 7.64 (d, J = 7.5 Hz, 2H, Ar-H), 7.42 (t, J = 7.5 Hz, 2H, Ar-H), 7.35 (t, J = 7.5 Hz, 2H, Ar-H), 5.76 (s, 1H, NCHCOOC $H_2$ ), 5.75 (s, 1H, NCHCOOC $H_2$ ), 4.43 (d, J = 4.3 Hz, 2H, COOC $H_2$ ), 4.23 (t, J = 6.8 Hz, 1H, COOCH<sub>2</sub>CH), 4.07 (d, J = 4.3 Hz, 1H, NCHCOOCH<sub>2</sub>), 2.35 (m, 1H, CH(CH<sub>3</sub>)<sub>2</sub>), 2.02 (2H, CH2CH(CH3)<sub>2</sub>, 1.09 (d, J = 6.8 Hz, 3H, CH(CH3)<sub>2</sub>), 0.99 (d, J = 6.8 Hz, 3H, CH(CH3)<sub>2</sub>); <sup>13</sup>C NMR (100 MHz, CD<sub>3</sub>OD)  $\delta$ 178.2, 155.6, 142.6, 126.7, 126.2, 125.2, 120.5, 95.6, 78.9, 67.3, 47.0, 27.9, 21.5, 18.9; LCMS: calculated for C<sub>22</sub>H<sub>23</sub>NO<sub>4</sub><sup>+</sup> 366.2, found 366.2 [MH<sup>+</sup>]

#### N-(((9H-Fluoren-9-yl)methoxy)carbonyl)-N-methyl-L-leucine (4.25)

(9*H*-Fluoren-9-yl)methyl (*S*)-4-isobutyl-5-oxooxazolidine-3-carboxylate (**4.23**) (1.0 g, 2.74 mmol, 1.0 equiv.) was dissolved in in CHC1<sub>3</sub> (15.0 mL), and trifluoroacetic acid (15.0 mL) and triethylsilane (1.36 mL, 0.76 g, 8.61 mmol, 3.2 equiv.) were added. The solution was stirred at room temperature for 24 h. Then additional fresh TFA (up to 50%) and one equivalent of TES was added and stirred for another 24 h followed by concentration in vacuo to an oil. The oil was dissolved in CH<sub>2</sub>C1<sub>2</sub> and re-concentrated three times. The resultant oil crystallized on standing. The crystals were dissolved in ether and concentrated to a crystalline solid which was washed with 5% ether in hexane and dried to give the product: yield (0.86 g, 90%); M.p. 147-149 °C; [α]<sub>D</sub><sup>23</sup> = -30.9° (c 1.0, CH<sub>2</sub>C1<sub>2</sub>); <sup>1</sup>H NMR (400 MHz, CD<sub>3</sub>OD) δ 7.82 (d, *J* = 7.5 Hz, 2H, Ar-H), 7.67 (d, *J* = 7.5 Hz, 2H, Ar-H), 7.42 (t, *J* = 7.5 Hz, 2H, Ar-H), 7.35 (t, *J* = 7.5 Hz, 2H, Ar-H), 4.43 (d, *J* = 4.3 Hz, 2H, COOC*H*<sub>2</sub>), 4.23 (t, *J* = 6.8 Hz, 1H, COOCH<sub>2</sub>C*H*), 4.07 (d, *J* = 4.3 Hz, 1H, NC*H*COOCH<sub>2</sub>), 3.21 (s, 3H, NC*H*<sub>3</sub>), 2.35 (m, 1H, C*H*(CH<sub>3</sub>)<sub>2</sub>), 2.02 (2H, C*H*<sub>2</sub>CH(C*H*<sub>3</sub>)<sub>2</sub>), 1.06 (d, *J* = 6.8 Hz, 3H, CH(C*H*<sub>3</sub>)<sub>2</sub>), 0.97 (d, *J* = 6.8 Hz, 3H, CH(C*H*<sub>3</sub>)<sub>2</sub>); <sup>13</sup>C NMR (100 MHz, CD<sub>3</sub>OD) δ178.4, 155.7, 142.6, 126.5, 126.2, 125.4, 120.6, 95.8, 78.9, 67.3, 47.0, 27.9, 21.5, 18.9; LCMS: calculated for C<sub>21</sub>H<sub>23</sub>NO<sub>4</sub><sup>+</sup> 354.1627, found 354.2 [MH<sup>+</sup>]

#### **Synthesis of Fmoc-L-homoleucine**

#### **N-Benzyl-(S)-proline** $(4.27)^{352}$

(*S*)-Proline (20.7 g, 179.80 mmol) was added to KOH (35.4 g, 630.01 mmol) in <sup>*i*</sup>PrOH (330.0 mL) and stirred at 45 °C. Benzyl chloride (24.8 mL, 216.0 mmol) in <sup>*i*</sup>PrOH (25.0 mL) was added dropwise over 1 h and the reaction mixture was subsequently left stirring at 45 °C for 5 h. With the aid of an ice bath, concentrated HCl was added to achieve pH 5-6, before CHCl<sub>3</sub> (170.0 mL) was added and the suspension left to settle overnight. The KCl was filtered off and the filtrate concentrated *in vacuo*. The resulting residue was triturated with acetone to yield product as a white powder (36.58 g, 89 %); M.p. 168-170 °C (lit.<sup>352</sup> M.p. 174-175 °C); R<sub>f</sub> = 0.08 (Hexane/EtOAc/AcOH, 1:1:0.01);  $[\alpha]_D^{23} = -25.5$  (c = 1, MeOH) (lit.<sup>352</sup>  $[\alpha]_D^{20} = -25.8$  (c = 1, EtOH)); <sup>1</sup>H NMR (400 MHz, CD<sub>3</sub>OD)  $\delta$  7.58-7.53 (m, 2H, Ph *Hs*), 7.49-7.45 (m, 3H, Ph *Hs*), 4.51 (d, *J* = 12.8 Hz, 1H, NCH<sub>A</sub>H<sub>B</sub>Ph), 4.28 (d, *J* = 12.8 Hz, 1H, NCH<sub>A</sub>H<sub>B</sub>Ph), 3.95 (dd, *J* = 9.4, 6.8 Hz, 1H, Pro<sub>8</sub>-*H*), 3.56-3.51 (m, 1H, Pro<sub>8</sub>-*H*), 3.28-3.21 (m, 1H, Pro<sub>8</sub>-*H*), 2.53-2.43 (m, 1H, Pro<sub>β</sub>-*H*), 2.19-2.08 (m, 2H, Pro<sub>β</sub>-*H*, Pro<sub>γ</sub>-*H*), 2.02-1.90 (m, 1H, Pro<sub>γ</sub>-*H*); <sup>13</sup>C NMR (100 MHz, CD<sub>3</sub>OD)  $\delta$  171.4, 130.6, 130.2, 129.5, 128.9, 68.4, 58.0, 53.8, 28.4, 22.4; LCMS: calculated for C<sub>12</sub>H<sub>16</sub>NO<sub>2</sub>+ 206.1, found 206.0 [MH<sup>+</sup>].

#### (S)-2-[N'-(N-Benzylprolyl)amino]benzophenone (BPB) $(4.28)^{352}$

*N*-Benzyl-(*S*)-proline (10.00 g, 49.0 mmol) had chlorobenzene (100.0 mL) added and cooled in an ice bath. To this phosphorus (V) pentachloride (10.15 g, 49.0 mmol) was added and left stirring at room temperature. The progress of the reaction was monitored after 30 min by LCMS. Then, 2-aminobenzophenone (9.61 g, 49.0 mmol) was added and stirred for a further 90 min.

The reaction was subsequently quenched with MeOH (8.0 mL) before being filtered to collect the crude precipitate, which was washed with acetone and dried *in vacuo*. Recrystallisation of this material in MeOH gave the pure product. Further product was recovered from the crude reaction filtrate by concentrating *in vacuo* and triturating the residual solid with acetone. The off-white solids obtained were combined (10.03 g, 54 %);  $R_f$ = 0.74 (Hexane/EtOAc 1:1);  $[\alpha]_D^{23}$  = -41.7 (c = 1, MeOH); <sup>1</sup>H NMR (400 MHz, CD<sub>3</sub>OD)  $\delta$  7.81-7.77 (m, 2H, Ph Hs), 7.68-7.58 (m, 2H, Ph Hs), 7.55-7.44 (m, 5H, Ph Hs), 7.43-7.35 (m, 5H, Ph Hs), 4.38-4.25 (m, 3H, NC $H_AH_B$ Ph, NCH<sub>A</sub> $H_B$ Ph, Pro $_\alpha$ -H), 3.61-3.53 (m, 1H, Pro $_\delta$ -H), 3.38-3.29 (m, 1H, Pro $_\delta$ -H), 2.47-2.35 (m, 1H, Pro $_\beta$ -H), 2.21-2.10 (m, 1H, Pro $_\gamma$ -H), 1.96-1.83 (m, 1H, Pro $_\gamma$ -H), 1.72-1.61 (m, 1H, Pro $_\beta$ -H); <sup>13</sup>C NMR (100 MHz, CD<sub>3</sub>OD)  $\delta$  196.2, 165.8, 137.2, 134.6, 132.9, 131.8, 131.7, 130.6, 130.2, 129.85, 129.81, 129.7, 128.9, 128.1, 125.5, 124.2, 66.7, 57.9, 54.4, 28.1, 22.4; LCMS: calculated for C<sub>25</sub>H<sub>25</sub>N<sub>2</sub>O<sub>2</sub>+ 385.2, found 385.0 [MH<sup>+</sup>].

# Ni (II)-Glycine-BPB complex (4.29)<sup>352,355</sup>

BPB•HCl salt (7.50 g, 17.8 mmol), glycine (4.02 g, 53.5 mmol) and Ni (NO<sub>3</sub>)<sub>2</sub>•6H<sub>2</sub>O (10.36 g, 35.7 mmol) had MeOH added (150 mL) and heated to 50 °C. K<sub>2</sub>CO<sub>3</sub> (36.97 g, 267.0 mmol) was added and heated to reflux at 65 °C. The green suspension quickly turned dark red. Additional K<sub>2</sub>CO<sub>3</sub> (12.32 g, 89.1 mmol) was added after 1 h. The reaction was cooled in an ice bath after an extra 2 h, before quenching with AcOH (15.0 mL). After filtering, H<sub>2</sub>O (450.0 mL) was added to the filtrate and stirred overnight. The resulting red precipitate was collected by vacuum filtration and dried in an oven at 45 °C to yield the product as a red solid (7.26 g, 80 %); M.p. 214-216°C (lit.<sup>355</sup> M.p. 217-220 °C); R<sub>f</sub> = 0.23 (Hexane/EtOAc/Acetone, 1:3:1); [α]<sub>D</sub><sup>24</sup> = +1792.3 (c = 0.29, MeOH) (lit.<sup>352</sup> [α]<sub>D</sub><sup>20</sup> = +2006 (c = 0.1, MeOH)); <sup>1</sup>H NMR (400 MHz, CDCl<sub>3</sub>) δ 8.31 (d, J = 8.7 Hz, 1H, Ph H), 8.09 (d, J = 7.3 Hz, 2H, Ph Hs), 7.58-7.50 (m, 3H, Ph Hs), 7.45 (t, J = 7.4 Hz, 2H, Ph Hs), 7.33 (t, J = 7.3 Hz, 1H, Ph H), 7.23 (t, J = 7.5 Hz, 1H, Ph H), 7.12 (d, J = 6.7 Hz, 1H, Ph H), 7.03-6.98 (m, 1H, Ph H), 6.82 (d, J = 7.8 Hz, 1H, Ph H), 6.72 (t, J = 7.4 Hz, 1H, Ph H), 4.51 (d, J = 12.7 Hz, 1H, NCH<sub>A</sub>H<sub>B</sub>Ph), 3.83-3.67 (m, 4H,

Pro<sub>δ</sub>-H, NC $H_A$ H<sub>B</sub>Ph, Gly<sub>α</sub>-H<sub>2</sub>), 3.50 (dd, J = 10.4, 4.9 Hz, 1H, Pro<sub>α</sub>-H), 3.43-3.31 (m, 1H, Pro<sub>γ</sub>-H), 2.64-2.56 (m, 1H, Pro<sub>β</sub>-H), 2.50-2.39 (m, 1H, Pro<sub>β</sub>-H), 2.21-2.05 (m, 2H, Pro<sub>γ</sub>-H, Pro<sub>δ</sub>-H); <sup>13</sup>C NMR (100 MHz, CDCl<sub>3</sub>) δ 181.4, 177.3, 171.7, 142.6, 134.7, 133.3, 133.2, 132.3, 131.8, 129.8, 129.6, 129.4, 129.2, 129.0, 126.4, 125.7, 125.2, 124.3, 120.9, 69.9, 63.1, 61.3, 57.5, 30.8, 23.7; LCMS: calculated for C<sub>27</sub>H<sub>26</sub>N<sub>3</sub>NiO<sub>3</sub><sup>+</sup> 498.1, found 498.1 [MH<sup>+</sup>].

## Ni (II)-(S)-BPB/(S)-2-amino-5-methylhexanoic acid Schiff's base complex (4.35)

To a solution of Ni (II)-Gly-BPB complex (2.21 g, 4.4 mmol) in anhydrous DMF (60.0 mL) was added NaOH (0.89 g, 22.2 mmol). After 5 min, isopentyl iodide (4.34) (0.56 mL, 4.8 mmol) in anhydrous DMF (10.0 mL) was added dropwise and stirred for 1 h. The reaction was monitored using RP-HPLC, quenched with saturated aqueous NH<sub>4</sub>Cl (110.0 mL) and extracted with EtOAc (3x50.0 mL). The organic layer was dried over MgSO4 and concentrated in vacuo. The residue was then re-dissolved in anhydrous MeOH (90 mL), K<sub>2</sub>CO<sub>3</sub> (3.07 g, 22.2 mmol) added and refluxed at 60 °C for 2 h. After quenching with 5 % AcOH in H<sub>2</sub>O (60.0 mL) at 0 °C, the reaction mixture was extracted with CH<sub>2</sub>Cl<sub>2</sub> (3x50.0 mL), dried over Na<sub>2</sub>SO<sub>4</sub> and concentrated in vacuo. Purification was achieved by column chromatography (hexane/ethyl acetate/acetone, 1:3:1) to give the product as a red solid (1.78 g, 68 %); M.p. 205-207 °C;  $R_f$ = 0.42 (Hexane/EtOAc/Acetone, 1:3:1); <sup>1</sup>H NMR (400 MHz, CDCl<sub>3</sub>)  $\delta$  8.15 (d, J = 8.6 Hz, 1H, Ph H), 8.08 (d, J = 7.5 Hz, 2H, Ph H), 7.57-7.48 (m, 3H, Ph Hs), 7.38 (t, J = 7.5 Hz, 2H, Ph Hs), 7.30-7.27 (m, 1H, Ph H), 7.24-7.15 (m, 2H, Ph Hs), 6.97 (d, J = 7.1 Hz, 1H, Ph H), 6.72-6.65 (m, 2H, Ph Hs), 4.45 (d, J = 12.7 Hz, 1H, NCH<sub>A</sub>H<sub>B</sub>Ph), 3.86 (dd, J = 9.7, 3.4 Hz, 1H, C<sub>\alpha</sub>-H), 3.63-3.48 (m, 4H,  $Pro_{\alpha}$ -H,  $Pro_{\gamma}$ -H,  $Pro_{\delta}$ -H,  $NCH_AH_BPh$ ), 2.80-2.64 (m, 1H,  $Pro_{\beta}$ -H), 2.62-2.51 (m, 1H, Pro<sub>8</sub>-H), 1.76-1.85 (m, 2H, CH<sub>2</sub>CH<sub>2</sub>CH), 1.60-1.65 (m, 1H, CH<sub>2</sub>CH<sub>2</sub>CH), 1.15.1.23 (m, 2H, CH<sub>2</sub>CH<sub>2</sub>CH), 1.05 (d, 6H, CH<sub>2</sub>CH(CH<sub>3</sub>)<sub>2</sub>), 2.29-2.21 (m, 1H, Pro<sub> $\gamma$ </sub>-H), 2.15-2.03 (m, 1H, Pro<sub>δ</sub>-H); <sup>13</sup>C NMR (100 MHz, CDCl<sub>3</sub>) δ 180.5, 178.4, 171.5, 142.4, 133.4, 133.2, 132.6, 131.5, 130.0, 129.2, 129.2, 129.0, 129.0, 127.2, 127.0, 126.1, 123.9, 120.9, 70.2, 68.6, 63.2, 57.2, 30.8, 30.3, 30.0, 28.1, 23.9; LCMS: calculated for C<sub>32</sub>H<sub>35</sub>N<sub>3</sub>NiO<sub>3</sub><sup>+</sup> 568.2, found 568.2 [MH<sup>+</sup>];

#### **Fmoc-L-Hle-OH (4.37)**

The alkylated Ni complex (2.50 g, 4.2 mmol) was dissolved in MeOH/2M HCl (3:1, 100.0 mL) and heated in a microwave reactor (50 W, 75 °C) for 30 min. After solvent removal in vacuo, the residue was re-dissolved in H<sub>2</sub>O (250.0 mL). Adjustment to pH 9 was achieved using saturated aqueous Na<sub>2</sub>CO<sub>3</sub> and the mixture was extracted with DCM (2x100.0 mL, 1x50.0 mL). EDTA disodium salt dihydrate (1.57 g, 4.2 mmol) was added to the aqueous layer and stirred for 1 h. Additional Na<sub>2</sub>CO<sub>3</sub> (1.34 g, 12.6 mmol) was added before dropwise addition of Fmoc-Oxyma (1.53 g, 4.2 mmol) in THF (140.0 mL) over 20 min at 0 °C. The reaction was stirred overnight at room temperature. Following THF removal in vacuo, the aqueous suspension was extracted with Et<sub>2</sub>O (2x100.0 mL). Acidification of the aqueous layer was carried out using saturate aqueous KHSO<sub>4</sub> until pH 1-2. This was subsequently extracted with EtOAc (2x100.0 mL, 1x50.0 mL), the combined organic extracts dried over MgSO<sub>4</sub> and concentrated in vacuo. Trituration of the resulting residue with H<sub>2</sub>O/MeOH (9:1) afforded the product as a white solid (0.85 g, 49 %); M.p. 125-127 °C;  $R_f = 0.26$  (Hexane/EtOAc/AcOH, 1:1:0.01);  $[\alpha]_D^{24} = -15.8$  (c = 0.45, MeOH); <sup>1</sup>H NMR (400 MHz, CD<sub>3</sub>OD)  $\delta$  7.77 (d, J = 7.5 Hz, 2H, Ar-H), 7.62 (d, J = 7.5 Hz, 2H, Ar-H), 7.42 (t, J = 7.5 Hz, 2H, Ar-H), 7.30 (t, J = 7.5 Hz, 2H, Ar-H), 5.78 (s, 1H, NCHCOOCH<sub>2</sub>), 5.73 (s, 1H, NCHCOOCH<sub>2</sub>), 1.75-1.88 (m, 2H, CH<sub>2</sub>CH<sub>2</sub>CH), 1.55-1.62 (m, 1H, CH<sub>2</sub>CH<sub>2</sub>CH), 1.18.1.27 (m, 2H, CH<sub>2</sub>CH<sub>2</sub>CH), 1.15 (d, 6H, CH<sub>2</sub>CH(CH<sub>3</sub>)<sub>2</sub>); <sup>13</sup>C NMR (100 MHz, CD<sub>3</sub>OD) δ δ178.5, 155.8, 142.9, 127.7, 125.2, 123.2, 118.5, 92.6, 77.9, 67.3, 47.0, 25.9, 22.5, 17.9; LCMS: calculated for C<sub>22</sub>H<sub>25</sub>NO<sub>4</sub><sup>+</sup> 368.2, found 368.2 [MH<sup>+</sup>]

# 8.5 Experimental for Chapter 5

(9H-Fluoren-9-yl)methyl (S)-(4-methyl-1-oxopentan-2-yl)carbamate (5.1)<sup>304</sup>

Fmoc-L-Leu-OH (2.0 g, 6.03 mmol, 1.0 equiv.) was dissolved in dry DCM (80.0 mL). The solution was cooled to 0°C and CDI (1.1 g, 6.63 mmol, 1.1 equiv.) was added. After stirring for 1 h at 0 °C, the reaction solution was cooled to -78°C (acetone/CO<sub>2</sub> bath) for 15 min. The DIBAL-H solution (1.0 M in toluene) (12.7 ml, 12.67 mmol, 2.1 equiv.) was added dropwise over 10 min under N<sub>2</sub> gas. The reaction mixture was stirred at -78°C for 1.5 h and monitored by TLC (Hexane: EtOAc 2:1). Upon completion, the reaction mixture diluted in EtOAc (80.0 mL) and quenched with the addition of tartaric acid solution (25% in H<sub>2</sub>O) (50.0 mL) with vigorous stirring. The mixture was warmed to room temperature and stirred at ambient temperature for 15 min. The organic phase was extracted with EtOAc (1×80.0 mL), and the combined organic layers were washed with 1M HCl aq (1×50.0 mL), 0.8M NaHCO<sub>3</sub> aq (1×50.0 mL), sat. NaCl aq (1×50.0 mL), dried over MgSO<sub>4</sub> and concentrated in vacuo. Purification was achieved by column chromatography (hexane/ethyl acetate, 3:1) to give 5.1 as white powder (1.75 g, 85% yield); M.p. 158-160 °C;  $R_f = 0.25$  (hexane/EtOAc = 2:1); <sup>1</sup>H NMR (CDCl<sub>3</sub>, 400 MHz)  $\delta$  9.65 (s, 1H, CHO), 7.75 (d, J = 7.5 Hz, 2H, Ar-H), 7.60 (d, J = 7.3Hz, 2H, Ar-H), 7.41 (t, J = 7.5 Hz, 2H, Ar-H), 7.32 (t, J = 7.5 Hz, 2H, Ar-H), 5.37 (brs, 1H, NH), 4.42 (d, J = 6.8 Hz, 2H, COOC $H_2$ ), 4.30-4.39 (m, 1H, NHCH), 4.20 (t, J = 6.8 Hz, 1H, COOCH<sub>2</sub>CH), 2.30 (m, 1H, CH(CH<sub>3</sub>)<sub>2</sub>), 1.72-1.78 (m, 2H, NHCHCH<sub>2</sub>), 1.04 (d, J = 6.8 Hz, 3H, CH(CH<sub>3</sub>)<sub>2</sub>), 0.97 (d, J = 6.8 Hz, 3H, CH(CH<sub>3</sub>)<sub>2</sub>); <sup>13</sup>C NMR (CDCl<sub>3</sub>, 100 MHz)  $\delta$  199.8, 156.4, 143.8, 141.3, 127.8, 127.1, 125.1, 120.0, 67.1, 65.1, 47.3, 29.1, 20.5, 17.6. LCMS: calcd. for  $C_{21}H_{23}NO_3 + 338.2$ , found 338.2 [MH<sup>+</sup>].

#### (9H-Fluoren-9-yl)methyl (S)-(5-methyl-1-oxohexan-2-yl)carbamate (5.2)

Fmoc-L-Hle-OH (1.0 g, 2.85 mmol, 1.0 equiv.) was dissolved in dry DCM (50.0 mL). The solution was cooled to 0°C and CDI (0.5 g, 3.14 mmol, 1.1 equiv.) was added. After stirring for 1 h at 0 °C, the reaction solution was cooled to -78°C (acetone/CO<sub>2</sub> bath) for 15 min. The DIBAL-H solution (1.0 M in toluene) (6.0 ml, 5.99 mmol, 2.1 equiv.) was added dropwise over 10 min under N<sub>2</sub> gas. The reaction mixture was stirred at -78°C for 1.5 h and monitored by TLC (Hexane: EtOAc 2:1). Upon completion, the reaction mixture diluted in EtOAc (80.0 mL) and quenched with the addition of tartaric acid solution (25% in H<sub>2</sub>O) (50.0 mL) with vigorous stirring. The mixture was warmed to room temperature and stirred at ambient temperature for 15 min. The organic phase was extracted with EtOAc (1×80.0 mL), and the combined organic layers were washed with 1M HCl aq (1×50.0 mL), 0.8M NaHCO<sub>3</sub> aq (1×50.0 mL), sat. NaCl aq (1×50.0 mL), dried over MgSO<sub>4</sub> and concentrated in vacuo. Purification was achieved by column chromatography (hexane/ethyl acetate, 2:1) to give 5.2 as white powder (0.65 g, 72% yield); M.p 158-160 °C;  $R_f = 0.25$  (hexane/EtOAc = 2:1); <sup>1</sup>H NMR (CDCl<sub>3</sub>, 400 MHz)  $\delta$  9.66 (s, 1H, CHO), 7.81 (d, J = 7.5 Hz, 2H, Ar-H), 7.54 (d, J = 7.3Hz, 2H, Ar-H), 7.40 (t, J = 7.5 Hz, 2H, Ar-H), 7.32 (t, J = 7.5 Hz, 2H, Ar-H), 5.35 (brs, 1H, NH), 4.42 (d, J = 6.8 Hz, 2H, COOCH<sub>2</sub>), 4.31-4.39 (m, 1H, NHCH), 4.20 (t, J = 6.8 Hz, 1H, COOCH<sub>2</sub>CH), 2.34 (m, 1H, CH(CH<sub>3</sub>)<sub>2</sub>), 1.75-1.79 (m, 2H, NHCHCH<sub>2</sub>), 1.05-1.18 (m, 2H, NHCHCH<sub>2</sub>CH<sub>2</sub>), 1.04 (d, J = 6.8 Hz, 3H, CH(CH<sub>3</sub>)<sub>2</sub>), 0.97 (d, J = 6.8 Hz, 3H, CH(CH<sub>3</sub>)<sub>2</sub>); <sup>13</sup>C NMR (CDCl<sub>3</sub>, 100 MHz) δ 199.8, 156.4, 143.8, 141.3, 127.7, 127.1, 125.2, 120.0, 67.3, 65.2, 47.3, 29.1, 25.4, 20.2, 17.6. LCMS: calcd. for  $C_{22}H_{25}NO_3 + 352.1834$ , found 352.2 [MH<sup>+</sup>].

#### (9H-Fluoren-9-yl)methyl (S)-(1-oxopentan-2-yl)carbamate (5.11)

Fmoc-L-Nva-OH (1.0 g, 3.09 mmol, 1.0 equiv.) was dissolved in dry DCM (40.0 mL). The solution was cooled to 0°C and CDI (0.6 g, 3.34 mmol, 1.1 equiv.) was added. After stirring for 1 h at 0 °C, the reaction solution was cooled to -78°C (acetone/CO<sub>2</sub> bath) for 15 min. The DIBAL-H solution (1.0 M in toluene) (6.5 ml, 6.49 mmol, 2.1 equiv.) was added dropwise over 10 min under N<sub>2</sub> gas. The reaction mixture was stirred at -78°C for 1.5 h and monitored by TLC (Hexane: EtOAc 2:1). Upon completion, the reaction mixture diluted in EtOAc (80.0 mL) and quenched with the addition of tartaric acid solution (25% in H<sub>2</sub>O) (50.0 mL) with vigorous stirring. The mixture was warmed to room temperature and stirred at ambient temperature for 15 min. The organic phase was extracted with EtOAc (1×80 mL), and the combined organic layers were washed with 1M HCl aq (1×50 mL), 0.8M NaHCO<sub>3</sub> aq (1×50 mL), sat. NaCl aq (1×50 mL), dried over MgSO<sub>4</sub> and concentrated in vacuo. Purification was achieved by column chromatography (hexane/ethyl acetate, 3:1) to give **5.10** as white powder  $(0.78 \text{ g}, 82\% \text{ yield}); \text{ M.p } 142-144 \text{ °C}; \text{ R}_f = 0.27 \text{ (hexane/EtOAc} = 2:1); {}^{1}\text{H NMR (CDCl}_3, 400)$ MHz)  $\delta$  9.67 (s, 1H, CHO), 7.87 (d, J = 7.5 Hz, 2H, Ar-H), 7.65 (d, J = 7.3 Hz, 2H, Ar-H), 7.47 (t, J = 7.5 Hz, 2H, Ar-H), 7.35 (t, J = 7.5 Hz, 2H, Ar-H), 5.37 (brd, J = 6.6 Hz, 1H, NH), 4.42 $(d, J = 6.8 \text{ Hz}, 2H, COOCH_2), 4.35-4.38 \text{ (m, 1H, NHC}H), 4.27 \text{ (t, } J = 6.8 \text{ Hz}, 1H, COOCH_2CH),$ 1.65-1.68 (m, 2H, NHCHC $H_2$ ), 1.15-1.23 (m, 2H, NHCHC $H_2$ C $H_2$ ), 0.98 (t, J = 6.8 Hz, 3H, CH<sub>2</sub>CH<sub>3</sub>); <sup>13</sup>C NMR (CDCl<sub>3</sub>, 400 MHz) δ 198.8, 157.4, 145.8, 141.7, 127.4, 127.0, 126.1, 122.4, 66.5, 64.1, 47.3, 29.1, 22.7, 19.5, 17.6. LCMS: calcd. for C<sub>20</sub>H<sub>21</sub>NO<sub>3</sub> + 324.1521, found 324.2 [MH<sup>+</sup>].

#### (9*H*-Fluoren-9-yl)methyl (*S*)-(1-oxohexan-2-yl)carbamate (5.12)

Fmoc-L-Nle-OH (1.0 g, 2.96 mmol, 1.0 equiv.) was dissolved in dry DCM (40.0 mL). The solution was cooled to 0°C and CDI (0.6 g, 3.26 mmol, 1.1 equiv.) was added. After stirring for 1 h at 0 °C, the reaction solution was cooled to -78°C (acetone/CO<sub>2</sub> bath) for 15 min. The DIBAL-H solution (1.0 M in toluene) (6.2 ml, 6.21 mmol, 2.1 equiv.) was added dropwise over 10 min under N<sub>2</sub> gas. The reaction mixture was stirred at -78°C for 1.5 h and monitored by TLC (Hexane: EtOAc 2:1). Upon completion, the reaction mixture diluted in EtOAc (80.0 mL) and quenched with the addition of tartaric acid solution (25% in H<sub>2</sub>O) (50.0 mL) with vigorous stirring. The mixture was warmed to room temperature and stirred at ambient temperature for 15 min. The organic phase was extracted with EtOAc (1×80.0 mL), and the combined organic layers were washed with 1M HCl aq (1×50.0 mL), 0.8M NaHCO<sub>3</sub> aq (1×50.0 mL), sat. NaCl aq (1×50.0 mL), dried over MgSO<sub>4</sub> and concentrated in vacuo. Purification was achieved by column chromatography (hexane/ethyl acetate, 3:1) to give 5.11 as white powder (0.75 g, 70% yield); M.p 135-137 °C;  $R_f = 0.25$  (hexane/EtOAc = 2:1); <sup>1</sup>H NMR (CDCl<sub>3</sub>, 400 MHz)  $\delta$  9.67 (s, 1H, CHO), 7.87 (d, J = 7.5 Hz, 2H, Ar-H), 7.65 (d, J = 7.3Hz, 2H, Ar-H), 7.47 (t, J = 7.5 Hz, 2H, Ar-H), 7.35 (t, J = 7.5 Hz, 2H, Ar-H), 5.37 (brd, J = 6.6Hz, 1H, NH), 4.42 (d, J = 6.8 Hz, 2H, COOCH<sub>2</sub>), 4.35-4.38 (m, 1H, NHCH), 4.27 (t, J = 6.8Hz ,1H, COOCH<sub>2</sub>CH), 1.65-1.68 (m, 2H, NHCHCH<sub>2</sub>), 1.15-1.23 (m, 2H, NHCHCH<sub>2</sub>CH<sub>2</sub>), 0.99-1.05 (m, 2H, NHCHCH<sub>2</sub>CH<sub>2</sub>CH<sub>2</sub>), 0.95 (t, J = 6.8 Hz, 3H, CH<sub>2</sub>CH<sub>3</sub>); <sup>13</sup>C NMR (CDCl<sub>3</sub>, 400 MHz) δ 198.8, 157.4, 145.8, 141.7, 127.4, 127.0, 126.1, 122.4, 66.5, 64.1, 47.3, 29.1, 24.7, 22.7, 19.5, 17.6. LCMS: calcd. for  $C_{21}H_{23}NO_3 + 338.1678$ , found 338.2 [MH<sup>+</sup>].

#### (9H-Fluoren-9-yl)methyl (S)-(1-(1H-indol-3-yl)-3-oxopropan-2-yl)carbamate (5.20)

Fmoc-L-Trp-OH (1.0 g, 2.44 mmol, 1.0 equiv.) was dissolved in dry DCM (50.0 mL). The solution was cooled to 0°C and CDI (0.5 g, 2.68 mmol, 1.1 equiv.) was added. After stirring for 1 h at 0 °C, the reaction solution was cooled to -78°C (acetone/CO<sub>2</sub> bath) for 15 min. The DIBAL-H solution (1.0 M in toluene) (5.1 ml, 5.12 mmol, 2.1 equiv.) was added dropwise over 10 min under N<sub>2</sub> gas. The reaction mixture was stirred at -78°C for 1.5 h and monitored by TLC (Hexane: EtOAc 2:1). Upon completion, the reaction mixture diluted in EtOAc (80.0 mL) and quenched with the addition of tartaric acid solution (25% in H<sub>2</sub>O) (50.0 mL) with vigorous stirring. The mixture was warmed to room temperature and stirred at ambient temperature for 15 min. The organic phase was extracted with EtOAc (1×80.0 mL), and the combined organic layers were washed with 1M HCl aq (1×50.0 mL), 0.8M NaHCO<sub>3</sub> aq (1×50.0 mL), sat. NaCl aq (1×50.0 mL), dried over MgSO<sub>4</sub> and concentrated in vacuo. Purification was achieved by column chromatography (hexane/ethyl acetate, 3:1) to give 5.20 as white powder (0.57 g, 47% yield); M.p 166-168 °C;  $R_f = 0.25$  (hexane/EtOAc = 2:1); <sup>1</sup>H NMR (CDCl<sub>3</sub>, 400 MHz)  $\delta$  10.82 (brs, 1H, Trp-N*H*), 9.57 (s, 1H, C*H*O), 7.76 (d, J = 7.5 Hz, 2H, Ar-H), 7.55 (d, J = 7.5 Hz, 2H, Ar-H), 7.52 (d, J = 7.5 Hz, 1H, Trp-Ar-H), 7.43 (t, J = 7.5Hz, 2H, Ar-H), 7.32 (t, J = 7.5 Hz, 2H, Ar-H), 7.30 (d, J = 7.5 Hz, 1H, Trp-Ar-H), 7.23 (m, 1H, Trp-Ar-H), 7.11 (m, 1H, Trp-Ar-H), 7.02 (m, 1H, Trp-Ar-H), 5.38 (brs, 1H, NH), 4.45 (d, J =4.3 Hz, 2H, COOC $H_2$ ), 4.25-4.36 (m, 1H, NHCH), 4.25 (t, J = 6.8 Hz, 1H, COOC $H_2$ CH), 3.30-3.40 (m, 1H, NHCHC $H_2$ ), 3.10-3.14 (m, 1H, NHCHC $H_2$ ); <sup>13</sup>C NMR (CDCl<sub>3</sub>, 100 MHz)  $\delta$ 199.0, 155.8, 143.8, 143.7, 141.4, 136.5, 127.8, 127.4, 127.1, 125.0, 124.3, 124.2, 120.0, 118.5, 116.4, 109.8, 106.4, 67.0, 56.0, 47.2, 27.5; LCMS: calcd. for C<sub>26</sub>H<sub>22</sub>N<sub>2</sub>O<sub>3</sub> + 411.1630, found 411.2 [MH<sup>+</sup>].

# (9H-Fluoren-9-yl)methyl (S)-(1-oxo-3-phenylpropan-2-yl)carbamate (5.21)<sup>304</sup>

Fmoc-L-Phe-OH (1.0 g, 2.69 mmol, 1.0 equiv.) was dissolved in dry DCM (40.0 mL). The solution was cooled to 0°C and CDI (0.5 g, 2.96 mmol, 1.1 equiv.) was added. After stirring for 1 h at 0 °C, the reaction solution was cooled to -78°C (acetone/CO<sub>2</sub> bath) for 15 min. The DIBAL-H solution (1.0 M in toluene) (5.7 ml, 5.65 mmol, 2.1 equiv.) was added dropwise over 10 min under N<sub>2</sub> gas. The reaction mixture was stirred at -78°C for 1.5 h and monitored by TLC (Hexane: EtOAc 2:1). Upon completion, the reaction mixture diluted in EtOAc (80.0 mL) and quenched with the addition of tartaric acid solution (25% in H<sub>2</sub>O) (50.0 mL) with vigorous stirring. The mixture was warmed to room temperature and stirred at ambient temperature for 15 min. The organic phase was extracted with EtOAc (1×80.0 mL), and the combined organic layers were washed with 1M HCl aq (1×50.0 mL), 0.8M NaHCO<sub>3</sub> aq (1×50.0 mL), sat. NaCl aq (1×50.0 mL), dried over MgSO<sub>4</sub> and concentrated in vacuo. Purification was achieved by column chromatography (hexane/ethyl acetate, 3:1) to give 5.21 as white powder (0.81 g, 85% yield); M.p 141-143 °C;  $R_f = 0.25$  (hexane/EtOAc = 2:1); <sup>1</sup>H NMR (CDCl<sub>3</sub>, 400 MHz)  $\delta$  9.58 (s, 1H, CHO), 7.78 (d, J = 7.5 Hz, 2H, Ar-H), 7.57 (d, J = 7.5Hz, 2H, Ar-H), 7.42 (t, J = 7.5 Hz, 2H, Ar-H), 7.34 (t, J = 7.5 Hz, 2H, Ar-H), 7.22 (m, 1H, Phe-Ar-H), 7.18 (m, 2H, Phe-Ar-H), 7.16 (m, 2H, Phe-Ar-H), 4.45 (d, J = 4.3 Hz, 2H, COOC $H_2$ ), 4.28-4.39 (m, 1H, NHCH), 4.25 (t, J = 6.8 Hz ,1H, COOCH<sub>2</sub>CH), 3.30-3.40 (m, 1H, NHCHCH<sub>2</sub>), 3.10-3.14 (m, 1H, NHCHCH<sub>2</sub>); <sup>13</sup>C NMR (CDCl<sub>3</sub>, 100 MHz) δ 199.7, 155.8, 143.6, 142.2, 138.5, 129.8, 127.4, 125.8, 125.3, 120.2, 75.2, 68.3, 47.5, 34.6; LCMS: calcd. for  $C_{24}H_{21}NO_3 + 372.1521$ , found 372.2 [MH<sup>+</sup>].

#### (9*H*-Fluoren-9-yl)methyl (*S*)-(1-cyclopropyl-3-oxopropan-2-yl)carbamate (5.22)

Fmoc-L-CPA-OH (1.0 g, 2.98 mmol, 1.0 equiv.) was dissolved in dry DCM (40.0 mL). The solution was cooled to 0°C and CDI (0.6 g, 3.28 mmol, 1.1 equiv.) was added. After stirring for 1 h at 0 °C, the reaction solution was cooled to -78°C (acetone/CO<sub>2</sub> bath) for 15 min. The DIBAL-H solution (1.0 M in toluene) (6.3 ml, 6.26 mmol, 2.1 equiv.) was added dropwise over 10 min under N<sub>2</sub> gas. The reaction mixture was stirred at -78°C for 1.5 h and monitored by TLC (Hexane: EtOAc 2:1). Upon completion, the reaction mixture diluted in EtOAc (80.0 mL) and quenched with the addition of tartaric acid solution (25% in H<sub>2</sub>O) (50.0 mL) with vigorous stirring. The mixture was warmed to room temperature and stirred at ambient temperature for 15 min. The organic phase was extracted with EtOAc (1×80.0 mL), and the combined organic layers were washed with 1M HCl aq (1×50 mL), 0.8M NaHCO<sub>3</sub> aq (1×50.0 mL), sat. NaCl aq (1×50.0 mL), dried over MgSO<sub>4</sub> and concentrated in vacuo. Purification was achieved by column chromatography (hexane/ethyl acetate, 3:1) to give **5.22** as white powder  $(0.77 \text{ g}, 75\% \text{ yield}); R_f = 0.29 \text{ (hexane/EtOAc} = 2:1); {}^{1}\text{H NMR (CDCl}_{3}, 400 \text{ MHz}) \delta 9.66 \text{ (s, }^{2})$ 1H, CHO), 7.75 (d, J = 7.5 Hz, 2H, Ar-H), 7.59 (d, J = 7.3 Hz, 2H, Ar-H), 7.39 (t, J = 7.5 Hz, 2H, Ar-H), 7.35 (t, J = 7.5 Hz, 2H, Ar-H), 5.37 (brd, J = 6.6 Hz, 1H, NH), 4.42 (d, J = 6.8 Hz, 2H, COOC $H_2$ ), 4.33-4.35 (m, 1H, NHCH), 4.26 (t, J = 6.8 Hz, 1H, COOC $H_2$ CH), 1.97 (m, 2H, NHCHCH<sub>2</sub>), 1.07 (m, 1H, CPA-CH<sub>2</sub>CH), 0.38-0.45 (m, 2H, CPA-CH<sub>2</sub>), 0.12-0.23 (m, 2H, CPA-CH<sub>2</sub>); <sup>13</sup>C NMR (CDCl<sub>3</sub>, 400 MHz) δ 199.5, 156.7, 143.2, 141.1, 127.7, 127.0, 125.1, 120.0, 67.1, 62.1, 47.3, 38.1, 5.3, 4.1; LCMS: calcd. for C<sub>21</sub>H<sub>21</sub>NO<sub>3</sub> + 336.1521, found 336.2  $[MH^+].$ 

Preparation of modified TG resin with different pre-loaded Fmoc-amino aldehydes.

#### General procedure

**TG** resin (2.27)

The dried Rink amide AM resin (Novagel) (1.0 equiv, loading = 0.7 mmol/g) was swollen in DMF (2.0 mL) for 15 h in a reaction column followed by washing with DMF (3.0 mL min<sup>-1</sup>) for 5-10 min. Then the resin wad attached by Fmoc-Gly-OH and Fmoc-Thr-OH via general Fmoc SPPS protocol. The washing and Fmoc-deprotection cycles were carried out using the manual peptide synthesiser NOVASYN® GEM with a post-column UV monitoring at 355 nM. The peptide chains were assembled by stepwise coupling of Nα-Fmoc-amino acid (4.0 eq) in DMF (0.6 mL) in the presence of carboxyl activating agent 1-[bis(dimethylamino)methylene]-1H-1,2,3-triazolo[4,5-b]pyridinium 3-oxid hexafluorophosphate (HATU; 3.9 eq) and DIPEA (8.0 eq). Each acylation reaction was carried out in the reaction column for 4 h at room temperature and was followed by the wash and deprotection steps. Following the assembly of the desired sequence, the resin washed with DMF (3.0 mL min<sup>-1</sup>) for 15 min. The modified TG resin is used for peptide synthesis without further checking.

#### Preloaded L-aa TG resin

A solution of Fmoc-amino aldehydes (4.0 equiv) and DIPEA (1% with respect to MeOH) in MeOH (final concentration of 0.1 M) was added to the TG resin and the resulting mixture was agitated at 60°C for 5 h. the resin was then washed with MeOH (5x3.0 mL), DMF (5x3.0 mL), DCM (5x3.0 mL), and THF (5x3.0 mL). The preloading TG resin was used for next step directly.

#### NH-Boc preloaded L-aa TG resin

A solution of Boc<sub>2</sub>O (5.0 equiv) and NMM (5.0 equiv) in THF was added to the preloading TG resin and agitated at 50°C for 5 h. the resulting resin was washed with THF and DMF. The loading efficiency was then evaluated.

## NH-Boc preloaded L-Leu TG resin (5.5)

Loading was performed as described in the general procedure, using Fmoc-L-Leu-H Theoretical loading = 0.42 mmol/g % yield = 84%

#### NH-Boc preloaded L-Hle TG resin (5.6)

Loading was performed as described in the general procedure, using Fmoc-L-Hle-H Theoretical loading = 0.39 mmol/g % yield =67%

#### NH-Boc preloaded L-Nva TG resin (5.13)

Loading was performed as described in the general procedure, using Fmoc-L-Nva-H Theoretical loading = 0.45 mmol/g % yield = 80%

#### NH-Boc preloaded L-Nle TG resin (5.14)

Loading was performed as described in the general procedure, using Fmoc-L-Nle-H Theoretical loading = 0.43 mmol/g

% yield = 86%

#### NH-Boc preloaded L-Trp TG resin (5.23)

Loading was performed as described in the general procedure, using Fmoc-L-Trp-H Theoretical loading = 0.35 mmol/g

% yield = 66%

#### NH-Boc preloaded L-Phe TG resin (5.24)

Loading was performed as described in the general procedure, using Fmoc-L-Phe-H Theoretical loading = 0.39 mmol/g

% yield = 58%

## NH-Boc preloaded L-CPA TG resin (5.25)

Loading was performed as described in the general procedure, using Fmoc-L-CPA-H Theoretical loading = 0.35 mmol/g

% yield = 54%

## NH-Boc preloaded L-N-Me-Val TG resin (5.33)

Loading was performed as described in the general procedure, using Fmoc-L-NMe-L-Val-H Theoretical loading = 0.32 mmol/g

% yield = 57%

## NH-Boc preloaded L-N-Me-Leu TG resin (5.34)

Loading was performed as described in the general procedure, using Fmoc-L-NMe-L-Leu-H Theoretical loading = 0.26 mmol/g

% yield = 46%

#### NH-Boc preloaded L-Thr TG resin (5.40)

Loading was performed as described in the general procedure, using Fmoc-L-Thr-H

Theoretical loading = 0.26 mmol/g

% yield = 37%

#### Synthesis of lugdunin analogues

## $(Leu)^7$ -lug (1.65)

Peptide chain with resin was filtered and washed with DMF, DCM and hexane. The resin was transferred into a round-bottom flask and dried in vacuo overnight. The dried resin was then suspended in TFA/H<sub>2</sub>O/TIPS (90:5:5) (10.0 mL) for 3 h. The suspension was then filtered by gravity and washed with TFA and DCM. The filtrate collected in a clean round-bottom flask was evaporated to dryness (DCM was added several times). The residue was triturated with cold diethyl ether (x3) to afford the crude product as white powder (58.8 mg, 81%). The peptide product was analysed by using LCMS and found [MH<sup>+</sup>]: 727.4 at retention time of 2.98 min. Compound was then purified by RP-HPLC and obtained 0.9 mg as pure product (3.2% recovery). <sup>1</sup>H NMR (500 MHz, DMSO-d<sub>6</sub>) δ 10.66-10.72 (m, 1H, L-Trp<sup>3</sup>-CCHNH), 8.54 (d, J  $= 8.5, 1H, L-Trp^3-NH), 8.50 (d, J = 8.5, 1H, D-Val^2-NH), 8.42 (d, J = 8.5, 1H, D-Leu^4-NH),$ 8.31-8.38 (m, 1H, L-Val<sup>5</sup>-NH), 8.22-8.25 (m, 1H, D-Val<sup>6</sup>-NH), 8.15-8.19 (m, 1H, L-Leu<sup>7</sup>-NH), 7.98 (d, J = 7.8, 1H, L-Trp<sup>3</sup>-Ar-H), 7.92 (dd, J = 8.1, 3.7, 1H, L-Trp<sup>3</sup>-Ar-H), 7.83 (d, J = 7.8, 1H, L-Trp<sup>3</sup>-Ar-H), 7.75 (dd, J = 8.0, 1.5, 1H, L-Trp<sup>3</sup>-Ar-H), 7.50 (d, J = 2.0, 1H, L-Trp<sup>3</sup>-NHCHC), 4.71-4.75 (m, 1H, L-Trp<sup>3</sup>-NHCHCH<sub>2</sub>), 4.60 (dd, J = 8.8, 4.5, 1H D-Val<sup>6</sup>-NHCHCH), 4.38 (t, J = 8.3, 1H, D-Leu<sup>4</sup>-NHCHCH<sub>2</sub>), 4.25 (t, J = 8.5, 1H, 1H L-Leu<sup>7</sup>-NHCHCH<sub>2</sub>), 4.05 $(d, J = 9.0, 1H, D-Val^2-NHCHCH), 3.95-4.02 (m, 1H, thiazolidine^1-NHCHCH<sub>2</sub>S), 3.85 (dd, J)$ = 9.0, 6.6, 1H, L-Val<sup>7</sup>-NHCHCH), 3.23 (dd, J = 10.5, 6.5, 1H, thiazolidine<sup>1</sup>-NHCHCH<sub>2</sub>S), 3.13  $(dd, J = 10.5, 6.5, 1H, thiazolidine^1-NHCHCH_2S), 3.05 (d, J = 7.8, 1H, L-Trp^3-NHCHCH_2),$  $3.01 \text{ (dd, } J = 13.5, 5.4, 1 \text{H, L-Trp}^3 \text{-NHCHC} H_2), 2.85 - 2.91 \text{ (m, 1H, thiazolidine}^1 - NHCHCH_2S),}$ 2.00-2.06 (m, 1H, D-Val<sup>6</sup>-CH(CH<sub>3</sub>)<sub>2</sub>), 1.92-1.99 (m, 1H, L-Val<sup>5</sup>-CH(CH<sub>3</sub>)<sub>2</sub>), 1.66-1.72 (m, 1H, D-Val<sup>2</sup>-CH(CH<sub>3</sub>)<sub>2</sub>), 1.52-1.61 (m, 1H, D-Leu<sup>4</sup>-CHCH<sub>2</sub>CH), 1.45-1.49 (m, 1H, L-Leu<sup>7</sup>-CHCH<sub>2</sub>CH), 1.27-1.42 (m, 1H, D-Leu<sup>4</sup>-CHCH<sub>2</sub>CH), 1.22-1.25 (m, 1H, 1-Leu<sup>7</sup>-CHCH<sub>2</sub>CH), 1.16 (d, J = 6.4, 3H, D-Val<sup>6</sup>-CH(CH<sub>3</sub>)<sub>2</sub>), 1.08 (d, J = 6.7, 3H, D-Leu<sup>4</sup>-CH(CH<sub>3</sub>)<sub>2</sub>), 1.05 (d, J =6.7, 3H, D-Leu<sup>4</sup>- CH(CH<sub>3</sub>)<sub>2</sub>), 1.03 (d, J = 6.5, 3H, D-Val<sup>6</sup>-CH(CH<sub>3</sub>)<sub>2</sub>), 1.01 (d, J = 6.6, 3H, L-

Leu<sup>7</sup>- CH(C $H_3$ )<sub>2</sub>), 0.96 (d, J = 6.6, 3H, L-Leu<sup>7</sup>- CH(C $H_3$ )<sub>2</sub>), 0.92 (d, J = 6.8, 3H, L-Val<sup>5</sup>- CH(C $H_3$ )<sub>2</sub>), 0.87 (d, J = 6.4, 3H, L-Val<sup>5</sup>-CH(C $H_3$ )<sub>2</sub>), 0.78 (d, J = 6.5, 3H, D-Val<sup>2</sup>-CH(C $H_3$ )<sub>2</sub>), 0.67 (d, J = 6.4, 3H, D-Val<sup>2</sup>-CH(C $H_3$ )<sub>2</sub>); HRMS: calculated for C<sub>36</sub>H<sub>54</sub>N<sub>8</sub>O<sub>6</sub>S<sub>1</sub><sup>+</sup> 727.3887, found 727.3889 [MH<sup>+</sup>]; Analytical RP-HPLC (**Method 1**)  $t_R = 4.62$  min.

## $(Hle)^7$ -lug (1.66)

Peptide chain with resin was filtered and washed with DMF, DCM and hexane. The resin was transferred into a round-bottom flask and dried in vacuo overnight. The dried resin was then suspended in TFA/H<sub>2</sub>O/TIPS (90:5:5) (10.0 mL) for 3 h. The suspension was then filtered by gravity and washed with TFA and DCM. The filtrate collected in a clean round-bottom flask was evaporated to dryness (DCM was added several times). The residue was triturated with cold diethyl ether x3) to afford the crude product as white powder (58.8 mg, 81%). The peptide product was analysed by using LCMS and found [MH<sup>+</sup>]: 741.5 at retention time of 2.88 min. Compound was then purified by RP-HPLC and obtained 0.4 mg as pure product (1.4% recovery). HRMS: calculated for  $C_{37}H_{56}N_8O_6S_1^+$  741.4044, found 741.4049 [MH<sup>+</sup>]; Analytical RP-HPLC (**Method 1**)  $t_R = 4.92$  min.

## $(Nva)^7$ -lug (1.67)

Peptide chain with resin was filtered and washed with DMF, DCM and hexane. The resin was transferred into a round-bottom flask and dried in vacuo overnight. The dried resin was then suspended in TFA/H<sub>2</sub>O/TIPS (90:5:5) (10.0 mL) for 3 h. The suspension was then filtered by gravity and washed with TFA and DCM. The filtrate collected in a clean round-bottom flask was evaporated to dryness (DCM was added several times). The residue was triturated with cold diethyl ether (x3) to afford the crude product as white powder (58.8 mg, 81%). The peptide product was analysed by using LCMS and found [MH<sup>+</sup>]: 713.4 at retention time of 2.75 min. Compound was then purified by RP-HPLC and obtained 0.6 mg as pure product (2.7% recovery). <sup>1</sup>H NMR (500 MHz, DMSO-d<sub>6</sub>) δ 10.64-10.68 (m, 1H, L-Trp<sup>3</sup>-CCHNH), 8.55 (d, J  $= 8.5, 1H, L-Trp^3-NH), 8.50 (d, J = 8.6, 1H, D-Val^2-NH), 8.42 (d, J = 8.5, 1H, D-Leu^4-NH),$ 8.30-8.34 (m, 1H, L-Val<sup>5</sup>-NH), 8.22-8.27 (m, 1H, D-Val<sup>6</sup>-NH), 8.15-8.19 (m, 1H, L-Val<sup>7</sup>-NH), 7.95 (d, J = 7.8, 1H, L-Trp<sup>3</sup>-Ar-H), 7.91 (dd, J = 8.0, 3.8, 1H, L-Trp<sup>3</sup>-Ar-H), 7.82 (d, J = 7.9, 1H, L-Trp<sup>3</sup>-Ar-H), 7.66 (dd, J = 8.0, 1.3, 1H, L-Trp<sup>3</sup>-Ar-H), 7.55 (d, J = 2.0, 1H, L-Trp<sup>3</sup>-NHCHC), 4.72-4.75 (m, 1H, L-Trp<sup>3</sup>-NHCHCH<sub>2</sub>), 4.59 (dd, J = 8.8, 4.5, 1H D-Val<sup>6</sup>-NHCHCH), 4.32 (t, J = 8.3, 1H, D-Leu<sup>4</sup>-NHCHCH<sub>2</sub>), 4.11 (d, J = 9.0, 1H, D-Val<sup>2</sup>-NHCHCH), 3.96-4.05(m, 1H, thiazolidine<sup>1</sup>-NHCHCH<sub>2</sub>S), 3.50-3.55 (m, 1H, L-Nva<sup>7</sup>-NHCHCH<sub>2</sub>), 3.23 (dd, J=10.5, 6.5, 1H, thiazolidine<sup>1</sup>-NHCHC $H_2$ S), 3.13 (dd, J = 10.5, 6.5, 1H, thiazolidine<sup>1</sup>-NHCHC $H_2$ S),  $3.05 \text{ (d, } J = 7.8, 1H, L-Trp^3-NHCHCH_2), 3.01 \text{ (dd, } J = 13.5, 5.4, 1H, L-Trp^3-NHCHCH_2), 2.91-$ 2.85 (m, 1H, thiazolidine<sup>1</sup>- NHCHCH<sub>2</sub>S), 2.00-2.06 (m, 1H, D-Val<sup>6</sup>-CH(CH<sub>3</sub>)<sub>2</sub>), 1.92-1.99 (m, 1H, L-Val<sup>5</sup>-CH(CH<sub>3</sub>)<sub>2</sub>), 1.66-1.72 (m, 1H, D-Val<sup>2</sup>-CH(CH<sub>3</sub>)<sub>2</sub>), 1.52-1.61 (m, 1H, D-Leu<sup>4</sup>-CHCH<sub>2</sub>CH), 1.42-1.49 (m, 2H, L-Nva<sup>7</sup>-NHCHCH<sub>2</sub>), 1.30-1.35 (m, 2H, L-Nva<sup>7</sup>-NHCHCH<sub>2</sub>CH<sub>2</sub>)1.27-1.42 (m, 1H, D-Leu<sup>4</sup>-CHCH<sub>2</sub>CH), 1.16 (d, J = 6.4, 3H, D-Val<sup>6</sup>- $CH(CH_3)_2$ ), 1.08 (d, J = 6.7, 3H, D-Leu<sup>4</sup>- $CH(CH_3)_2$ ), 1.05 (d, J = 6.7, 3H, D-Leu<sup>4</sup>- $CH(CH_3)_2$ ), 1.03 (d, J = 6.5, 3H, D-Val<sup>6</sup>-CH(CH<sub>3</sub>)<sub>2</sub>), 0.92 (d, J = 6.8, 3H, L-Val<sup>5</sup>-CH(CH<sub>3</sub>)<sub>2</sub>), 0.87 (d, J =6.4, 3H, L-Val<sup>5</sup>-CH(C $H_3$ )<sub>2</sub>), 0.82 (t, J = 6.6, 3H, L-Nva<sup>7</sup>-NHCHCH<sub>2</sub>CH<sub>2</sub>C $H_3$ ), 0.78 (d, J = 6.5,

3H, D-Val<sup>2</sup>-CH(C $H_3$ )<sub>2</sub>), 0.67 (d, J = 6.4, 3H, D-Val<sup>2</sup>-CH(C $H_3$ )<sub>2</sub>); HRMS: calculated for C<sub>35</sub>H<sub>52</sub>N<sub>8</sub>O<sub>6</sub>S<sub>1</sub><sup>+</sup> 713.3731, found 713.3736 [MH<sup>+</sup>]; Analytical RP-HPLC (**Method 1**)  $t_R = 4.35$  min.

## $(Nle)^7$ -lug (1.68)

Peptide chain with resin was filtered and washed with DMF, DCM and hexane. The resin was transferred into a round-bottom flask and dried in vacuo overnight. The dried resin was then suspended in TFA/H<sub>2</sub>O/TIPS (90:5:5) (10.0 mL) for 3 h. The suspension was then filtered by gravity and washed with TFA and DCM. The filtrate collected in a clean round-bottom flask was evaporated to dryness (DCM was added several times). The residue was triturated with cold diethyl ether (x3) to afford the crude product as white powder (58.8 mg, 81%). The peptide product was analysed by using LCMS and found [MH<sup>+</sup>]: 727.5 at retention time of 2.92 min. Compound was then purified by RP-HPLC and obtained 0.9 mg as pure product (3.2% recovery). <sup>1</sup>H NMR (500 MHz, DMSO-d<sub>6</sub>) δ 10.62-10.66 (m, 1H, L-Trp<sup>3</sup>-CCHN*H*), 8.53 (d, *J*  $= 8.5, 1H, L-Trp^3-NH), 8.48 (d, J = 8.6, 1H, D-Val^2-NH), 8.38 (d, J = 8.5, 1H, D-Leu^4-NH),$ 8.28-8.32 (m, 1H, L-Val<sup>5</sup>-NH), 8.22-8.25 (m, 1H, D-Val<sup>6</sup>-NH), 8.11-8.18 (m, 1H, L-Nle<sup>7</sup>-NH), 7.92 (d, J = 7.8, 1H, L-Trp<sup>3</sup>-Ar-H), 7.87 (dd, J = 8.0, 3.8, 1H, L-Trp<sup>3</sup>-Ar-H), 7.82 (d, J = 7.9, 1H, L-Trp<sup>3</sup>-Ar-H), 7.66 (dd, J = 8.0, 1.3, 1H, L-Trp<sup>3</sup>-Ar-H), 7.55 (d, J = 2.0, 1H, L-Trp<sup>3</sup>-NHCHC), 4.72-4.75 (m, 1H, L-Trp<sup>3</sup>-NHCHCH<sub>2</sub>), 4.59 (dd, J = 8.8, 4.5, 1H D-Val<sup>6</sup>-NHCHCH), 4.32 (t, J = 8.3, 1H, D-Leu<sup>4</sup>-NHCHCH<sub>2</sub>), 4.11 (d, J = 9.0, 1H, D-Val<sup>2</sup>-NHCHCH), 3.96-4.05(m, 1H, thiazolidine<sup>1</sup>-NHCHCH<sub>2</sub>S), 3.50-3.55 (m, 1H, L-Nle<sup>7</sup>-NHCHCH<sub>2</sub>), 3.23 (dd, J = 10.5, 6.5, 1H, thiazolidine<sup>1</sup>-NHCHC $H_2$ S), 3.13 (dd, J = 10.5, 6.5, 1H, thiazolidine<sup>1</sup>-NHCHC $H_2$ S),  $3.05 (d, J = 7.8, 1H, L-Trp^3-NHCHCH_2), 3.01 (dd, J = 13.5, 5.4, 1H, L-Trp^3-NHCHCH_2), 2.91$ 2.85 (m, 1H, thiazolidine<sup>1</sup>- NHCHCH<sub>2</sub>S), 2.00-2.06 (m, 1H, D-Val<sup>6</sup>-CH(CH<sub>3</sub>)<sub>2</sub>), 1.92-1.99 (m, 1H, L-Val<sup>5</sup>-CH(CH<sub>3</sub>)<sub>2</sub>), 1.70-1.75 (m, 1H, D-Val<sup>2</sup>-CH(CH<sub>3</sub>)<sub>2</sub>), 1.65-1.67 (m, 2H, L-Nle<sup>7</sup>-

NHCHC $H_2$ ), 1.52-1.61 (m, 1H, D-Leu<sup>4</sup>-CHC $H_2$ CH), 1.29-1.32 (m, 2H, L-Nle<sup>7</sup>-NHCHCH<sub>2</sub>CH<sub>2</sub>CH<sub>2</sub>), 1.20-1.25 (m, 1H, D-Leu<sup>4</sup>-CHC $H_2$ CH), 1.15-1.18 (m, 2H, L-Nle<sup>7</sup>-NHCHCH<sub>2</sub>CH<sub>2</sub>), 1.13 (d, J = 6.4, 3H, D-Val<sup>6</sup>-CH(C $H_3$ )<sub>2</sub>), 1.09 (d, J = 6.7, 3H, D-Leu<sup>4</sup>-CH(C $H_3$ )<sub>2</sub>), 1.02 (d, J = 6.7, 3H, D-Leu<sup>4</sup>-CH(C $H_3$ )<sub>2</sub>), 1.01 (d, J = 6.5, 3H, D-Val<sup>6</sup>-CH(C $H_3$ )<sub>2</sub>), 0.95 (d, J = 6.8, 3H, L-Val<sup>5</sup>-CH(C $H_3$ )<sub>2</sub>), 0.86 (d, J = 6.4, 3H, L-Val<sup>5</sup>-CH(C $H_3$ )<sub>2</sub>), 0.85 (t, J = 6.6, 3H, L-Nle<sup>7</sup>-NHCHCH<sub>2</sub>CH<sub>2</sub>CH<sub>2</sub>CH<sub>3</sub>), 0.79 (d, J = 6.5, 3H, D-Val<sup>2</sup>-CH(C $H_3$ )<sub>2</sub>), 0.65 (d, J = 6.4, 3H, D-Val<sup>2</sup>-CH(C $H_3$ )<sub>2</sub>); HRMS: calculated for C<sub>36</sub>H<sub>54</sub>N<sub>8</sub>O<sub>6</sub>S<sub>1</sub><sup>+</sup> 727.3887, found 727.3892 [MH<sup>+</sup>]; Analytical RP-HPLC (**Method 1**)  $t_R = 4.66$  min.

# $(Trp)^7$ -lug (1.69)

Peptide chain with resin was filtered and washed with DMF, DCM and hexane. The resin was transferred into a round-bottom flask and dried in vacuo overnight. The dried resin was then suspended in TFA/H<sub>2</sub>O/TIPS (90:5:5) (10.0 mL) for 3 h. The suspension was then filtered by gravity and washed with TFA and DCM. The filtrate collected in a clean round-bottom flask was evaporated to dryness (DCM was added several times). The residue was triturated with cold diethyl ether (x3) to afford the crude product as white powder (78.8 mg, 82%). The peptide product was analysed by using LCMS and found [MH<sup>+</sup>]: 800.6 at retention time of 2.95 min. Compound was then purified by RP-HPLC and obtained 0.9 mg as pure product (3.2% recovery). <sup>1</sup>H NMR (500 MHz, DMSO-d<sub>6</sub>)  $\delta$  10.62-10.69 (m, 1H, L-Trp<sup>3</sup>-CCHN*H*), 10.42-10.55 (m, 1H, L-Trp<sup>7</sup>-CCHN*H*), 8.53 (d, J = 8.5, 1H, L-Trp<sup>3</sup>-N*H*), 8.52 (d, J = 8.5, 1H, D-Val<sup>2</sup>-N*H*), 8.51 (d, J = 8.5, 1H, L-Trp<sup>7</sup>-NHC, 8.44 (d, J = 8.5, 1H, D-Leu<sup>4</sup>-N*H*), 8.32-8.36 (m, 1H, L-Val<sup>5</sup>-N*H*), 8.27-8.31 (m, 1H, D-Val<sup>6</sup>-N*H*), 7.5-7.95 (m, 8H, L-Trp<sup>3</sup>-Ar-*H*, L-Trp<sup>7</sup>-Ar-*H*), 7.52 (d, J = 2.0, 1H, L-Trp<sup>3</sup>-NHC*HC*), 7.35 (d, J = 2.5, 1H, L-Trp<sup>7</sup>-NHC*HC*), 4.71-4.77 (m, 1H, L-Trp<sup>3</sup>-NHC*HCH*<sub>2</sub>), 4.52-4.58 (m, 1H, L-Trp<sup>7</sup>-NHC*HCH*<sub>2</sub>), 4.57 (dd, J = 8.8, 4.5, 1H, D-Val<sup>6</sup>-NHC*HCH*<sub>2</sub>), 4.36 (t, J = 8.3, 1H, D-Leu<sup>4</sup>-NHC*HCH*<sub>2</sub>), 4.09 (d, J = 9.0, 1H, D-Val<sup>2</sup>-NHC*HCH*<sub>2</sub>),

3.92-4.05 (m, 1H, thiazolidine<sup>1</sup>-NHCHCH<sub>2</sub>S), 3.25 (dd, J = 10.5, 6.5, 1H, thiazolidine<sup>1</sup>-NHCHCH<sub>2</sub>S), 3.11 (dd, J = 10.5, 6.5, 1H, thiazolidine<sup>1</sup>-NHCHCH<sub>2</sub>S), 3.02 (d, J = 7.8, 1H, L-Trp<sup>3</sup>-NHCHCH<sub>2</sub>), 2.97 (dd, J = 13.5, 5.4, 1H, L-Trp<sup>3</sup>-NHCHCH<sub>2</sub>), 2.82-2.89 (m, 1H, thiazolidine<sup>1</sup>- NHCHCH<sub>2</sub>S), 2.05-2.08 (m, 1H, D-Val<sup>6</sup>-CH(CH<sub>3</sub>)<sub>2</sub>), 1.92-1.95 (m, 1H, L-Val<sup>5</sup>-CH(CH<sub>3</sub>)<sub>2</sub>), 1.65-1.70 (m, 1H, D-Val<sup>2</sup>-CH(CH<sub>3</sub>)<sub>2</sub>), 1.54-1.60 (m, 1H, D-Leu<sup>4</sup>-CHCH<sub>2</sub>CH), 1.28-1.45 (m, 1H, D-Leu<sup>4</sup>-CHCH<sub>2</sub>CH), 1.15 (d, J = 6.4, 3H, D-Val<sup>6</sup>-CH(CH<sub>3</sub>)<sub>2</sub>), 1.08 (d, J = 6.7, 3H, D-Leu<sup>4</sup>-CH(CH<sub>3</sub>)<sub>2</sub>), 1.05 (d, J = 6.7, 3H, D-Leu<sup>4</sup>-CH(CH<sub>3</sub>)<sub>2</sub>), 1.03 (d, J = 6.5, 3H, D-Val<sup>6</sup>-CH(CH<sub>3</sub>)<sub>2</sub>), 0.95 (d, J = 6.8, 3H, L-Val<sup>5</sup>-CH(CH<sub>3</sub>)<sub>2</sub>), 0.89 (d, J = 6.4, 3H, L-Val<sup>5</sup>-CH(CH<sub>3</sub>)<sub>2</sub>), 0.77 (d, J = 6.5, 3H, D-Val<sup>2</sup>-CH(CH<sub>3</sub>)<sub>2</sub>), 0.65 (d, J = 6.4, 3H, D-Val<sup>2</sup>-CH(CH<sub>3</sub>)<sub>2</sub>); HRMS: calculated for C<sub>41</sub>H<sub>53</sub>N<sub>9</sub>O<sub>6</sub>S<sub>1</sub><sup>+</sup> 800.3840, found 800.3845 [MH<sup>+</sup>]; Analytical RP-HPLC (**Method 1**)  $t_R = 5.11$  min.

## $(Phe)^7$ -lug (1.70)

Peptide chain with resin was filtered and washed with DMF, DCM and hexane. The resin was transferred into a round-bottom flask and dried in vacuo overnight. The dried resin was then suspended in TFA/H<sub>2</sub>O/TIPS (90:5:5) (10.0 mL) for 3 h. The suspension was then filtered by gravity and washed with TFA and DCM. The filtrate collected in a clean round-bottom flask was evaporated to dryness (DCM was added several times). The residue was triturated with cold diethyl ether (x3) to afford the crude product as white powder (48.7 mg, 70%). The peptide product was analysed by using LCMS and found [MH<sup>+</sup>] : 761.6 at retention time of 2.92 min. Compound was then purified by RP-HPLC and obtained 0.84 mg as pure product (2.9% recovery). <sup>1</sup>H NMR (500 MHz, DMSO-d<sub>0</sub>)  $\delta$  10.63-10.68 (m, 1H, L-Trp<sup>3</sup>-CCHN*H*), 8.55 (d, *J* = 8.5, 1H, L-Trp<sup>3</sup>-N*H*), 8.57 (d, *J* = 8.5, 1H, D-Val<sup>2</sup>-N*H*), 8.42 (d, *J* = 8.5, 1H, D-Leu<sup>4</sup>-N*H*), 8.29-8.32 (m, 1H, L-Val<sup>5</sup>-N*H*), 8.23-8.26 (m, 1H, D-Val<sup>6</sup>-N*H*), 8.11-8.15 (m, 1H, L-Phe<sup>7</sup>-N*H*), 7.92 (d, *J* = 7.8, 1H, L-Trp<sup>3</sup>-Ar-*H*), 7.85 (dd, *J* = 8.1, 3.7, 1H, L-Trp<sup>3</sup>-Ar-*H*), 7.83 (d, *J* = 7.9,

1H, L-Trp³-Ar-H), 7.75 (dd, J = 8.0, 1.3, 1H, L-Trp³-Ar-H), 7.56 (d, J = 2.0, 1H, L-Trp³-NHCHC), 7.15-7.25 (m, 5H, L-Phe<sup>7</sup>-Ar-H), 4.75-4.79 (m, 1H, L-Phe<sup>7</sup>-NHCHCH<sub>2</sub>), 4.68-4.73 (m, 1H, L-Trp³-NHCHCH<sub>2</sub>), 4.54 (dd, J = 8.8, 4.5, 1H D-Val<sup>6</sup>-NHCHCH), 4.38 (t, J = 8.3, 1H, D-Leu<sup>4</sup>-NHCHCH<sub>2</sub>), 4.03 (d, J = 9.0, 1H, D-Val<sup>2</sup>-NHCHCH), 3.98-4.05 (m, 1H, thiazolidine<sup>1</sup>-NHCHCH<sub>2</sub>S), 3.32 (d, J = 8.5, 1H, L-Phe<sup>7</sup>-NHCHCH<sub>2</sub>), 3.23 (dd, J = 10.5, 6.5, 1H, thiazolidine<sup>1</sup>-NHCHCH<sub>2</sub>S), 3.17 (d, J = 8.6, 1H, L-Phe<sup>7</sup>-NHCHCH<sub>2</sub>), 3.11 (dd, J = 10.5, 6.5, 1H, thiazolidine<sup>1</sup>-NHCHCH<sub>2</sub>S), 3.04 (d, J = 7.8, 1H, L-Trp³-NHCHCH<sub>2</sub>), 2.98 (dd, J = 13.5, 5.4, 1H, L-Trp³-NHCHCH<sub>2</sub>), 2.84-2.89 (m, 1H, thiazolidine<sup>1</sup>-NHCHCH<sub>2</sub>S), 2.07-2.11 (m, 1H, D-Val<sup>6</sup>-CH(CH<sub>3</sub>)<sub>2</sub>), 1.90-1.95 (m, 1H, L-Val<sup>5</sup>-CH(CH<sub>3</sub>)<sub>2</sub>), 1.65-1.71 (m, 1H, D-Val<sup>2</sup>-CH(CH<sub>3</sub>)<sub>2</sub>), 1.57-1.62 (m, 1H, D-Leu<sup>4</sup>-CHCHCHCH), 1.29-1.35 (m, 1H, D-Leu<sup>4</sup>-CHCHCHCH), 1.18 (d, J = 6.4, 3H, D-Val<sup>6</sup>-CH(CH3)<sub>2</sub>), 1.05 (d, J = 6.7, 3H, D-Leu<sup>4</sup>-CHC(H3)<sub>2</sub>), 1.05 (d, J = 6.7, 3H, D-Leu<sup>4</sup>-CHC(H3)<sub>2</sub>), 0.88 (d, J = 6.4, 3H, L-Val<sup>5</sup>-CH(CH3)<sub>2</sub>), 0.80 (d, J = 6.5, 3H, D-Val<sup>2</sup>-CH(CH3)<sub>2</sub>), 0.69 (d, J = 6.4, 3H, D-Val<sup>2</sup>-CH(CH3)<sub>2</sub>), 1.69 (d, J = 6.4, 3H, D-Val<sup>2</sup>-CH(CH3)<sub>2</sub>), 1.69 (d, J = 6.5, 3H, D-Val<sup>2</sup>-CHC(CH3)<sub>2</sub>), 0.69 (d, J = 6.4, 3H, D-Val<sup>2</sup>-CHC(CH3)<sub>2</sub>), 1.80 (d, J = 6.5, 3H, D-Val<sup>2</sup>-CHC(CH3)<sub>2</sub>), 0.69 (d, J = 6.4, 3H, D-Val<sup>2</sup>-CHC(CH3)<sub>2</sub>), 1.65 (d, J = 6.5, 3H, D-Val<sup>2</sup>-CHC(CH3)<sub>2</sub>), 0.69 (d, J = 6.4, 3H, D-Val<sup>2</sup>-CHC(CH3)<sub>2</sub>), 1.80 (d, J = 6.5, 3H, D-Val<sup>2</sup>-CHC(CH3)<sub>2</sub>), 0.69 (d, J = 6.4, 3H, D-Val<sup>2</sup>-CHC(CH3)<sub>2</sub>), 1.65 (d, J = 6.5, 3H, D-Val<sup>2</sup>-CHC(CH3)<sub>2</sub>), 0.69 (d, J = 6.4, 3H, D-Val<sup>2</sup>-CHC(CH3)<sub>2</sub>), 1.65 (d, J = 6.5, 3H, D-Val<sup>2</sup>-CHC(CH3)<sub>2</sub>), 0.69 (d, J = 6.4, 3H, D-Val<sup>2</sup>-CHC(CH3)<sub>2</sub>), 1.65 (d, J = 6.5, 3H, D-Val<sup>2</sup>-CHC(CH3)<sub>2</sub>), 0.69 (d, J = 6.4, 3H, D-Val<sup>2</sup>-CHC(C

# $(L-CPA)^7$ -lug (1.71)

Peptide chain with resin was filtered and washed with DMF, DCM and hexane. The resin was transferred into a round-bottom flask and dried in vacuo overnight. The dried resin was then suspended in TFA/H<sub>2</sub>O/TIPS (90:5:5) (10.0 mL) for 3 h. The suspension was then filtered by gravity and washed with TFA and DCM. The filtrate collected in a clean round-bottom flask was evaporated to dryness (DCM was added several times). The residue was triturated with cold diethyl ether (x3) to afford the crude product as white powder (62.7 mg, 75%). The peptide product was analysed by using LCMS and found [MH<sup>+</sup>]: 725.5 at retention time of 2.90 min. Compound was then purified by RP-HPLC and obtained 0.65 mg as pure product (2.7% recovery). <sup>1</sup>H NMR (500 MHz, DMSO-d<sub>6</sub>) δ 10.62-10.68 (m, 1H, L-Trp<sup>3</sup>-CCHN*H*), 8.57 (d, *J* 

 $= 8.5, 1H, L-Trp^3-NH), 8.55 (d, J = 8.5, 1H, D-Val^2-NH), 8.39 (d, J = 8.5, 1H, D-Leu^4-NH),$ 8.28-8.32 (m, 1H, L-Val<sup>5</sup>-NH), 8.22-8.25 (m, 1H, D-Val<sup>6</sup>-NH), 8.12-8.15 (m, 1H, L-Val<sup>7</sup>-NH), 7.95 (d, J = 7.8, 1H, L-Trp<sup>3</sup>-Ar-H), 7.91 (dd, J = 8.1, 3.7, 1H, L-Trp<sup>3</sup>-Ar-H), 7.83 (d, J = 7.9, 1H, L-Trp<sup>3</sup>-Ar-H), 7.68 (dd, J = 8.0, 1.3, 1H, L-Trp<sup>3</sup>-Ar-H), 7.57 (d, J = 2.0, 1H, L-Trp<sup>3</sup>-NHCHC), 4.70-4.75 (m, 1H, L-Trp<sup>3</sup>-NHCHCH<sub>2</sub>), 4.55 (dd, J = 8.8, 4.5, 1H D-Val<sup>6</sup>-NHCHCH), 4.36 (t, J = 8.3, 1H, D-Leu<sup>4</sup>-NHCHCH<sub>2</sub>), 4.02 (d, J = 9.0, 1H, D-Val<sup>2</sup>-NHCHCH), 3.95-4.05(m, 1H, thiazolidine<sup>1</sup>-NHCHCH<sub>2</sub>S), 3.85 (dd, J = 9.0, 6.6, 1H, L-Val<sup>7</sup>-NHCHCH), 3.23 (dd, J= 10.5, 6.5, 1H, thiazolidine<sup>1</sup>-NHCHC $H_2S$ ), 3.15 (dd, J = 10.5, 6.5, 1H, thiazolidine<sup>1</sup>-NHCHC $H_2$ S), 3.05 (d, J = 7.8, 1H, L-Trp<sup>3</sup>-NHCHC $H_2$ ), 3.01 (dd, J = 13.5, 5.4, 1H, L-Trp<sup>3</sup>-NHCHCH<sub>2</sub>), 2.87-2.95 (m, 1H, thiazolidine<sup>1</sup>- NHCHCH<sub>2</sub>S), 2.02-2.06 (m, 1H, D-Val<sup>6</sup>- $CH(CH_3)_2$ ), 1.92-1.97 (m, 1H, L-Val<sup>5</sup>- $CH(CH_3)_2$ ), 1.81-1.85 (m, 2H, L-CPA<sup>7</sup>-NHCHC $H_2$ ), 1.68-1.72 (m, 1H, D-Val<sup>2</sup>-CH(CH<sub>3</sub>)<sub>2</sub>), 1.58-1.61 (m, 1H, D-Leu<sup>4</sup>-CHCH<sub>2</sub>CH), 1.31-1.42 (m, 1H, D-Leu<sup>4</sup>-CHC $H_2$ CH), 1.19 (d, J = 6.4, 3H, D-Val<sup>6</sup>-CH(C $H_3$ )<sub>2</sub>), 1.06 (d, J = 6.7, 3H, D-Leu<sup>4</sup>- $CH(CH_3)_2$ ), 1.02 (d, J = 6.7, 3H, D-Leu<sup>4</sup>-  $CH(CH_3)_2$ ), 0.98 (d, J = 6.5, 3H, D-Val<sup>6</sup>- $CH(CH_3)_2$ ), 0.94-0.96 (m, 1H, L-CPA<sup>7</sup>-NHCHCH<sub>2</sub>CH), 0.93 (d, J = 6.8, 3H, L-Val<sup>5</sup>-CH(CH<sub>3</sub>)<sub>2</sub>), 0.85 (d, J= 6.4, 3H, L-Val<sup>5</sup>-CH(C $H_3$ )<sub>2</sub>), 0.76 (d, J = 6.5, 3H, D-Val<sup>2</sup>-CH(C $H_3$ )<sub>2</sub>), 0.64 (d, J = 6.4, 3H, D- $Val^2$ -CH(CH<sub>3</sub>)<sub>2</sub>), 0.25-0.39 (m, 4H, L-CPA<sup>7</sup>-CH(CH<sub>2</sub>)<sub>2</sub>); HRMS: calculated for C<sub>36</sub>H<sub>52</sub>N<sub>8</sub>O<sub>6</sub>S<sub>1</sub><sup>+</sup> 725.3731, found 725.3738 [MH<sup>+</sup>]; Analytical RP-HPLC (**Method 1**)  $t_R = 4.46$  min.

# $(L-N-Me-Val)^7-lug (5.29)$

Peptide chain with resin was filtered and washed with DMF, DCM and hexane. The resin was transferred into a round-bottom flask and dried in vacuo overnight. The dried resin was then suspended in TFA/H<sub>2</sub>O/TIPS (90:5:5) (10.0 mL) for 3 h. The suspension was then filtered by gravity and washed with TFA and DCM. The filtrate collected in a clean round-bottom flask was evaporated to dryness (DCM was added several times). The residue was triturated with cold diethyl ether (x3) to afford the crude product as white powder (78.8 mg, 85%). The peptide product was analysed by using LCMS and found [MH<sup>+</sup>]: 727.4 at retention time of 2.88 min.

Compound was then purified by RP-HPLC and obtained 1.2 mg as pure product (4.1% recovery). <sup>1</sup>H NMR (500 MHz, DMSO-d<sub>6</sub>) δ 10.66-10.75 (m, 1H, L-Trp<sup>3</sup>-CCHNH), 8.56 (d, J  $= 8.5, 1H, L-Trp^3-NH), 8.51 (d, J = 8.5, 1H, D-Val^2-NH), 8.46 (d, J = 8.5, 1H, D-Leu^4-NH),$ 8.37-8.39 (m, 1H, L-Val<sup>5</sup>-NH), 8.32-8.37 (m, 1H, D-Val<sup>6</sup>-NH), 7.94 (d, J = 7.8, 1H, L-Trp<sup>3</sup>-Ar-H), 7.91 (dd,  $J = 8.1, 3.7, 1H, L-Trp^3-Ar-H)$ , 7.86 (d,  $J = 7.9, 1H, L-Trp^3-Ar-H)$ , 7.71 (dd,  $J = 8.0, 1.3, 1H, L-Trp^3-Ar-H), 7.52$  (d,  $J = 2.0, 1H, L-Trp^3-NHCHC$ ), 4.71-4.75 (m, 1H, L- $Trp^3$ -NHCHCH<sub>2</sub>), 4.59 (dd, J = 8.8, 4.5, 1H D-Val<sup>6</sup>-NHCHCH), 4.34 (t, J = 8.3, 1H, D-Leu<sup>4</sup>-NHCHCH<sub>2</sub>), 4.05 (d, J = 9.0, 1H, D-Val<sup>2</sup>-NHCHCH), 3.95-4.02 (m, 1H, thiazolidine<sup>1</sup>-NHCHCH<sub>2</sub>S), 3.85 (dd, J = 9.0, 6.6, 1H, L-N-Me-Val<sup>7</sup>-NHCHCH), 3.38 (s, 3H, L-N-Me-Val<sup>7</sup>-NCH3), 3.25 (dd, J = 10.5, 6.5, 1H, thiazolidine<sup>1</sup>-NHCHCH<sub>2</sub>S), 3.19 (dd, J = 10.5, 6.5, 1H, thiazolidine<sup>1</sup>-NHCHC $H_2$ S), 3.09 (d, J = 7.8, 1H, L-Trp<sup>3</sup>-NHCHC $H_2$ ), 3.04 (dd, J = 13.5, 5.4, 1H, L-Trp<sup>3</sup>-NHCHCH<sub>2</sub>), 2.89-2.93 (m, 1H, thiazolidine<sup>1</sup>- NHCHCH<sub>2</sub>S), 2.19-2.24 (m, 1H, L-N-Me-Val<sup>7</sup>-CH(CH<sub>3</sub>)<sub>2</sub>), 2.05-2.12 (m, 1H, D-Val<sup>6</sup>-CH(CH<sub>3</sub>)<sub>2</sub>), 1.89-1.86 (m, 1H, L-Val<sup>5</sup>- $CH(CH_3)_2$ ), 1.62-1.71 (m, 1H, D-Val<sup>2</sup>- $CH(CH_3)_2$ ), 1.51-1.58 (m, 1H, D-Leu<sup>4</sup>- $CHCH_2CH$ ), 1.29-1.44 (m, 1H, D-Leu<sup>4</sup>-CHC $H_2$ CH), 1.16 (d, J = 6.4, 3H, D-Val<sup>6</sup>-CH(C $H_3$ )<sub>2</sub>), 1.05 (d, J =6.7, 3H, D-Leu<sup>4</sup>-CH(C $H_3$ )<sub>2</sub>), 1.02 (d, J = 6.7, 3H, D-Leu<sup>4</sup>-CH(C $H_3$ )<sub>2</sub>), 1.01 (d, J = 6.5, 3H, D- $Val^6$ -CH(CH<sub>3</sub>)<sub>2</sub>), 0.95 (d, J = 6.8, 3H, L-Val<sup>5</sup>-CH(CH<sub>3</sub>)<sub>2</sub>), 0.89 (d, J = 6.4, 3H, L-Val<sup>5</sup>- $CH(CH_3)_2$ ), 0.83 (d, J = 8.5, 3H, L-N-Me-Val<sup>7</sup>-CH(CH<sub>3</sub>)<sub>2</sub>), 0.79 (d, J = 6.4, 3H, L-N-Me-Val<sup>7</sup>- $CH(CH_3)_2$ , 0.74 (d, J = 6.5, 3H, D- $Val^2$ - $CH(CH_3)_2$ ), 0.66 (d, J = 6.4, 3H, D- $Val^2$ - $CH(CH_3)_2$ ); HRMS: calculated for C<sub>36</sub>H<sub>54</sub>N<sub>8</sub>O<sub>6</sub>S<sub>1</sub><sup>+</sup> 727.3887, found 727.3892 [MH<sup>+</sup>]; Analytical RP-HPLC (**Method 1**)  $t_R = 4.55$  min.

## $(L-N-Me-Leu)^7-lug (5.30)$

Peptide chain with resin was filtered and washed with DMF, DCM and hexane. The resin was transferred into a round-bottom flask and dried in vacuo overnight. The dried resin was then suspended in TFA/H<sub>2</sub>O/TIPS (90:5:5) (10.0 mL) for 3 h. The suspension was then filtered by gravity and washed with TFA and DCM. The filtrate collected in a clean round-bottom flask was evaporated to dryness (DCM was added several times). The residue was triturated with cold diethyl ether (x3) to afford the crude product as white powder (62.5 mg, 72%). The peptide product was analysed by using LCMS and found [MH<sup>+</sup>]: 741.4 at retention time of 2.86 min. Compound was then purified by RP-HPLC and obtained 1.1 mg as pure product (3.7% recovery). <sup>1</sup>H NMR (500 MHz, DMSO-d<sub>6</sub>) δ 10.71-10.79 (m, 1H, L-Trp<sup>3</sup>-CCHNH), 8.56 (d, J  $= 8.5, 1H, L-Trp^3-NH), 8.52 (d, J = 8.5, 1H, D-Val^2-NH), 8.41 (d, J = 8.5, 1H, D-Leu^4-NH),$ 8.33-8.37 (m, 1H, L-Val<sup>5</sup>-NH), 8.25-8.29 (m, 1H, D-Val<sup>6</sup>-NH), 7.98 (d, J = 7.8, 1H, L-Trp<sup>3</sup>-Ar-H), 7.95 (dd,  $J = 8.1, 3.7, 1H, L-Trp^3-Ar-H)$ , 7.83 (d,  $J = 7.8, 1H, L-Trp^3-Ar-H)$ , 7.77 (dd,  $J = 8.0, 1.5, 1H, L-Trp^3-Ar-H), 7.53$  (d,  $J = 2.0, 1H, L-Trp^3-NHCHC$ ), 4.72-4.76 (m, 1H, L- $Trp^3$ -NHCHCH<sub>2</sub>), 4.58 (dd,  $J = 8.8, 4.5, 1H D-Val^6$ -NHCHCH), 4.35 (t,  $J = 8.3, 1H, D-Leu^4$ -NHCHCH<sub>2</sub>), 4.11 (d, J = 9.0, 1H, D-Val<sup>2</sup>-NHCHCH), 3.95-4.02 (m, 1H, thiazolidine<sup>1</sup>-NHCHCH<sub>2</sub>S), 3.86 (dd, J = 9.0, 6.6, 1H, L-N-Me-Leu<sup>7</sup>-NHCHCH<sub>2</sub>), 3.33 (s, 3H, L-N-Me-Leu<sup>7</sup>-NCH<sub>3</sub>), 3.23 (dd, J = 10.5, 6.5, 1H, thiazolidine<sup>1</sup>-NHCHCH<sub>2</sub>S), 3.15 (dd, J = 10.5, 6.5, 1H, thiazolidine<sup>1</sup>-NHCHC $H_2$ S), 3.09 (d, J = 7.8, 1H, L-Trp<sup>3</sup>-NHCHC $H_2$ ), 3.02 (dd, J = 13.5, 5.4, 1H, L-Trp<sup>3</sup>-NHCHCH<sub>2</sub>), 2.88-2.95 (m, 1H, thiazolidine<sup>1</sup>- NHCHCH<sub>2</sub>S), 2.09-2.15 (m, 1H, D-Val<sup>6</sup>-CH(CH<sub>3</sub>)<sub>2</sub>), 1.86-1.92 (m, 1H, L-Val<sup>5</sup>-CH(CH<sub>3</sub>)<sub>2</sub>), 1.63-1.69 (m, 1H, D-Val<sup>2</sup>-CH(CH<sub>3</sub>)<sub>2</sub>), 1.49-1.56 (m, 1H, D-Leu<sup>4</sup>-CHCH<sub>2</sub>CH), 1.40-1.45 (m, 1H, L-N-Me-Leu<sup>7</sup>-CHCH<sub>2</sub>CH), 1.29-1.45 (m, 1H, D-Leu<sup>4</sup>-CHCH<sub>2</sub>CH), 1.21-1.24 (m, 1H, L-N-Me-Leu<sup>7</sup>-CHC $H_2$ CH), 1.18 (d, J = 6.4, 3H, D-Val<sup>6</sup>-CH(C $H_3$ )<sub>2</sub>), 1.09 (d, J = 6.7, 3H, D-Leu<sup>4</sup>-CH(C $H_3$ )<sub>2</sub>),  $1.06 \text{ (d, } J = 6.7, 3H, D-Leu^4-CH(CH_3)_2), 1.04 \text{ (d, } J = 6.5, 3H, D-Val^6-CH(CH_3)_2), 0.99 \text{ (d, } J = 6.5, 3H, D$ 6.6, 3H, L-Leu<sup>7</sup>- CH(CH<sub>3</sub>)<sub>2</sub>), 0.94 (d, J = 6.6, 3H, L-N-Me-Leu<sup>7</sup>-CH(CH<sub>3</sub>)<sub>2</sub>), 0.91 (d, J = 6.8,

3H, L-Val<sup>5</sup>-CH(C $H_3$ )<sub>2</sub>), 0.85 (d, J = 6.4, 3H, L-Val<sup>5</sup>-CH(C $H_3$ )<sub>2</sub>), 0.76 (d, J = 6.5, 3H, D-Val<sup>2</sup>-CH(C $H_3$ )<sub>2</sub>), 0.64 (d, J = 6.4, 3H, D-Val<sup>2</sup>-CH(C $H_3$ )<sub>2</sub>); HRMS: calculated for C<sub>37</sub>H<sub>56</sub>N<sub>8</sub>O<sub>6</sub>S<sub>1</sub><sup>+</sup> 741.4044, found 741.4049 [MH<sup>+</sup>]; Analytical RP-HPLC (**Method 1**)  $t_R = 4.72$  min.

# $(Thr)^7$ -lug (5.37)

Peptide chain with resin was filtered and washed with DMF, DCM and hexane. The resin was transferred into a round-bottom flask and dried in vacuo overnight. The dried resin was then suspended in TFA/H<sub>2</sub>O/TIPS (90:5:5) (10.0 mL) for 3 h. The suspension was then filtered by gravity and washed with TFA and DCM. The filtrate collected in a clean round-bottom flask was evaporated to dryness (DCM was added several times). The residue was triturated with cold diethyl ether (x3) to afford the crude product as white powder (38.8 mg, 52%). The peptide product was analysed by using LCMS and found [MH<sup>+</sup>]: 685.4 at retention time of 2.62 min. Compound was then purified by RP-HPLC and obtained 0.52 mg as pure product (2.4% recovery). HRMS: calculated for  $C_{34}H_{50}N_8O_7S_1^+$  715.3523, found 715.3226 [MH<sup>+</sup>]; Analytical RP-HPLC (**Method 1**)  $t_R$  = 4.05 min.

## $(D-Leu)^6$ -lug (1.72)

Peptide chain with resin was filtered and washed with DMF, DCM and hexane. The resin was transferred into a round-bottom flask and dried in vacuo overnight. The dried resin was then suspended in TFA/H<sub>2</sub>O/TIPS (90:5:5) (10.0 mL) for 3 h. The suspension was then filtered by gravity and washed with TFA and DCM. The filtrate collected in a clean round-bottom flask was evaporated to dryness (DCM was added several times). The residue was triturated with cold diethyl ether (x3) to afford the crude product as white powder (58.2 mg, 80%). The peptide product was analysed by using LCMS and found [MH<sup>+</sup>]: 727.5 at retention time of 2.88 min. Compound was then purified by RP-HPLC and obtained 0.63 mg as pure product (2.2% recovery). <sup>1</sup>H NMR (500 MHz, DMSO-d<sub>6</sub>) δ 10.68-10.79 (m, 1H, L-Trp<sup>3</sup>-CCHN*H*), 8.56 (d, *J*  $= 8.5, 1H, L-Trp^3-NH), 8.48 (d, J = 8.5, 1H, D-Val^2-NH), 8.45 (d, J = 8.5, 1H, D-Leu^4-NH),$ 8.35-8.39 (m, 1H, L-Val<sup>5</sup>-NH), , 8.27-8.31 (m, 1H, D-Leu<sup>6</sup>-NH), 8.19-8.22 (m, 1H, L-Val<sup>7</sup>-NH), 7.96 (d, J = 7.8, 1H, L-Trp<sup>3</sup>-Ar-H), 7.91 (dd, J = 8.1, 3.7, 1H, L-Trp<sup>3</sup>-Ar-H), 7.85 (d, J =7.8, 1H, L-Trp<sup>3</sup>-Ar-H), 7.77 (dd, J = 8.0, 1.5, 1H, L-Trp<sup>3</sup>-Ar-H), 7.56 (d, J = 2.0, 1H, L-Trp<sup>3</sup>-NHCHC), 4.73-4.77 (m, 1H, L-Trp<sup>3</sup>-NHCHCH<sub>2</sub>), 4.36 (t, J = 8.3, 1H, D-Leu<sup>4</sup>-NHCHCH<sub>2</sub>), 4.25 (t, J = 8.5, 1H, 1H D-Leu<sup>6</sup>- NHCHCH<sub>2</sub>), 4.05 (d, J = 9.0, 1H, D-Val<sup>2</sup>-NHCHCH), 3.95-4.05 (m, 1H, thiazolidine<sup>1</sup>-NHCHCH<sub>2</sub>S), 3.88 (dd, J = 9.0, 6.6, 1H, L-Val<sup>7</sup>-NHCHCH), 3.25 $(dd, J = 10.5, 6.5, 1H, thiazolidine^1-NHCHCH_2S), 3.15 (dd, J = 10.5, 6.5, 1H, thiazolidine^1-$ NHCHC $H_2$ S), 3.09 (d, J = 7.8, 1H, L-Trp<sup>3</sup>-NHCHC $H_2$ ), 3.04 (dd, J = 13.5, 5.4, 1H, L-Trp<sup>3</sup>-NHCHCH<sub>2</sub>), 2.80-2.84 (m, 1H, thiazolidine<sup>1</sup>- NHCHCH<sub>2</sub>S), 2.12-2.18 (m, 1H, D-Val<sup>6</sup>-CH(CH<sub>3</sub>)<sub>2</sub>), 1.99-2.02 (m, 1H, L-Val<sup>5</sup>-CH(CH<sub>3</sub>)<sub>2</sub>), 1.72-1.79 (m, 1H, D-Val<sup>2</sup>-CH(CH<sub>3</sub>)<sub>2</sub>), 1.55-1.65 (m, 1H, D-Leu<sup>4</sup>-CHCH<sub>2</sub>CH), 1.47-1.51 (m, 1H, D-Leu<sup>6</sup>-CHCH<sub>2</sub>CH), 1.32-1.42 (m, 1H, D-Leu<sup>4</sup>-CHC $H_2$ CH), 1.25-1.29 (m, 1H, D-Leu<sup>6</sup>-CHC $H_2$ CH), 1.19 (d, J = 6.4, 3H, L-Val<sup>7</sup>- $CH(CH_3)_2$ ), 1.08 (d, J = 6.7, 3H, D-Leu<sup>4</sup>- $CH(CH_3)_2$ ), 1.06 (d, J = 6.7, 3H, D-Leu<sup>4</sup>- $CH(CH_3)_2$ ),  $1.02 \text{ (d, } J = 6.5, 3H, L-Val^7-CH(CH_3)_2), 0.97 \text{ (d, } J = 6.6, 3H, D-Leu^6-CH(CH_3)_2), 0.93 \text{ (d, } J = 6.6, 3H, D$ 6.6, 3H, D-Leu<sup>6</sup>- CH(CH<sub>3</sub>)<sub>2</sub>), 0.89 (d, J = 6.8, 3H, L-Val<sup>5</sup>-CH(CH<sub>3</sub>)<sub>2</sub>), 0.85 (d, J = 6.4, 3H, L- $Val^5$ -CH(CH<sub>3</sub>)<sub>2</sub>), 0.76 (d, J = 6.5, 3H, D-Val<sup>2</sup>-CH(CH<sub>3</sub>)<sub>2</sub>), 0.66 (d, J = 6.4, 3H, D-Val<sup>2</sup>-

CH(C $H_3$ )<sub>2</sub>); HRMS: calculated for C<sub>36</sub>H<sub>54</sub>N<sub>8</sub>O<sub>6</sub>S<sub>1</sub><sup>+</sup> 727.3887, found 727.3892 [MH<sup>+</sup>]; Analytical RP-HPLC (**Method 1**)  $t_R = 4.52$  min.

## $(D-Trp)^6$ -lug (1.46)

Peptide chain with resin was filtered and washed with DMF, DCM and hexane. The resin was transferred into a round-bottom flask and dried in vacuo overnight. The dried resin was then suspended in TFA/H<sub>2</sub>O/TIPS (90:5:5) (10.0 mL) for 3 h. The suspension was then filtered by gravity and washed with TFA and DCM. The filtrate collected in a clean round-bottom flask was evaporated to dryness (DCM was added several times). The residue was triturated with cold diethyl ether (x3) to afford the crude product as white powder (60.2 mg, 75%). The peptide product was analysed by using LCMS and found [MH<sup>+</sup>]: 800.5 at retention time of 2.92 min. Compound was then purified by RP-HPLC and obtained 1.3 mg as pure product (4.1% recovery). <sup>1</sup>H NMR (500 MHz, DMSO-d<sub>6</sub>) δ 10.62-10.69 (m, 1H, L-Trp<sup>3</sup>-CCHN*H*), 10.42- $10.55 \text{ (m, 1H, D-Trp}^6\text{-CCHN}H), 8.57 \text{ (d, } J = 8.5, 1H, L-Trp}^3\text{-N}H), 8.49 \text{ (d, } J = 8.5, 1H, D-Val}^2\text{-}$ NH), 8.46 (d, J = 8.5, 1H, D-Trp<sup>6</sup>-NH), 8.40 (d, J = 8.5, 1H, D-Leu<sup>4</sup>-NH), 8.32-8.37 (m, 1H, L-Val<sup>5</sup>-NH), 8.21-8.27 (m, 1H, L-Val<sup>7</sup>-NH), 7.65-7.8 (m, 8H, L-Trp<sup>3</sup>-Ar-H, D-Trp<sup>6</sup>-Ar-H), 7.51  $(d, J = 2.0, 1H, L-Trp^3-NHCHC), 7.42 (d, J = 2.5, 1H, D-Trp^6-NHCHC), 4.73-4.79 (m, 1H, L-Trp^6-NHCHC), 4$  $Trp^3$ -NHCHCH<sub>2</sub>), 4.52-4.58 (m, 1H, D-Trp<sup>6</sup>-NHCHCH<sub>2</sub>), 4.57 (dd,  $J = 8.8, 4.5, 1H, L-Val^7$ -NHCHCH), 4.36 (t, J = 8.5, 1H, D-Leu<sup>4</sup>-NHCHCH<sub>2</sub>), 4.08 (d, J = 9.0, 1H, D-Val<sup>2</sup>-NHCHCH), 3.92-4.05 (m, 1H, thiazolidine<sup>1</sup>-NHCHCH<sub>2</sub>S), 3.27 (dd, J = 10.5, 6.6, 1H, thiazolidine<sup>1</sup>-NHCHC $H_2$ S), 3.11 (dd, J = 10.5, 6.5, 1H, thiazolidine<sup>1</sup>-NHCHC $H_2$ S), 3.07 (d, J = 7.9, 1H, L- $Trp^3$ -NHCHC $H_2$ ), 2.97 (dd, J = 13.5, 5.4, 1H, L- $Trp^3$ -NHCHC $H_2$ ), 2.85-2.89 (m, 1H, thiazolidine<sup>1</sup>- NHCHCH<sub>2</sub>S), 2.05-2.0 (m, 1H, L-Val<sup>7</sup>-CH(CH<sub>3</sub>)<sub>2</sub>), 1.91-1.97 (m, 1H, L-Val<sup>5</sup>- $CH(CH_3)_2$ ), 1.68-1.72 (m, 1H, D-Val<sup>2</sup>- $CH(CH_3)_2$ ), 1.58-1.62 (m, 1H, D-Leu<sup>4</sup>- $CHCH_2CH$ ), 1.33-1.45 (m, 1H, D-Leu<sup>4</sup>-CHC $H_2$ CH), 1.19 (d, J = 6.4, 3H, L-Val<sup>7</sup>-CH(C $H_3$ )<sub>2</sub>), 1.13 (d, J =6.9, 3H, D-Leu<sup>4</sup>-CH(C $H_3$ )<sub>2</sub>), 1.07 (d, J = 6.8, 3H, D-Leu<sup>4</sup>- CH(C $H_3$ )<sub>2</sub>), 1.04 (d, J = 6.5, 3H, L-

Val<sup>7</sup>-CH(C $H_3$ )<sub>2</sub>), 0.98 (d, J = 6.8, 3H, L-Val<sup>5</sup>-CH(C $H_3$ )<sub>2</sub>), 0.92 (d, J = 6.6, 3H, L-Val<sup>5</sup>-CH(C $H_3$ )<sub>2</sub>), 0.83 (d, J = 6.5, 3H, D-Val<sup>2</sup>-CH(C $H_3$ )<sub>2</sub>), 0.72 (d, J = 6.5, 3H, D-Val<sup>2</sup>-CH(C $H_3$ )<sub>2</sub>); HRMS: calculated for C<sub>41</sub>H<sub>53</sub>N<sub>9</sub>O<sub>6</sub>S<sub>1</sub><sup>+</sup> 800.3840, found 800.3845 [MH<sup>+</sup>]; Analytical RP-HPLC (**Method 1**)  $t_R = 5.12$  min.

#### $(D-Phe)^6$ -lug (1.73)

Peptide chain with resin was filtered and washed with DMF, DCM and hexane. The resin was transferred into a round-bottom flask and dried in vacuo overnight. The dried resin was then suspended in TFA/H<sub>2</sub>O/TIPS (90:5:5) (10.0 mL) for 3 h. The suspension was then filtered by gravity and washed with TFA and DCM. The filtrate collected in a clean round-bottom flask was evaporated to dryness (DCM was added several times). The residue was triturated with cold diethyl ether (x3) to afford the crude product as white powder (56.2 mg, 74%). The peptide product was analysed by using LCMS and found [MH<sup>+</sup>]: 761.6 at retention time of 2.90 min. Compound was then purified by RP-HPLC and obtained 0.72 mg as pure product (3.7% recovery). <sup>1</sup>H NMR (500 MHz, DMSO-d<sub>6</sub>) δ 10.69-10.75 (m, 1H, L-Trp<sup>3</sup>-CCHNH), 8.59 (d, J  $= 8.5, 1H, L-Trp^3-NH), 8.52 (d, J = 8.5, 1H, D-Val^2-NH), 8.45 (d, J = 8.5, 1H, D-Leu^4-NH),$ 8.25-8.29 (m, 1H, L-Val<sup>5</sup>-NH), 8.16-8.21 (m, 1H, D-Phe<sup>6</sup>-NH), 8.09-8.13 (m, 1H, L-Val<sup>7</sup>-NH), 7.95 (d, J = 7.8, 1H, L-Trp<sup>3</sup>-Ar-H), 7.89 (dd, J = 8.1, 3.7, 1H, L-Trp<sup>3</sup>-Ar-H), 7.85 (d, J = 8.0, 1H, L-Trp<sup>3</sup>-Ar-H), 7.72 (dd, J = 7.9, 1.3, 1H, L-Trp<sup>3</sup>-Ar-H), 7.61 (d, J = 2.0, 1H, L-Trp<sup>3</sup>-NHCHC), 7.17-7.22 (m, 5H, D-Phe<sup>6</sup>-Ar-H), 4.72-4.77 (m, 1H, D-Phe<sup>6</sup>-NHCHCH<sub>2</sub>), 4.65-4.71 (m, 1H, L-Trp<sup>3</sup>-NHCHCH<sub>2</sub>), 4.51 (dd,  $J = 8.7, 4.5, 1H L-Val^7-NHCHCH$ ), 4.42 (t, J = 8.3, 1H, D-Leu<sup>4</sup>-NHCHCH<sub>2</sub>), 4.19 (d, J = 8.9, 1H, D-Val<sup>2</sup>-NHCHCH), 3.94-4.02 (m, 1H, thiazolidine<sup>1</sup>-NHCHCH<sub>2</sub>S), 3.45 (d, J = 8.5, 1H, D-Phe<sup>6</sup>-NHCHCH<sub>2</sub>), 3.36 (dd, J = 10.5, 6.6, 1H, thiazolidine<sup>1</sup>-NHCHC $H_2$ S), 3.26 (d, J = 8.6, 1H, D-Phe<sup>6</sup>-NHCHC $H_2$ ), 3.19 (dd, J = 10.5, 6.5, 1H, thiazolidine<sup>1</sup>-NHCHC $H_2$ S), 3.07 (d, J = 7.8, 1H, L-Trp<sup>3</sup>-NHCHC $H_2$ ), 2.99 (dd, J = 13.5, 5.4, 1H, L-Trp<sup>3</sup>-NHCHCH<sub>2</sub>), 2.82-2.85 (m, 1H, thiazolidine<sup>1</sup>- NHCHCH<sub>2</sub>S), 2.15-2.22 (m, 1H,

L-Val<sup>7</sup>-CH(CH<sub>3</sub>)<sub>2</sub>), 1.96-2.01 (m, 1H, L-Val<sup>5</sup>-CH(CH<sub>3</sub>)<sub>2</sub>), 1.79-1.83 (m, 1H, D-Val<sup>2</sup>-CH(CH<sub>3</sub>)<sub>2</sub>), 1.58-1.67 (m, 1H, D-Leu<sup>4</sup>-CHCH<sub>2</sub>CH), 1.32-1.44 (m, 1H, D-Leu<sup>4</sup>-CHCH<sub>2</sub>CH), 1.26 (d, J = 6.5, 3H, L-Val<sup>7</sup>-CH(CH<sub>3</sub>)<sub>2</sub>), 1.17 (d, J = 6.6, 3H, D-Leu<sup>4</sup>-CH(CH<sub>3</sub>)<sub>2</sub>), 1.12 (d, J = 6.5, 3H, D-Leu<sup>4</sup>- CH(CH<sub>3</sub>)<sub>2</sub>), 1.08 (d, J = 6.5, 3H, L-Val<sup>7</sup>-CH(CH<sub>3</sub>)<sub>2</sub>), 0.97 (d, J = 6.8, 3H, L-Val<sup>5</sup>-CH(CH<sub>3</sub>)<sub>2</sub>), 0.91 (d, J = 6.4, 3H, L-Val<sup>5</sup>-CH(CH<sub>3</sub>)<sub>2</sub>), 0.86 (d, J = 6.6, 3H, D-Val<sup>2</sup>-CH(CH<sub>3</sub>)<sub>2</sub>), 0.79 (d, J = 6.6, 3H, D-Val<sup>2</sup>-CH(CH<sub>3</sub>)<sub>2</sub>); HRMS: calculated for C<sub>39</sub>H<sub>52</sub>N<sub>8</sub>O<sub>6</sub>S<sub>1</sub><sup>+</sup> 761.3731, found 761.3736 [MH<sup>+</sup>]; Analytical RP-HPLC (**Method 1**)  $t_R$  = 4.53 min.

# $(D-Trp)^6-(L-Leu)^7-lug (5.44)$

Peptide chain with resin was filtered and washed with DMF, DCM and hexane. The resin was transferred into a round-bottom flask and dried in vacuo overnight. The dried resin was then suspended in TFA/H<sub>2</sub>O/TIPS (90:5:5) (10.0 mL) for 3 h. The suspension was then filtered by gravity and washed with TFA and DCM. The filtrate collected in a clean round-bottom flask was evaporated to dryness (DCM was added several times). The residue was triturated with cold diethyl ether (x3) to afford the crude product as white powder (46.2 mg, 57%). The peptide product was analysed by using LCMS and found [MH<sup>+</sup>]: 814.5 at retention time of 2.97 min. Compound was then purified by RP-HPLC and obtained 0.35 mg as pure product (1.4% recovery). HRMS: calculated for  $C_{42}H_{55}N_9O_6S_1^+$  814.3996, found 814.3988 [MH<sup>+</sup>]; Analytical RP-HPLC (**Method 1**)  $t_R = 5.14$  min.

# 8.6 Biological evaluations of lugdunin and analogues

#### Antimicrobial peptide stock solutions and bacterial strains

The lugdunin and analogues were prepared as 10 mM stock solutions in DMSO. Vancomycin (3.45 mM stock in H<sub>2</sub>O) was used as a positive control. Frozen stocks of *S. aureus* SH1000, MRSA USA300 JE2, Newman, Mu50 and PM54 were obtained from the Centre for Biomolecular Sciences, University of Nottingham.

#### **Growth Inhibition Assay**

*S. aureus* SH1000/USA 300 JE2

A single colony was incubated in Luria Bertani (LB) broth (5 mL) overnight in a shaking incubator at 37 °C and 200 rpm. The optical density (OD) of this overnight culture was measured at 600 nm, before LB broth was used to dilute the culture to achieve an OD600 of 0.01 ( $\approx 10^6$  CFU/mL). Typically, 10  $\mu$ L of the 10 mM stock peptide solution was then diluted with this bacterial culture (990  $\mu$ L) to give a concentration of 100  $\mu$ M. Two-fold serial dilutions were done seven times in eppendorf tubes, keeping the DMSO concentration constant at 1 %. An aliquot of each treated culture (200  $\mu$ L) was transferred into a 96-well microtitre plate in duplicate. In addition, vancomycin treated culture was set up as a positive control and LB media, untreated culture and culture with 1 % DMSO were set up as negative controls. The plate was incubated at 37 °C for 20 h and OD600 measurements were taken every 15 min using a TECAN microplate reader. Three independent assays were performed for each analogue. The percentage growth of bacteria at 13 h was calculated for each concentration of peptide and the IC50 was determined using GraphPad Prism (version 7.05).

## **Broth Microdilution Assay**

The minimum inhibitory concentration (MIC) of the analogues was determined using the broth microdilution method, according to CLSI guidelines.<sup>5</sup> For *S. aureus*, 3-5 colonies from a 24 h Mueller Hinton agar plate were incubated in CAMHB (5 mL) at 37 °C and 200 rpm for 4-6 h. The optical density at 600 nm was measured before the culture was diluted in CAMHB to achieve an OD<sub>600</sub> of 0.001 ( $\approx 10^6$  CFU/mL). For *C. acnes*, colonies from a 48 h plate (blood agar base no.2 with 7 % horse blood, OXOID CM0271) were suspended in CAMHB (5 mL) and the optical density measured at 600 nm, before the culture was directly diluted to achieve

an OD<sub>600</sub> of 0.1 ( $\approx 10^8$  CFU/mL). The 10 mM stock peptide solution was diluted in CAMHB to achieve a concentration of 64 µg/mL. An aliquot of this (200 µL) was transferred to a 96-well microtitre plate in triplicate. Two-fold serial dilutions were done into CAMHB across the plate, resulting in 100 µL of 2x the required concentration in each well. The concentration of DMSO was adjusted so that it was constant across all test compound concentrations. 100 µL of the bacterial culture was then added to each well containing the test compound. This resulted in the test compound concentrations being halved, as well as the bacterial concentrations ( $\approx 5$  x  $10^5$  CFU/mL for *S. aureus* and  $\approx 5$  x  $10^7$  CFU/mL for *C. acnes*). In addition, vancomycin treated culture was set up as a positive control and CAMHB media, untreated culture and culture with DMSO were set up as negative controls. The plate was incubated at 37 °C for 24 h for *S. aureus*. The MIC was determined as the lowest concentration that inhibited visible growth, as detected by unaided eyes.

# Chapter 9

## References

- 1. Saga, T.; Yamaguchi, K., History of antimicrobial agents and resistant bacteria. *JMAJ.* **2009**, *52*, 103-108.
- 2. Rea, M. C.; Ross, R. P.; Cotter, P. D.; Hill, C., Classification of bacteriocins from Gram-positive bacteria. In: *Prokaryotic antimicrobial peptides: From genes to applications*, Springer: **2011**, 29-53.
- 3. Fair, R. J.; Tor, Y., Antibiotics and bacterial resistance in the 21st century. *Perspect. Med. Chem.* **2014**, *6*, 25-64.
- 4. Leekha, S.; Terrell, C. L.; Edson, R. S. In General principles of antimicrobial therapy, *Mayo Clin Proc*, Elsevier: **2011**, 86, 156-167.
- 5. Moellering Jr, R. C., What is inadequate antibacterial therapy?, *Clinic Infect Dis*. **2009**, 1006-1008
- 6. Ventola, C. L., The antibiotic resistance crisis: part 1: causes and threats. *PT.* **2015**, 40, 277-283.
- 7. Li, B.; Webster, T. J., Bacteria antibiotic resistance: New challenges and opportunities for implant-associated orthopedic infections. *J. Orthop. Res.* **2018**, *36*, 22-32.
- 8. Rai, J.; Randhawa, G. K.; Kaur, M., Recent advances in antibacterial drugs. *Int. J. Appl. Basic Med. Res.* **2013**, *3*, 3.
- 9. Ligon, B. L. In *Penicillin: its discovery and early development*, Seminars in pediatric infectious diseases, Elsevier: **2004**, 52-57.
- 10. World Health Organization. Lack of new antibiotics threatens global efforts to contain drug-resistant infections; **2020** Available from: https://www.who.int/news-room/detail/17-01-2020-17-01-2020-lack-of-new-antibiotics-threatens-global-efforts-to-contain-drug-resistant-infections.

- 11. Cassell, G. H.; Mekalanos, J., Development of antimicrobial agents in the era of new and reemerging infectious diseases and increasing antibiotic resistance. *JMAJ.* 2001, 285, 601-605.
- 12. Fosgerau, K.; Hoffmann, T., Peptide therapeutics: current status and future directions. *Drug Discov. Today.* **2015**, *20*, 122-128.
- 13. Breijyeh, Z.; Jubeh, B.; Karaman, R., Resistance of gram-negative bacteria to current antibacterial agents and approaches to resolve it. *Molecules*. **2020**, *25*, 1340.
- 14. Belete, T. M., Novel targets to develop new antibacterial agents and novel alternatives to antibacterial agents. *Hum. Microbiome J.* **2019**, *11*, 100052.
- 15. Moellering Jr, R. C., Discovering new antimicrobial agents. *Int. J. Antimicrob. Agents.* **2011**, *37*, 2-9.
- 16. Steckbeck, J. D.; Deslouches, B.; Montelaro, R. C., Antimicrobial peptides: new drugs for bad bugs?, *Expert Opin. Biol.* **2014**, *14*, 11.
- 17. Harvey, A. L., Natural products in drug discovery. *Drug Discov. Today.* **2008**, *13*, 894-901.
- 18. Diamond, G., Nature's antibiotics: the potential of antimicrobial peptides as new drugs. *Biologist.* **2001**, *48*, *209-212*.
- 19. Lei, J.; Sun, L.; Huang, S.; Zhu, C.; Li, P.; He, J.; Mackey, V.; Coy, D. H.; He, Q., The antimicrobial peptides and their potential clinical applications.

  Am. J. Transl. Res. 2019, 11, 3919-3931.
- Zipperer, A.; Konnerth, M. C.; Laux, C.; Berscheid, A.; Janek, D.; Weidenmaier, C.; Burian, M.; Schilling, N. A.; Slavetinsky, C.; Marschal, M., Human commensals producing a novel antibiotic impair pathogen colonization. *Nature*.
  2016, 535, 511-516.
- 21. Beveridge, T. J., Use of the Gram stain in microbiology. *Biotech. Histochem.* **2001**, *76*, 111-118.

- 22. Moyes, R. B.; Reynolds, J.; Breakwell, D. P., Differential staining of bacteria: gram stain. *Curr Protoc Microbiol.* **2009**, *15*.
- 23. Greenwood, D.; Slack, R. C.; Barer, M. R.; Irving, W. L., *Medical Microbiology, A Guide to Microbial Infections: Pathogenesis, Immunity, Laboratory Diagnosis and Control.* Churchill Livingstone, Philadelphia, Pa USA. **2007**.
- 24. Thairu, Y.; Nasir, I. A.; Usman, Y., Laboratory perspective of gram staining and its significance in investigations of infectious diseases. *SAMJ, S. Afr. Med.* **2014**, *1*, 168.
- 25. Silhavy, T. J.; Kahne, D.; Walker, S., The bacterial cell envelope. *Cold Spring Harb. Perspect. Biol.* **2010**, 2, a000414.
- 26. Madigan, M. T.; Martinko, J. M.; Parker, J., *Brock Biology of Microorganisms Plus Masteringmicrobiology With Etext*, Benjamin-Cummings Pub Co. **2014**.
- 27. Vollmer, W.; Blanot, D.; De Pedro, M. A., Peptidoglycan structure and architecture. *FEMS Microbiol. Rev.* **2008**, *32*, 149-167.
- 28. Bradley, K., Reproduction in Bacteria. Scientific e-Resources: **2019.**
- 29. Liu, Y.; Qin, R.; Zaat, S. A.; Breukink, E.; Heger, M., Antibacterial photodynamic therapy: overview of a promising approach to fight antibiotic-resistant bacterial infections. *J. Clin. Tran.s Res.* **2015**, *1*, 140-167.
- 30. Wilson, L. G., The early recognition of streptococci as causes of disease. *Med Hist.* **1987**, *31*, 403-414.
- 31. Licitra, G., Etymologia: Staphylococcus. *Emerg. Infect. Dis.* **2013**, *19*, 1553.
- 32. Chambers, H. F.; DeLeo, F. R., Waves of resistance: Staphylococcus aureus in the antibiotic era. *Nat. Rev. Microbiol.* **2009**, *7*, 629-641.
- 33. Masalha, M.; Borovok, I.; Schreiber, R.; Aharonowitz, Y.; Cohen, G., Analysis of Transcription of theStaphylococcus aureus Aerobic Class Ib and Anaerobic Class III Ribonucleotide Reductase Genes in Response to Oxygen. *J. Bacteriol* 2001, 183, 7260-7272.

- 34. Schaumburg, F.; Pauly, M.; Anoh, E.; Mossoun, A.; Wiersma, L.; Schubert, G.; Flammen, A.; Alabi, A. S.; Muyembe-Tamfum, J.-J.; Grobusch, M. P., Staphylococcus aureus complex from animals and humans in three remote African regions. *Clin. Microbiol. Infect.* **2015**, *21*, 345.e1–345.e8.
- 35. Friendship, B.; Weese, S., Methicillin Resistant Staphylococcus aureus (MRSA). *Adv. Pork Production.* **2009**, *20*, 173-180.
- 36. Kluytmans, J.; Van Belkum, A.; Verbrugh, H., Nasal carriage of Staphylococcus aureus: epidemiology, underlying mechanisms, and associated risks. *Clin. Microbiol. Rev.* **1997**, *10*, 505-520.
- 37. Kong, C.; Neoh, H.-m.; Nathan, S., Targeting Staphylococcus aureus toxins: a potential form of anti-virulence therapy. *Toxins.* **2016**, *8*, 72.
- 38. Tong, S. Y.; Davis, J. S.; Eichenberger, E.; Holland, T. L.; Fowler, V. G., Staphylococcus aureus infections: epidemiology, pathophysiology, clinical manifestations, and management. *Clin. Microbiol. Rev.* **2015**, *28*, 603-661.
- 39. Weems Jr, J. J., The many faces of Staphylococcus aureus infection: recognizing and managing its life-threatening manifestations. *Postgrad Med.* **2001**, *110*, 24-36.
- 40. Defres, S.; Marwick, C.; Nathwani, D., MRSA as a cause of lung infection including airway infection, community-acquired pneumonia and hospital-acquired pneumonia. *Eur. Respir. J.* **2009**, *34*, 1470-1476.
- 41. Schlecht, L. M.; Peters, B. M.; Krom, B. P.; Freiberg, J. A.; Hänsch, G. M.; Filler, S. G.; Jabra-Rizk, M. A.; Shirtliff, M. E., Systemic Staphylococcus aureus infection mediated by Candida albicans hyphal invasion of mucosal tissue. *Microbiol.* **2015**, *161*, 168-181.
- 42. Klein, E.; Smith, D. L.; Laxminarayan, R., Hospitalizations and deaths caused by methicillin-resistant Staphylococcus aureus, United States, 1999–2005. *Emerg. Infect. Dis.* **2007**, *13*, 1840-1846.
- 43. Dalton, K.R., Rock, C., Carroll, K.C. *et al.* One Health in hospitals: how understanding the dynamics of people, animals, and the hospital built-environment

- can be used to better inform interventions for antimicrobial-resistant gram-positive infections. *Antimicrob Resist Infect Control* **9**, 78 (2020). https://doi.org/10.1186/s13756-020-00737-2
- 44. Scarsbrook, C.; Raja, N. S.; Hardman, M.; Hughes, K., An Audit of Staphylococcus aureus Bacteraemia Treatment in a UK District General Hospital. *J. Microbiol. Infect. Dis.* **2017**, *7*, 188-193.
- 45. Styers, D.; Sheehan, D. J.; Hogan, P.; Sahm, D. F., Laboratory-based surveillance of current antimicrobial resistance patterns and trends among Staphylococcus aureus: 2005 status in the United States. *Ann. clin. Microbiol. Antimicrob.* **2006**, *5*, 2.
- 46. Rossolini, G. M.; Arena, F.; Pecile, P.; Pollini, S., Update on the antibiotic resistance crisis. *Curr. Opin. Pharmacol.* **2014**, *18*, 56-60.
- 47. Stewart, P. S.; Costerton, J. W., Antibiotic resistance of bacteria in biofilms. *The Lancet.* **2001**, *358*, 135-138.
- 48. Van Duin, D.; Paterson, D. L., Multidrug-resistant bacteria in the community: trends and lessons learned. *Infect. Dis. Clin.* **2016**, *30*, 377-390.
- 49. Organization, W. H., Antimicrobial resistance: global report on surveillance. *World Health Organization*: **2014**.
- 50. Borer, A.; Saidel-Odes, L.; Riesenberg, K.; Eskira, S.; Peled, N.; Nativ, R.; Schlaeffer, F.; Sherf, M., Attributable mortality rate for carbapenem-resistant Klebsiella pneumoniae bacteremia. *Infect Control Hosp Epidemiol.* **2009**, *30*, 972.
- 51. Cecchini, M.; Langer, J.; Slawomirski, L., Antimicrobial resistance in G7 countries and beyond: economic issues, policies and options for action. *Paris: Organization for Economic Co-operation and Development* **2015**. Available from: https://www.oecd.org/els/health-systems/Antimicrobial-Resistance-in-G7-Countries-and-Beyond.pdf.
- 52. Solomon, S. L.; Oliver, K. B., Antibiotic resistance threats in the United States: stepping back from the brink. *Am. Fam. Physician.* **2014**, *89*, 938-941.

- 53. Roberts, R. R.; Hota, B.; Ahmad, I.; Scott, R. D.; Foster, S. D.; Abbasi, F.; Schabowski, S.; Kampe, L. M.; Ciavarella, G. G.; Supino, M., Hospital and societal costs of antimicrobial-resistant infections in a Chicago teaching hospital: implications for antibiotic stewardship. *Clin. Infect. Dis.* **2009**, *49*, 1175-1184.
- 54. Blair, J. M.; Webber, M. A.; Baylay, A. J.; Ogbolu, D. O.; Piddock, L. J., Molecular mechanisms of antibiotic resistance. *Nat. Rev. Microbiol.* **2015**, *13*, 42-51.
- Davies, S. C.; Fowler, T.; Watson, J.; Livermore, D. M.; Walker, D., Annual Report of the Chief Medical Officer: infection and the rise of antimicrobial resistance. *The Lancet.* **2013**, *381*, 1606-1609.
- 56. Salmanov, A.; Shchehlov, D.; Svyrydiuk, O.; Bortnik, I.; Mamonova, M.; Korniyenko, S.; Rud, V.; Artyomenko, V.; Gudym, M.; Maliarchuk, R., Epidemiology of healthcare-associated infections and mechanisms of antimicrobial resistance of responsible pathogens in Ukraine: a multicentre study. *J. Hosp. Infect.* 2023, *131*, 129-138.
- 57. Lowy, F. D., Staphylococcus aureus infections. *N. Engl. J. Med.* **1998**, *339*, 520-532.
- 58. Yang, D.; Wijenayaka, A. R.; Solomon, L. B.; Pederson, S. M.; Findlay, D. M.; Kidd, S. P.; Atkins, G. J., Novel insights into Staphylococcus aureus deep bone infections: the involvement of osteocytes. *MBio.* 2018, 9, e00415-18.
- 59. Harris, L. G.; Foster, S.; Richards, R. G., An introduction to Staphylococcus aureus, and techniques for identifying and quantifying S. aureus adhesins in relation to adhesion to biomaterials: review. *Eur. Cell. Mater.* **2002**, *4*, 39-60.
- 60. Honeyman, A.; Friedman, H.; Bendinelli, M., *Staphylococcus aureus infection and disease*. Springer Science & Business Media: Berlin/Heidelberg, Germany, **2006**; ISBN 9780306468483.
- 61. Zhou, K.; Li, C.; Chen, D.; Pan, Y.; Tao, Y.; Qu, W.; Liu, Z.; Wang, X.; Xie, S., A review on nanosystems as an effective approach against infections of Staphylococcus aureus. *Int. J. Nanomedicine*. **2018**, *13*, 7333-7347.

- 62. Löffler, B.; Tuchscherr, L.; Niemann, S.; Peters, G., Staphylococcus aureus persistence in non-professional phagocytes. *Int. J. Med. Microbiol.* **2014**, *304*, 170-176.
- 63. Speziale, P.; Pietrocola, G.; Rindi, S.; Provenzano, M.; Provenza, G.; Di Poto, A.; Visai, L.; Arciola, C. R., Structural and functional role of Staphylococcus aureus surface components recognizing adhesive matrix molecules of the host. *Future Microbiol.* **2009**, *4*, 1337-1352.
- 64. Zecconi, A.; Scali, F., Staphylococcus aureus virulence factors in evasion from innate immune defenses in human and animal diseases. *Immunol. Lett.* **2013**, *150*, 12-22.
- 65. Clarke, S. R.; Brummell, K. J.; Horsburgh, M. J.; McDowell, P. W.; Mohamad, S. A. S.; Stapleton, M. R.; Acevedo, J.; Read, R. C.; Day, N. P.; Peacock, S. J., Identification of in vivo—expressed antigens of Staphylococcus aureus and their use in vaccinations for protection against nasal carriage. *J. Infect. Dis.* 2006, 193, 1098-1108.
- 66. Garzoni, C.; Kelley, W. L., Staphylococcus aureus: new evidence for intracellular persistence. *Trends Microbiol.* **2009**, *17*, 59-65.
- 67. Bank, T.; Dosen, A.; Giese, R.; Haase, E.; Sojar, H., Atomic force spectroscopy evidence of non-specific adhesion of Aggregatibacter actinomycetemcomitans. *J. Nanosci. Nanotechnol.* **2011**, *11*, 8450-8456.
- 68. Shinji, H.; Yosizawa, Y.; Tajima, A.; Iwase, T.; Sugimoto, S.; Seki, K.; Mizunoe, Y., Role of fibronectin-binding proteins A and B in in vitro cellular infections and in vivo septic infections by Staphylococcus aureus. *Infect Immun.* **2011**, *79*, 2215-2223.
- 69. Proctor, R. A., Fibronectin: a brief overview of its structure, function, and physiology. *Rev. Infect. Dis.* **1987**, *9* (Supplement 4), S317-S321.
- 70. Clarke, S. R.; Wiltshire, M. D.; Foster, S. J., IsdA of Staphylococcus aureus is a broad spectrum, iron-regulated adhesin. *Mol. Microbiol* **2004**, *51*, 1509-1519.

- 71. Clarke, S. R.; Mohamed, R.; Bian, L.; Routh, A. F.; Kokai-Kun, J. F.; Mond, J. J.; Tarkowski, A.; Foster, S. J., The Staphylococcus aureus surface protein IsdA mediates resistance to innate defenses of human skin. *Cell Host Microbe* **2007**, *1*, 199-212.
- 72. Andrade, M. A.; Ciccarelli, F. D.; Perez-Iratxeta, C.; Bork, P., NEAT: a domain duplicated in genes near the components of a putative Fe 3+ siderophore transporter from Gram-positive pathogenic bacteria. *Genome Biol.* **2002**, *3*, 1-5.
- 73. Zinkernagel, A. S.; Nizet, V., Staphylococcus aureus: a blemish on skin immunity. *Cell Host Microbe*. **2007**, *1*, 161-162.
- 74. Grigg, J. C.; Vermeiren, C. L.; Heinrichs, D. E.; Murphy, M. E., Haem recognition by a Staphylococcus aureus NEAT domain. *Mol. Microbiol.* **2007**, *63*, 139-149.
- 75. Wiltshire, M. D.; Foster, S. J., Identification and analysis of Staphylococcus aureus components expressed by a model system of growth in serum. *Infect Immun.* **2001**, *69*, 5198-5202.
- 76. Clarke, S. R.; Andre, G.; Walsh, E. J.; Dufrêne, Y. F.; Foster, T. J.; Foster, S. J., Iron-regulated surface determinant protein A mediates adhesion of Staphylococcus aureus to human corneocyte envelope proteins. *Infect Immun.* **2009**, *77*, 2408-2416.
- 77. Argudín, M. Á.; Mendoza, M. C.; Rodicio, M. R., Food poisoning and Staphylococcus aureus enterotoxins. *Toxins*. **2010**, *2*, 1751-1773.
- 78. Bergdoll, M.; Reiser, R.; Crass, B.; Robbins, R.; Davis, J., A new staphylococcal enterotoxin, enterotoxin F, associated with toxic-shock-syndrome Staphylococcus aureus isolates. *The Lancet.* **1981**, *317*, 1017-1021.
- 79. Balaban, N.; Rasooly, A., Staphylococcal enterotoxins. *Int. J. Food Microbiol.* **2000**, *61*, 1-10.
- 80. Laarman, A. J.; Ruyken, M.; Malone, C. L.; van Strijp, J. A.; Horswill, A. R.; Rooijakkers, S. H., Staphylococcus aureus metalloprotease aureolysin cleaves complement C3 to mediate immune evasion. *J. Immunol.* **2011**, *186*, 6445-6453.

- 81. Arvidson, S.; Holme, T.; Lindholm, B., Studies on extracellular proteolytic enzymes from Staphylococcus aureus: I. Purification and characterization of one neutral and one alkaline protease. *Biochim Biophys Acta.* **1973**, *302*, 135-148.
- 82. Drapeau, G., Role of metalloprotease in activation of the precursor of staphylococcal protease. *J. Bacteriol.* **1978**, *136*, 607-613.
- 83. Jusko, M.; Potempa, J.; Kantyka, T.; Bielecka, E.; Miller, H. K.; Kalinska, M.; Dubin, G.; Garred, P.; Shaw, L. N.; Blom, A. M., Staphylococcal proteases aid in evasion of the human complement system. *J. Innate Immun.* **2014**, *6*, 31-46.
- 84. Dubin, G., Extracellular proteases of *Staphylococcus spp. Biol Chem.* **2002**, 383, 1075-1086.
- 85. Chavakis, T.; Hussain, M.; Kanse, S. M.; Peters, G.; Bretzel, R. G.; Flock, J.-I.; Herrmann, M.; Preissner, K. T., Staphylococcus aureus extracellular adherence protein serves as anti-inflammatory factor by inhibiting the recruitment of host leukocytes. *Nat. Med.* **2002**, *8*, 687-693.
- 86. Athanasopoulos, A. N.; Economopoulou, M.; Orlova, V. V.; Sobke, A.; Schneider, D.; Weber, H.; Augustin, H. G.; Eming, S. A.; Schubert, U.; Linn, T., The extracellular adherence protein (Eap) of Staphylococcus aureus inhibits wound healing by interfering with host defense and repair mechanisms. *Blood.* 2006, 107, 2720-2727.
- 87. Liu, G. Y., Molecular pathogenesis of Staphylococcus aureus infection. *Pediatr. Res.* **2009**, *65*, 71-77.
- 88. Kane, T. L.; Carothers, K. E.; Lee, S. W., Virulence factor targeting of the bacterial pathogen Staphylococcus aureus for vaccine and therapeutics. *Curr. Drug Targets*. **2018**, *19*, 111-127.
- 89. Bhakdi, S.; Tranum-Jensen, J., Alpha-toxin of Staphylococcus aureus. *Microbiol. Mol. Biol. Rev.* **1991**, *55*, 733-751.
- 90. Bantel, H.; Sinha, B.; Domschke, W.; Peters, G.; Schulze-Osthoff, K.; Jänicke, R.U., α-Toxin is a mediator of Staphylococcus aureus—induced cell death and

- activates caspases via the intrinsic death pathway independently of death receptor signaling. *J. Cell. Biol.* **2001**, *155*, 637-648.
- 91. Fraunholz, M.; Sinha, B., Intracellular Staphylococcus aureus: live-in and let die. *Front. Cell. Infect. Microbiol.* **2012**, *2*, 43.
- 92. Rasmussen, G.; Monecke, S.; Brus, O.; Ehricht, R.; Söderquist, B., Long term molecular epidemiology of methicillin-susceptible Staphylococcus aureus bacteremia isolates in Sweden. *PLoS One.* **2014**, *9*, e114276.
- 93. Srivastava, S. S.; Pany, S.; Sneh, A.; Ahmed, N.; Rahman, A.; Musti, K. V., Membrane bound monomer of staphylococcal α-hemolysin induces caspase activation and apoptotic cell death despite initiation of membrane repair pathway. *PLoS One.* **2009**, *4*, e6293.
- 94. Silva, M. T., Secondary necrosis: the natural outcome of the complete apoptotic program. *FEBS Lett.* **2010**, *584*, 4491-4499.
- 95. Harraghy, N.; Hussain, M.; Haggar, A.; Chavakis, T.; Sinha, B.; Herrmann, M.; Flock, J.-I., The adhesive and immunomodulating properties of the multifunctional Staphylococcus aureus protein Eap. *Microbiol.* **2003**, *149*, 2701-2707.
- 96. Giese, B.; Glowinski, F.; Paprotka, K.; Dittmann, S.; Steiner, T.; Sinha, B.; Fraunholz, M. J., Expression of δ-toxin by Staphylococcus aureus mediates escape from phago-endosomes of human epithelial and endothelial cells in the presence of β-toxin. *Cell Microbiol.* 2011, 13, 316-329.
- 97. Roy, C. R.; Kagan, J. C., Evasion of phagosome lysosome fusion and establishment of a replicative organelle by the intracellular pathogen Legionella pneumophila. In *Madame Curie Bioscience Database [Internet]*, Landes Bioscience: 2013. Available from: https://www.ncbi.nlm.nih.gov/books/NBK6111/
- 98. Pauwels, A.-M.; Trost, M.; Beyaert, R.; Hoffmann, E., Patterns, receptors, and signals: regulation of phagosome maturation. *Trends Immunol.* **2017**, *38*, 407-422.
- 99. Von Eiff, C., Staphylococcus aureus small colony variants: a challenge to microbiologists and clinicians. *Int. J. Antimicrob. Agents.* **2008**, *31*, 507-510.

- Kahl, B. C.; Becker, K.; Löffler, B., Clinical significance and pathogenesis of staphylococcal small colony variants in persistent infections. *Clin. Microbiol. Rev.* 2016, 29, 401-427.
- 101. Proctor, R. A.; van Langevelde, P.; Kristjansson, M.; Maslow, J. N.; Arbeit, R. D., Persistent and relapsing infections associated with small-colony variants of Staphylococcus aureus. *Clin. Infect. Dis.* **1995**, *20*, 95-102.
- 102. Sadowska, B.; Bonar, A.; von Eiff, C.; Proctor, R. A.; Chmiela, M.; Rudnicka, W.; Róźalska, B., Characteristics of Staphylococcus aureus, isolated from airways of cystic fibrosis patients, and their small colony variants. *FEMS Microbiol. Immunol.* 2002, 32, 191-197.
- 103. Kahl, B. C.; Duebbers, A.; Lubritz, G.; Haeberle, J.; Koch, H. G.; Ritzerfeld, B.; Reilly, M.; Harms, E.; Proctor, R. A.; Herrmann, M., Population dynamics of persistent Staphylococcus aureus isolated from the airways of cystic fibrosis patients during a 6-year prospective study. J. Clin. Microbiol. 2003, 41, 4424-4427.
- 104. Lattar, S. M.; Tuchscherr, L. P.; Caccuri, R. L.; Centrón, D.; Becker, K.; Alonso, C. A.; Barberis, C.; Miranda, G.; Buzzola, F. R.; von Eiff, C., Capsule expression and genotypic differences among Staphylococcus aureus isolates from patients with chronic or acute osteomyelitis. *Infect Immun.* 2009, 77, 1968-1975.
- 105. Holten, K. B.; Onusko, E. M., Appropriate prescribing of oral beta-lactam antibiotics. *Am. Fam. Physician.* **2000**, *62*, 611-620.
- 106. Elander, R., Industrial production of β-lactam antibiotics. *Appl. Microbiol. Biotechnol.* **2003**, *61*, 385-392.
- 107. Denyer, S. P.; Hodges, N. A.; Gorman, S. P., Hugo and Russell's pharmaceutical microbiology. John Wiley & Sons: **2008**.
- 108. Neu, H. C., β-Lactam antibiotics: structural relationships affecting in vitro activity and pharmacologic properties. *Rev. Infect. Dis.* **1986**, 8 (Supplement\_3), S237-S259.

- 109. Donowitz, G. R.; Mandell, G. L., Beta-lactam antibiotics. *N. Engl. J. Med.* **1988**, *318*, 419-426.
- 110. Ambler, R. P., The structure of β-lactamases. *Philos. Trans. R. Soc. Lond. B Biol. Sci.* **1980**, *289*, 321-331.
- 111. Massova, I.; Mobashery, S., Kinship and diversification of bacterial penicillinbinding proteins and β-lactamases. *Antimicrob Agents Chemother.* **1998**, *42*, 1-17.
- 112. Tooke, C. L.; Hinchliffe, P.; Bragginton, E. C.; Colenso, C. K.; Hirvonen, V. H.; Takebayashi, Y.; Spencer, J., β-Lactamases and β-Lactamase Inhibitors in the 21st Century. *J. Mol. Biol* **2019**, *431*, 3472-3500.
- 113. Lowy, F. D., Antimicrobial resistance: the example of Staphylococcus aureus. *J. Clin. Investig.* **2003**, *111*, 1265-1273.
- 114. Stapleton, P. D.; Taylor, P. W., Methicillin resistance in Staphylococcus aureus: mechanisms and modulation. *Sci. Prog.* **2002**, *85*, 57-72.
- 115. Michel, M.; Gutmann, L., Methicillin-resistant Staphylococus aureus and vancomycin-resistant enterococci: therapeutic realities and possibilities. *The Lancet.* **1997**, *349*, 1901-1906.
- 116. Jarrahpour, A.; Aye, M.; Sinou, V.; Latour, C.; Brunel, J. M., Synthesis of some new monocyclic β-lactams as antimalarial agents. *J. Iran. Chem. Soc.* **2015**, *12*, 2083-2092.
- 117. Tiemersma, E. W.; Bronzwaer, S. L.; Lyytikäinen, O.; Degener, J. E.; Schrijnemakers, P.; Bruinsma, N.; Monen, J.; Witte, W.; Grundmann, H.; Participants, E. A. R. S. S., Methicillin-resistant Staphylococcus aureus in Europe, 1999–2002. Emerg. Infect. Dis. 2004, 10, 1627.
- 118. Harkins, C. P.; Pichon, B.; Doumith, M.; Parkhill, J.; Westh, H.; Tomasz, A.; de Lencastre, H.; Bentley, S. D.; Kearns, A. M.; Holden, M. T., Methicillin-resistant Staphylococcus aureus emerged long before the introduction of methicillin into clinical practice. *Genome Biol.* **2017**, *18*, 130.
- 119. Jubeh, B.; Breijyeh, Z.; Karaman, R., Resistance of gram-positive bacteria to

- current antibacterial agents and overcoming approaches. *Molecules*. **2020**, *25*, 2888.
- 120. Krause, K. M.; Serio, A. W.; Kane, T. R.; Connolly, L. E., Aminoglycosides: an overview. *Cold Spring Harb. Perspect. Med.* **2016**, *6*, a027029.
- 121. Kroppenstedt, R. M.; Mayilraj, S.; Wink, J. M.; Kallow, W.; Schumann, P.; Secondini, C.; Stackebrandt, E., Eight new species of the genus Micromonospora, Micromonospora citrea sp. nov., Micromonospora echinaurantiaca sp. nov., Micromonospora echinofusca sp. nov. Micromonospora fulviviridis sp. nov., Micromonospora inyonensis sp. nov., Micromonospora peucetia sp. nov., Micromonospora sagamiensis sp. nov., and Micromonospora viridifaciens sp. nov. Syst. Appl. Microbiol. 2005, 28, 328-339.
- 122. Dewick, P.M. Medicinal Natural Products; Wiley: Chichester, UK. 2009, 550.
- 123. Jadhav, R. W.; Kobaisi, M. A.; Jones, L. A.; Vinu, A.; Bhosale, S. V., The Supramolecular Self-Assembly of Aminoglycoside Antibiotics and their Applications. *ChemistryOpen.* **2019**, *8*, 1154-1166.
- 124. Schatz, A.; Robinson, K., The true story of the discovery of streptomycin. *Actinomycetes.* **1993**, *4*, 27-39.
- 125. Mingeot-Leclercq, M.-P.; Glupczynski, Y.; Tulkens, P. M., Aminoglycosides: activity and resistance. *Antimicrob Agents Chemother.* **1999**, *43*, 727-737.
- 126. Li, M.; E. Duc, A.-C. c.; Klosi, E.; Pattabiraman, S.; Spaller, M. R.; Chow, C. S., Selection of peptides that target the aminoacyl-tRNA site of bacterial 16S ribosomal RNA. *Biochemistry.* 2009, 48, 8299-8311.
- 127. King, D. E.; Malone, R.; Lilley, S. H., New classification and update on the quinolone antibiotics. *Am. Fam. Physician.* **2000**, *61*, 2741-2748.
- 128. Pham, T. D.; Ziora, Z. M.; Blaskovich, M. A., Quinolone antibiotics. *MedChemComm.* **2019**, *10*, 1719-1739.
- 129. Emmerson, A.; Jones, A., The quinolones: decades of development and use. *J. Antimicrob. Chemother.* **2003**, *51*, 13-20.

- 130. Fedorowicz, J.; Sączewski, J., Modifications of quinolones and fluoroquinolones: hybrid compounds and dual-action molecules. *Monatsh. Chem.* **2018**, *149*, 1199-1245.
- 131. Aldred, K. J.; Kerns, R. J.; Osheroff, N., Mechanism of quinolone action and resistance. *Biochemistry.* **2014**, *53*, 1565-1574.
- 132. Kadhim, N. J.; Aziz, D. Z.; Hadi, M. A., HPLC Fractioning to Study the Synergy and Antagonism of Rue Plant Seeds Alkaloid to Inhibit Topoisomerase II as Antitumor. *Am. J. Biomed.* **2016**, *4*, 253-262.
- 133. Fournier, B.; Zhao, X.; Lu, T.; Drlica, K.; Hooper, D. C., Selective targeting of topoisomerase IV and DNA gyrase in Staphylococcus aureus: different patterns of quinolone-induced inhibition of DNA synthesis. *Antimicrob Agents Chemother*: **2000**, *44*, 2160-2165.
- 134. Dinos, G. P., The macrolide antibiotic renaissance. *Br. J. Pharmacol* **2017**, *174*, 2967-2983.
- 135. Mahajan, G. B.; Balachandran, L., Antibacterial agents from actinomycetes-a review. *Front Biosci (Elite Ed).* **2012**, *4*, 240-53.
- 136. Wanger, A.; Chavez, V.; Huang, R.; Wahed, A.; Actor, J.; Dasgupta, A. Antibiotics, Antimicrobial Resistance, Antibiotic Susceptibility Testing, and Therapeutic Drug Monitoring for Selected Drugs. Microbiol Mol Diagnosis Pathol. 2017, 119-153.
- 137. Garza-Ramos, G.; Xiong, L.; Zhong, P.; Mankin, A., Binding site of macrolide antibiotics on the ribosome: new resistance mutation identifies a specific interaction of ketolides with rRNA. *J. Bacteriol.* **2001**, *183*, 6898-6907.
- 138. Nakajima, Y., Mechanisms of bacterial resistance to macrolide antibiotics. *J. Infect. Chemother.* **1999**, *5*, 61-74.
- 139. Omura, S., Ed.; *Macrolide Antibiotics. Chemistry, Biology, and Practice*, 2nd ed.; Academic Press. **2002**.
- 140. Wang, F.; Zhou, H.; Olademehin, O. P.; Kim, S. J.; Tao, P., Insights into key interactions between vancomycin and bacterial cell wall structures. *ACS omega*.

- **2018**, *3*, 37-45.
- 141. Chang, S.; Sievert, D. M.; Hageman, J. C.; Boulton, M. L.; Tenover, F. C.; Downes, F. P.; Shah, S.; Rudrik, J. T.; Pupp, G. R.; Brown, W. J., Infection with vancomycin-resistant Staphylococcus aureus containing the vanA resistance gene. N. Engl. J. Med. 2003, 348, 1342-1347.
- 142. Menichetti, F., Current and emerging serious Gram-positive infections. *Clin. Microbiol. Infect.* **2005**, *11*, 22-28.
- 143. Zeng, D.; Debabov, D.; Hartsell, T. L.; Cano, R. J.; Adams, S.; Schuyler, J. A.; McMillan, R.; Pace, J. L., Approved glycopeptide antibacterial drugs: mechanism of action and resistance. *Cold Spring Harb. Perspect. Med.* **2016**, *6*, a026989.
- 144. Courvalin, P., Vancomycin resistance in gram-positive cocci. *Clin. Infect. Dis.* **2006**, *42* (Supplement\_1), S25-S34.
- 145. Sarkar, P.; Yarlagadda, V.; Ghosh, C.; Haldar, J., A review on cell wall synthesis inhibitors with an emphasis on glycopeptide antibiotics. *Medchemcomm.* **2017**, *8*, 516-533.
- 146. Lau, J. L.; Dunn, M. K., Therapeutic peptides: Historical perspectives, current development trends, and future directions. *Bioorg. Med. Chem.* **2018**, *26*, 2700-2707.
- 147. Mayer, J. P.; Zhang, F.; DiMarchi, R. D., Insulin structure and function. *Biopolymers*. **2007**, *88*, 687-713.
- 148. Bruno, B. J.; Miller, G. D.; Lim, C. S., Basics and recent advances in peptide and protein drug delivery. *Ther. Deliv.* **2013**, *4*, 1443-1467.
- 149. Lee, A. C.-L.; Harris, J. L.; Khanna, K. K.; Hong, J.-H., A comprehensive review on current advances in peptide drug development and design. *Int J Mol Sci.* **2019**, *20*, 2383.
- 150. Craik, D. J.; Fairlie, D. P.; Liras, S.; Price, D., The future of peptide-based drugs. *Chem. Biol. Drug Des.* **2013**, *81*, 136-147.

- 151. Muttenthaler, M.; King, G. F.; Adams, D. J.; Alewood, P. F., Trends in peptide drug discovery. *Nat. Rev. Drug Discov.* **2021,** *20*, 309-325.
- 152. Chelliah, R.; Daliri, E. B.-M.; Elahi, F.; Yeon, S.-J.; Tyagi, A.; Oh, D.-H., Current Advances in Therapeutic Peptides: Past and Future Trends. *Preprints.org.* **2021**.
- 153. Apostolopoulos, V.; Bojarska, J.; Chai, T.-T.; Elnagdy, S.; Kaczmarek, K.; Matsoukas, J.; New, R.; Parang, K.; Lopez, O. P.; Parhiz, H., A global review on short peptides: frontiers and perspectives. *Molecules*. **2021**, *26*, 430.
- 154. Baker, D. D.; Chu, M.; Oza, U.; Rajgarhia, V., The value of natural products to future pharmaceutical discovery. *Nat. Prod. Rep.* **2007**, *24*, 1225-1244.
- 155. Henninot, A.; Collins, J. C.; Nuss, J. M., The current state of peptide drug discovery: back to the future? *J. Med. Chem.* **2018**, *61*, 1382-1414.
- 156. De la Torre, B. G.; Albericio, F., Peptide Therapeutics 2.0. *Molecules*. **2020**, *25*, 2293.
- D'Hondt, M.; Bracke, N.; Taevernier, L.; Gevaert, B.; Verbeke, F.; Wynendaele,
  E.; De Spiegeleer, B., Related impurities in peptide medicines. *J. Pharm. Biomed.*2014, 101, 2-30.
- 158. Mahlapuu, M.; Håkansson, J.; Ringstad, L.; Björn, C., Antimicrobial peptides: an emerging category of therapeutic agents. *Front. Cell. Infect. Microbiol.* **2016**, *6*, 194.
- 159. Lai, Y.; Gallo, R. L., AMPed up immunity: how antimicrobial peptides have multiple roles in immune defense. *Trends Immunol.* **2009**, *30*, 131-141.
- 160. Fjell, C. D.; Hiss, J. A.; Hancock, R. E.; Schneider, G., Designing antimicrobial peptides: form follows function. *Nat. Rev. Drug Discov.* **2012**, *11*, 37-51.
- 161. Mahlapuu, M.; Björn, C.; Ekblom, J., Antimicrobial peptides as therapeutic agents: Opportunities and challenges. *Crit. Rev. Biotechnol.* **2020**, *40*, 978-992.
- 162. Molchanova, N.; Hansen, P. R.; Franzyk, H., Advances in development of antimicrobial peptidomimetics as potential drugs. *Molecules.* **2017**, *22*, 1430.

- 163. Fox, J. L., Antimicrobial peptides stage a comeback: Better understanding of the mechanisms of action, modification and synthesis of antimicrobial peptides is reigniting commercial development. *Nat. Biotechnol.* **2013**, *31*, 379-383.
- 164. Huan, Y.; Kong, Q.; Mou, H.; Yi, H., Antimicrobial peptides: classification, design, application and research progress in multiple fields. *Front Microbiol.* **2020**, 2559.
- 165. Moretta, A.; Scieuzo, C.; Petrone, A. M.; Salvia, R.; Manniello, M. D.; Franco, A.; Lucchetti, D.; Vassallo, A.; Vogel, H.; Sgambato, A., Antimicrobial peptides: A new hope in biomedical and pharmaceutical fields. *Front. Cell. Infect. Microbiol.* 2021, 11, 453.
- 166. Hancock, R. E.; Chapple, D. S., Peptide antibiotics. *Antimicrob Agents Chemother* **1999,** *43*, 1317-1323.
- 167. McIntosh, J. A.; Donia, M. S.; Schmidt, E. W., Ribosomal peptide natural products: bridging the ribosomal and nonribosomal worlds. *Nat. Prod. Rep.* **2009**, *26*, 537-559.
- 168. Martínez-Núñez, M. A., Nonribosomal peptides synthetases and their applications in industry. *Sustain. Chem. Process.* **2016**, *4*, 1-8.
- 169. Papagianni, M., Ribosomally synthesized peptides with antimicrobial properties: biosynthesis, structure, function, and applications. *Biotechnol. Adv.* **2003**, *21*, 465-499.
- 170. Boman, H. G., Peptide antibiotics and their role in innate immunity. *Annu. Rev. Immunol.* **1995**, *13*, 61-92.
- 171. Cammue, B. P.; De Bolle, M. F.; Schoofs, H. M.; Terras, F. R.; Thevissen, K.; Osborn, R.; Rees, S.; Broekaert, W., Gene-encoded antimicrobial peptides from plants. *Antimicrobial peptides*. **1994**, *186*, 91-101.
- 172. Singh, N.; Abraham, J., Ribosomally synthesized peptides from natural sources. *J. Antibiot.* **2014**, *67*, 277-289.
- 173. Hancock, R. E.; Sahl, H.-G., Antimicrobial and host-defense peptides as new anti-

- infective therapeutic strategies. Nat. Biotechnol. 2006, 24, 1551-1557.
- 174. Zasloff, M., Antimicrobial peptides of multicellular organisms. *Nature* **2002**, *415*, 389-395.
- 175. Nissen-Meyer, J.; Nes, I. F., Ribosomally synthesized antimicrobial peptides: their function, structure, biogenesis, and mechanism of action. *Arch. Microbiol.* **1997**, *167*, 67-77.
- 176. Li, Y.; Xiang, Q.; Zhang, Q.; Huang, Y.; Su, Z., Overview on the recent study of antimicrobial peptides: origins, functions, relative mechanisms and application. *Peptides* **2012**, *37*, 207-215.
- 177. Rinaldi, A. C., Antimicrobial peptides from amphibian skin: an expanding scenario: Commentary. *Curr. Opin. Chem. Biol.* **2002**, *6*, 799-804.
- 178. Hoffmann, J. A.; Kafatos, F. C.; Janeway Jr, C. A.; Ezekowitz, R., Phylogenetic perspectives in innate immunity. *Science* **1999**, *284*, 1313-1318.
- 179. Boman, H., Peptide antibiotics: holy or heretic grails of innate immunity? *Scand. J. Immunol.* **1996**, *43*, 475-482.
- 180. Ageitos, J.; Sánchez-Pérez, A.; Calo-Mata, P.; Villa, T., Antimicrobial peptides (AMPs): Ancient compounds that represent novel weapons in the fight against bacteria. *Biochem. Pharmacol.* **2017**, *133*, 117-138.
- 181. Simons, A.; Alhanout, K.; Duval, R. E., Bacteriocins, antimicrobial peptides from bacterial origin: overview of their biology and their impact against multidrugresistant bacteria. *Microorganisms*. **2020**, *8*, 639.
- 182. Marr, A. K.; Gooderham, W. J.; Hancock, R. E., Antibacterial peptides for therapeutic use: obstacles and realistic outlook. *Curr. Opin. Pharmacol.* **2006**, *6*, 468-472.
- 183. Lien, S.; Lowman, H. B., Therapeutic peptides. *Trends Biotechnol.* **2003**, *21*, 556-562.
- 184. Matsunaga, S.; Fusetani, N., Nonribosomal peptides from marine sponges.

- Curr. Org. Chem. 2003, 7, 945-966.
- 185. Nikolouli, K.; Mossialos, D., Bioactive compounds synthesized by non-ribosomal peptide synthesizes and type-I polyketide synthases discovered through genomemining and metagenomics. *Biotechnology Lett.* **2012**, *34*, 1393-1403.
- 186. Martínez-Núñez, M. A.; López, V. E. L. y., Nonribosomal peptides synthetases and their applications in industry. *Sustain. Chem. Process.* **2016**, *4*, 1-8.
- 187. Finking, R.; Marahiel, M. A., Biosynthesis of nonribosomal peptides. *Annu. Rev. Microbiol.* **2004**, *58*, 453-488.
- 188. Felnagle, E. A.; Jackson, E. E.; Chan, Y. A.; Podevels, A. M.; Berti, A. D.; McMahon, M. D.; Thomas, M. G., Nonribosomal peptide synthetases involved in the production of medically relevant natural products. *Mol. Pharmaceutics.* 2008, 5, 191-211.
- 189. Sieber, S. A.; Marahiel, M. A., Learning from Nature's Drug Factories: Nonribosomal Synthesisof MacrocyclicPeptides. *J. Bacteriol.* 2003, 185, 7036-7043.
- 190. Grünewald, J.; Marahiel, M. A., Chemoenzymatic and template-directed synthesis of bioactive macrocyclic peptides. *Microbiol. Mol. Biol. Rev.* **2006**, *70*, 121-146.
- 191. Mach, B.; Reich, E.; Tatum, E., Separation of the biosynthesis of the antibiotic polypeptide tyrocidine from protein biosynthesis. *Proc. Natl. Acad. Sci. U. S. A.* **1963**, *50*, 175.
- 192. Mankelow, D. P.; Neilan, B. A., Non-ribosomal peptide antibiotics. *Expert. Opin. Ther. Pat.* **2000**, *10*, 1583-1591.
- Condurso, H. L.; Bruner, S. D., Structure and noncanonical chemistry of nonribosomal peptide biosynthetic machinery. *Nat. Prod. Rep.* 2012, 29, 1099-1110.
- 194. Agrawal, S.; Acharya, D.; Adholeya, A.; Barrow, C. J.; Deshmukh, S. K., Nonribosomal peptides from marine microbes and their antimicrobial and anticancer potential. *Front. Pharmacol.* **2017**, *8*, 828.

- 195. Liu, Y.; Ding, S.; Shen, J.; Zhu, K., Nonribosomal antibacterial peptides that target multidrug-resistant bacteria. *Nat. Prod. Rep.* **2019**, *36*, 573-592.
- 196. Stennicke, H.; Salvesen, G., Catalytic properties of the caspases. *Cell Death Differ.* **1999**, *6*, 1054-1059.
- 197. Lucana, M. C.; Arruga, Y.; Petrachi, E.; Roig, A.; Lucchi, R.; Oller-Salvia, B., Protease-resistant peptides for targeting and intracellular delivery of therapeutics. *Pharmaceutics* **2021**, *13*, 2065.
- 198. Di, L., Strategic approaches to optimizing peptide ADME properties. *The AAPS Journal* **2015**, *17*, 134-143.
- 199. Lenci, E.; Trabocchi, A., Peptidomimetic toolbox for drug discovery. *Chem. Soc. Rev.* **2020**, *49*, 3262-3277.
- 200. Avan, I.; Hall, C. D.; Katritzky, A. R., Peptidomimetics via modifications of amino acids and peptide bonds. *Chem. Soc. Rev.* **2014**, *43*, 3575-3594.
- 201. McGrath, D. M.; Barbu, E. M.; Driessen, W. H.; Lasco, T. M.; Tarrand, J. J.; Okhuysen, P. C.; Kontoyiannis, D. P.; Sidman, R. L.; Pasqualini, R.; Arap, W., Mechanism of action and initial evaluation of a membrane active all-D-enantiomer antimicrobial peptidomimetic. *Proc. Natl. Acad. Sci.* 2013, *110*, 3477-3482.
- 202. Wei, X.; Zhan, C.; Shen, Q.; Fu, W.; Xie, C.; Gao, J.; Peng, C.; Zheng, P.; Lu, W., A d-Peptide Ligand of Nicotine Acetylcholine Receptors for Brain-Targeted Drug Delivery. *Angew. Chem.* 2015, 127, 3066-3070.
- 203. Chow, H. Y.; Zhang, Y.; Matheson, E.; Li, X., Ligation technologies for the synthesis of cyclic peptides. *Chem. Rev.* **2019**, *119*, 9971-10001.
- 204. Dougherty, P. G.; Sahni, A.; Pei, D., Understanding cell penetration of cyclic peptides. *Chem. Rev.* **2019**, *119*, 10241-10287.
- 205. Malde, A. K.; Hill, T. A.; Iyer, A.; Fairlie, D. P., Crystal structures of protein-bound cyclic peptides. *Chem. Rev.* **2019**, *119*, 9861-9914.
- 206. Joo, S.-H., Cyclic peptides as therapeutic agents and biochemical tools.

- Biomol. Therap. 2012, 20, 19-26.
- 207. Khatri, B.; Nuthakki, V. R.; Chatterjee, J., Strategies to enhance metabolic stabilities. *Methods Mol. Biol.* **2019**, *2001*, 17-40.
- 208. Bird, G. H.; Christian Crannell, W.; Walensky, L. D., Chemical Synthesis of Hydrocarbon-Stapled Peptides for Protein Interaction Research and Therapeutic Targeting. *Curr. protoc. chem. Biol.* **2011**, *3*, 99-117.
- 209. Qian, Z.; Rhodes, C. A.; McCroskey, L. C.; Wen, J.; Appiah-Kubi, G.; Wang, D. J.; Guttridge, D. C.; Pei, D., Enhancing the cell permeability and metabolic stability of peptidyl drugs by reversible bicyclization. *Angew. Chem. Int. Ed. Engl.* 2017, 56, 1525-1529.
- 210. Velkov, T.; Dai, C.; Ciccotosto, G. D.; Cappai, R.; Hoyer, D.; Li, J., Polymyxins for CNS infections: pharmacology and neurotoxicity. *Pharmacol. Ther.* **2018**, *181*, 85-90.
- 211. Moon, S. H.; Zhang, X.; Zheng, G.; Meeker, D. G.; Smeltzer, M. S.; Huang, E., Novel linear lipopeptide paenipeptins with potential for eradicating biofilms and sensitizing Gram-negative bacteria to rifampicin and clarithromycin.

  J. Med. Chem. 2017, 60, 9630-9640.
- 212. Fleming, A., On the antibacterial action of cultures of a penicillium, with special reference to their use in the isolation of B. influenzae. *Br. J. Exp. Pathol.* **1929**, *10*, 226-236
- 213. Schilling, N. A.; Berscheid, A.; Schumacher, J.; Saur, J. S.; Konnerth, M. C.; Wirtz, S. N.; Beltrán-Beleña, J. M.; Zipperer, A.; Krismer, B.; Peschel, A., Synthetic lugdunin analogues reveal essential structural motifs for antimicrobial action and proton translocation capability. *Angew. Angew. Chem. Int. Ed.* 2019, 58, 9234-9238.
- 214. Stansly, P.; Shepherd, R.; White, H., Polymyxin: a new chemotherapeutic agent. *Bull. Johns Hopkins Hosp.* **1947**, *81*, 43-54.
- 215. McCormick, M. H., Vancomycin, a new antibiotic. I. Chemical and biologic

- properties. Antibiot Annu. 1956, 3, 606-611.
- 216. Ehlert, F.; Neu, H., In vitro activity of LY146032 (daptomycin), a new peptolide. *Eur. J. Clin. Microbiol.* **1987**, *6*, 84-90.
- 217. Müller, A.; Wenzel, M.; Strahl, H.; Grein, F.; Saaki, T. N.; Kohl, B.; Siersma, T.; Bandow, J. E.; Sahl, H.-G.; Schneider, T., Daptomycin inhibits cell envelope synthesis by interfering with fluid membrane microdomains. *Proc. Natl. Acad. Sci.* 2016, 113, 7077-7086.
- 218. Barsby, T.; Kelly, M. T.; Gagné, S. M.; Andersen, R. J., Bogorol A produced in culture by a marine Bacillus sp. reveals a novel template for cationic peptide antibiotics. *Organic Lett.* **2001**, *3*, 437-440.
- Barsby, T.; Warabi, K.; Sørensen, D.; Zimmerman, W. T.; Kelly, M. T.; Andersen, R. J., The bogorol family of antibiotics: template-based structure elucidation and a new approach to positioning enantiomeric pairs of amino acids. *J. Org. Chem.*2006, 71, 6031-6037.
- 220. Xie, Y.; Chen, R.; Si, S.; Sun, C.; Xu, H., A new nucleosidyl-peptide antibiotic, sansanmycin. *J. Antibiot.* **2007**, *60*, 158-161.
- 221. Vallet-Gely, I.; Novikov, A.; Augusto, L.; Liehl, P.; Bolbach, G.; Péchy-Tarr, M.; Cosson, P.; Keel, C.; Caroff, M.; Lemaitre, B., Association of hemolytic activity of Pseudomonas entomophila, a versatile soil bacterium, with cyclic lipopeptide production. *Appl. Environ. Microbiol.* 2010, 76, 910-921.
- 222. Janek, T.; Łukaszewicz, M.; Rezanka, T.; Krasowska, A., Isolation and characterization of two new lipopeptide biosurfactants produced by Pseudomonas fluorescens BD5 isolated from water from the Arctic Archipelago of Svalbard. *Bioresour. Technol.* 2010, 101, 6118-6123.
- 223. Garcia-Gonzalez, E.; Müller, S.; Ensle, P.; Süssmuth, R. D.; Genersch, E., Elucidation of sevadicin, a novel non-ribosomal peptide secondary metabolite produced by the honey bee pathogenic bacterium P aenibacillus larvae. *Environ. Microbiol.* 2014, 16, 1297-1309.

- 224. Ling, L. L.; Schneider, T.; Peoples, A. J.; Spoering, A. L.; Engels, I.; Conlon, B. P.; Mueller, A.; Schäberle, T. F.; Hughes, D. E.; Epstein, S., A new antibiotic kills pathogens without detectable resistance. *Nature* **2015**, *517*, 455-459.
- 225. Johnston, C. W.; Skinnider, M. A.; Dejong, C. A.; Rees, P. N.; Chen, G. M.; Walker, C. G.; French, S.; Brown, E. D.; Berdy, J.; Liu, D. Y., Assembly and clustering of natural antibiotics guides target identification. *Nat. Chem. Biol.* 2016, 12, 233-239.
- 226. Huang, E.; Yang, X.; Zhang, L.; Moon, S. H.; Yousef, A. E., New Paenibacillus strain produces a family of linear and cyclic antimicrobial lipopeptides: cyclization is not essential for their antimicrobial activity. *FEMS Microbiology Lett.* **2017**, *364*, fnx049.
- 227. Liu, Y.; Ding, S.; Dietrich, R.; Märtlbauer, E.; Zhu, K., A biosurfactant-inspired heptapeptide with improved specificity to kill MRSA. *Angew. Chem.* **2017**, *129*, 1508-1512.
- 228. Pantel, L.; Florin, T.; Dobosz-Bartoszek, M.; Racine, E.; Sarciaux, M.; Serri, M.; Houard, J.; Campagne, J.-M.; de Figueiredo, R. M.; Midrier, C., Odilorhabdins, antibacterial agents that cause miscoding by binding at a new ribosomal site. *Mol. Cell.* 2018, 70, 83-94.
- 229. Lewis, K.; Strandwitz, P., Microbiology: Antibiotics right under our nose. *Nature* **2016**, *535* (7613), 501-502.
- 230. Frank, K. L.; Del Pozo, J. L.; Patel, R., From clinical microbiology to infection pathogenesis: how daring to be different works for Staphylococcus lugdunensis. *Clin. Microbiol. Rev.* **2008**, *21*, 111-133.
- 231. Babu, E.; Oropello, J., Staphylococcus lugdunensis: the coagulase-negative staphylococcus you don't want to ignore. *Expert. Rev. Anti. Infect. Ther.* **2011**, *9*, 901-907.
- 232. Davis, C. P., "Normal flora in medical microbiology," in *Normal Flora in Medical Microbiology*, S. Baron, Ed., University of Texas Medical Branch, Galveston, Tex, USA, 1996.

- 233. Ohara-Nemoto, Y.; Haraga, H.; Kimura, S.; Nemoto, T., Occurrence of staphylococci in the oral cavities of healthy adults and nasal—oral trafficking of the bacteria. *J. Med. Microbiol.* **2008**, *57*, 95-99.
- 234. Taha, L.; Stegger, M.; Söderquist, B., Staphylococcus lugdunensis: antimicrobial susceptibility and optimal treatment options. *Eur. J. Clin. Microbiol.* **2019**, *38*, 1449-1455.
- 235. Saur, J. S.; Wirtz, S. N.; Schilling, N. A.; Krismer, B.; Peschel, A.; Grond, S., Distinct Lugdunins from a New Efficient Synthesis and Broad Exploitation of Its MRSA-Antimicrobial Structure. *J. Med. Chem.* 2021, 64, 4034-4058.
- 236. Malins, L. R.; deGruyter, J. N.; Robbins, K. J.; Scola, P. M.; Eastgate, M. D.; Ghadiri, M. R.; Baran, P. S., Peptide macrocyclization inspired by non-ribosomal imine natural products. *J. Am. Chem. Soc.* 2017, *139*, 5233-5241.
- 237. Ivkovic, J.; Lembacher-Fadum, C.; Breinbauer, R., A rapid and efficient one-pot method for the reduction of N-protected α-amino acids to chiral α-amino aldehydes using CDI/DIBAL-H. *Org. Biomol. Chem.* **2015**, *13*, 10456-10460.
- 238. Freidinger, R. M.; Hinkle, J. S.; Perlow, D. S., Synthesis of 9-fluorenylmethyloxycarbonyl-protected N-alkyl amino acids by reduction of oxazolidinones. *J. Org. Chem.* **1983**, *48*, 77-81.
- 239. Fischer, E.; Fourneau, E., Ueber einige derivate des glykocolls. In Untersuchungen über Aminosäuren, Polypeptide und Proteïne (1899–1906), Springer. **1906**, 279-289.
- 240. Chan, W. C.; White, P. D., Fmoc Solid Phase Peptide Synthesis: A Practical Approach. OUP Oxford, UK. **2000**; ISBN 978-0-19-963724-9.
- 241. Bergmann, M.; Zervas, L., Über ein allgemeines Verfahren der Peptid-synthese. *Ber. Dtsch. Chem. Ges.* **1932**, *65*, 1192-1201.
- 242. Vigneaud, V. d.; Ressler, C.; Swan, C. J. M.; Roberts, C. W.; Katsoyannis, P. G.; Gordon, S., The synthesis of an octapeptide amide with the hormonal activity of oxytocin. *J. Am. Chem. Soc.* 1953, 75, 4879-4880.

- 243. Amblard, M.; Fehrentz, J.-A.; Martinez, J.; Subra, G., Methods and protocols of modern solid phase peptide synthesis. *Mol. Biotechnol.* **2006**, *33*, 239-254.
- 244. Merrifield, R. B., Solid phase peptide synthesis. I. The synthesis of a tetrapeptide. J. Am. Chem. Soc. 1963, 85, 2149-2154.
- 245. Korzeniowski, O.; Sande, M. A., Combination antimicrobial therapy for Staphylococcus aureus endocarditis in patients addicted to parenteral drugs and in nonaddicts: a prospective study. *Ann. Intern. Med.* **1982**, *97*, 496-503.
- 246. Isidro-Llobet, A.; Alvarez, M.; Albericio, F., Amino acid-protecting groups. *Chem. Rev.* **2009**, *109*, 2455-2504.
- 247. Sakakibara, S.; Shimonishi, Y.; Kishida, Y.; Okada, M.; Sugihara, H., Use of anhydrous hydrogen fluoride in peptide synthesis. I. Behavior of various protective groups in anhydrous hydrogen fluoride. *Bull. Chem. Soc. Jpn.* **1967**, *40*, 2164-2167.
- 248. Carpino, L. A.; Han, G. Y., 9-Fluorenylmethoxycarbonyl amino-protecting group. *J. Org. Chem.* **1972**, *37*, 3404-3409.
- 249. Masui, Y.; Chino, N.; Sakakibara, S., The Modification of Tryptophyl Residues during the Acidolytic Cleavage of Boc-groups. I. Studies with Boc-Tryptophan. *Bull. Chem. Soc. Jpn.* **1980**, *53*, 464-468.
- 250. Wünsch, E.; Jaeger, E.; Kisfaludy, L.; Löw, M., Side Reactions in Peptide Synthesis: tert-Butylation of Tryptophan. *Angew. Chem. Int. Ed. Engl.* **1977**, *16*, 317-318.
- 251. Stawikowski, M.; Fields, G. B., Introduction to peptide synthesis. *Curr. Protoc. Protein Sci.* **2012**, *69*, 18.1.1-18.1.13.
- 252. Fields, G. B., Methods for removing the Fmoc group. *Methods Mol. Biol.* **1994**, 35, 17-27.
- 253. Palladino, P.; Stetsenko, D. A., New TFA-free cleavage and final deprotection in Fmoc solid-phase peptide synthesis: Dilute HCl in fluoro alcohol. *Org. Lett.* **2012**, *14*, 6346-6349.

- 254. Gross, E.; Meienhofer, J., The Peptides Analysis, Synthesis, Biology, Academic Press, New York. **2012**.
- 255. Stewart, J. M., [3] Cleavage methods following Boc-based solid-phase peptide synthesis. *Meth. Enzymol.* **1997**, *289*, 29-44.
- 256. King, D. S.; FIELDS, C. G.; FIELDS, G. B., A cleavage method which minimizes side reactions following Fmoc solid phase peptide synthesis. *Int. J. Pept. Protein Res.* **1990**, *36*, 255-266.
- 257. Fields, C. G.; Fields, G. B.; Noble, R. L.; Cross, T., Solid phase peptide synthesis of 15N-gramicidins A, B, and C and high performance liquid chromatographic purification. *Int. J. Pept. Protein Res.* **1989**, *33*, 298-303.
- 258. Podorieszach, A. P.; Huttunen-Hennelly, H. E., The effects of tryptophan and hydrophobicity on the structure and bioactivity of novel indolicidin derivatives with promising pharmaceutical potential. *Org. Biomol. Chem.* **2010**, *8*, 1679-1687.
- 259. Abel, R. J. V.; Tang, Y. Q.; Rao, V.; Dobbs, C. H.; Tran, D.; Barany, G.; Selsted, M. E., Synthesis and characterization of indolicidin, a tryptophan-rich antimicrobial peptide from bovine neutrophils. *Int. J. Pept. Protein Res.* 1995, 45, 401-409.
- 260. Hermkens, P. H.; Ottenheijm, H. C.; Rees, D. C., Solid-phase organic reactions II: A review of the literature Nov 95–Nov 96. *Tetrahedron* **1997**, *53*, 5643-5678.
- 261. Fischer, P. M., Diketopiperazines in peptide and combinatorial chemistry. *J. Pept. Sci.* **2003**, *9*, 9-35.
- 262. White, C. J.; Yudin, A. K., Contemporary strategies for peptide macrocyclization. *Nat. Chem.* **2011**, *3*, 509-524.
- 263. Davies, J. S., The cyclization of peptides and depsipeptides. *J. Pept. Sci.* **2003**, *9*, 471-501.
- 264. Wen, S.; Packham, G.; Ganesan, A., Macrolactamization versus macrolactonization: total synthesis of FK228, the depsipeptide histone deacetylase inhibitor. *J. Org. Chem.* **2008**, *73*, 9353-9361.

- 265. Marti-Centelles, V.; Pandey, M. D.; Burguete, M. I.; Luis, S. V., Macrocyclization reactions: the importance of conformational, configurational, and template-induced preorganization. *Chem. Rev.* **2015**, *115*, 8736-8834.
- 266. Carbain, B.; Schütznerová, E.; Přibylka, A.; Krchňák, V., Solid-Phase Synthesis of 3, 4-Dihydroquinoxalin-2 (1H)-ones via the Cyclative Cleavage of N-Arylated Carboxamides. Adv. Synth. Catal. 2016, 358, 701-706.
- 267. Schmidt, U.; Langner, J., Cyclotetrapeptides and cyclopentapeptides: occurrence and synthesis. *J. Pept. Res.* **1997**, *49*, 67-73.
- 268. Hoffmann, R. W., Flexible molecules with defined shape-conformational design. *Angew. Chem. Int. Ed. Engl.* **1992**, *31*, 1124-1134.
- 269. Al-Warhi, T. I.; Al-Hazimi, H. M.; El-Faham, A., Recent development in peptide coupling reagents. *J. Saudi Chem. Soc.* **2012**, *16*, 97-116.
- 270. Valeur, E.; Bradley, M., Amide bond formation: beyond the myth of coupling reagents. *Chem. Soc. Rev.* **2009**, *38*, 606-631.
- 271. Benz, G., *Synthesis of amides and related compounds*. Comprehensive Organic Synthesis. *Compr. Org. Synth.* **1991**, 381-417.
- 272. Sharma, A.; Kumar, A.; de la Torre, B. G.; Albericio, F., Liquid-Phase Peptide Synthesis (LPPS): A Third Wave for the Preparation of Peptides *Chem. Rev.* **2022**, *122*, 13516-13546.
- 273. Montalbetti, C. A.; Falque, V., Amide bond formation and peptide coupling. *Tetrahedron* **2005**, *61*, 10827-10852.
- 274. Sehgal, D.; Vijay, I. K., A method for the high efficiency of water-soluble carbodiimide-mediated amidation. *Anal. Biochem.* **1994**, *218*, 87-91.
- 275. Sheehan, J. C.; Hess, G. P., A new method of forming peptide bonds. *J. Am. Chem. Soc.* **1955**, 77, 1067-1068.
- 276. Anderson, G. W.; Callahan, F. M., Racemization by the dicyclohexylcarbodiimide method of peptide synthesis. *J. Am. Chem. Soc.* **1958**, *80*, 2902-2903.

- 277. Williams, A.; Ibrahim, I. T., Carbodiimide chemistry: recent advances. *Chem. Rev.* **1981**, *81*, 589-636.
- 278. Carpino, L. A.; El-Faham, A., The diisopropylcarbodiimide/1-hydroxy-7-azabenzotriazole system: segment coupling and stepwise peptide assembly. *Tetrahedron* **1999**, *55*, 6813-6830.
- 279. Pu, Y. J.; Vaid, R. K.; Boini, S. K.; Towsley, R. W.; Doecke, C. W.; Mitchell, D., A Practical Method for Functionalized Peptide or Amide Bond Formation in Aqueous— Ethanol Media with EDC as Activator. *Org. Process Res. Dev.* 2009, 13, 310-314.
- 280. Hojo, K.; Ichikawa, H.; Fukumori, Y.; Kawasaki, K., Development of a method for the solid-phase peptide synthesis in water. *Int. J. Pept. Res. Ther.* **2008**, *14*, 373-380.
- 281. Subirós-Funosas, R.; Khattab, S. N.; Nieto-Rodriguez, L.; El-Faham, A.; Albericio, F., Advances in acylation methodologies enabled by oxyma-based reagents. *Aldrichimica Acta.* **2013**, *46*, 21-41.
- 282. Carpino, L. A.; Imazumi, H.; El-Faham, A.; Ferrer, F. J.; Zhang, C.; Lee, Y.; Foxman, B. M.; Henklein, P.; Hanay, C.; Mügge, C., The uronium/guanidinium peptide coupling reagents: finally the true uronium salts. *Angew. Chem. Int. Ed.* **2002**, *41*, 441-445.
- 283. Sewald, N.; Jakubke, H.-D., *Peptides: chemistry and biology*. John Wiley & Sons: **2015**.
- 284. El-Faham, A.; Funosas, R. S.; Prohens, R.; Albericio, F., COMU: a safer and more effective replacement for benzotriazole-based uronium coupling reagents. *Chem. Eur. J.* **2009**, *15*, 9404-9416.
- 285. Carpino, L. A., 1-Hydroxy-7-azabenzotriazole. An efficient peptide coupling additive. *J. Am. Chem. Soc.* **1993**, *115*, 4397-4398.
- 286. Albericio, F.; Bofill, J. M.; El-Faham, A.; Kates, S. A., Use of onium salt-based coupling reagents in peptide Synthesis1. *J. Org. Chem.* **1998**, *63*, 9678-9683.

- 287. Abdelmoty, I.; Albericio, F.; Carpino, L. A.; Foxman, B. M.; Kates, S. A., Structural studies of reagents for peptide bond formation: Crystal and molecular structures of HBTU and HATU. *J. Pept. Sci.* **1994**, *1*, 57-67.
- 288. Poulain, R. F.; Tartar, A. L.; Déprez, B. t. P., Parallel synthesis of 1, 2, 4-oxadiazoles from carboxylic acids using an improved, uronium-based, activation. *Tetrahedron Lett.* **2001**, *42*, 1495-1498.
- 289. Subiros-Funosas, R.; Acosta, G. A.; El-Faham, A.; Albericio, F., Microwave irradiation and COMU: a potent combination for solid-phase peptide synthesis. *Tetrahedron Lett.* **2009**, *50*, 6200-6202.
- 290. Twibanire, J.-d. A. K.; Grindley, T. B., Efficient and controllably selective preparation of esters using uronium-based coupling agents. *Organic Lett.* **2011**, *13*, 2988-2991.
- 291. Høeg-Jensen, T.; Jakobsen, M. H.; Olsen, C. E.; Holm, A., Formation of peptide thioamides by use of Fmoc amino monothioacids and PyBOP. *Tetrahedron Lett.* **1991**, *32*, 7617-7620.
- 292. Albericio, F.; Cases, M.; Alsina, J.; Triolo, S. A.; Carpino, L. A.; Kates, S. A., On the use of PyAOP, a phosphonium salt derived from HOAt, in solid-phase peptide synthesis. *Tetrahedron Lett.* **1997**, *38*, 4853-4856.
- 293. Subirós-Funosas, R.; El-Faham, A.; Albericio, F., PyOxP and PyOxB: the Oxymabased novel family of phosphonium salts. *Org. Biomol. Chem.* **2010**, *8*, 3665-3673.
- 294. Chantell, C. A.; Onaiyekan, M. A.; Menakuru, M., Fast conventional Fmoc solid-phase peptide synthesis: a comparative study of different activators. *J. Pept. Sci.* 2012, 18, 88-91.
- 295. Arujõe, M.; Ploom, A.; Mastitski, A.; Järv, J., Comparison of various coupling reagents in solid-phase aza-peptide synthesis. *Tetrahedron Lett.* **2017**, *58*, 3421-3425.
- 296. Coste, J.; Frérot, E.; Jouin, P.; Castro, B., Oxybenzotriazole free peptide coupling

- reagents for N-methylated amino acids. Tetrahedron Lett. 1991, 32, 1967-1970.
- 297. Coste, J.; Dufour, M.-N.; Pantaloni, A.; Castro, B., Brop: A new reagent for coupling N-methylated amino acids. *Tetrahedron Lett.* **1990**, *31*, 669-672.
- 298. Tohma, H.; Kita, Y., Hypervalent iodine reagents for the oxidation of alcohols and their application to complex molecule synthesis. *Adv. Synth. Catal.* **2004**, *346*, 111-124.
- 299. Nahm, S.; Weinreb, S. M., N-Methoxy-N-methylamides as effective acylating agents. *Tetrahedron Lett.* **1981**, *22*, 3815-3818.
- 300. Cui, Y.; Kang, L.; Lan, S.; Rodrigues, S.; Cai, W., Giant chiral optical response from a twisted-arc metamaterial. *Nano Lett.* **2014**, *14*, 1021-1025.
- 301. Polavarapu, P. L., Optical rotation: recent advances in determining the absolute configuration. *Chirality* **2002**, *14*, 768-781.
- 302. Mukhopadhyay, P.; Zuber, G.; Goldsmith, M. R.; Wipf, P.; Beratan, D. N., Solvent effect on optical rotation: a case study of methyloxirane in water. *Chem. Phys. Chem.* **2006**, *7*, 2483-2486.
- 303. Wu, Y.; Xu, J.-C., Synthesis of chiral peptide nucleic acids using Fmoc chemistry. *Tetrahedron* **2001**, *57*, 8107-8113.
- 304. Douat, C.; Heitz, A.; Martinez, J.; Fehrentz, J.-A., Synthesis of N-protected α-amino aldehydes from their morpholine amide derivatives. *Tetrahedron Lett.* **2000**, *41*, 37-40.
- 305. Schmidt, B.; Hauke, S.; Muehlenberg, N., Imino glycals via ruthenium-catalyzed RCM and isomerization. *Synthesis* **2014**, *46*, 1648-1658.
- 306. Moore, C. L.; Leatherwood, D. D.; Diehl, T. S.; Selkoe, D. J.; Wolfe, M. S., Difluoro ketone peptidomimetics suggest a large S1 pocket for Alzheimer's γ-secretase: implications for inhibitor design. *J. Med. Chem.* **2000**, *43*, 3434-3442.
- 307. Porcheddu, A.; Taddei, M.; Falorni, M.; Giacomelli, G., A simple method for the reduction of carboxylic acids to aldehydes or alcohols using H 2 and Pd/C. *J. Org.*

- Chem. 1999, 64, 8962-8964.
- 308. Fehrentz, J.-A.; Paris, M.; Heitz, A.; Velek, J.; Winternitz, F.; Martinez, J., Solid phase synthesis of C-terminal peptide aldehydes. *J. Org. Chem.* **1997**, *62*, 6792-6796.
- 309. Conroy, T.; Guo, J. T.; Linington, R. G.; Hunt, N. H.; Payne, R. J., Total synthesis, stereochemical assignment, and antimalarial activity of gallinamide A. *Chem. Eur. J.* **2011**, *17*, 13544-13552.
- 310. Wen, J. J.; Crews, C. M., Synthesis of 9-fluorenylmethoxycarbonyl-protected amino aldehydes. *Tetrahedron: Asymmetry* **1998**, *9*, 1855-1858.
- 311. Zlatoidsky, P., Preparation of N2-protected amino acid aldehydes via reduction of corresponding acid halides with lithium tris-(tert. butoxy)-aluminium hydride. *Tetrahedron Lett.* **1995**, *36*, 7281-7284.
- 312. Morita, T.; Nagasawa, Y.; Yahiro, S.; Matsunaga, H.; Kunieda, T., Versatile Synthons for Optically Pure α-Amino Aldehydes and α-Amino Acids:(+)-and (-)-4, 5-Dialkoxy-2-oxazolidinones. *Organic Lett.* **2001**, *3*, 897-899.
- 313. Fehrentz, J.-A.; Pothion, C.; Califano, J.-C.; Loffet, A.; Martinez, J., Synthesis of chiral N-protected α-amino aldehydes by reduction of N-protected N-carboxyanhydrides (UNCAs). *Tetrahedron Lett.* **1994**, *35*, 9031-9034.
- 314. Ede, N. J.; Bray, A. M., A simple linker for the attachment of aldehydes to the solid phase. Application to solid phase synthesis by the multipin<sup>TM</sup> method. *Tetrahedron Lett.* **1997**, *38*, 7119-7122.
- 315. Morrison, K. L.; Weiss, G. A., Combinatorial alanine-scanning. *Curr. Opin. Chem. Biol.* **2001**, *5*, 302-307.
- 316. Kayikci, M.; Venkatakrishnan, A.; Scott-Brown, J.; Ravarani, C. N.; Flock, T.; Babu, M. M., Visualization and analysis of non-covalent contacts using the Protein Contacts Atlas. *Nat. Struct. Mol. Biol.* **2018**, *25*, 185-194.
- 317. Jhoti, H.; Cleasby, A.; Verdonk, M.; Williams, G., Fragment-based screening using X-ray crystallography and NMR spectroscopy. *Curr. Opin. Chem. Biol.* **2007**, *11*,

- 485-493.
- 318. Riley, K. E.; Hobza, P., On the importance and origin of aromatic interactions in chemistry and biodisciplines. *Acc. Chem. Res.* **2013**, *46*, 927-936.
- 319. Massova, I.; Kollman, P. A., Computational alanine scanning to probe protein—protein interactions: a novel approach to evaluate binding free energies. *J. Am. Chem. Soc.* **1999**, *121*, 8133-8143.
- 320. Migoń, D.; Jaśkiewicz, M.; Neubauer, D.; Bauer, M.; Sikorska, E.; Kamysz, E.; Kamysz, W., Alanine scanning studies of the antimicrobial peptide aurein 1.2. *Probiotics Antimicrob.* **2019**, *11*, 1042-1054.
- 321. Chatterjee, J.; Gilon, C.; Hoffman, A.; Kessler, H., N-methylation of peptides: a new perspective in medicinal chemistry. *Acc. Chem. Res.* **2008**, *41*, 1331-1342.
- 322. Mindt, M.; Risse, J. M.; Gruß, H.; Sewald, N.; Eikmanns, B. J.; Wendisch, V. F., One-step process for production of N-methylated amino acids from sugars and methylamine using recombinant Corynebacterium glutamicum as biocatalyst. *Sci. Rep.* **2018**, *8*, 1-11.
- 323. Räder, A. F.; Reichart, F.; Weinmüller, M.; Kessler, H., Improving oral bioavailability of cyclic peptides by N-methylation. *Bioorg. Med. Chem.* **2018**, *26*, 2766-2773.
- 324. Di, L., Strategic approaches to optimizing peptide ADME properties. *AAPS J.* **2015**, *17*, 134-143.
- 325. Gentilucci, L.; De Marco, R.; Cerisoli, L., Chemical modifications designed to improve peptide stability: incorporation of non-natural amino acids, pseudopeptide bonds, and cyclization. *Curr. Pharm. Des.* **2010**, *16*, 3185-3203.
- 326. Dong, Q.-G.; Zhang, Y.; Wang, M.-S.; Feng, J.; Zhang, H.-H.; Wu, Y.-G.; Gu, T.-J.; Yu, X.-H.; Jiang, C.-L.; Chen, Y., Improvement of enzymatic stability and intestinal permeability of deuterohemin-peptide conjugates by specific multi-site N-methylation. *Amino Acids* **2012**, *43*, 2431-2441.
- 327. Bockus, A.T.; Schwochert, J.A.; Pye, C.R.; Townsend, C.E.; Sok, V.; Bednarek,

- M.A.; Lokey, R.S. Going Out on a Limb: Delineating The Effects of beta-Branching, N-Methylation, and Side Chain Size on the Passive Permeability, Solubility, and Flexibility of Sanguinamide A Analogues. *J. Med. Chem.* **2015**, *58*, 7409–7418.
- 328. Malakoutikhah, M.; Prades, R.; Teixidó, M.; Giralt, E., N-methyl phenylalaninerich peptides as highly versatile blood-brain barrier shuttles. *J. Med. Chem.* **2010**, 53, 2354-2363.
- 329. Fischer, E.; Lipschitz, W., Optisch-aktive N-Monomethyl-Derivate von Alanin, Leucin, Phenyl-alanin und Tyrosin. *Ber. Dtsch. Chem. Ges.* **1915**, *48*, 360-378.
- 330. Fischer, E.; Mechel, L., Formation of active secondary amino acids from halogen acids and primary amines. *Chem Ber.* **1916**, *49*, 1355-66.
- 331. Izumiya, N.; Nagamatsu, A., Walden inversion of amino acids. VI. The synthesis of D-Surinamine (N-methyl-D-tyrosine). *Bull. Chem. Soc. Jpn.* **1952**, *25*, 265-267.
- 332. Winstein, S.; Lucas, H., The Loss of Optical Activity in the Reaction of the Optically Active erythro-and threo-3-Bromo-2-butanols with Hydrobromic Acid. *J. Am. Chem. Soc.* **1939**, *61*, 2845-2848.
- 333. Heravi, M. M.; Ghalavand, N.; Ghanbarian, M.; Mohammadkhani, L., Applications of mitsunobu reaction in total synthesis of natural products. *Appl. Organomet. Chem.* **2018**, *32*, e4464.
- 334. Swamy, K. K.; Kumar, N. B.; Balaraman, E.; Kumar, K. P., Mitsunobu and related reactions: advances and applications. *Chem. Rev.* **2009**, *109*, 2551-2651.
- 335. Papaioannou, D.; Athanassopoulos, C.; Magafa, V.; Karamanos, N.; Stavropoulos, G.; Napoli, A.; Sindona, G.; Aksnes, D.; Francis, G., Redox N-Alkylation of Tosyl Protected Amino Acid and Peptide Esters. *Acta Chem. Scand.* 1994, 48, 324-333.
- 336. Mitsunobu, O., The use of diethyl azodicarboxylate and triphenylphosphine in synthesis and transformation of natural products. *Synthesis* **1981**, *1981*, 1-28.
- 337. Olah, G. A.; Narang, S. C., Iodotrimethylsilane-a versatile synthetic reagent. *Tetrahedron* **1982**, *38*, 2225-2277.

- 338. Biron, E.; Kessler, H., Convenient synthesis of N-methylamino acids compatible with Fmoc solid-phase peptide synthesis. *J. Org. Chem.* **2005**, *70*, 5183-5189.
- 339. Quitt, V. P.; Hellerbach, J.; Vogler, K., Die Synthese optisch aktiver N-Monomethyl-Aminosäuren. *Helv. Chem. Acta.* **1963**, *46*, 327-333.
- 340. Hlaváček, J.; Poduška, K.; Šorm, F.; Sláma, K., N-Methyl analogues of some peptide juvenoids. *Collect. Czech. Commun.* **1976**, *41*, 2079-2087.
- 341. Ben-Ishai, D., Reaction of acylamino acids with paraformaldehyde. *J. Am. Chem. Soc.* **1957**, *79*, 5736-5738.
- 342. Itoh, M., I. Selective Protection of α-or Side-chain Carboxyl Groups of Aspartic and Glutamic Acid. A Facile Synthesis of β-Aspartyl and γ-Glutamyl Peptides. *Chem. Pharm. Bull.* **1969**, *17*, 1679-1686.
- 343. Allevi, P.; Cighetti, G.; Anastasia, M., Cleavage of benzyloxycarbonyl-5-oxazolidinones to α-benzyloxycarbonylamino-α-alkyl esters by alcohols and sodium hydrogen carbonate. *Tetrahedron Lett.* **2001**, *42*, 5319-5321.
- 344. Aurelio, L.; Brownlee, R. T.; Hughes, A. B., Synthetic preparation of N-methyl-α-amino acids. *Chem. Rev.* **2004**, *104*, 5823-5846.
- 345. Reddy, G. V.; Rao, G. V.; Iyengar, D., A practical approach for the optically pure N-Methyl-α-amino acids. *Tetrahedron Lett.* **1998**, *39*, 1985-1986.
- 346. Reddy, G. V.; Iyengar, D., A Simple and Rapid Protocol for N-Methyl-α-Amino Acids. *Chemistry Lett.* **1999**, *28*, 299-300.
- 347. Houck, D., Luis Aceña, J., & Soloshonok, V. A., Alkylations of Chiral Nickel (II) Complexes of Glycine under Phase-Transfer Conditions. *Helv. Chim. Acta*. **2012**, *95*, 2672-2679.
- 348. Ueki, H.; Ellis, T. K.; Martin, C. H.; Boettiger, T. U.; Bolene, S. B.; Soloshonok, V. A., Improved synthesis of proline-derived Ni (II) complexes of glycine: versatile chiral equivalents of nucleophilic glycine for general asymmetric synthesis of α-amino acids. *J. Org. Chem.* **2003**, *68*, 7104-7107.

- 349. Sorochinsky, A. E.; Acena, J. L.; Moriwaki, H.; Sato, T.; Soloshonok, V. A., Asymmetric synthesis of alpha-amino acids via homologation of Ni(II) complexes of glycine Schiff bases; part 1: alkyl halide alkylations. *Amino Acids* **2013**, *45*, 691-718.
- 350. Soloshonok, V. A.; Cai, C.; Yamada, T.; Ueki, H.; Ohfune, Y.; Hruby, V. J., Michael addition reactions between chiral equivalents of a nucleophilic glycine and (S)-or (R)-3-[(E)-enoyl]-4-phenyl-1, 3-oxazolidin-2-ones as a general method for efficient preparation of β-substituted pyroglutamic acids. Case of topographically controlled stereoselectivity. *J. Am. Chem. Soc.* **2005**, *127*, 15296-15303.
- 351. Tanaka, K.; Ahn, M.; Watanabe, Y.; Fuji, K., Asymmetric synthesis of uncommon α-amino acids by diastereoselective alkylations of a chiral glycine equivalent. *Tetrahedron: Asymmetry* **1996**, *7*, 1771-1782.
- 352. Belokon, Y. N.; Tararov, V. I.; Maleev, V. I.; Savel'eva, T. F.; Ryzhov, M. G., Improved procedures for the synthesis of (S)-2-[N-(N'-benzylprolyl)amino]benzophenone (BPB) and Ni(II) complexes of Schiff's bases derived from BPB and amino acids. *Tetrahedron: Asymmetry* **1998**, *9*, 4249-4252.
- 353. Wang, J.; Lin, D.; Zhou, S.; Ding, X.; Soloshonok, V. A.; Liu, H., Asymmetric synthesis of sterically and electronically demanding linear omega-trifluoromethyl containing amino acids via alkylation of chiral equivalents of nucleophilic glycine and alanine. *J. Org. Chem.* **2011**, *76*, 684-687.
- 354. Romoff, T. T.; Palmer, A. B.; Mansour, N.; Creighton, C. J.; Miwa, T.; Ejima, Y.; Moriwaki, H.; Soloshonok, V. A., Scale-up synthesis of (R)- and (S)-N-(2-benzoyl-4-chlorophenyl)-1-(3,4-dichlorobenzyl)pyrrolidine-2-carboxamide hydrochloride, a versatile reagent for the preparation of tailor-made α- and β-amino acids in an enantiomerically pure form. *Org. Process Res. Dev.* **2017**, *21*, 732-739.
- 355. Ng, V.; Kuehne, S. A.; Chan, W. C., Rational design and synthesis of modified teixobactin analogues: in vitro antibacterial activity against Staphylococcus aureus, Propionibacterium acnes and Pseudomonas aeruginosa. *Chem. Eur. J.*

- **2018**, *24*, 9136-9147.
- 356. Sorochinsky, A. E.; Aceña, J. L.; Moriwaki, H.; Sato, T.; Soloshonok, V. A., Asymmetric synthesis of α-amino acids via homologation of Ni (II) complexes of glycine Schiff bases; Part 1: alkyl halide alkylations. *Amino Acids* **2013**, *45*, 691-718.
- 357. Nian, Y.; Wang, J.; Zhou, S.; Dai, W.; Wang, S.; Moriwaki, H.; Kawashima, A.; Soloshonok, V. A.; Liu, H., Purely chemical approach for preparation of D-α-amino acids via (S)-to-(R)-interconversion of unprotected tailor-made α-amino acids. *J. Org. Chem.* **2016**, *81*, 3501-3508.
- 358. Novo, D.; Perlmutter, N. G.; Hunt, R. H.; Shapiro, H. M., Accurate flow cytometric membrane potential measurement in bacteria using diethyloxacarbocyanine and a ratiometric technique. *Cytometry* **1999**, *35*, 55-63.
- 359. Shapiro, H. M., Membrane potential estimation by flow cytometry. *Methods* **2000**, *21*, 271-279.
- 360. Weinstein, J. N.; Klausner, R. D.; Innerarity, T.; Ralston, E.; Blumenthal, R., Phase transition release, a new approach to the interaction of proteins with lipid vesicles Application to lipoproteins. *Biochim Biophys Acta.* **1981**, *647*, 270-284.
- 361. Stocks, S., Mechanism and use of the commercially available viability stain, BacLight. *Cytometry A.* **2004**, *61*, 189-195.
- 362. Rosenberg, M.; Azevedo, N. F.; Ivask, A., Propidium iodide staining underestimates viability of adherent bacterial cells. *Sci. Rep.* **2019**, *9*, 1-12.
- 363. Wenzel, M.; Rautenbach, M.; Vosloo, J. A.; Siersma, T.; Aisenbrey, C. H.; Zaitseva, E.; Laubscher, W. E.; Van Rensburg, W.; Behrends, J. C.; Bechinger, B., The multifaceted antibacterial mechanisms of the pioneering peptide antibiotics tyrocidine and gramicidin S. *MBio.* **2018**, *9*, e00802-18.
- 364. Kano, K.; Fendler, J. H., Pyranine as a sensitive pH probe for liposome interiors and surfaces. pH gradients across phospholipid vesicles. *Biochim. Biophys. Acta.* **1978**, *509*, 289-299.

- 365. Overly, C. C.; Lee, K.-D.; Berthiaume, E.; Hollenbeck, P. J., Quantitative measurement of intraorganelle pH in the endosomal-lysosomal pathway in neurons by using ratiometric imaging with pyranine. *Proc. Natl. Acad. Sci.* **1995**, *92*, 3156-3160.
- 366. O'Neill, A., Staphylococcus aureus SH1000 and 8325-4: comparative genome sequences of key laboratory strains in staphylococcal research.

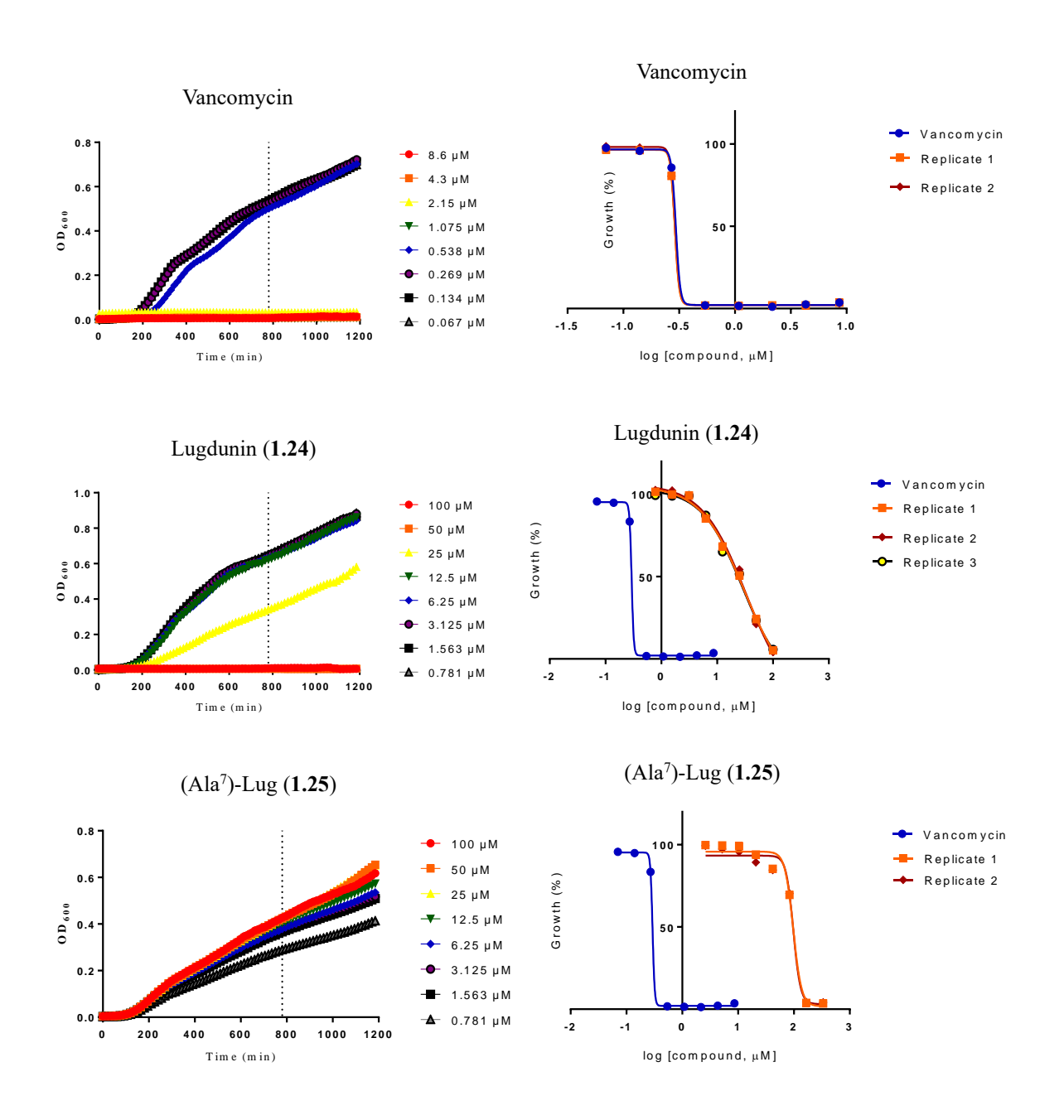
  Lett. Appl. Microbiol. 2010, 51, 358-361.
- 367. Roberts, G. A.; Houston, P. J.; White, J. H.; Chen, K.; Stephanou, A. S.; Cooper, L. P.; Dryden, D. T.; Lindsay, J. A., Impact of target site distribution for Type I restriction enzymes on the evolution of methicillin-resistant Staphylococcus aureus (MRSA) populations. *Nucleic Acids Res.* **2013**, *41*, 7472-7484.
- 368. Baker, J.; Sengupta, M.; Jayaswal, R. K.; Morrissey, J. A., The Staphylococcus aureus CsoR regulates both chromosomal and plasmid-encoded copper resistance mechanisms. *Enviro. Microbiol.* **2011**, 2495-2507.
- 369. Baba, T.; Bae, T.; Schneewind, O.; Takeuchi, F.; Hiramatsu, K., Genome sequence of Staphylococcus aureus strain Newman and comparative analysis of staphylococcal genomes: polymorphism and evolution of two major pathogenicity islands. *J. Bacteriol.* **2008**, *190*, 300-310.
- 370. Hiramatsu, K., Vancomycin-resistant Staphylococcus aureus: a new model of antibiotic resistance. *Lancet Infect. Dis.* **2001**, *1*, 147-155.
- 371. Miller, L. S.; Pietras, E. M.; Uricchio, L. H.; Hirano, K.; Rao, S.; Lin, H.; O'Connell, R. M.; Iwakura, Y.; Cheung, A. L.; Cheng, G., Inflammasomemediated production of IL-1β is required for neutrophil recruitment against Staphylococcus aureus in vivo. *J. Immunol.* **2007**, *179*, 6933-6942.
- 372. Adessi, C.; Soto, C., Converting a peptide into a drug: strategies to improve stability and bioavailability. *Curr. Med. Che.* **2002**, *9*, 963-978.
- 373. Uchiyama, T.; Sugiyama, T.; QUAN, Y. S.; Kotani, A.; Okada, N.; Fujita, T.; Muranishi, S.; Yamamoto, A., Enhanced permeability of insulin across the rat intestinal membrane by various absorption enhancers: Their intestinal mucosal

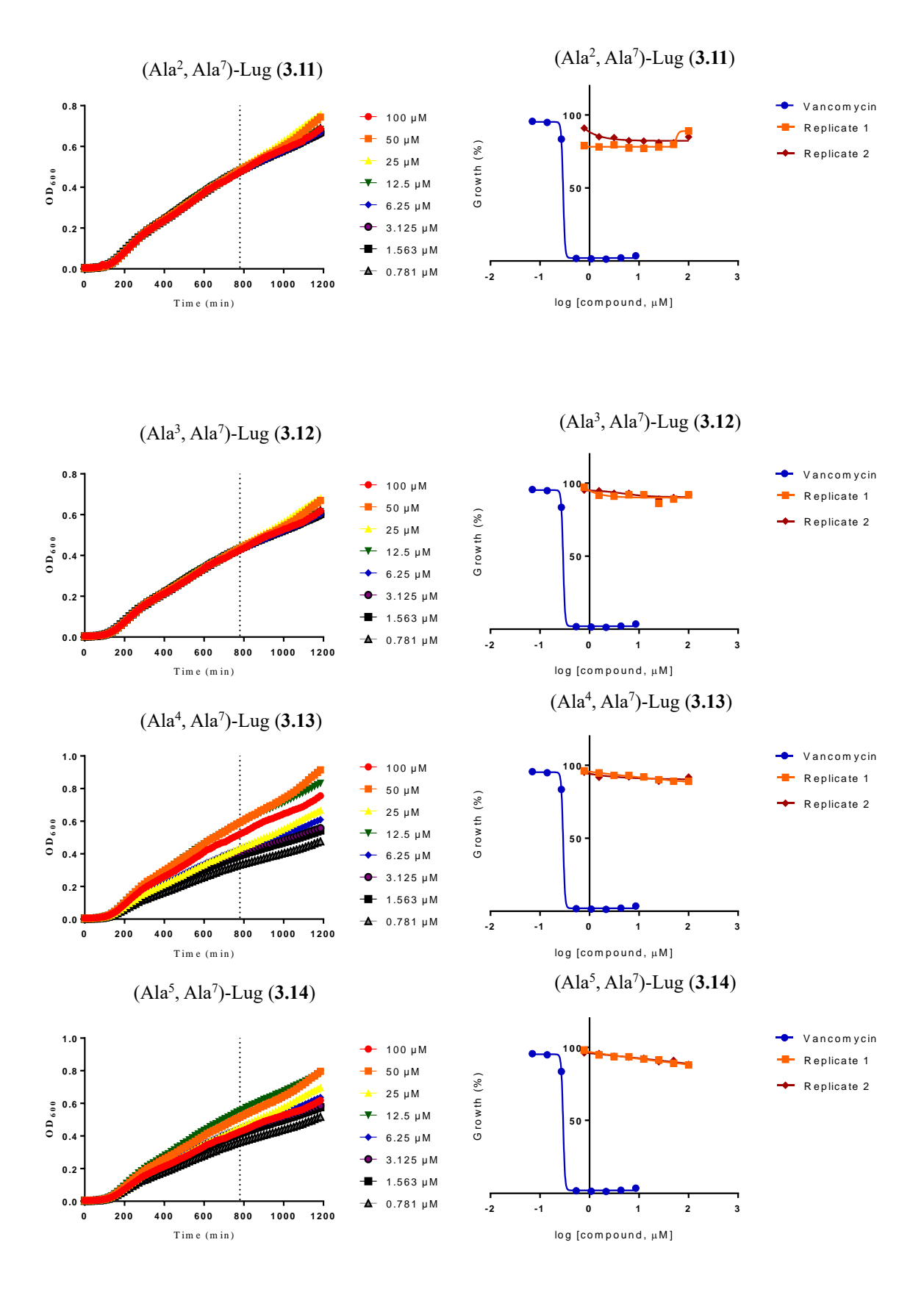
- toxicity and absorption-enhancing mechanism of N-lauryl- $\beta$ -d-maltopyranoside. J. *Pharm. Pharmacol.* **1999,** *51*, 1241-1250.
- 374. Sarnowski, M. P.; Del Valle, J. R., *N*-Hydroxy peptides: solid-phase synthesis and β-sheet propensity. *Org. Biomol. Chem.* **2020**, *18*, 3690-3696
- 375. Detomaso, A.; Curci, R., Oxidation of natural targets by dioxiranes. Part 4: A novel approach to the synthesis of *N*-hydroxyamino acids using dioxiranes. *Tetrahedron Letters* **2001**, *42*, 755-758.
- 376. Nicolaou, K. C.; Estrada, A. A.; Zak, M.; Lee, S. H.; Safina, B. S., A mild and selective method for the hydrolysis of esters with trimethyltin hydroxide. *Angewandte Chemie* **2005**, *117*, 1402-1406.
- 377. Chmiel, T., food Mieszkowska, A., Kempińska-Kupczyk, D., Kot-Wasik, A., Namieśnik, J., & Mazerska, Z., The impact of lipophilicity on environmental processes, drug delivery and bioavailability of components. Microchem. J., **2019**, *146*, 393-406.
- 378. Xiao, J., Cao, H., Wang, Y., Zhao, J., & Wei, X., Glycosylation of dietary flavonoids decreases the affinities for plasma protein. *J. Agric. Food Chem* **2009**, *57*, 6642-6648.
- 379. Griffin, S., Wyllie, S. G., & Markham, J., Determination of octanol—water partition coefficient for terpenoids using reversed-phase high-performance liquid chromatography. *J. Chromatogr. A.* **1999**, *864*, 221-228.
- 380. ACD/Log*P*, www.acdlabs.com/logp/ Advanced Chemistry Development, Inc., Toronto, ON, Canada.

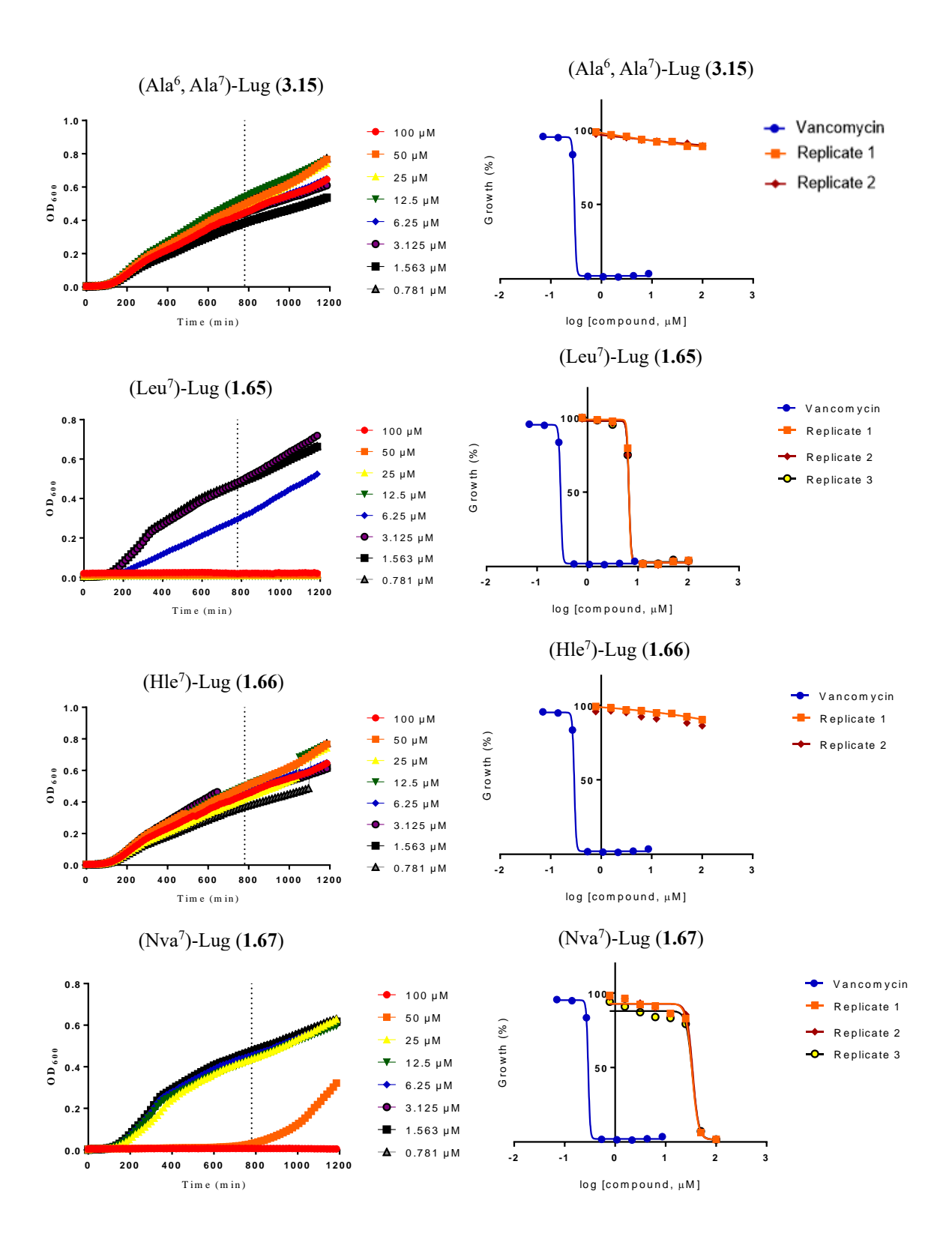
## **Appendix**

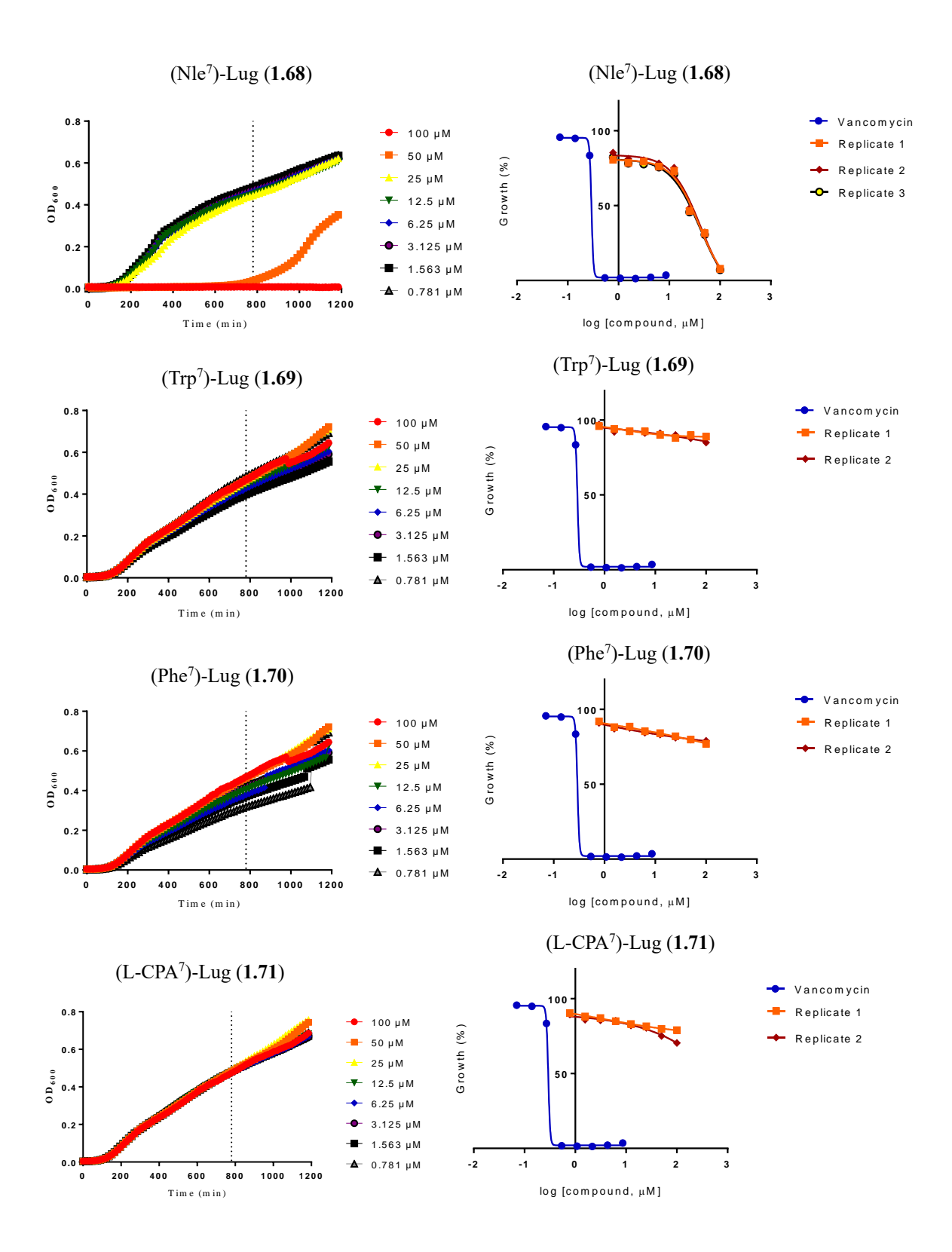
Appendix 1

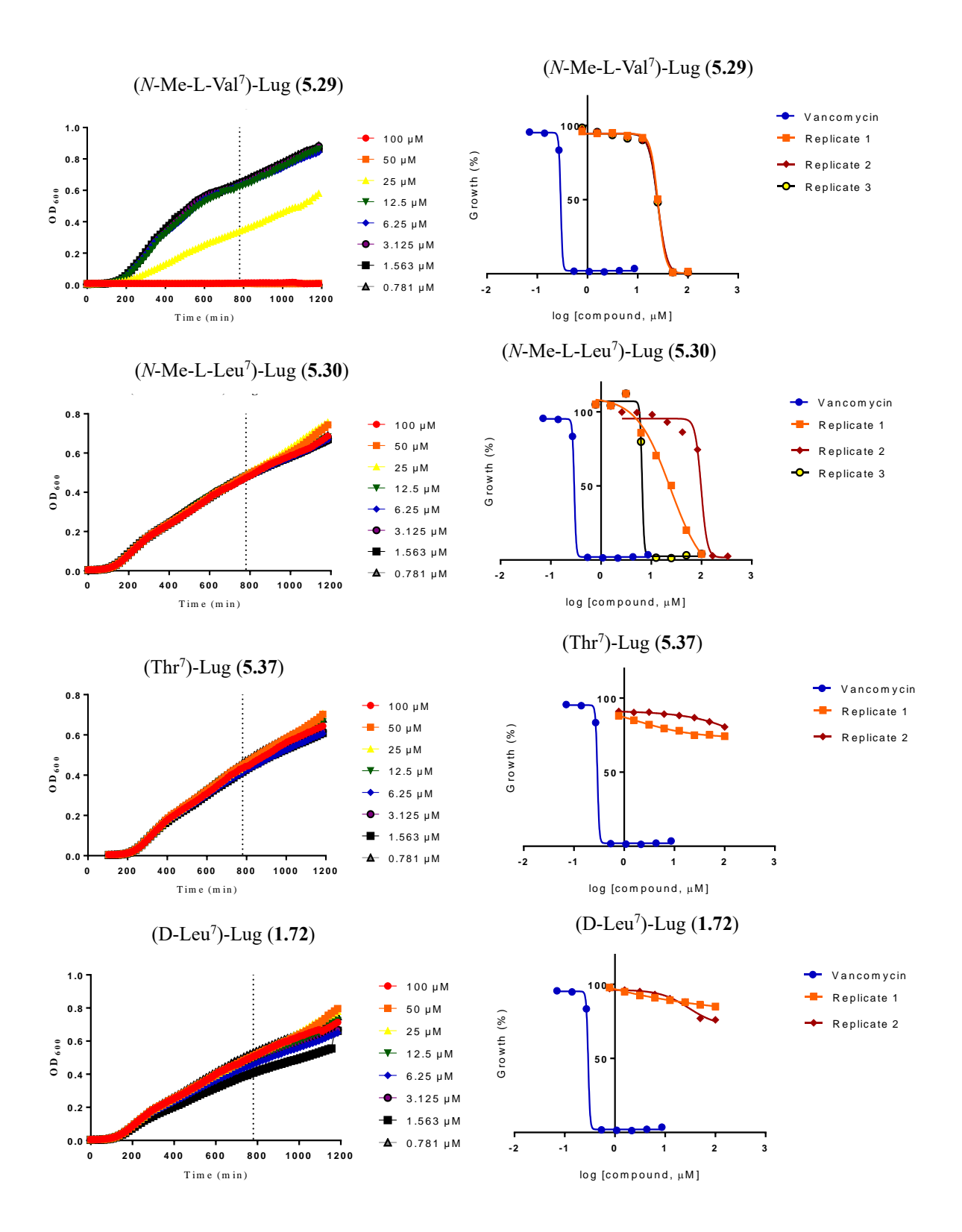
Growth curves and dose-response curves generated from all two/three independent assessments against *S. aureus* SH1000

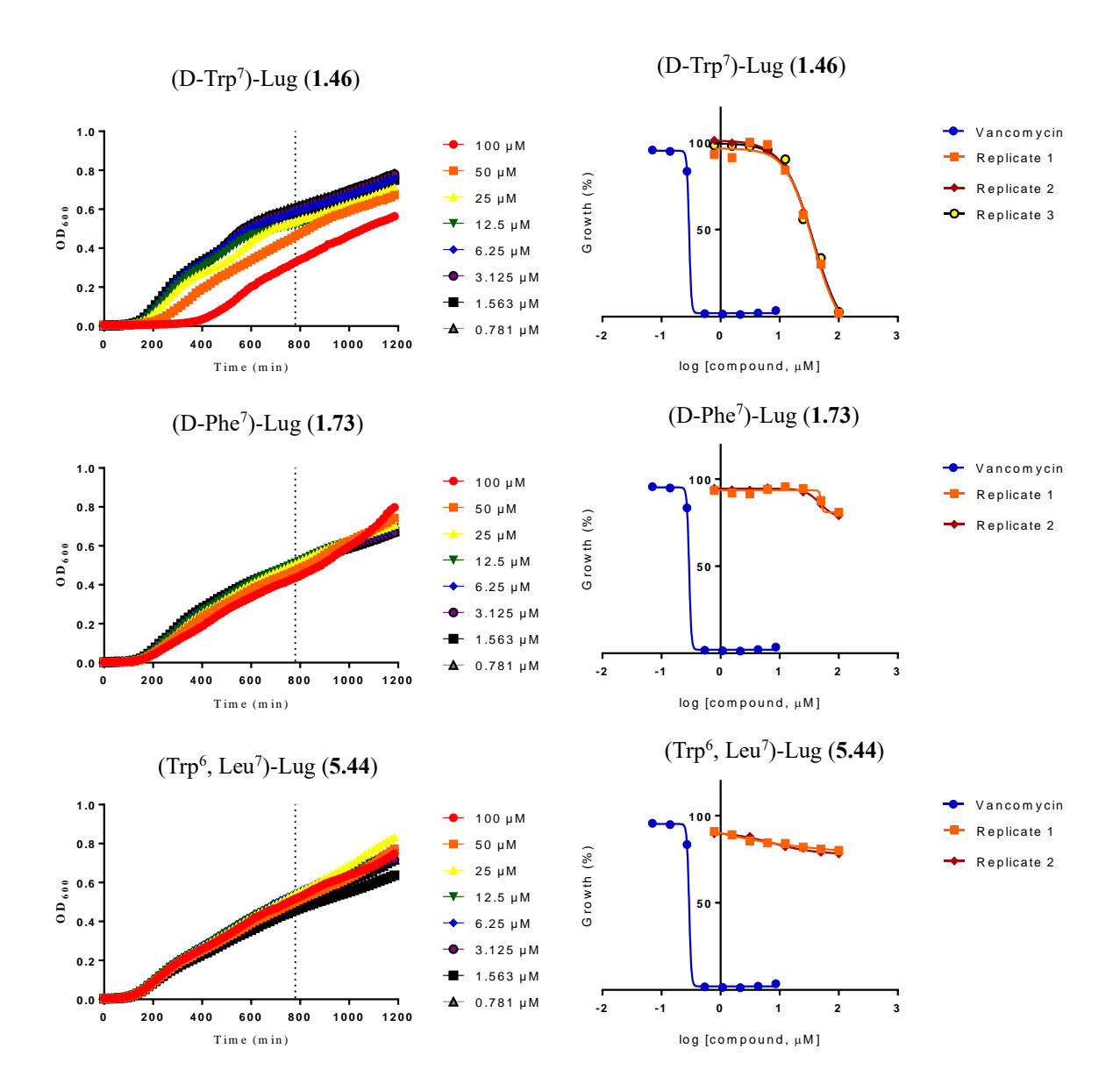












Appendix 2

Growth curves and dose-response curves generated from all two/three independent assessments against *S. aureus* USA300 JE2

